Methods in Molecular Biology 697

Springer Protocols

Scott E. McNeil
Editor

Characterization of Nanoparticles Intended for Drug Delivery

Humana Press

METHODS IN MOLECULAR BIOLOGY™

Series Editor
John M. Walker
School of Life Sciences
University of Hertfordshire
Hatfield, Hertfordshire, AL10 9AB, UK

For other titles published in this series, go to
www.springer.com/series/7651

Characterization of Nanoparticles Intended for Drug Delivery

Edited by

Scott E. McNeil

Nanotechnology Characterization Laboratory, SAIC-Frederick, Inc., National Cancer Institute at Frederick, Frederick, MD, USA

Humana Press

Editor
Scott E. McNeil, Ph.D.
Nanotechnology Characterization Laboratory
SAIC-Frederick, Inc.,
National Cancer Institute at Frederick
Frederick, MD
USA
ncl@mail.nih.gov

ISSN 1064-3745 e-ISSN 1940-6029
ISBN 978-1-60327-197-4 e-ISBN 978-1-60327-198-1
DOI 10.1007/978-1-60327-198-1
Springer New York Dordrecht Heidelberg London

Library of Congress Control Number: 2010938916

Humana Press is part of Springer Science+Business Media (www.springer.com)

Preface

The intent of this book is to provide a basic set of methods for the characterization of nanomaterials for medical use. This is offered to scientists as a survey of methods important in the preclinical characterization of nanomedicines. The chapters will provide methods to characterize the physicochemical properties (e.g., size, aggregation, and surface chemistry), and in vitro immunological and biological characteristics of nanomaterials

Chapter 1 of this volume presents some of the exciting opportunities that are now being realized in the application of nanotechnology to medicine. Nanotechnology is revolutionizing traditional pharmaceutical design by giving drug developers the toolsets and flexibility of engineering. On the nanoscale, medical researchers can "build" new drugs and diagnostics in ways that seem more akin to constructing a machine than to traditional synthetic chemistry. And in certain ways, nanotech pharmaceuticals behave more like tiny, complex, multipart systems than like traditional small molecule drugs.

Characterizing these complex, multipart systems to ensure they are pure, reproducible, safe, and effective can be challenging. Chapters 2 and 3 outline some of these challenges, including interference – nanoparticles often interfere with standardized methods with long histories of use in the pharmaceutical industry. The remainder of this volume contains protocols for nanomaterial characterization, many of which have been developed at the National Cancer Institute's Nanotechnology Characterization Laboratory (NCL) – an interagency collaboration among NCI, FDA and the National Institute of Standards and Technology (NIST). NCL scientists developed these protocols to rigorously characterize nanoparticle physicochemical properties, as well as in vitro immunological and cytotoxic characteristics. These methods have undergone extensive in-house validation and are subjected to regular revision to ensure applicability to a variety of nanomaterial types.

As the reader will appreciate, multiple man-years of effort are incorporated into these chapters. Accordingly, I would like to thank all the authors who have contributed to this work and recognize the efforts that made this publication possible. Specifically, I would like to thank the staff at NCL for their heroic dedication over the years to nanoparticle characterization: Drs. Anil Patri, Stephan Stern, and Marina Dobrovolskaia are the key scientists who developed the majority of these methods. Hands-on support to develop and qualify the protocols was also provided on a daily basis by Chris McLeland, Tim Potter, Barry Neun, Sarah Skoczen, Jamie Rodriguez, and Drs. Jeffrey Clogston and Jiwen Zheng. Within the parent organization of the NCL, SAIC-Frederick, thanks go to Kunio Nagashima, David Parmiter, King Chan, and Drs. Haleem Issaq and Jack Simpson. Other important contributors include Drs. Nakissa Sadrieh and Katherine Tyner at FDA for their very informative overview of how nanotech products are regulated and reviewed. At NIST this list of valuable contributors includes Drs. Vince Hackley, Robert Cook and Jaroslaw Grobelny. Finally, let me also thank Dr. Jennifer Hall at NCL for her extensive help coordinating, assembling, and editing this work.

Scott E. McNeil

Acknowledgment

This project has been funded in whole or in part with federal funds from the National Cancer Institute, National Institutes of Health, under contract HHSN261200800001E. The content of this publication does not necessarily reflect the views or policies of the Department of Health and Human Services, nor does mention of trade names, commercial products, or organizations imply endorsement by the U.S. Government.

Contents

Contributors

Parag Aggarwal, Ph.D. • *Nanotechnology Characterization Laboratory, Advanced Technology Program, SAIC – Frederick, Inc., National Cancer Institute at Frederick, Frederick, MD, USA*

King C. Chan, Ph.D. • *Laboratory of Proteomics and Analytical Technologies, Advanced Technology Program, SAIC – Frederick, Inc., National Cancer Institute at Frederick, Frederick, MD, USA*

Jeffrey D. Clogston, Ph.D. • *Nanotechnology Characterization Laboratory, Advanced Technology Program, SAIC – Frederick, Inc., National Cancer Institute at Frederick, Frederick, MD, USA*

Robert F. Cook, Ph.D. • *Ceramics Division, National Institute of Standards and Technology, Gaithersburg, MD, USA*

Jason de la Cruz • *Electron Microscopy Laboratory, Advanced Technology Program, SAIC – Frederick, Inc., National Cancer Institute at Frederick, Frederick, MD, USA*

Frank W. DelRio, Ph.D. • *Ceramics Division, National Institute of Standards and Technology, Gaithersburg, MD, USA*

Marina A. Dobrovolskaia, Ph.D. • *Nanotechnology Characterization Laboratory, Advanced Technology Program, SAIC – Frederick, Inc., National Cancer Institute at Frederick, Frederick, MD, USA*

Jaroslaw Grobelny, Ph.D. • *Ceramics Division, National Institute of Standards and Technology, Gaithersburg, MD, USA*

Vincent A. Hackley, Ph.D. • *Ceramics Division, National Institute of Standards and Technology, Gaithersburg, MD, USA*

Haleem J. Issaq, Ph.D. • *Laboratory of Proteomics and Analytical Technologies, Advanced Technology Program, SAIC – Frederick, Inc., National Cancer Institute at Frederick, Frederick, MD, USA*

Doo-In Kim, Ph.D. • *Ceramics Division, National Institute of Standards and Technology, Gaithersburg, MD, USA*

Christopher B. McLeland • *Nanotechnology Characterization Laboratory, Advanced Technology Program, SAIC – Frederick, Inc., National Cancer Institute at Frederick, Frederick, MD, USA*

Scott E. McNeil, Ph.D. • *Nanotechnology Characterization Laboratory, Advanced Technology Program, SAIC – Frederick, Inc., National Cancer Institute at Frederick, Frederick, MD, USA*

Kunio Nagashima • *Electron Microscopy Laboratory, Advanced Technology Program, SAIC – Frederick, Inc., National Cancer Institute at Frederick, Frederick, MD, USA*

Barry W. Neun • *Nanotechnology Characterization Laboratory, Advanced Technology Program, SAIC – Frederick, Inc., National Cancer Institute at Frederick, Frederick, MD, USA*
David Parmiter • *Nanotechnology Characterization Laboratory, Advanced Technology Program, SAIC – Frederick, Inc., National Cancer Institute at Frederick, Frederick, MD, USA*
Anil K. Patri, Ph.D. • *Nanotechnology Characterization Laboratory, Advanced Technology Program, SAIC – Frederick, Inc., National Cancer Institute at Frederick, Frederick, MD, USA*
Timothy M. Potter • *Nanotechnology Characterization Laboratory, Advanced Technology Program, SAIC – Frederick, Inc., National Cancer Institute at Frederick, Frederick, MD, USA*
Namboodiri Pradeep, Ph.D. • *Ceramics Division, National Institute of Standards and Technology, Gaithersburg, MD, USA*
Uma Ramalinga, Ph.D. • *Nanotechnology Characterization Laboratory, Advanced Technology Program, SAIC – Frederick, Inc., National Cancer Institute at Frederick, Frederick, MD, USA*
Jamie Rodriguez • *Nanotechnology Characterization Laboratory, Advanced Technology Program, SAIC – Frederick, Inc., National Cancer Institute at Frederick, Frederick, MD, USA*
Nakissa Sadrieh, Ph.D. • *Center for Drug Evaluation and Research, US Food and Drug Administration, Silver Spring, MD, USA*
John T. Simpson, Ph.D. • *Protein Chemistry Laboratory, Advanced Technology Program, SAIC – Frederick, Inc., National Cancer Institute at Frederick, Frederick, MD, USA*
Sarah L. Skoczen • *Nanotechnology Characterization Laboratory, Advanced Technology Program, SAIC – Frederick, Inc., National Cancer Institute at Frederick, Frederick, MD, USA*
Stephan T. Stern, Ph.D. • *Nanotechnology Characterization Laboratory, Advanced Technology Program, SAIC – Frederick, Inc., National Cancer Institute at Frederick, Frederick, MD, USA*
Katherine Tyner, Ph.D. • *Center for Drug Evaluation and Research, US Food and Drug Administration, Silver Spring, MD, USA*
Timothy D. Veenstra, Ph.D. • *Laboratory of Proteomics and Analytical Technologies, Advanced Technology Program, SAIC – Frederick, Inc., National Cancer Institute at Frederick, Frederick, MD, USA*
Jiwen Zheng, Ph.D. • *Nanotechnology Characterization Laboratory, Advanced Technology Program, SAIC – Frederick, Inc., National Cancer Institute at Frederick, Frederick, MD, USA*

Part I

Introduction and Discussion

Chapter 1

Unique Benefits of Nanotechnology to Drug Delivery and Diagnostics

Scott E. McNeil

Abstract

Nanotechnology offers many potential benefits to medical research by making pharmaceuticals more efficacious and by decreasing their adverse side-effects. Preclinical characterization of nanoparticles intended for medical applications is complicated – due to the variety of materials used, their unique surface properties and multifunctional nature. This chapter serves as an introduction to the volume, giving a broad overview of applications of nanotechnology to medicine, and describes some of the beneficial aspects of nanotechnology-based drug delivery. We define nanotechnology and provide brief descriptions of the major classes of nanomaterials used for medical applications. The following two chapters discuss scientific and regulatory hurdles involved in the use of nanotechnology in medicine. The remaining bulk of the volume provides the reader with protocols that have been tested against clinically relevant nanoparticles and describes some of the nuances of nanoparticle types and necessary controls.

Key words: Nanoparticles, nanomedicine, active and passive targeting, efficacy, toxicity

Prior to an involved discussion of protocols for nanotechnology, a definition of terms is in order. The SI prefix "nano" means a billionth (10^{-9}) part, and a nanometer is thus a billionth of a meter (about one hundred thousandth the thickness of a sheet of paper). An object is nanoscale, then, when it is of a size convenient to measure in nanometers – generally less in size than a micron. The nanoscale is also the size scale at which the properties of a material are often different than they are for the bulk (or "macroscale") phase. For many materials, this is approximately in the 1–300 nm size range. In this size range, properties change because as things become very small, their surfaces shrink more slowly than their volumes, causing nanoscale materials ("nanomaterials") to have far larger surface-to-volume ratios than larger objects. More surface area can mean that nanomaterials have higher reactivity; different elastic, tensile, and magnetic properties; increased conductivity; or increased tendency to reflect and refract light.

The nanoscale is a size scale that a cellular biologist is quite familiar with – it is the size range of important cellular components,

Scott E. McNeil (ed.), *Characterization of Nanoparticles Intended for Drug Delivery*, Methods in Molecular Biology, vol. 697,
DOI 10.1007/978-1-60327-198-1_1,

such as DNA (double-stranded DNA is about 2.5 nm in diameter), proteins (hemoglobin is about 5 nm in diameter), cell walls, cell membranes, and compartments. Biological macromolecules were known to display properties and behavior different than macroscale objects far before they were termed "nanoparticles." For example, the way in which proteins fold into globular forms is a process with no analog among larger objects.

The US National Nanotechnology Initiative has defined the nanoscale as 1–100 nm (1). This includes particles which are naturally occurring, such as proteins, particles in smoke, volcanic ash, sea spray, and from anthropogenic sources such as industrial combustion products and automotive exhaust.

The term "nanotechnology" involves manipulating and controlling nanoscale objects. The particles themselves are often engineered, such as those created by chemical reactions, electron beam lithography, or single-molecule manipulation. These nanoparticles can be put to use in a broad spectrum of applications, including aerospace, energy, healthcare, transportation, defense and information technology. They are also found in food additives and sunscreens.

Relevant to this volume, nanoparticles are used as medical devices, as imaging agents and diagnostics, and as drug carriers for therapeutics for many different types of diseases. For this latter application, molecules such as chemotherapeutic agents can be selectively adsorbed or attached to the nanoparticle surface or interior. The drug is affixed to the nanoparticle by covalent conjugation or noncovalent attachment (e.g., encapsulation). Polymer coatings can also be bound to nanoparticle drug carriers – to increase their solubility and biocompatibility.

The major classes of nanoparticles used for nanotech medical applications include: liposomes, nanoshells (including quantum dots), metals and metal oxides, carbon-based particles (carbon nanotubes and fullerenes), nanoemulsions, nanocrystals, and polymer-based nanomaterials (including dendrimers). Table 1 outlines some of the primary clinical uses of each of these types.

One reason why nanotechnology is gaining popularity is that there are great benefits to being able to engineer at the scale of individual macromolecules. For medicine especially, building tiny molecular-scale devices capable of delivering drugs specifically to areas of disease can make conventional pharmaceuticals more efficacious and decrease their adverse side effects. A nanoparticle coated with hydrophilic molecules, for example, can be an effective carrier for an otherwise insoluble drug (2). Similarly, nanoparticle drug carriers can improve therapeutic outcomes by modulating drug distribution to tumor target sites via passive and active targeting. Passive targeting refers to the process whereby nanoscaled particles accumulate in tumors or sites of inflammation simply due to their size. For tumors, this phenomenon is

Table 1
Major classes of nanoparticles used in clinical applications

Nanoparticle class	Examples	Indications and uses
Liposomes	Doxil®	Liposomes provide both hydrophilic and hydrophobic environments, enhancing drug solubility High carrying capacity – each liposome can entrap up to tens of thousands of drug molecules (11)
Nanoshells	Quantum dots Nanospectra AuroShell®	Laser ablation Quantum dots can be used as imaging agents with fluorescence energy proportional to size Semiconductor properties In vitro imaging
Metal colloids and metal oxides	Gold colloid Iron oxide Aurimune®	Biocompatible drug-delivery platform Laser ablation Imaging properties Electron dense
Carbon structures	Carbon nanotubes Fullerenes	Efficient heat conductors; high tensile strength and elastic modulus
Nanoemulsions	Propofol/Diprivan®	Both hydrophilic and hydrophobic environments
Nanocrystals	Rapamune®	Single crystalline Electrical and thermal properties depend on size
Polymer- or protein-based	Abraxane®, Cyclosert®, Avidimer®	Provide both hydrophilic and hydrophobic environments, enhancing drug solubility
Viral vector	Rexin-G®	Commonly used tool of molecular biology to deliver genetic material into cells

referred to as the enhanced permeability and retention (EPR) effect and is caused by the leaky vasculature and incomplete lymphatic system surrounding tumors of soft-tissue and epithelial cell origin (3, 4). The EPR effect allows nanoscale particles to permeate into tumor interstitia and accumulate there (see Fig. 1). Nanotech-based drugs taking advantage of EPR are already demonstrating pronounced improvements in efficacy.

Active targeting works through the attachment of biochemical moieties, such as monoclonal antibodies, which facilitate delivery to diseased tissues expressing biomarkers that distinguish it from the surrounding healthy tissue (5, 6). Examples of these biomarkers include membrane receptors and mutated cellular proteins. Both active and passive targeting can lower a drug's adverse effects by reducing its systemic exposure to healthy tissues and organ systems.

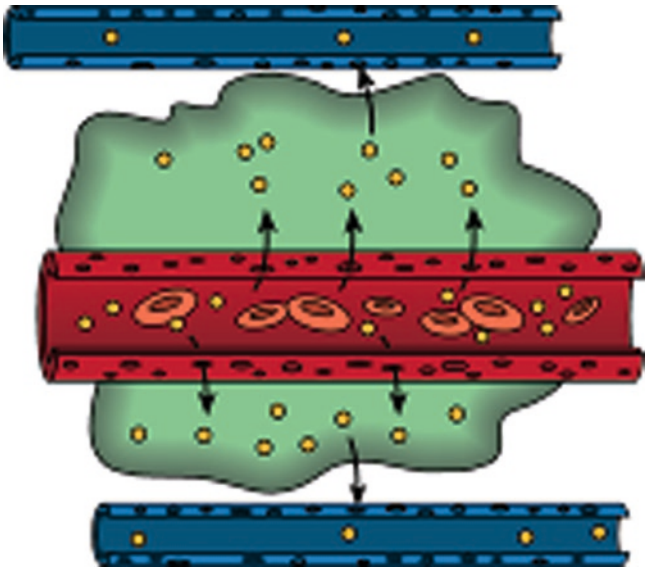

Fig.1. *Illustration of the enhanced permeability and retention* (*EPR*) *effect*. Nanoscale particles (represented here as *gold spheres*) may penetrate leaky tumor vasculature and accumulate in diseased tissue (teal). If the nanoparticle is a drug carrier for a chemotherapeutic, that chemotherapeutic may be more efficacious than in its free (non-nanotech) form due to the high concentrations of the carrier-bound particles which build up in the tumor.

Certain nanotech reformulations of existing drugs show remarkably decreased toxicity in comparison to their free (sometimes termed "native") forms. An excellent example of this is a drug in development by CytImmune Sciences, Inc. under the trade name Aurimune® (7). Aurimune consists of tumor necrosis factor alpha (TNF-α) bound to polyethylene glycol (PEG)-coated nanosized colloidal gold. Almost ten years ago, TNF-α in its free form was discontinued during clinical trials due to severe immunotoxicity. Using the nanotech formulation (Aurimune), this same quantity of TNF-α was given to patients – but with minimal ill effect. This illustrates the utility of nanoparticle platforms in decreasing toxicity and adverse side effects.

Another way a nanoparticle platform may be used to improve a drug formulation is through serving as an alternative to conventional administration vehicles, which are sometimes toxic. For example, the potent chemotherapeutic paclitaxel is not soluble in water. Under the trade name Taxol®, paclitaxel is dissolved in Cremophor EL, a polyoxyethylated castor oil, which is toxic. Abraxane®, an albumin-bound form of paclitaxel uses the nanotech platform of albumin as an alternative to Cremophor EL. Abraxane (which gained FDA approval in 2005) has been shown to be both more efficacious and less toxic than Taxol (8, 9) (Fig. 2).

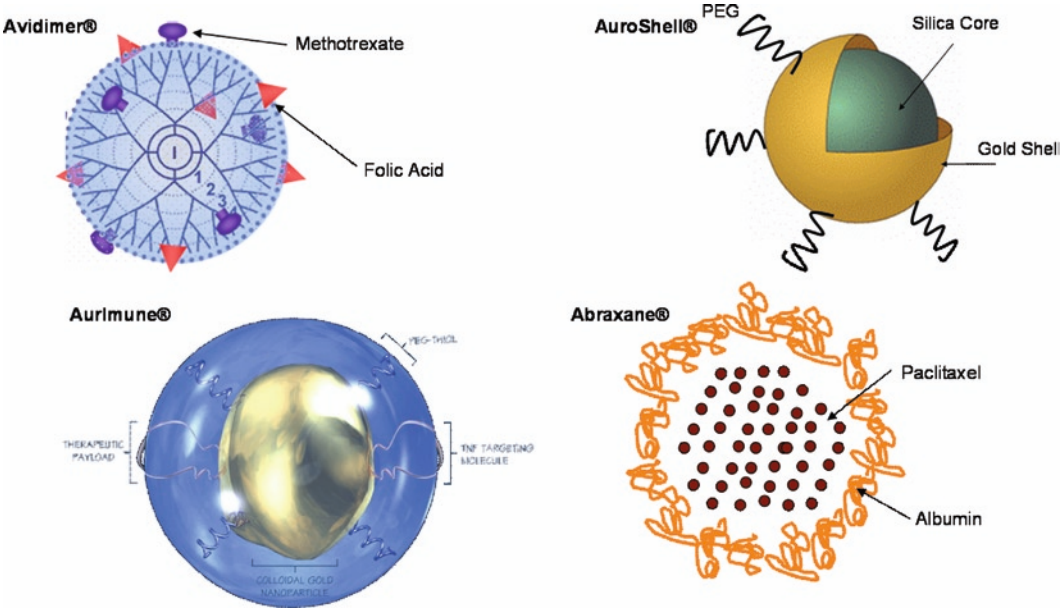

Fig. 2. *Schematic illustrations of nanotech cancer applications.* Not drawn to scale. From *top left*, Avidimer's folic acid and methotrexate functionalized dendrimers, Nanospectra AuroShells® used for thermal ablation of tumors, CytImmune Sciences' AurImmune®, and Abraxane®, which is albumin-stabilized paclitaxel.

Finally, the ability to engineer at the nanoscale confers the ability to combine several beneficial features into one multicomponent, multifunctional nanoparticle. The nanoparticle can serve as a scaffold for attachment of a variety of chemical moieties, each of which performs an individual medical function. For example, ligands for particular cellular receptors can be attached to the nanoparticle to facilitate active targeting to tissues expressing those receptors (10). Additionally, hydrophilic molecules, such as polyethylene glycol (PEG), can be bound to the nanoparticle surface to increase solubility and biocompatibility. Finally, image contrast agents, such as chelated gadolinium, can be conjugated to the nanoparticles for diagnostic purposes. The resulting nanoparticle is a multifunctional entity engineered to have greater biocompatibility and efficacy than a conventional small-molecule drug.

Because nanoparticle-based drugs represent novel medical entities, they pose novel challenges for scientists, developers, and regulatory agencies. In particular, the FDA and pharmaceutical industries have used standardized tests to assess material biocompatibility for several decades. Nanoparticle developers and manufacturers leverage these well-established methods whenever possible, but the unique properties of nanomaterials often complicate this seemingly straightforward process. Some of the challenges involved in nanoparticle characterization are detailed in

the following two chapters. The remainder of the volume consists of protocols specifically developed for nanoparticle characterization, and intended for use by the research community, drug developers, and regulatory agencies. Such methods are needed to speed up the translation of nanoparticle drugs from discovery to development, accelerating the conversion of the benefits of nanotechnology to drug delivery and diagnostics into real benefits for patients.

Acknowledgments

This project has been funded in whole or in part by federal funds from the National Cancer Institute, National Institutes of Health, under contract N01-CO-12400. The content of this publication does not necessarily reflect the views or policies of the Department of Health and Human Services, nor does the mention of trade names, commercial products, or organizations imply endorsement by the US Government.

References

1. http://www.nano.gov/html/facts/whatIsNano.html
2. Harris, J.M., Chess, R.B. (2003) Effect of pegylation on pharmaceuticals. *Nat Rev Drug Discov* **2**, 214–21.
3. Fang, J., Sawa, T., Maeda, H. (2003) Factors and mechanism of "EPR" effect and the enhanced antitumor effects of macromolecular drugs including SMANCS. *Adv Exp Med Biol* **519**, 29–49.
4. Maeda, H., Wu, J., Sawa, T., Matsumura, Y., Hori, K. (2000) Tumor vascular permeability and the EPR effect in macromolecular therapeutics: a review. *J Control Release* **65**, 271–84.
5. Sahoo, S.K., Labhasetwar, V. (2003) Nanotech approaches to drug delivery and imaging. *Drug Discov Today* **8**, 1112–20.
6. Ravi Kumar, M., Hellermann, G., Lockey, R.F., Mohapatra, S.S. (2004) Nanoparticle-mediated gene delivery: state of the art. *Expert Opin Biol Ther* **4**, 1213–24.
7. Paciotti, G.F., Myer, L., Weinreich, D., Goia, D., Pavel, N., McLaughlin, R.E., Tamarkin, L. (2004) Colloidal gold: a novel nanoparticle vector for tumor directed drug delivery. *Drug Deliv* **11**, 169–83.
8. Desai, N., Trieu, V., Yao, Z., Louie, L., Ci, S., Yang, A., Tao, C., De, T., Beals, B., Dykes, D., Noker, P., Yao, R., Labao, E., Hawkins, M., Soon-Shiong, P. (2006) Increased antitumor activity, intratumor paclitaxel concentrations, and endothelial cell transport of cremophor-free, albumin-bound paclitaxel, ABI-007, compared with cremophor-based paclitaxel. *Clin Cancer Res* **12**, 1317–24.
9. Green, M.R., Manikhasm, G.M., Orlovm, S., Afanasyev, B., Makhson, A.M., Bhar, P., Hawkins, M.J. (2006) Abraxane, a novel Cremophor-free, albumin-bound particle form of paclitaxel for the treatment of advanced non-small-cell lung cancer. *Ann Oncol* **17**, 1263–8.
10. Patri, A.K., Kukowska-Latallo, J.F., Baker, J.R. Jr. (2005) Targeted drug delivery with dendrimers: comparison of the release kinetics of covalently conjugated drug and non-covalent drug inclusion complex. *Adv Drug Deliv Rev* **57**, 2203–14.
11. Huwyler, J., Wu, D., Pardridge, W.M. (1996) Brain drug delivery of small molecules using immunoliposomes. *Proc Natl Acad Sci USA* **93**, 14164–9.

Chapter 2

Challenges for Nanoparticle Characterization

Scott E. McNeil

Abstract

The Food and Drug Administration (FDA) and pharmaceutical industry have used standards to assess material biocompatibility, immunotoxicity, purity, and sterility (as well as many other properties) for several decades. Nanoparticle developers and manufacturers leverage well-established methods as much as possible. However, the unique properties of nanomaterials often interfere with standardized protocols, giving false-positive or false-negative results. This chapter provides details of some of the problems which can arise during the characterization of nanoparticle samples. Additionally, we discuss ways to identify, avoid, and resolve such interference, with emphasis on the use of inhibition and enhancement controls.

Key words: Nanoparticles, nanomedicine, active and passive targeting, efficacy, toxicity

Nanotechnology offers the potential to significantly transform diagnostics and therapeutics, as described in the previous chapter. The ability to manipulate the biological and physicochemical properties at the macromolecular size-scale allows for efficient drug targeting and delivery, which result in greater potency and decreased adverse side effects. Nanoparticles intended for clinical applications consist of a wide variety of materials, for which preclinical characterization is particularly challenging. Many of these particles scatter light (e.g., gold colloids) or have optical properties which may invalidate colorimetric assays that rely on absorbance measurements (e.g., quantum dots). Other nanoparticles, such as dendrimers, can have catalytic properties that interfere with enzymatic tests.

Most nanoparticle formulations include surfactants to promote dispersion (i.e., prevent agglomeration) of the primary particles. These compounds too can interfere with conventional characterization methods. Impurities and contaminants which adsorb to nanoparticle surfaces can also contribute to ambiguous analytical results. These difficulties tend to hamper the development of standards for characterization and the subsequent clinical application of nanoparticles.

An investigational new drug (IND) or investigative device exemption (IDE) application is the first step in the FDA approval

Scott E. McNeil (ed.), *Characterization of Nanoparticles Intended for Drug Delivery*, Methods in Molecular Biology, vol. 697,
DOI 10.1007/978-1-60327-198-1_2,

process which is required by law before a developer can test a candidate drug's therapeutic or diagnostic potential in humans (1). Preclinical testing data in the IND must demonstrate that the new drug will not expose humans to unreasonable risks during initial use, and, in the case of therapeutics, that the drug exhibits sufficient pharmacological activity to justify first-in-man clinical trials. For small-molecule drugs, the FDA has criteria for the types of preclinical data which should be presented in an IND. For nanomaterials, an IND can be less straightforward, since there is no standardized set of characterization methods for these materials. Until such standards become available, nanotech developers have to design and validate their own novel characterization methods to assess safety, toxicity, and quality control. The FDA then faces the difficulty of interpreting data generated by a variety of unfamiliar techniques without a substantial history of acceptance in scientific literature. All of this complicates the preclinical development process and can increase the time preceding first-in-man trials for nanotech-based drugs.

One of the chief complications for preclinical characterization is the multicomponent nature of many nanoparticle-based therapeutics. The nanoparticle can serve as a scaffold for attachment of chemical moieties that each perform a particular medical function (e.g., targeting ligands, hydrophilic coatings that improve solubility, imaging agents, drugs, etc.). The resulting nanoparticle therapeutic is a multipart, multifunctional entity with greater complexity than a conventional small-molecule drug. Assessing the safety and efficacy of such a complex entity can be a daunting task. Ultimately, the realization of the use of these multicomponent nanoparticles in clinical trials is highly dependent on rigorous preclinical characterization.

Thorough characterization is also key for evaluating the safety of nanoparticles for incidental exposure and addressing concerns about environmental health and safety (EHS). Whether or not nanomaterials are more toxic than their macroscale counterparts has been a matter of extensive debate in the EHS community. The scientific literature contains a wide range of research findings, which are often conflicting due to the variety of methods used and to subtle variations in test materials. Arriving at a definitive answer to this question will depend on thorough characterization using standardized methods and materials.

A rational characterization strategy for biomedical nanoparticles contains three elements: physicochemical characterization, in vitro assays, and in vivo studies. Each of these is essential to a comprehensive understanding of nanoparticle safety and efficacy. For example, without physicochemical characterization there can be no meaningful interpretation of in vitro or in vivo biological data or interlaboratory comparison. The simplicity and amplified reactions of in vitro assays may help elucidate the biological

mechanism of action of a therapeutic or toxicant. Testing in in vitro physiological models can also give an initial estimate of formulation efficacy and toxicity. Realistically though, it is not possible for the laboratory bench to exactly match the complex biological interplay found in vivo. It is therefore necessary to characterize the absorption, distribution, metabolism, and excretion and toxicity (ADME) of a drug formulation in animal models.

In terms of physicochemical properties, traditional small-molecule drugs are characterized by their molecular weight, chemical composition, purity, solubility, and stability. These data form the basis of the chemistry, manufacturing, and controls (CMC) section of the IND application with the FDA. For small molecules, the instrumentation to ascertain these properties have been well established and the techniques are standardized. Techniques like nuclear magnetic resonance (NMR), mass spectrometry, ultraviolet-visible (UV-Vis) spectroscopy, infrared spectroscopy (IR), and gas chromatography (GC) can be run in a high-throughput fashion to analyze such molecules. For nanomaterials, alternate instrumentation is required to obtain information on the same properties (composition, purity, stability, etc.). These properties influence biological activity, and may depend on parameters such as particle size, size distribution, surface area, surface charge, surface functionality, shape, and aggregation state. Additionally, since many nanoparticle concepts are multifunctional (with targeting, imaging, and therapeutic components), the stability and distribution of these components can have dramatic effects on nanoparticle biological activity as well.

It is now widely acknowledged that physicochemical properties such as size and surface chemistry can dramatically affect nanoparticle behavior in biological systems (2–7) and influence biodistribution, safety and efficacy. For instance, a decrease in particle size leads to an exponential increase in surface area per unit mass, and a concomitant increase in the availability of reactive surface groups. Nanoparticles with cationic surfaces have a notably increased tendency to permeate (and perforate) cellular membranes compared to neutral or anionic nanoparticles (8). Physicochemical characterization of properties such as size, surface area, surface chemistry, and aggregation state can provide the basis for better understanding of structure–activity relationships. In this volume, methods are presented for determining nanoparticle size in solution by dynamic light scattering (DLS), molecular weight via mass spectrometry, surface charge through zeta potential measurement and topology by atomic force microscopy (AFM). Methods are also presented for transmission electron microscopy (TEM) and scanning electron microscopy (SEM) examination of nanoparticle samples, and elemental identification using energy dispersive X-ray spectroscopy (EDX).

Another important and challenging area of nanoparticle characterization is measurement under physiological conditions that resemble or mimic the physical state in vivo. Many properties of nanoparticles are environment and condition dependent; for example, the particle's hydrodynamic size at physiological pH and ionic strength may differ from the size in water or the dry state. Surface charge may also depend on the pH and ionic strength of the suspending solution. Plasma proteins are known to bind nanoparticles in the blood, and the protein-bound size is expected to be a more relevant determinant of disposition and clearance than the free-particle size. The release profile of an encapsulated therapeutic may even be environment dependent (9). That is, there may be faster or slower release of the therapeutic as the temperature, pH, and/or ionic strength of the solution surrounding the nanoparticle formulation is varied.

Because the results of in vitro biological assays often don't correlate with in vivo endpoints, in vitro characterization is performed to elucidate mechanisms, not necessarily to screen for biocompatibility. In vitro studies may also be used to identify areas requiring attention for in vivo animal studies. Unfortunately, nanoparticle-based therapeutics frequently interfere with conventional in vitro pharmacologic assays. For instance, many nanoparticles aggregate or adsorb proteins. Other nanoparticles scatter light or have optical properties, which may invalidate colorimetric assays that rely on absorbance measurements. Some nanoparticles have catalytic properties that may interfere with enzymatic tests, such as those that evaluate endotoxin contamination. These many interferences necessitate the use of inhibition and enhancement controls. These are control samples with known properties included in an in vitro assay along with analyte samples to ensure accurate results. For example, in tests to evaluate endotoxin contamination, known amounts of endotoxin can be spiked into nanoparticle samples. If the endotoxin assay reliably measures the true (i.e., known) amount then the researcher can be reasonably sure that the nanoparticles are not interfering with the test method. However, if the test returns a measurement substantially higher (enhancement) or lower (inhibition) than the true amount in the control samples, then the test must be modified before the results can be meaningful.

Figure 1 illustrates the use of inhibition and enhancement controls in a test for endotoxin contamination. Bacterial endotoxin or lipopolysaccharide (LPS) is a membrane component of most bacteria. Administration of a drug contaminated with bacterial endotoxin can cause fever, shock, and even death. Accordingly, the FDA sets limits on the number of endotoxin units (EU), which may be present in a drug or device product. Detection of the products of the Limulus amoebocyte lysate (LAL) reaction can be an effective means of quantifying the endotoxin units present in a drug formulation.

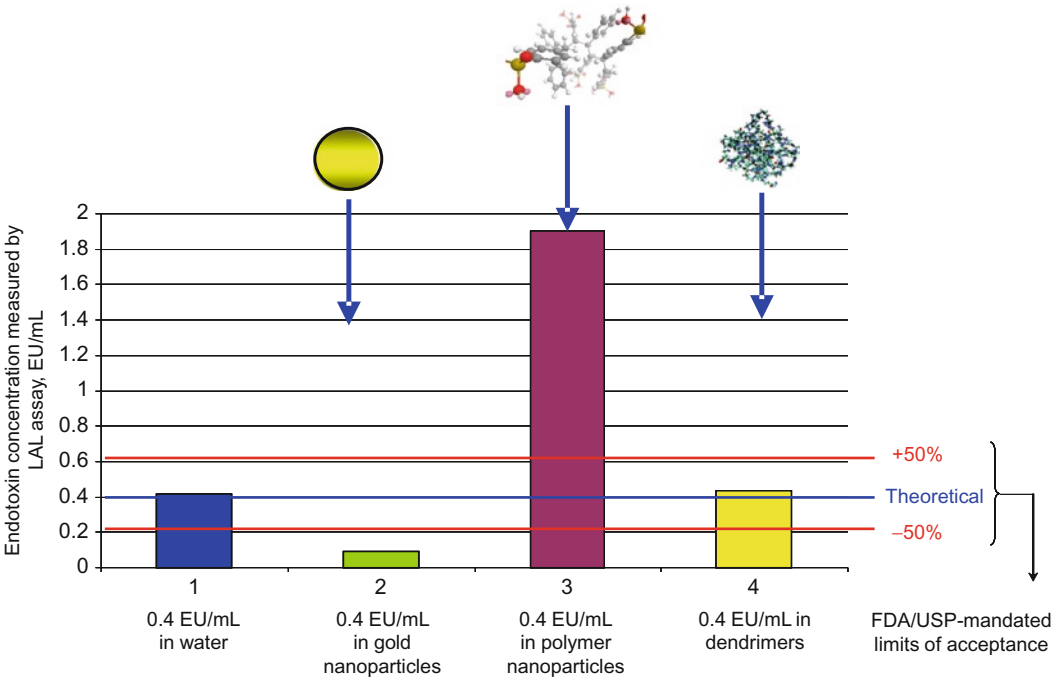

Fig. 1. The line at 0.4 EU/mL represents the assay response which would reflect the true amount of spiked endotoxin in the samples (0.4 EU/mL endotoxin). The lines at ± 50% represent the FDA/USP mandated limits for assay acceptance (±50%). The gold colloid interferes with the assay, the polymer greatly enhances the result, and the dendrimer yields acceptable values.

However, many nanoparticles interfere with the reactivity of endotoxin, the LAL reaction, or the detection of the reaction products. Known amounts of endotoxin can be spiked into samples as inhibition and enhancement controls to evaluate if the particles interfere with the LAL assay. In Fig. 1, water, gold colloid, polymeric, and dendrimeric nanoparticles were spiked with endotoxin inhibition and enhancement controls (a known amount of endotoxin). As can be seen, the LAL test on the water and dendrimeric samples yield a result near the true amount of spiked sample. The gold colloid nanoparticles, however, inhibit the assay, returning an endotoxin reading which is less than the known amount spiked into the sample. The test on the polymeric nanoparticles yields an endotoxin concentration corresponding to a much greater amount of endotoxin than was spiked into the sample. It cannot be concluded from this test alone if the polymeric particles enhance the assay or are in fact contaminated with endotoxin.

Biocompatibility of nanomaterials with blood can be evaluated in vitro, and the methods presented in this volume make use of a variety of cell-based in vitro systems including immortalized cell

lines or combinations of cell lines and primary cell preparations freshly derived from organ and tissue sources. This volume includes 20 methods for in vitro characterization of nanoparticle samples. These are assays to evaluate sterility, toxicity, and explore immunological properties. Protocols for in vitro assessment of hemolysis, complement activation, and thrombogenicity are presented as these tests are required by the FDA for conventional pharmaceuticals (10). There is also an in vitro test for nanoparticle phagocytosis, which can be predictive of recognition by the immune system and clearance by the reticuloendothelial system (RES).

In summary, the characterization of nanoparticle-based drugs poses a host of novel challenges for scientists, developers, and regulatory agencies. This volume contains protocols for nanoparticle characterization, many of which have been developed at the National Cancer Institute's Nanotechnology Characterization Laboratory (NCL) – an interagency collaboration among NCI, FDA and the National Institute of Standards and Technology (NIST). NCL scientists developed these protocols to rigorously characterize nanoparticle physicochemical properties (e.g., size, aggregation, and surface chemistry), as well as in vitro immunological and cytotoxic characteristics, and ADME/Tox profiles in animal models (Fig. 2). These methods have undergone extensive

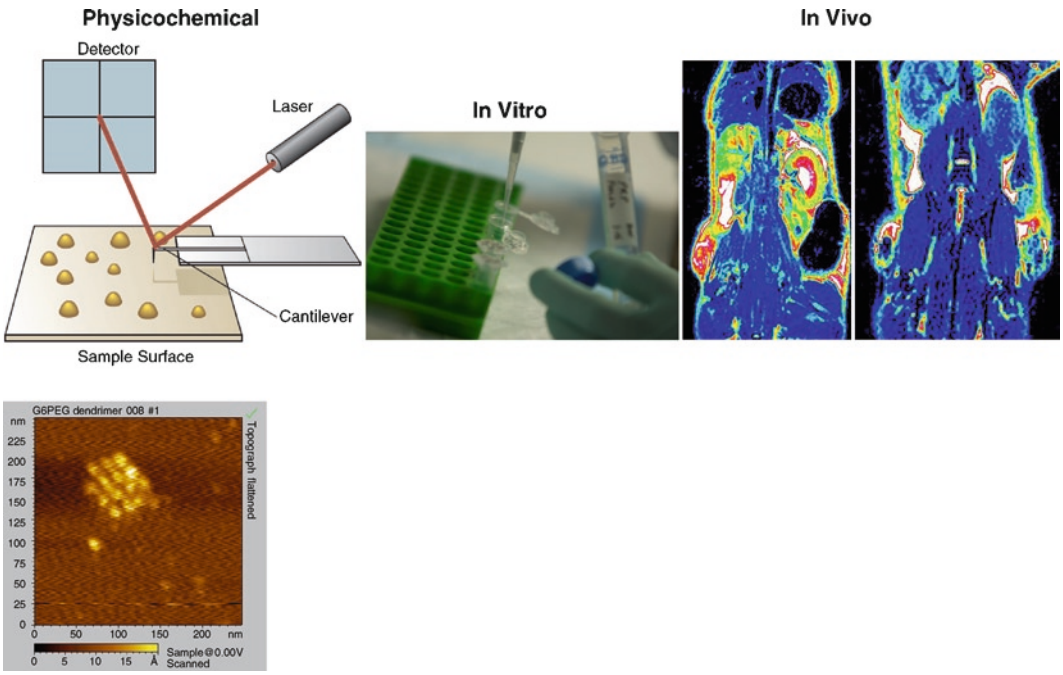

Fig. 2. Characterizing nanoparticles in the NCL assay cascade. Nanotechnology strategies submitted to NCL are characterized in a standardized assay cascade developed in collaboration with the National Institute of Standards and Technology and the Food and Drug Administration. This three-tiered system for nanoparticle characterization consists of physicochemical, in vitro, and in vivo testing.

in-house validation and are subjected to regular revision to ensure applicability to a variety of nanomaterial types. Standardized protocols specific to nanoparticles, such as those presented in this volume, can be employed along with appropriate controls to avoid and overcome many of the challenges described in this chapter.

Acknowledgments

This project has been funded in whole or in part with federal funds from the National Cancer Institute, National Institutes of Health, under contract N01-CO-12400. The content of this publication does not necessarily reflect the views or policies of the Department of Health and Human Services, nor does mention of trade names, commercial products, or organizations imply endorsement by the US Government.

References

1. For the remainder of the chapter we confine the discussion to the IND process for drugs regulated through the FDA's Center for Drug Evaluation and Research (CDER). A similar process is required in the Investigational Device Exemption (IDE) filing for a device regulated through the FDA's Center for Devices and Radiological Health (CDRH).
2. Kobayashi H, Kawamoto S, Jo SK, Bryant HL, Jr, Brechbiel MW, Star RA. Macromolecular MRI contrast agents with small dendrimers: pharmacokinetic differences between sizes and cores. Bioconjugate Chemistry 2003; 14: 388–394.
3. Oberdorster G, Oberdorster E, Oberdorster J. Nanotoxicology: an emerging discipline evolving from studies of ultrafine particles. Environmental Health Perspectives 2005; 113: 823–839.
4. Furumoto K, Nagayama S, Ogawara K, Takakura Y, Hashida M, Higaki K, Kimura T. Hepatic uptake of negatively charged particles in rats: possible involvement of serum proteins in recognition by scavenger receptor. Journal of Controlled Release 2004; 97: 133–141.
5. Oberdorster G. Toxicology of ultrafine particles: in vivo studies. Philosophical Transactions of the Royal Society of London Series A, Mathematical Physical and Engineering Sciences 2000; 358: 2719–2739.
6. Ogawara K, Yoshida M, Higaki K, Kimura T, Shiraishi K, Nishikawa M, Takakura Y, Hashida M. Hepatic uptake of polystyrene microspheres in rats: effect of particle size on intrahepatic distribution. Journal of Controlled Release 1999; 59: 15–22.
7. Ogawara K, Yoshida M, Kubo J, Nishikawa M, Takakura Y, Hashida M, Higaki K, Kimura T. Mechanisms of hepatic disposition of polystyrene microspheres in rats: effects of serum depend on the sizes of microspheres. Journal of Controlled Release 1999; 61: 241–250.
8. Fenart L, Casanova A, Dehouck B, Duhem C, Slupek S, Cecchelli R, Betbeder D. Evaluation of effect of charge and lipid coating on ability of 60-nm nanoparticles to cross an in vitro model of the blood-brain barrier. Journal of Pharmacology and Experimental Therapeutics 1999; 291: 1017–1022.
9. Rajananthanan P, Attard GS, Sheikh NA, Morrow WJ. Novel aggregate structure adjuvants modulate lymphocyte proliferation and Th1 and Th2 cytokine profiles in ovalbumin immunized mice. Vaccine 1999; 18: 140–152.
10. ASTM International Standard Practice F748-98. "Selecting generic biological test methods for materials and devices."

Chapter 3

Considerations When Submitting Nanotherapeutics to FDA/CDER for Regulatory Review

Katherine Tyner and Nakissa Sadrieh

Abstract

The Food and Drug Administration (FDA) does not, as yet, have specific guidances for products containing nanoscale materials. As announced in the report issued by the FDA Nanotechnology Task Force (July 2007), however, there are recommendations to various centers within the FDA to develop guidances for industry. Regardless of the lack of explicit FDA guidances, there are therapeutics currently on the market containing nanoscale materials, and additional novel nanomaterial-containing therapeutics are being developed with the hopes of being submitted for regulatory review and approval. While, for the most part, these novel nanomaterial-containing products are being evaluated using the same regulatory requirements as products that do not contain nanomaterials, it is increasingly evident that at least in the area of characterization of nanomaterials used in drug products, there may be areas where special focus is needed. Specific areas include the validity of applying small molecule principles and methodologies to nanomaterial-containing products, the effects the nanomaterial will impart to the rest of the formulation (or vice versa), and how the physicochemical properties may be impacted by biological settings. Similarly, for safety evaluation, biodistribution studies will be at the core of any evaluation of products containing nanomaterials. These biodistribution studies will, in effect, be indicative of where the nanoparticles are traveling and possibly accumulating, therefore subjecting those sites to increased likelihood of toxicological effects. This chapter focuses on questions and considerations that may arise for sponsors during product characterization, as well as considerations for the appropriate design and conduct of in vivo toxicology studies. This chapter will also review how current FDA guidances apply to nanotherapeutics.

This chapter reflects the current thinking and experience of the authors. However, this is not a policy document and should not be used in lieu of regulations, published FDA guidances, or direct discussions with the agency.

Key words: Nano-therapeutic, nano-pharmaceutics, characterization, regulatory, safety assessment

1. Introduction

Nanomedicine has emerged as a promising field for future therapeutics, with applications that could impact many products regulated by the Center for Drug Evaluation and Research

Scott E. McNeil (ed.), *Characterization of Nanoparticles Intended for Drug Delivery*, Methods in Molecular Biology, vol. 697,
DOI 10.1007/978-1-60327-198-1_3, © Springer Science+Business Media, LLC 2011

(CDER), within the Food and Drug Administration (FDA). Currently, the FDA does not have an official definition of nanotechnology or nanomedicine (http://www.fda.gov/nanotechnology/), although the agency has reviewed and is currently reviewing products that would fall into traditional definitions of nanotechnology (1, 2) (http://www.nano.gov/html/facts/whatIsNano.html, http://nihroadmap.nih.gov/nanomedicine/). Similarly, there are over-the-counter products on the market that have been described by some as containing nanoparticles (specifically cosmetics and other topical products such as sunscreens). Whether these materials, or products containing these materials, need to be evaluated differently from "traditional products" has not been established, despite much discussion within and outside the agency. This chapter attempts to address some, but not all, of the notable issues that may arise when a nanotherapeutic is being developed and later submitted for regulatory review.

2. Initial Product Characterization

Physicochemical characterization of therapeutics is fundamental for understanding resulting safety issues stemming from product use. As such, manufacturers of all regulated products are required to provide basic physiochemical characterization as part of investigational new drug (IND) or new drug applications (NDA) submitted to the FDA for review (3). Included in the characterization is proper identification of the therapeutic including, but not limited to, structure, composition, crystal structure, quality, stability, and purity as well as the synthetic route of the therapeutic. Products containing nanotherapeutics are not currently subject to additional regulatory requirements or exempt from any of the regulatory review steps, and the "necessary" product characterization is expected to be completed as a part of the regulatory submissions. The product characterization consists of all the factors listed above, as well as other features that may be identified during the review process by the reviewing division. For example, in addition to the standard physiochemical information normally required for small molecules, it has been proposed that products containing nanomaterials may need to be additionally characterized to include information related to their unique features such as particle size and particle size distribution, particle shape (morphology), surface effects (including surface area, reactivity, and coatings), and aggregation/agglomeration effects in relevant systems (4, 5). There may also be several specific questions concerning the novel properties of specific nanotherapeutics that need to be addressed on a case-by-case basis during characterization procedures.

2.1. How Is the Product Performance and Quality Impacted by the Fact that It Contains Nanoscale Features?

There are bonafide reasons to formulate a nanosized therapeutic over a larger-sized drug. Biodistribution and the pharmacokinetic profile of an I.V. injectable nanotherapeutic may be altered by changing the particle size (6). By taking advantage of the substantially increased surface area of nanoparticles, bioavailability of poorly soluble drugs may also be enhanced (7, 8). In addition, surface effects and coatings (including multifunctional coatings) can further enhance a nanotherapeutic in terms of active targeting, increased plasma half-life, controlled release of drugs, and multifunctional activity (9, 10). During initial characterization, novel properties should be identified and noted for subsequent analysis. For example, if the size of the therapeutic is crucial for correct biodistribution, then an analytical method that provides statistical information about individual particles may be more appropriate than one that provides bulk or average results of the entire formulation.

2.2. Will the Formulation Procedure and/or Product Use Change the Nanotherapeutic?

Nanotherapeutics should be characterized in the form to which the end-user will be exposed, which means in the final formulation. Although this statement holds true for all regulated materials (i.e., the final product must be tested), it is especially important to emphasize for nanomaterials. This is because the high surface-to-bulk ratio for nanomaterials and the subsequent increased importance of surface effects may result in the raw nanomaterial differing significantly from the formulated product. Aggregation/agglomeration effects alone can significantly alter the behavior of otherwise perfectly behaved materials. Therefore, if the nanotherapeutic will be delivered in an I.V. injectable format, the product should be characterized in the I.V. solution, containing all excipients and other inactive ingredients. If the therapeutic is formulated into a cream or gel, the therapeutic should be characterized in this matrix, and so forth. Furthermore, a determination must be made with regards as to what could change in the product during normal use. Stability information for drug products is usually requested for all submitted applications including the expected shelf life of the product and any compositional changes such as crystal phase changes or product degradation. Specific nanotherapeutic considerations with regards to stability include aggregation/agglomeration and their potential effects on a product's effectiveness and toxicity. Additionally, surface coatings, if applicable, may also need to be monitored for stability issues both for the coating itself and the potential effects from exposure to the core material and released coating after the coating has degraded (11).

There is an effort in the nanotherapeutic field to develop multifunctional or "smart" drugs, which would have a combination of features including targeting, therapy, imaging, sensing, controlled delivery, and controlled degradation (leading to elimination). The benefits to such drugs include reducing the overall

quantity of drug delivered systemically, while increasing the activity at the targeted dosing site and reducing the drug concentration at sites that are not diseased (9, 10, 12). This fact alone could significantly reduce the dose of a drug needed to be administered as well as reduce any possible side effects or toxicities associated with the use of that product. For products such as chemotherapeutics and cytotoxic drugs, this consideration is by no means trivial, and constitutes a major advantage for the use of nanotechnology-based delivery systems. In addition to reducing the therapeutic dose, when multifunctional moieties are incorporated into a nanotherapeutic, the number of injections/administrations given to a patient can potentially be reduced, providing yet another advantage to the patient.

In terms of multifunctional nanomaterials, all novel components, including the nanoparticle delivery system (or carrier) and surface moieties, need to be considered and examined in detail, since these moieties will impart properties to the product that can potentially impact performance and quality. This analysis should include any interactions with other components in the formulation and any potential release, whether intentional or not. In addition, significant changes to a formulation (i.e., a new surface coating) may also need to be evaluated both separately and in the final formulation. Of course, the extent of the analysis will have to be decided on a case-by-case basis and agreed to by both the sponsor and the reviewing division, and may depend on factors such as prior knowledge about the ligands and the base nanoparticle. Most importantly, the requested studies must be guided by sound science.

When a product is expected to change during use (such as controlled delivery or degradation), the changes should be characterized and quantified. Therefore, the fate of all the components of a multifunctional construct needs to be understood and evaluated. If a construct is metabolized to its individual components, then it becomes necessary to fully understand where these components localize, how they are cleared, and whether they may be responsible for some of the observed findings in preclinical studies. This type of information will help provide a complete preclinical characterization, as well as facilitate the monitoring of subjects in clinical trials. As therapeutics are continuously modified during development, in order to achieve the optimal formulation, it is possible that the above analysis may present significant challenges in terms of time, resources, and instrumentation. The development of high-throughput testing and lab-on-a-chip technology may hopefully alleviate some of the time and resource constraints.

It only stands to reason that the amount of characterization for an NME (new molecular entity) is likely to be different than for a previously approved molecule. It is worth noting, however,

that even a previously approved ligand, when formulated as a targeted nanotherapeutic, may have a different pharmacokinetic profile, biodistribution and possible toxicological profile, as compared to the free ligand. In some cases, the incorporation of a ligand into a nanotherapeutic may improve efficacy and reduce overall toxicity of the drug. On the other hand, previously inaccessible areas of the body may now be exposed to the ligand. For example, if a targeted nanotherapeutic incorporates a previously approved ligand into its structure, but the entire moiety concentrates in a particular tissue that would have not been exposed to the free ligand, then that particular tissue would potentially be exposed to a larger dose of the ligand, especially if it is released from its carrier through degradation. In this case, existing preclinical data of the ligand would not be able to support the clinical development of the nanotherapeutic. This is a clear example that even if the toxicology of a free ligand is known (from a previously approved product), this information may not suffice to support the development of a nanotherapeutic that incorporates the ligand as part of its construct. For this reason, it is only upon the evaluation of pharmacokinetic and ADME profile (absorption, distribution, metabolism, and excretion) of the complete nanotherapeutic, that one can truly estimate the need for additional studies.

2.3. How will Components in the Product Formulation Affect Characterization Procedures and Choice of Instrumentation?

The size and complexity of nanotherapeutics can sometimes cause the resulting product to fall between the range and sensitivity of traditional instrumentation used for small molecules and/or bulk materials. Recent advances as well as application/modification of older technologies have emerged to address this issue, but there still can be shortcomings in terms of adequate characterization of different aspects of nanotherapeutics. Traditional nanocharacterization techniques such as electron microscopy and scanning probe microscopy are not always amenable to in-line processing or high-throughput analysis. Advances in instrumentation, however, are allowing for automated analysis in traditionally time-consuming methods such as particle size, morphology, surface features, and compositional statistics using scanning electron microscopy coupled with energy dispersive X-ray analysis (13) and atomic force microscopy for complex phase analysis (14). In addition, methods traditionally used for small molecule characterization such as chromatography and analytical centrifugation may be adapted for characterizing nanopharmaceuticals. As technology advances, further methods will become available for in-line characterization, and these methods will need to be evaluated and validated for generalized use. The current FDA thinking on analytical method validation may be found in a draft guidance (15).

As the FDA has no definitive guidance on instrumentation for complete nanotherapeutic characterization, the sponsor's

understanding of the product and justification of the chosen instrumentation for analysis will play a role in the review process. The benefits of this approach is that the choice is left to the sponsor, thus relieving obstacles of meeting established requirements as well as fostering innovation in methods and process development for nanotherapeutics.

In the near future, many of the nanotherapeutics submitted for review are expected to be I.V. injectables for cancer therapies. This is partly due to the high benefit-to-risk ratio for that patient population. Solutions of nanoparticles have some of the most well-defined characterization pathways in terms of size and aggregation/agglomeration effects (16–18). Difficulties may be encountered with especially dilute or concentrated systems; however, advances in the above technologies can now often handle these situations.

When the nanotherapeutic is incorporated into a complex formulation such as a cream, gel, or a solid dosage form, such as a tablet, the difficulty of characterization increases (and will increase further when particles are roughly the same size as other features in the bulk matrix or are of the same basic composition of the matrix). Traditional light-scattering techniques often would not be appropriate in these cases, and care needs to be taken to ensure that the nanotherapeutic is correctly identified from the matrix. For example, if particles are placed in an oil and water emulsion, the particles of interest should be identified as separate entities from the other features (i.e., do not mistake an emulsion droplet for a drug nanoparticle). Chemical analysis can be beneficial in these cases (X-ray analysis, confocal Raman analysis, etc.) although the resolution for many methods is not always sufficient to resolve individual particles. If the formulation is further complicated by the particles having a similar composition to the matrix, additional information such as crystal structure or phase analysis of the bulk material may be useful to positively identify different components within the formulation.

A major factor in the production of a drug product, regardless of whether it contains nanoparticles, is the assurance of product quality during the manufacturing process and upon completion of manufacturing. The techniques that have been used in the past to ensure product quality during manufacture have included chromatography and spectroscopy, amongst others. While these methods have been proven adequate for small molecules, their usefulness for evaluating nanotherapeutic constructs remains to be determined.

Finally, care must be taken during analytical evaluation that the overall product is not significantly changed by the method. If the product is not diluted during use, then it should not be diluted during testing. If the product is not dried during use, then it should be analyzed in environmental conditions, etc. Figure 1

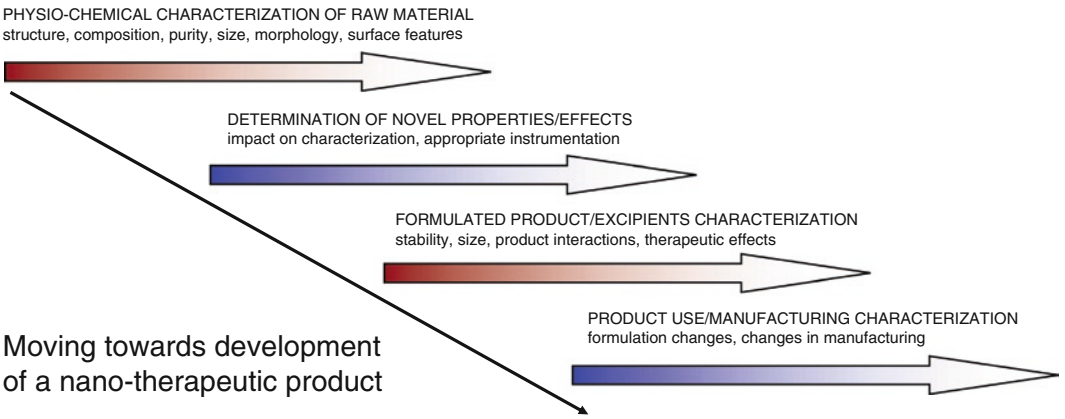

Fig. 1. Suggested chronology for nanotherapeutic characterization.

shows a basic timeline for characterization steps when developing a nanotherapeutic. In general, the bulk of the physicochemical characterization will occur early in the development stage. As formulations are modified and manufacturing steps are identified, characterization procedures will focus more on final product characterization and quality control.

In summary, nanotherapeutics should be characterized in biologically relevant systems. Characterization should focus on aspects of the nanotherapeutic that are expected to impart novel activity, and instrumentation should be chosen to appropriately characterize this activity or any potential changes to the therapeutic during use in the as-formulated product.

3. Animal Toxicology Studies

3.1. Biological Relevance

Depending on the formulation of the nanopharmaceutical being developed, there may be a need for more or less extensive preclinical evaluation of the product. There are cases where sponsors have reformulated previously approved drugs into "new" nanopharmaceuticals, simply by milling the active pharmaceutical ingredient (API) into nanoparticles. An example of this is seen in formulations using nanocrystal colloidal dispersions for several recently approved products, which were previously approved as formulations that did not contain nanoparticles. In other situations, constructs are being developed using delivery systems made up of nanoparticles (such as dendrimers or gold) to which ligands comprised of previously approved drugs have been attached. In both cases, because of prior information available on some of the components of the nanopharmaceutical, some parts of the preclinical development may have been streamlined, with respect

to the types of animal studies needed. However, if both the nanoparticle and the ligands are novel entities, never before used in humans, it is likely that the preclinical development will be more involved. One can argue that because a nanoparticle-based reformulation of a previously approved product has novel properties that are being exploited, such as better solubility, targeting, or biodistribution, there exist enough reasons to evaluate the product based on its own, new, merits, independent of those of a previously approved product. At the heart of additional evaluations for nanoreformulations of previously approved products are the bridging biodistribution and toxicology studies. These studies should directly compare the previously approved formulation to the new formulation. The requirements for additional preclinical data can be modified based on the findings of these bridging studies.

There are, however, studies that may need to be conducted in order to understand the behavior of nanotherapeutic formulations in biological systems. If there are suitable methods available, these studies may be conducted in vitro, in order to help fully describe the physical behavior of nanoparticle-containing formulations in blood and tissues. Previous chapters in this volume have addressed some of these techniques. These studies are of particular importance to the proper understanding of pharmacokinetic and toxicology studies. Factors that may impact the physical behavior of nanopharmaceuticals can include the following.

3.1.1. Aggregation/ Agglomeration

Due to the high aggregation/agglomeration potential of most nanomaterials, the addition of particles into biological solutions (saline, etc.) can cause aggregation and agglomeration that can significantly alter the performance of the therapeutic as well as the overall formulation itself (19). As mentioned in the previous section, the nanotherapeutic must be characterized in biologically relevant environments, in part to assess such agglomeration/aggregation effects.

3.1.2. Opsonization

If a nanoparticle has the potential to be opsonized in vivo, it becomes necessary to evaluate any effects prior to studies in animals and humans. These studies are necessary as opsonization is likely to affect certain characteristics of the nanopharmaceutical, especially its surface properties, including charge, targeting effectiveness, and agglomeration potential. Similarly, the impact of opsonization on characterization parameters and preclinical findings needs to be fully assessed. Clearly, opsonization may also impact issues such immune system modulation, which may present significant challenges to developing nanoparticle-based drugs.

3.1.3. Sufficient Concentration

In order to allow for proper administration and exposure of preclinical species to a nanoformulation, it is necessary to ensure that

the product can be dissolved in a biological matrix (buffer, saline), such that it can be administered to animals. In the event that dissolution at a high enough concentration cannot be achieved, dosing the animals at sufficiently high concentrations to result in biological effects may become impossible. In order to ensure sufficient concentration, there needs to be some effort put into developing methods that allow nanoparticle-based formulations to be suspended in biological media at biologically and toxicologically relevant concentrations.

3.2. Biodistribution Studies

Biodistribution studies are crucial in helping sponsors interpret toxicological findings and design adequate monitoring procedures for clinical studies. It is imperative to know where in the body the nanotherapeutic is distributing, how long it remains at the sites to which it is distributing, if it is transformed (metabolized), and when and how it is cleared from the sites to which it is distributing. This information would allow sponsors to more accurately interpret any toxicological finding that may be observed in the preclinical studies, particularly if the findings for a multifunctional nanotherapeutic are significantly different that those of the free ligand(s). If lesions are observed in a tissue where a nanoparticle has been found to distribute and accumulate, then it is likely that a direct link can be established between the nanoparticle and the observed toxicity. On the other hand, if a nanoparticle is found to be present in a tissue in the absence of apparent lesions, it may mean one of two things: either the nanoparticles are not toxicologically relevant, or the study was terminated too early, and insufficient time was allowed for the pathology to manifest itself. In the latter case, knowing this information will allow the sponsor to better design future toxicology studies aimed at establishing whether there may or may not be a toxicological relevance to the presence of nanoparticles in a particular organ where nanoparticles are accumulating. The following section lists several guidance documents that are currently published, some of which are specifically focused on the conduct and interpretation of pharmacokinetic and toxicokinetic studies. While these guidances are not intended for nanopharmaceuticals exclusively, the general principles do apply to these products as much as to small molecules.

3.2.1. Current Guidances as Applied to Nanoparticle Preclinical Drug Development

It needs to be emphasized that all the currently published guidance documents that are applicable for the development of small molecule drugs will also apply to the development of nanopharmaceuticals. A complete review of all FDA guidances is beyond the scope of this chapter. Below is a list of selected guidance documents that may be most relevant when considering how to plan the early stages of a program for nanopharmaceutical development. Additionally, as many multifunctional nanomaterials may

Table 1
Examples of relevant guidance documents useful in the early stages of nanopharmaceutical development

M3 nonclinical safety studies for the conducts of human clinical trials for pharmaceuticals	http://www.fda.gov/cder/guidance/1855fnl.pdf
Pharmacokinetics and tissue distribution	http://www.fda.gov/cder/guidance/ichs3b.pdf
Toxicokinetics	http://www.fda.gov/cder/guidance/ichs3a.pdf
Estimating the maximal safe starting dose in initial clinical trials for therapeutics in adult healthy volunteers	http://www.fda.gov/cder/guidance/5541fnl.pdf
Content and format of investigational new drug applications (INDs) for Phase 1 studies of drugs, including well-characterized, therapeutic biotechnology-derived products	http://www.fda.gov/cder/guidance/clin2.pdf
Single dose acute toxicity testing for pharmaceuticals	http://www.fda.gov/cder/guidance/pt1.pdf
Liposome guidance	http://www.fda.gov/cder/guidance/2191dft.pdf

be considered innovative combination products, the guidances given in Table 1 may be applicable (20).

To date, there have been no guidances issued by CDER, or any part of the FDA which focus specifically on nanomaterial-containing products. While there are discussions about the need for guidances for products with nanoscale materials and there are definite plans to develop such documents, no guidances are currently under preparation for the specific purpose of nanopharmaceutical development. One of the main reasons for this is that there have been no compelling reasons to believe that nanopharmaceuticals need to be treated in a fundamentally different manner from small molecules, despite some academic reports in the published literature (using mostly in vitro models which are not often predictive of in vivo behavior). It is believed that the reported differences, which stem from features such as their small size, the capacity to target tissues, and their multifunctionality, do not lead to compelling reasons to regulate these pharmaceutical products outside of the current rigorous preclinical requirements that apply to small molecules, as the current tests should still be able to identify potential hazards and efficacy issues. It is believed, however, that the Chemistry, Manufacturing and Controls (CMC) of nanopharmaceuticals may pose novel challenges to the regulatory requirements for CMC data This belief is mainly due to the fact that the novel features of the nanotherapeutic (structure, shape, composition, and surface properties), are often evaluated

with methods not traditionally found in small-molecule CMC procedures. For this reason, it is felt that the first guidance documents that will be issued by CDER are likely to be ones that will focus on product characterization and the methodologies that can be used to assess physicochemical properties of nanoscale drugs.

The list of guidance documents in Table 1 is solely provided to illustrate the point that existing guidance documents will most likely cover many aspects of the nanopharmaceutical development process. However, as mentioned above, there will be situations, as with nanomaterial characterization, where specific guidances may be necessary. In light of the current paucity of data on nanomaterial manufacturing and nanopharmaceutical characterization, FDA is counting on input from interested parties, to help develop guidance documents on these topics.

Of the guidances listed above, the ICH M3 (http://www.fda.gov/cder/guidance/1855fnl.pdf) document, which relates to the timing of nonclinical studies during the clinical development of pharmaceuticals, is of particular value. In this document, the timing of preclinical studies such as single and repeat dose toxicity studies, reproduction toxicity studies, genotoxicity studies, local tolerance studies, carcinogenicity studies, safety pharmacology studies, and pharmacokinetic studies (absorption, distribution, metabolism, and excretion) is discussed. It is likely that all the issues mentioned in the M3 document, including the timing of the conduct of preclinical studies will apply to nanopharmaceuticals, as they apply to small molecule drugs.

When preparing a package for submission to the agency, the guidance document on the content and format of INDs is very valuable in that it provides a near step-by-step description of how current regulations at 21 CFR 312.22 and 312.23 should be interpreted with respect to data submission in support of an application. This guidance document details the great flexibility in the amount and depth of data required in an IND, depending on the phase of investigation and the specific human testing proposed. The guidance clarifies that in order to expedite the entry of new drugs into clinical testing, the Agency will accept integrated summary reports of toxicology findings based upon unaudited draft toxicological reports of completed animal studies as initial support for human studies, and specifies the manufacturing data appropriate for a Phase 1 investigation. Other guidance documents listed above, and those not listed, need to be referenced by product developers for their applicability and relevance to the specific nanotherapeutic under development.

3.2.2. Qualitative Methods to Evaluate Nanoparticle Biodistribution

As discussed above, in order to correctly interpret the pharmacology and toxicology studies submitted in support of drug applications for nanopharmaceuticals, a comprehensive knowledge of the absorption, distribution, metabolism, and excretion (ADME) of

the compound is necessary. To obtain information on potential sites of action, it is important to conduct tissue distribution studies. Nanopharmaceutical products are often composed of carrier particles (the nanoparticle) attached to therapeutic drug molecules as well as targeting ligands. These constructs are designed to achieve targeted delivery of therapeutic molecules. In such cases, it is theoretically possible that the construct may only accumulate at the site of action. In order to evaluate the distribution of such targeted therapies, it is necessary to conduct appropriate biodistribution studies. Traditionally, qualitative methods such as histopathology have been used in order to detect possible lesions in tissues, resulting from exposure to a drug. The presence of a lesion has often been directly linked with tissue exposure to drugs, although secondary lesions, resulting from the drug's pharmacological effects at another site are also likely. Due to some of the unique applications of nanopharmaceuticals, it is possible that these conventional methods for detection of qualitative changes in tissues could be complemented with additional modalities, such as in vivo imaging of dosed animals. If such modalities were to be exploited, then imaging methods such as MR (magnetic resonance) or PET (positron emission tomography) would greatly enhance the capacity to assess the biodistribution of a nanopharmaceutical product. While some imaging modalities may be qualitative in nature, there are advances that could allow for quantitative assessments via imaging tools, thus allowing for superior evaluation of the biodistribution of nanopharmaceuticals. Some of these methods are discussed in the following section.

Whereas for traditional therapies, qualitative evaluation of biodistribution would be mainly based upon secondary information such as histopathology (i.e., lesions, etc.), nanoparticles are large enough that they can often be directly imaged in tissues. By visualizing the nanoparticles, the presence of particles can be simultaneously detected and evaluated for damage or changes to the surrounding tissues. Electron microscopy, and in particular transmission electron microscopy (TEM), is often considered the standard for this type of evaluation. Advances in instrumentation, however, can allow for particle identification and tissue evaluation without going through the laborious sample preparation typical for TEM. The advent of environmental scanning electron microscopy (ESEM) allows samples to be directly imaged without going through traditional fixative and embedding processes (although at a cost of lower resolution). Depending upon particle composition and aggregation/agglomeration status, various types of optical microscopy may sometimes be sufficient for particle identification. In addition, if the particle composition is different than that of the surrounding tissues, biodistribution determinations may be made solely through compositional analysis.

For most compounds, it is expected that single dose tissue distribution studies would provide an adequate assessment of tissue distribution and potential accumulation. However, because of the reported higher specificity of targeted therapies using nanoparticles, it is also possible that levels of the nanopharmaceutical may not reach a concentration that allows adequate detection. In these cases, repeat dose studies in animals may be necessary in order to be able to adequately characterize the biodistribution. In fact, this issue is mentioned in the pharmacokinetics guidance for industry on repeat dose tissue distribution studies, which is mentioned above (http://www.fda.gov/cder/guidance/ichs3b.pdf).

3.2.3. Quantitative Methods for Evaluation of Nanoparticles in Tissues

As with small molecules, quantitative biodistribution determinations may be made with radiolabeled experiments. In this case, it is important to ensure that the radio labeling does not impact the physicochemical properties of the nanoparticles. In addition, if the nanoparticles do not degrade within the body, they may be extracted from the tissue and analyzed. Again, if the particle composition is sufficiently different than that of the surrounding tissue, methods such as inductively coupled plasma mass spectrometry (ICPMS), X-ray fluorescence (XRF), or neutron activation analysis (NAA) can quantitatively evaluate nanoparticle levels in tissue.

4. Conclusions

Products containing nanomaterials are being investigated for potential applications as therapeutics. While some of these nanomaterials are nanoscale versions of larger materials used in approved products, other nanomaterials are novel and have never been used in drug products. The regulatory requirements to ensure preclinical safety for products containing such novel materials remain identical to those requirements for products that do not contain nanoparticles. It is, however, well appreciated by scientists within CDER and FDA that because there are unique features associated with nanotherapeutic products, there may be future challenges for the development, manufacturing, safety evaluation, and review of nanomaterial-containing products. These challenges are likely to be encountered by sponsors of nanotechnology-based products, as well as for regulatory agencies. The areas of challenge fall into three categories, including safety assessment, characterization and manufacturing, and environmental impact assessment. This chapter focused on identifying some of the possible issues related to characterization and preclinical safety assessment. The chapter, however, does not represent a complete list of issues, as each product is unique and has to be treated on a case-by-case basis. Similarly, it is up to the reviewing

division to make decisions regarding the need for studies, which will heavily depend on the total package of information submitted by the sponsor. Currently, at FDA and within each center, efforts are under way to identify areas where guidance development could help product development, such that innovation which may enhance public health can be encouraged. It is therefore likely that in the next few years, there may be several guidance documents issued, once the specific areas of focus are identified. Steps are actively under way to identify these specific areas of focus, which would help structure and develop future guidance documents.

References

1. Siegel, R.W., Hu, E., Roco, M.C. (eds.) (1999) *Nanostructure Science and Technology. A Worldwide Study. National Science and Technology Council Committee on Technology, The Interagency working group on nanoscience, engineering and technology.* International Technology Research Institute World Technology Division, Baltimore, MD.
2. Vogel, V., Baird, B. (eds.) (2003) *Nanobiotechnology. Report of the National Nanotechnology Initiative Workshop.* National Nanotechnology Initiative, Arlington, VA.
3. US Department of Health and Human Services, Food and Drug Administration, Center for Drug Evaluation and Research, and Center for Biologics Evaluation and Research. Guidance for Industry Content and format of investigational new drug applications for phase 1 studies of drugs, including well-characterized, therapeutic, biotechnology-derived products. 1995 http://www.fda.gov/cder/guidance/phase1.pdf accessed February, 2008.
4. Warheit, D. (2008) How meaningful are results of nanotoxicity studies in the absence of adequate material characterization? *Toxicol Sci* **101**, 183–185.
5. Oberdorster, G., Oberdorster, E., Oberdorster, J. (2005) Nanotoxicology: An emerging discipline evolving from studies of ultrafine particles. *Environ Health Perspect* **113**, 823–839.
6. Gaur, U., Sahoo, S., De, T., Ghosh, P., Maitra, A., Ghosh, P. (2000) Biodistribution of fluoresceinated dextran using novel nanoparticles evading reticuloendothelial system. *Int J Pharm* **202**, 1–10.
7. Liversidge, G., Cundy, K. (1995) Particle size reduction for improvement of oral bioavailability of hydrophobic drugs: I. Absolute oral bioavailability of nanocrystalline danazol in beagle dogs. *Int J Pharm* **125**, 91–97.
8. Hu, J., Johnston, K., Williams, R. (2004) Nanoparticle engineering processes for enhancing the dissolution rates of poorly water soluble drugs. *Drug Dev Ind Pharm* **30**, 233–245.
9. LaVan, D., McGuire, T., Langer, R. (2003) Small-scale systems for in vivo drug delivery. *Nat Biotechnol* **21**, 1184–1191.
10. Nishiyama, N., Kataoka, K. (2006) Current state, achievements, and future prospects of polymeric micelles as nanocarriers for drug and gene delivery. *Pharmacol Ther* **112**, 630–648.
11. Hezinger, A., Tebmar, J., Gopferich, A. (2008) Polymer coating of quantum dots – a powerful tool toward diagnostics and sensorics. *Eur J Pharm Biopharm* **68**, 138–152.
12. Dobson, J. (2006) Magnetic nanoparticles for drug delivery. *Drug Dev Res* **67**, 55–60.
13. Castaldo, D. (2008) Identification of foreign particles below 10 microns key to inhaled drug quality. *Pharmaceutical Processing.* http://www.pharmpro.com/ShowPR.aspx?PUBCODE=021&ACCT=0000100&ISSUE=0405&RELTYPE=PR&Cat=0&SubCat=0&ProdCode=0000&PRODLETT=R&SearchText=aspex accessed April 1, 2008.
14. Adams, N., De Gans, B.-J., Kozodaev, D., Sanchez, C., Bastiaansen, C., Broer, D., Schubert, U. (2006) High-throughput screening and optimization of photoembossed relief structures. *J Comb Chem* **8**, 184–191.
15. Draft Guidance Guidance for Industry, Analytical Procedures and Methods Validation, Chemistry, Manufacturing, and Controls Documentation, August 2000.
16. Magenheim, B., Benita, S. (1991) Nanoparticle characterization: A comprehensive physiochemical approach. *STP Pharma Sci.* **1**, 221–241.

17. Bootz, A., Vogel, V., Schubert, D., Kreuter, J. (2004) Comparison of scanning electron microscopy, dynamic light scattering, and analytical ultracentrifugation for the sizing of poly(butyl cyanoacrylate) nanoparticles. *Eur J Pharm Biopharm* **57**, 369–375.
18. Jillavenkatesa, J., Dapkunas, S., Lum, L.-S. (2001) NIST recommended practice guide special publication 960-1 Particle size characterization. NIST.
19. Murdock, R., Braydich-Stolle, L., Schrand, A., Schlager, J., Hussain, S. (2008) Characterization of nanomaterial dispersion in solution prior to *in vitro* exposure using dynamic light scattering technique. *Toxicol Sci* **101**, 239–253.
20. Guidance for Industry and FDA Staff, Early Development Considerations for Innovative Combination Products, September 2006 (http://www.fda.gov/oc/combination/innovative.html.

Part II

Assays to Determine Physical and Chemical Properties

Chapter 4

Measuring the Hydrodynamic Size of Nanoparticles in Aqueous Media Using Batch-Mode Dynamic Light Scattering

Vincent A. Hackley and Jeffrey D. Clogston

Abstract

Particle size characterization is of particular importance to nanomedicine. The size similarity of nanoparticles to biological moieties is believed to impart many of their unique medical properties. Here we present a method for sample preparation and the determination of mean nanoparticle size (hydrodynamic diameter) using batch-mode dynamic light scattering (DLS) in dilute aqueous suspensions. We then demonstrate this method for 30 nm colloidal gold.

Key words: Hydrodynamic size, dynamic light scattering, photon correlation spectroscopy, quasi-elastic light scattering, DLS, PCS, QELS, diffusion, diffusion coefficient

1. Introduction

The size of a nanoparticle can have important consequences for how it behaves in clinical applications. Size influences particle uptake, deposition, and clearance. For example, dendrimeric nanoparticles less than 5 nm in diameter quickly transit through blood vessel walls into surrounding tissue (1). Dendrimeric nanoparticles with diameters from 3 to 6 nm are rapidly excreted through the kidneys (2). In the 6–8 nm diameter range, dendrimeric nanoparticles permeate hyperpermeable tumor vessels. Continuing to change the particle size, up to 15 nm in diameter, has been shown to alter permeability across the vascular wall, affect excretion route, and influence recognition by the reticuloendothelial system (RES) (3).

Relatively few techniques are capable of determining the size of nanoparticles *in solution*; of these, fewer still are widely available or cost-effective for routine on-site analysis. One technique that can

Scott E. McNeil (ed.), *Characterization of Nanoparticles Intended for Drug Delivery*, Methods in Molecular Biology, vol. 697,
DOI 10.1007/978-1-60327-198-1_4,

provide an accurate measure of nanoparticle hydrodynamic size is dynamic light scattering (DLS), also referred to in the literature as photon correlation spectroscopy (PCS) or quasielastic light scattering (QELS).

In DLS, the nanoparticle solution is illuminated by a monochromatic laser and its scattering intensity is recorded with a photon detector at a fixed or variable scattering angle. The scattered intensity is time-dependent when observed on a microsecond timescale due to the Brownian motion of the nanoparticles. On this timescale, intensity fluctuations reflect the rate of diffusion of the particles. These fluctuations are captured using the method of autocorrelation, in which the scattered intensity at time t is compared to itself at time $t+\tau$, where τ is the correlation delay time. The process is repeated over the period of observation and for a (typically logarithmically spaced) range of values τ to generate a correlation function, which is displayed graphically as a correlogram (see e.g., Fig. 1). From the decay of the correlation function, the rate of diffusion (i.e., the translational diffusion coefficient, D) is calculated:

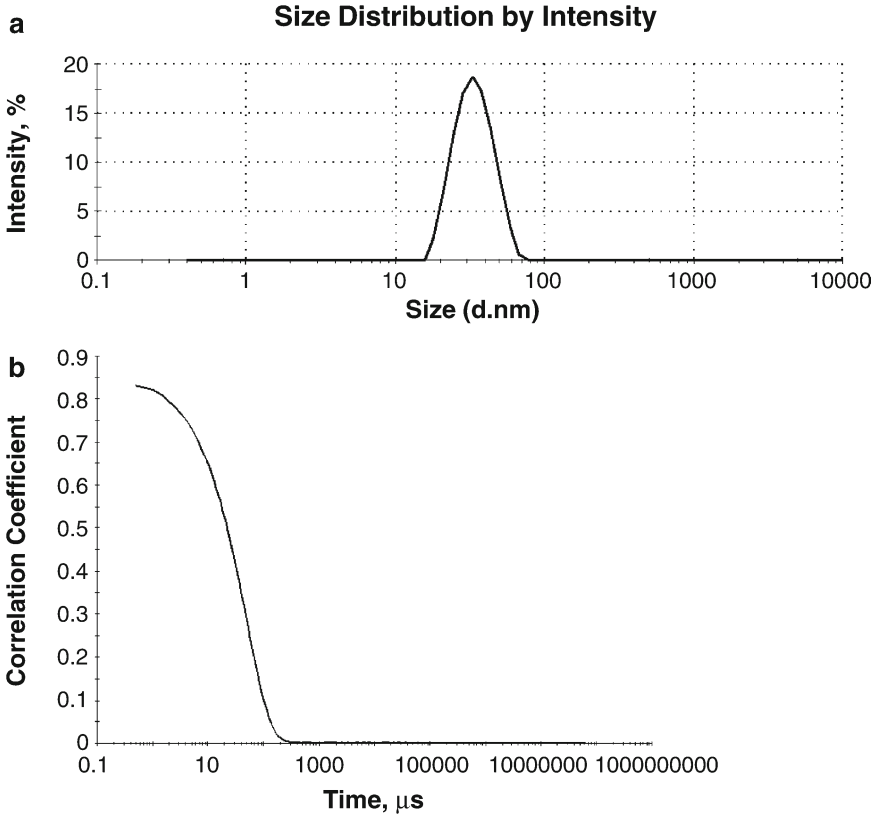

Fig. 1. The averaged ($n=10$) intensity distribution plot (**a**) and correlation curve (**b**) for 30 nm colloidal gold. Samples were prepared at 100 μg/mL in 2 mmol/L NaCl and filtered with a 0.45 μm filter. The samples were transferred to a 10 mm path length quartz cuvette and measured at 25°C. The DLS instrument employed a 633 nm laser wavelength at a scattering angle of 173°. The z-average was 29.6 ± 0.2 nm with a PI of 0.162 ± 0.008. A refractive index of 1.332 and a viscosity of 0.890 cP were used for size calculations.

$$\Gamma = q^2 D,$$

where Γ is the exponential decay rate and q is the modulus of the scattering vector (defined by the scattering angle and wavelength of light). The Stokes–Einstein equation can then be used to relate D to the hydrodynamic diameter (d_H) of the particle, taking into account the viscosity of the sample solution and the temperature at which the measurement is performed.

$$d_H = kT/3\pi\eta D,$$

where k is the Boltzmann constant, T is the absolute temperature, and η is the absolute zero-shear viscosity of the medium. The quantity d_H is the diameter of an *equivalent rigid sphere* that diffuses at the same rate as the analyte.

Generally, nanoparticle samples contain a distribution of sizes as a result of imperfections in synthesis and due to natural conformational variations in the large number of atoms involved (nanoparticle-based drugs contain thousands of atoms, many more than small-molecule drugs, which usually contain fewer than 100). It is therefore of interest to characterize both the central tendency and the degree of particle-to-particle size variability present in the sample. The mean decay rate, from which the mean size is determined, is derived by least-squares fitting of the measured correlation function using the cumulants method (4). A metric for size variability is the polydispersity index (PI), a unitless quantity derived from the cumulants analysis *and equivalent to the relative variance of the distribution*. For a more detailed explanation of the parameters and relationships utilized in DLS, refer to refs. (4–13). Although the standard is to report the z-average size, algorithms exist to calculate intensity-, volume-, and number-weighted distributions. Of these, the intensity-weighted distribution is preferred.

Although particle size is the primary determinant of the measured diffusion coefficient, sample handling and preparation can impact these measurements and thus influence the determined size. Therefore, this chapter describes a procedure and guidelines for sample preparation and the subsequent determination of mean nanoparticle size (hydrodynamic diameter) using batch-mode DLS in dilute aqueous suspensions. The method can be applied to any suitable DLS instrument with batch measurement capability. In addition, methods for measuring long- and short-term, pH, and thermal stability of nanoparticles via batch-mode DLS are described. Stability is defined relative to changes in hydrodynamic size in response to changes in the sample environment. Temporal stability is measured under two different sets of storage conditions. The first condition is designated as long-term and is an indicator of shelf-life, where the stability of the stock sample *in its native medium* is monitored periodically. The second condition examines the stability of prepared dilutions in media at different

storage temperatures (ambient, 4, and 37°C) over 1 to several days and is referred to as short-term stability. The latter test is relevant to application scenarios in which the stock sample has been diluted and stored for use in subsequent studies or for purposes of characterization.

2. Materials and Instrumentation

1. DLS instrument – Fixed-angle or multiangle system equipped with a suitable correlator, coherent laser source, photon detector and optics, ability to control and maintain sample temperature, and software compliant with ISO 13321-1996 for application of the cumulants analysis algorithm.
2. pH electrode and meter or autotitrator equipped with pH electrode (for pH stability method).
3. Quartz or optical-quality glass cuvettes with caps.
4. Disposable cuvettes (if appropriate).
5. Syringe filters of appropriate pore size and membrane type or optionally a microcentrifuge with low-binding microfuge tubes.
6. Sample medium (filtered demineralized water, 10 mM NaCl, phosphate buffered saline (PBS), etc.).
7. 0.1 M HCl.
8. 0.1 M NaOH.

3. Methods

3.1. Sample Preparation

1. Use a cuvette with quartz or optical-quality glass windows. Choose the appropriate cuvette capacity depending on your available sample volume and instrument requirements. Prerinse cuvette with filtered solvent at least three times.
2. Measurement cuvettes should be cleaned with filtered demineralized water and stored dry (see Note 1). Periodic use of commercial cleaning agents formulated specifically for optical cells and components is recommended to remove difficult residues, but care must be taken to remove all traces of the cleaning detergent as this may impact the nanomaterial properties. Keep cleaned cuvette sealed/capped until needed. If available, store cuvette under HEPA-filtered air.
3. Suspending medium (i.e., solvent, dispersant, or solution) should be filtered *prior* to sample preparation using a 0.1 μm or smaller pore size membrane and should be tested for scattering

contributions to the measured signal in the absence of the analyte (see Note 2). As a general rule, one should filter the medium to at least the nominal size of the analyte to be measured. This may not be practical for particles smaller than 20 nm, and so the suspending medium should always be measured separately to ensure the absence of, or to account for, interfering particles or nanoscale surfactant structures present at significant concentrations.

4. A typical starting sample concentration is 1 mg/mL (see Note 3). This concentration should be adjusted to accommodate the scattering properties of your sample (e.g., 100 μg/mL for colloidal gold and 2 mg/mL for dendrimers is typical see Note 4) and/or the optical requirements of your specific instrument (i.e., according to instrument manufacturer's specifications for acceptable count rate range). Use caution in handling and disposal of all nanomaterials (see Note 5).
5. Samples should be filtered with a 0.2 μm or smaller pore size membrane, preferably in conjunction with loading sample into the cuvette (see Note 2). The choice of pore size depends on the maximum dimension of the test particles and their tendency to adhere to the filter membrane. Whichever procedure is used, it should be validated for the test material prior to measurement to ensure that the analyte is not being removed or otherwise modified by the process.

3.2. Sample Loading

1. Prerinse filter with solvent (at least 1 mL, depending on filter size and dead volume of filter holder or cartridge).
2. After loading syringe with sample and inserting syringe filter, allow the first four drops to go to waste. If possible, use the next four drops to prerinse the cuvette, and discard. The remainder can be used for the sample measurement.
3. Load sample into cuvette using minimum volume necessary to ensure liquid level is at least 2 mm above the entrance height of the laser beam for your particular instrument configuration. Typically, the beam center height is either 8.5 mm or 15 mm from the cuvette bottom; refer to the instrument manual or contact manufacturer to confirm beam height at the cuvette. For microcuvettes with a sample well insert, fill the well with sample, but do not fill beyond the well lip. Overfilling of a cuvette can lead to thermal gradients that will adversely impact measurement accuracy.
4. Take care not to touch the cuvette windows with your bare hands while loading. Wipe outside of cuvette with lens paper if needed (see Note 1).
5. Cap the cuvette to prevent dust contamination and solvent evaporation (see Note 2).

6. Inspect the cuvette to ensure that air bubbles are not clinging to the optical window area. If necessary, *gently* tap cuvette on a padded surface to release bubbles before placing cuvette in the sample holder. Never shake cuvette, as this may introduce air bubbles or entrap air in the sample well of microcuvettes. Make sure to place the cuvette correctly in the sample holder (i.e., quartz windows should be facing the incident beam and detector).

3.3. Measurement Procedure

1. The correct performance of the instrument should be verified under experimental conditions on a periodic basis to ensure that accuracy and precision are maximized (see Notes 6 and 7).
2. For a nominal sample volume of 1 mL or less, an equilibration time of 4 min at each temperature is recommended prior to starting measurements. Larger sample volumes or large temperature changes may require longer equilibration times; this should be determined using the cuvette and medium under relevant experimental conditions. The temperature should be controlled and measured with an accuracy and precision of 0.3°C or better.
3. Perform three to ten independent measurements per sample per temperature setting to establish measurement repeatability (see Note 8). Measurement duration should be set according to instrument manufacturer's recommendations and will differ depending on particle size and scattering characteristics, as well as the optical characteristics of the instrument itself (e.g., detector sensitivity, scattering angle, etc.). A *minimum* duration (measurement time) of 60 s is recommended for nanosize particles.

3.4. Stability Assessment

Long-term stability assesses the shelf-life of a stock nanoparticle suspension over a period of weeks to months. Short-term measures the stability of a prepared dilution of a stock suspension at different storage temperatures over a period of days. All DLS measurements are performed at a sample temperature of 25°C. The sample preparation and measurement procedures are identical to the standard batch-mode sizing measurement, with the following exceptions.

3.4.1. Long/Short-Term Stability

1. Long-term stability is assessed on samples appropriately diluted from the stock suspension into the chosen medium. Measurements on freshly prepared dilutions of the stock are made once a week for 4 weeks, followed by every other week for 2 months, and finally once a month for the duration of the study. For short-term stability, three samples are prepared in the same manner as that in the long-term study, but the samples are analyzed immediately and then subsequently stored in the

measurement cuvettes at room temperature, 4°C, and at 37°C. The latter two storage conditions are achieved by using an incubator set to the desired temperature; room temperature corresponds to the ambient temperature of the user's laboratory. The samples are removed from storage once each day and allowed to equilibrate at room temperature before performing size measurements. This procedure is repeated for the duration of the study (typically several days).

2. The cuvette to be used should be able to handle the temperature range being studied. The cuvette should also have a well-fitted cap to prevent evaporative loss of solvent at elevated temperatures or over long periods of storage. For this purpose, the authors recommend using disposable low volume cuvettes (see Note 9). Make sure the cuvette is properly sealed by capping the cuvette and sealing with laboratory film (e.g., Parafilm), if necessary.
3. Size measurements should normally be made in the range (20–25)°C; thus, it is important to determine beforehand the time it takes for the sample to reach this temperature if stored at other than room temperature. As a rule of thumb, double the determined equilibration time for the experiment. For samples stored at, or already equilibrated to, room temperature, follow recommendations given in Subheading 3.3.
4. Check the cuvette periodically for solvent evaporation and sample settling. In the former case, gently tap the cuvette to recover the evaporated solvent that has condensed on the cuvette walls. For the case of sample settling (due to instability), the sample is no longer suitable for DLS.

3.4.2. Thermal Stability

1. The cuvette to be used should be able to handle the temperature range being studied. The cuvette should also have a well-fitted cap. For this purpose, the authors recommend using a quartz or glass cuvette with a tight fitting cap or insert for all temperature-dependent measurements. Make sure the cuvette is properly sealed to prevent evaporative loss of solvent.
2. Determine beforehand the time it takes for your sample to reach each temperature. This should be determined in the actual cuvette to be used containing the same sample solvent and volume. The actual temperature profile should be used, i.e., if you are studying a range from 20 to 40°C in 5°C increments, the equilibration times for each temperature step should be determined. As a rule of thumb, double the determined equilibration time for each step (i.e., use 10 min if the determined equilibration time is 5 min).
3. Check the cuvette periodically for solvent evaporation and sample settling. In the former case, gently tap the cuvette to recover evaporated solvent that has condensed on the cuvette

wall. For the case of sample settling (due to instability at different temperatures), the sample is no longer suitable for DLS.

3.4.3. pH Stability

1. Sample is titrated with either acid or base (0.1 M HCl or NaOH, respectively) to the desired pH. This can be done manually and the pH measured with an appropriate pH electrode and meter, or using an autotitrator. Samples are transferred from the titration cell to the cuvette at each target pH value and measured as described above. Optionally, a flow-type cuvette can be used if available and integrated with an autotitrator. The number of pH data points is dependent on the range and level of accuracy required.
2. It is recommended to run fresh samples for each pH titration range. For example, if the sample's native pH is 7, one sample is titrated with acid to cover the lower pH range. The higher pH range is examined with a fresh sample titrated with base.
3. The pH reading should be stable to ±0.2 pH units over the period of measurement. The size measurements can be repeated until a stable pH is obtained.
4. Check the cuvette periodically for sample settling. Settling indicates that the sample is not stable at that pH and therefore not suitable for DLS. A sharp decrease in scattering intensity often indicates that the sample has destabilized and sedimented. This is typically preceded by an increase in both intensity and hydrodynamic size due to the formation of large clusters prior to sedimentation.

3.5. Data Analysis

A detailed description of data analysis is beyond the present scope. There are many methods available to analyze the autocorrelation data in order to extract size information, and these methods will process the data differently using different inherent assumptions. It is left for the reader to identify the data analysis algorithms provided by the instrument vendor or to seek third party software solutions. However, a few issues regarding data analysis are worth discussing within the context of the methods described herein:

1. Whichever model the instrument software uses to fit the measured correlation data, ultimately the Stokes–Einstein relationship will be employed to calculate the hydrodynamic diameter, d_H. Thus, it is important to ensure that the correct temperature and viscosity values are used in this calculation. Temperature is usually handled automatically by the instrument software, and good temperature control of the sample is critical for accurate measurement. On the other hand, viscosity is typically a user input or selected value. One should therefore input correct values of viscosity for the particular

solvent used at the measurement temperature. Generally, for maximum accuracy, viscosity values should be accurate to within about 1%. For solutions containing significant amounts of salt (e.g., buffers, isotonic solutions), viscosity will be slightly dependent on salt concentration. For instance, use of bulk water viscosity for a sample dispersed in PBS results in an error of about 2% in the viscosity at room temperature.

2. Similarly, it is important to input the correct refractive index (RI) for the suspending medium, as this value is used in the primary calculations yielding the diffusion coefficient. RI values should be accurate to within about 0.5%, or to two decimal places for water. There is a slight dependence of RI on salt concentration (and other nonlight-absorbing soluble additives) in dilute aqueous solutions, but the difference between PBS, for instance, and water is less than 0.2%. Similarly, the temperature dependence of the RI is very weak over the normal measurement temperature range for water and varies only about 0.2% from 20 to 37°C. RI is also wavelength-dependent, but for water this dependence is sufficiently weak over the normal range of wavelengths used in DLS instruments (typically from 488 to 750 nm), such that values reported for the sodium D line (589.3 nm) are usually acceptable (with an error of less than 0.3% over the entire range). The RI for pure water at 20°C is 1.332 (calculated based on IAPWS 1997 for a wavelength of 632.8 nm), and this value can be used for most dilute salt solutions over the temperature range from 20 to 37°C. The refractive index for the particle phase is only required for transformation of size distribution results from the intensity-weighted measurement basis to a volume- or number-weighted distribution; it does not impact the calculation of the diffusion coefficient or the z-average size. For small particles, where all physical dimensions are smaller than about 60 nm (based on use of He–Ne or similar wavelength lasers), the angular dependence of scattering is negligible and the RI value input for the particles will not greatly affect the transformation to a volume-weighted distribution using the Mie model or Rayleigh–Gans–Debye (RGD) approximation (i.e., the exact value of the particle RI is not critical). On the other hand, this does not indicate that the model employed is appropriate for the particles being analyzed.
3. For the reader's convenience, Table 1 provides recommended values for the absolute viscosity and refractive index as a function of temperature and solvent composition for several common aqueous suspending media. Viscosity is given in SI units of mPa s, which are equivalent to the c.g.s. units of centiPoise (cP). The base values for the viscosity of pure water are derived from the NIST Chemistry WebBook (2005). The contributions of dissolved salt to the viscosity of pure water

Table 1
Properties of common aqueous media (absolute viscosity and refractive index as a function of temperature) useful for DLS measurement. Viscosity is given in SI units of mPa s, which are equivalent to the c.g.s. units of centi-Poise (cP). The base values for the viscosity of pure water are derived from the NIST Chemistry WebBook (2005)

	Absolute viscosity (mPa s)			
Aqueous medium	20°C	25°C	37°C	Refractive index
Pure water	1.002	0.890	0.692	1.332
10 mmol/L NaCl	1.003	0.891	0.693	1.332
Isotonic saline (154 mmol/L NaCl)	1.020	0.908	0.710	1.334
Phosphate buffered saline (PBS)	1.023	0.911	0.713	1.334

are assumed to be additive, and are based on values interpolated from data available in the CRC Handbook of Chemistry and Physics (2006), and fit using a third order polynomial. Therefore, to calculate the viscosity of a salt solution presented in the table below, at a different temperature between 0 and 100°C, simply subtract the value of pure water at 20°C from the corresponding value for the salt solution. This will provide the incremental increase in viscosity for a particular salt composition. The incremental value can then be added to the viscosity for pure water at temperatures not reported below, but available from sources such as the CRC Handbook, NIST WebBook or the IAPWS (14–16).

4. Presently, the only recognized standard for the analysis of measured autocorrelation data is the *cumulants* method as stipulated in ISO 13321:1996 Annex A. Cumulants analysis yields a mean intensity-weighted size (commonly called the z-average diameter but identified in the standard as the average PCS diameter, x_{PCS}, or the *harmonic* z-average) and a measure of the broadness of the distribution (PI). The latter is the relative variance of the size polydispersity. Cumulants does not generate a size distribution per se; it provides a mean value and the distribution variance. With the assumption of a single-mode Gaussian function, these values can be used to construct a *hypothetical* size distribution.
5. Beyond the cumulants approach, an array of distribution analysis algorithms have been developed for DLS (11), including widely used methods such as CONTIN and Non-Negative Least Squares (NNLS). These methods invert the measured correlograms in order to extract size distribution information,

and they typically apply some degree of predetermined smoothing that impacts the resolution and noise level in the resulting distribution. The utility of these methods is highly dependent on the quality of the input data and on the selection of predetermined fitting parameters to which the user may or may not have access. Therefore, distribution analysis methods should be used with caution and they are most appropriate when utilized for comparative rather than analytical purposes. Furthermore, the subsequent conversion of intensity distribution results to volume- or number-weighted distributions is subject to significant uncertainties and artifacts. In particular, number-weighted distributions should generally be avoided due to the high potential for error and misuse. General guidelines to data analysis for DLS can be found in the References section (4–13).

3.6. Reporting Particle Size Data

International standard ISO 13321:1996 gives specific recommendations for reporting of test results derived from DLS. At a minimum, the mean z-average diameter (or radius) and mean PI should be reported, along with their standard deviations based on three to ten replicate measurements; the number of replicate measurements should also be reported. If a size distribution analysis algorithm is applied, it should be identified along with any key parameter values used in the analysis. Although the ISO standard recommends reporting the z-average size, algorithms exist to calculate intensity-, volume-, and number-weighted distributions. Of these, the intensity-weighted distribution is preferred for reporting size. The volume-weighted (or mass-weighted) distribution should be used to determine relative amounts of multimodal sample distributions. The transformation from the intensity to the number and/or volume involves several assumptions (8). For nanoparticles, the size derived from the number-weighted distribution is typically not used. Other critical information that should be reported includes: particle concentration (mass or volume based), dispersion medium composition, refractive index values for the particles and the dispersion medium, viscosity value for the medium, measurement temperature, filtration or other procedure used to remove extraneous particulates/dust prior to analysis (including pore size and filter type if relevant), cuvette type and size (i.e., optical path length in millimeters), instrument make and model, scattering angle(s), and laser wavelength. Additional information that can be helpful to include in a report includes: measured autocorrelation *y*-intercept (amplitude), mean count rate during measurement of sample and dispersing medium, duration of a single measurement, and mean signal-to-noise ratio if available. An example correlation curve and intensity size distribution are shown in Fig. 1. This represents a measurement for nominal 30 nm diameter colloidal gold.

4. Notes

1. Minimize the time for which uncapped cuvettes are exposed to the ambient environment so as to reduce the likelihood of dust contamination. Handle cuvettes in a manner that avoids unnecessary contact with any cuvette surface that is in the pathway of the incident or scattered laser beam. It is recommended to wear nonpowder-containing latex or nitrile gloves at all times when handling the cuvettes. Cuvettes should be inspected periodically for surface scratches or coatings that might interfere with optical measurements. Use only good quality lens paper to wipe/dry external surfaces and nonabrasive particle-free clean room swabs to wipe internal surfaces.

   It is not recommended to use ultrasonics to clean quartz or glass cuvettes used for optical measurements. This can degrade the surface finish or cause the cuvette to crack at joints. Cuvette suppliers offer specially formulated cleaning solutions that can be used to remove difficult residues, such as proteins.

   If possible, dry the cleaned cuvettes in a HEPA-filtered clean bench. Extraneous dust can be removed from dry cuvettes by applying a short-duration blast of filtered nonreactive gas, e.g., from a pressurized air canister of the type typically used in critical clean room applications.

   As a general rule, always remove the sample from the cuvette as soon as possible following the measurements, and immediately rinse the cuvette with the filtered medium or with filtered demineralized water. Never allow a sample to dry in the cuvette.

2. The intensity of light scattered by nanosize particles is proportional to the square of the molecular mass or d^6, where d is the particle diameter; thus larger particles will scatter much more strongly than smaller particles. Additionally, water, as a polar solvent, is an excellent medium for "dust" particles (a collective term used here to refer to any foreign particulate matter originating from normal environmental contact). Although state-of-the-art DLS instruments are equipped with some form of "dust rejection" algorithm, experience shows that the best practice to achieve good reproducibility is to eliminate dust prior to analysis. This is especially important for samples that scatter weakly due to extremely small size and/or low refractive index contrast with the medium. Cuvettes, sample vials, solvent bottles, etc. should remain closed as much as possible to minimize dust contamination. Dispersion media should be filtered to a 0.1 μm pore size or smaller. The solvent storage container should, if possible, be outfitted with an air intake filter with a 1 μm or smaller pore size.

It is recommended that the dispersion medium should be periodically checked for background scattering; ensure that it is within the instrument guidelines and record its average count rate for future comparison.

Additionally, the prepared sample should be filtered to remove large interfering particulate matter whenever: (a) contamination may be associated with the source material rather than the solvent, (b) the sample to be analyzed was not prepared under clean conditions as specified above, or (c) the sample is of uncertain origin. Select an appropriate filter membrane and pore size such that the principal analyte is not removed from the solution or otherwise modified during filtration. For many aqueous applications, a 0.2 μm detergent-free polycarbonate or polyethersulfone filter will suffice, where the latter is a good choice for low protein-binding requirements. For extremely small hydrodynamic sizes (<5 nm diameter), where the scattered intensity is low, a 0.02 μm pore size may be necessary to remove all interfering extraneous particles. For samples that bind strongly to filters (e.g., colloidal gold), use a larger pore size or try a different membrane material to reduce interaction between the sample and the filter surface.

One should always validate the filtration procedure for a material or material class prior to proceeding with the analysis. Sample filtration may only be necessary if preliminary DLS results indicate the presence of contaminating large particles.

Centrifugation is an alternative to filtration for removing large size contaminants. The parameters for correct use (speed and duration) depend on the specific rotor and tube used (and on the size and density of the contamination), and thus can be more difficult to stipulate in advance. Centrifugation is recommended for extremely small low-density particles (e.g., bovine serum albumin – BSA – or other folded proteins – where adsorption by the filter may be an issue), or low generation dendrimers. Dust particles can be removed by spinning at moderate speeds (e.g., relative centrifugal force of $2500 \times g$) for 30 min in a microcentrifuge without affecting such small analytes. Centrifugation may also be preferred in situations where emulsions or other "soft" particles exist, which can deform or disintegrate to pass through a membrane and then reform afterwards.

Another option to minimize dust contamination is to perform sample preparation and transfer operations within a HEPA-filtered clean bench and to seal the sample cuvette against further contamination prior to removing it from the clean area for analysis.

3. A typical starting sample concentration is 1 mg/mL, but this value should be modified accordingly to account for the scattering

properties of your sample (e.g., intensity indicated by the average count rate at the detector). Scattering intensity will depend on particle size, refractive index, and concentration of your sample; only the latter can be modified for analysis. Too low a concentration may degrade the signal-to-noise ratio and subject the analysis to the effects of extraneous particles that might be present in solution. This will result in noisy and inconsistent results. On the other hand, too high a concentration can lead to multiple scattering effects and particle interactions, both of which can produce changes in the measured (apparent) hydrodynamic size.

It is therefore recommended to execute a validation procedure for measurement of a given type of sample in a given instrument. In this procedure, multiple concentrations are analyzed to bracket the target concentration (over at least a decade in concentration range), to ensure that the measured size is not concentration-dependent, or to establish the applicable concentration range. This procedure is recommended in ISO 13321:1996. In the case of an observed concentration effect, extrapolation of the apparent measured size to zero concentration may be appropriate, in order to obtain a concentration-independent (unbiased) size. Instrumental approaches to diminish the effects of multiple scattering include use of backscatter optics with an adjustable measurement depth or implementation of a cross-correlation technique.

The user is reminded that by diluting a sample (e.g., to obtain reduced particle concentrations), the effective particle size may change due to changes in the chemistry of the medium or changes in the electrical double layer of charged particles. It is therefore generally recommended for dilution purposes to use *conductivity matching*, a *compositionally equivalent medium*, or to use the sample *supernatant* extracted after centrifugation removal of the analyte.

Furthermore, the hydrodynamic size derived from DLS can depend on the salt concentration of the suspending medium. This effect arises due to the electrical double-layer surrounding charged particles in an aqueous medium. At extremely low salt concentrations (e.g., in demineralized water), the additional drag induced by the extension of the double layer into adjacent bulk solution causes a decrease in the diffusion coefficient and an apparent increase in size. This effect tends to increase with decreasing actual particle size. Adding a small amount of inert "supporting" monovalent electrolyte (e.g., 10 mmol/L NaCl) to screen the double layer will eliminate this issue for most systems.

A similar effect is the hindered diffusion that occurs at high particle concentrations due to interaction between

neighboring particles. This effect is enhanced by low salt concentrations and can lead to an apparent increase in particle size.

On the other hand, too high a salt concentration (e.g., ≈0.1 mol/L or greater monovalent salt) may destabilize charged particles leading to salt-induced aggregation and an increase in both particle size and polydispersity. It is generally considered good practice to perform DLS measurements with some inert monovalent electrolyte present, whereas pure deionized or distilled water should generally be avoided as a dispersion medium or used for qualitative comparisons only. The conditions under which a supporting electrolyte is used should be validated for your specific test material.

4. Recording the visible transmission spectrum of your sample is recommended if it is colored. Check to see if your sample absorbs strongly at the DLS instrument's laser wavelength. If this is the case, use of a different size-measuring instrument or laser may be necessary, or sample concentration may be increased.
5. Always wear appropriate personal protective equipment and take appropriate precautions when handling your nanomaterial. Also, be sure to follow your facility's recommended disposal procedure for a specific nanomaterial. Most fixed-angle instruments will accommodate microcuvettes, and this can help reduce the overall volume of waste material generated.
6. The instrument should be powered up at least 30 min in advance of measurements to allow the laser to stabilize (note: stability may be less of an issue for diode lasers compared with gas lasers such as the commonly used He–Ne, but as a matter of practice this procedure ensures stability of the instrument). Additional time may be needed to bring the sample holder up to the desired temperature if the measurement temperature is not set at the time of power-up.
7. DLS is a first-principles measurement technique, and as such, does not require calibration in the usual sense of the word. However, it is recommended that users periodically run standards to provide qualification (i.e., verification) of correct instrument operation within manufacturer specifications and to validate your measurement procedure.

   For this purpose, latex size standards down to nominally 20 nm (NIST-traceable polystyrene spheres) are available from a number of commercial suppliers. For standards below 20 nm, proteins such as cytochrome c and BSA are recommended. These materials are also commercially available and are relatively inexpensive, and their hydrodynamic size has been thoroughly characterized and reported in the scientific literature. Colloidal gold is commercially available in a wide range of

sizes down to nominally 2 nm. Certified reference materials are also available from NIST (http://www.nist.gov/ts/msd/srm/), including SRMs 1963a and 1964 (100 and 60 nm polystyrene lattices) and RMs 8011, 8012, and 8013 (gold nanoparticles, nominally 10, 30, and 60 nm, respectively).

ISO 22412:2008 recommends that a polystyrene latex with narrow size distribution and average diameter as measured by DLS of about 100 nm be used for qualification purposes on a periodic basis. The measured average diameter (z-average size) of the latex sample should be within 2% of the stated size and the repeatability should be better than 2%; additionally, the PI should be less than 0.1. Deviations beyond the above-stated limits indicate that a problem may exist with the instrument performance, the measurement cell, or the water used to dilute the standard prior to measurement; in this case, the user should address possible sources of error and contact the manufacturer if cell or water issues prove inconsequential. All water-dispersed standards are subject to instabilities over time and shelf-life limitations. Check that the reference standard has not exceeded the stated expiration date.

Particle size results obtained from DLS measurements may not coincide with those obtained from other techniques (e.g., electron microscopy). This is due in part to differences in the weighted averages determined in each case (e.g., number versus intensity), as well as differences in the physical property that is actually measured (e.g., hydrodynamic diffusion versus projected area). DLS is especially sensitive to the presence of small quantities of large particles or clusters of smaller particles, whereas electron microscopy, for instance, typically reflects the size of primary particles and may not include a statistically relevant sampling of larger clusters.

8. A minimum of three measurements 60 s or longer in duration and up to ten measurements per sample is recommended (ISO 13321:1996 recommends six replicate measurements, but this has been revised down in ISO 22412:2008). Check the raw correlation data to ensure that the amplitude (y-intercept, extrapolated $\tau = 0$ value for the measured correlation function) is stable and the correlograms are smooth (i.e., they decay exponentially to a flat baseline). Noisy correlograms and/or fluctuating amplitudes for a given sample can be attributed to the presence of dust/foreign particles in the sample, concentration variations from sample precipitation or aggregation, solvent evaporation (if measuring at temperatures greater than ambient temperature), or dirty cuvettes.
The repeatability for a set of N replicate measurements, defined as $100 \cdot s / \langle x_{PCS} \rangle$ (where s is the estimated standard deviation at $N-1$ degrees of freedom, $\langle x_{PCS} \rangle$ is the mean

z-average size, and brackets indicate an ensemble average), should be better than 5% for samples other than the reference material used to qualify the instrument performance.

If sediment is visible at the bottom of the cuvette following measurement, the data should be discarded; sediment indicates that the sample either contains a significant portion of large (micrometer) size particles or the target particles are unstable during the time frame of the experiment. DLS is applicable *only* to particles that undergo Brownian diffusional motion and remain fully suspended throughout the measurement; samples containing larger size particles should be analyzed using more appropriate techniques, such as laser diffraction, electrical sensing zone method, or gravitational sedimentation.

9. Although plastic disposable cuvettes are available in a range of sizes and materials, they are not constructed to high optical tolerance and should not be used for samples that are weak scatterers (e.g., sub-20 nm in size, low refractive index contrast with medium, low particle concentration). Refer to the instrument manufacturer's recommendations for optimal scattering intensity as a guide. Generally speaking, quartz or optical-quality glass cuvettes will provide higher quality data with better precision and fewer artifacts. The use of disposable cuvettes should be validated for a particular sample or material class.

Acknowledgments

This project has been funded in whole or in part with federal funds from the National Cancer Institute, National Institutes of Health, under contract N01-CO-12400. The content of this publication does not necessarily reflect the views or policies of the Department of Health and Human Services, nor does mention of trade names, commercial products, or organizations imply endorsement by the U.S. Government.

References

1. Dong, Q., Hurst, D., Weinmann, H., Chenevert, T., Londy, F. and Prince, M. (1998) Magnetic resonance angiography with gadomer-17. An animal study original investigation. *Invest Radiol* **33**, 699–708.
2. Sato, N., Kobayashi, H. and Hiraga A. et al. (2001) Pharmacokinetics and enhancement patterns of macromolecular MR contrast agents with various sizes of polyamidoamine dendrimer cores. *Magn Reson Med* **46**, 1169–1173.
3. Kobayashi, H. and Brechbiel, M. (2005) Nano-sized MRI contrast agents with dendrimer cores. *Adv Drug Deliv Rev* **57**, 2271–2286.
4. ISO 13321:1996(E). *Particle Size Analysis – Photon Correlation Spectroscopy*. International Organization for Standardization (provides

information and guidance on instrumentation, sample preparation, measurement, and data analysis – available for electronic purchase and download at http://www.iso.org/).

5. Lomakin, A., Teplow, D.B. and Benedek, G.B. (2005) Quasielastic light scattering for protein assembly study in *Amyloid Proteins: Methods and Protocols*, *Methods in Molecular Biology*, *vol. 299* (edited by Sigurdsson, E.M.), Humana, Totowa, NJ, pp. 153–174.
6. Berne, J. and Pecora, R. (2000) *Dynamic Light Scattering – with Applications to Chemistry, Biology, and Physics.* Dover Publications, Mineola, NY.
7. ISO 22412:2008. *Particle Size Analysis – Dynamic Light Scattering (DLS)*. Updates and extends ISO 13321:1996(E).
8. Santos, N.C. and Castanho, M.A.R.B. (1996) Teaching light scattering spectroscopy: the dimension and shape of tobacco mosaic virus. *Biophys J* **71**, 1641–1646.
9. Finsy, R. (1994) Particle sizing by quasi-elastic light scattering. *Adv Colloid Interface Sci* **52**, 79–143.
10. Brown, W. (ed.) (1993) *Dynamic Light Scattering – The Method and Some Applications.* Clarendon Press, Oxford, UK.
11. Johnsen, R.M. and Brown, W. (1992) An overview of current methods of analyzing QLS data in *Laser Light Scattering in Biochemistry* (edited by Harding, S.E., Sattelle, D.B. and Bloomfield, V.A.), The Royal Society of Chemistry, Cambridge, UK, pp. 78–91.
12. Weiner, B.B. and Tscharnuter, W.W. (1987) Uses and abuses of photon correlation spectroscopy in particle sizing in *Particle Size Distribution: Assessment and Characterization* (edited by Provder, T.), American Chemical Society, Washington, DC, pp. 49–61.
13. Morrison, I.D., Grabowski, E.F. and Herb, C.A. (1985) Improved techniques for particle size determination by quasi-elastic light scattering. *Langmuir* **1**, 496–501.
14. Lide, D.R. (ed.). (2006) Concentrative properties of aqueous solutions: density, refractive index, freezing point depression, and viscosity in *CRC Handbook of Chemistry and Physics*, Internet Version 2006 (http://www.hbcpnetbase.com/), Taylor and Francis, Boca Raton, FL.
15. Lemmon, E.W., McLinden, M.O. and Friend, D.G. (2005) Thermophysical properties of fluid systems in *NIST Chemistry WebBook*, NIST Standard Reference Database Number 69 (edited by Linstrom, P.J. and Mallard, W.G.). National Institute of Standards and Technology, Gaithersburg MD (http://www.webbook.nist.gov/).
16. IAPWS. (1997) *Release on Refractive Index of Ordinary Water Substance as a Function of Wavelength, Temperature and Pressure*, International Association for the Properties of Water and Steam (IAPWS), Erlangen, Germany.

Chapter 5

Characterization of Nanoparticles by Matrix Assisted Laser Desorption Ionization Time-of-Flight Mass Spectrometry

Uma Ramalinga, Jeffrey D. Clogston, Anil K. Patri, and John T. Simpson

Abstract

Determining the molecular weight of nanoparticles can be challenging. The molecular weight characterization of dendrimers, for example, with varying covalent and noncovalent modifications is critical to their use as therapeutics. As such, we describe in this chapter a protocol for the analysis of these molecules by matrix assisted laser desorption ionization time-of-flight mass spectrometry (MALDI-TOF MS).

Key words: mass spectrometry, MALDI, electrospray, nanotechnology, dendrimers

1. Introduction

The field of nanotechnology has been expanding at an almost exponential rate over the last several years. Applications of this technology span such diverse fields as physics, chemistry, material science, biotechnology, medicine, and robotics. As with any new or emerging material(s), the need for analytical characterization is at the forefront. The focus of this chapter will be the analysis of a particular type of nanoparticle, dendrimers, by matrix assisted laser desorption ionization (MALDI) time-of-flight mass spectrometry. Dendrimers are a class of macromolecules that have found recent applications in the cancer and biomedical fields (1–5). Their use as potential targeting therapeutics has made their analytical characterization of critical importance. However, due to the complex and heterogeneous nature of many dendrimers, this characterization has proven challenging. One approach has been the application of mass spectrometry, in particular, MALDI-TOF mass spectrometry to the analysis of these molecules (6–8). Due to the heterogeneous nature of many dendrimer preparations, the

Scott E. McNeil (ed.), *Characterization of Nanoparticles Intended for Drug Delivery*, Methods in Molecular Biology, vol. 697,
DOI 10.1007/978-1-60327-198-1_5,

MALDI-TOF spectra for higher order dendrimers usually contain a distribution of masses rather than a distinct peak at a particular mass. This can add uncertainty to the mass assignment. In addition, fragmentation of dendrimers has led some investigators to use matrix additives such as fucose, to help cool the ionization process and minimize fragmentation (7).

While the reader is directed to sources beyond the scope of this chapter, a short introduction to the mechanisms of MALDI and electrospray will be given. MALDI is a solid-phase technique whereby sample and matrix are cocrystallized on a solid support, usually a stainless steel target. Irradiation with a nitrogen laser (typically 337 nm), sublimates the matrix/sample mixture into the gas phase where ionization of the sample, usually by simple proton transfer, takes place. MALDI data is characterized by relatively simple spectra, usually with a dominant pseudomolecular ion ($[M+H]^+$ for instance), and perhaps a doubly-charged +2 ion and in some cases, a $[2M+H]^+$ dimer. In general, MALDI is not used in conjunction with chromatography. In contrast, electrospray ionization (ESI) is used almost exclusively in-line with high performance liquid chromatography (HPLC). Ions are formed in electrospray by application of a voltage to a liquid flow, usually in the presence of acid, which nebulizes the flow into fine droplets. Drops in pressure through the ion source of the mass spectrometer desolvate the droplets, and finally release the ions into the gas phase. ESI spectra, in contrast to MALDI spectra, are characterized by a multiply charged envelope, with any basic residue in a molecule serving as a potential site for protonation (in the case of positive ion analysis). A distinct advantage of electrospray is its ease of use with on line chromatography. The technique is, however, sensitive to nonvolatile salts and other contaminants which may foul the ion source of the mass spectrometer. MALDI is more forgiving in this regard, due to the different mechanism of ionization and ion source geometries.

Following is a detailed protocol for the MALDI-TOF mass spectrometric analysis of PAMAM based dendrimers. This protocol can be extended to other types of nanoparticles such as fullerenes and polymers.

2. Materials

1. Voyager-DE PRO time-of-flight mass spectrometer (Applied Biosystems, Inc.) or equivalent.
2. MALDI matrix: 2,5-dihydroxybenzoic acid (DHB) (Aldrich Chemicals, cat. no. 14,935-7, see Note 4).
3. Water, 18 MΩ (Millipore Milli-Q System or equivalent).
4. Bovine serum albumin (mass spec standard, Sigma Chemical, cat. no. A-8471) used for instrument calibration.

5. Microcentrifuge (Clover Laboratories), single speed (2940 × *g*) or equivalent.

3. Methods

3.1. MALDI Matrix Preparation

1. Weigh 20 mg DHB (see Note 1) and dissolve in 1 mL 18 MΩ water in a 1.5 mL microcentrifuge tube and vortex on high for 30 s–1 min.
2. Centrifuge the matrix mixture for 1 min at 2940 × *g*.

3.2. Sample and Matrix Application to MALDI Plate

Sample, 0.3 µL (see Note 2), is first applied to the MALDI plate (stainless steel), followed by 0.3 µL of the DHB matrix directly on the sample. The sample/matrix mixture is then allowed to air dry. This is a modified version of the "dried droplet" method (9).

3.3. Mass Spectrometry Analysis of Dendrimers

1. Following loading of the MALDI target plate into the mass spectrometer, the following instrument parameters were used: the accelerating voltage was 25 kV, guide wire 0.15%, and grid voltage 91.5%. The instrument was operated in linear mode under positive ion conditions (see Note 5) from 10 to 100 kDa with the low mass gate set at 5 kDa. A nitrogen laser was used at 337 nm with 250 laser shots averaged per spectrum. External calibration was performed using bovine serum albumin as a standard.
2. Data analysis was carried out using "Data Explorer" software resident on the Voyager mass spectrometer. Equivalent software should be available on other mass spectrometers. Briefly, the sample spectrum was noise filtered/smoothed using the "Default" setting and a mass peak resolution of 1,000. The spectrum was then mass calibrated using the calibration file created by the analysis of bovine serum albumin. Peak masses were automatically assigned by the software following these procedures.
3. Example dendrimer data from the use of the above protocol follow. These examples were chosen as representative of current applications of dendrimers as carriers for small molecule drugs (10). Figure 1 illustrates two potential schemes by which a dendrimer can be associated with a small molecule drug (here, the chemotherapeutic molecule, methotrexate (MTX)). In Fig. 1a the dendrimer is covalently linked to the drug, while in Fig. 1b the drug is encapsulated in the branches of the dendrimer (these illustrations are schematic and molecules are not drawn to scale). The MALDI-TOF spectra of these molecules are shown in Figs. 2–5, respectively. The broad peak shapes of the molecular ion regions (m/z 31,371

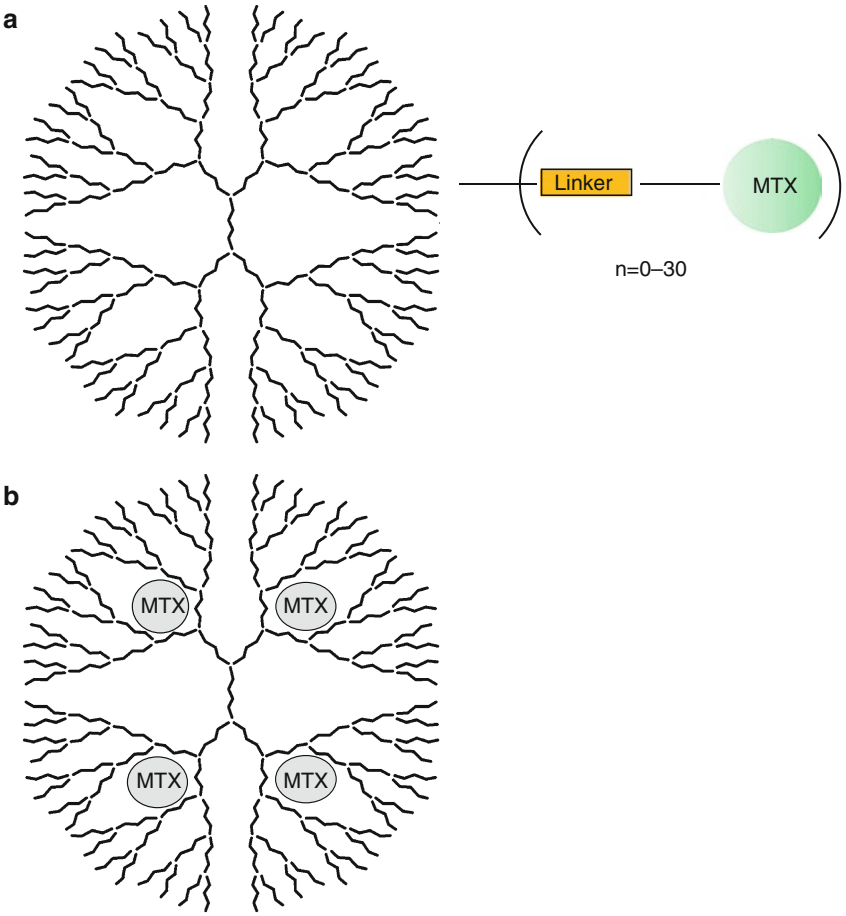

Fig. 1. Cartoon structures depicting the molecules under study. (**a**) Covalent attachment of the drug (methotrexate, abbreviated MTX) to the PAMAM dendrimer, and (**b**) an inclusion complex of the drug (MTX) in the interstitial space of a PAMAM dendrimer structure.

for PAMAM dendrimer UR-01-09, and *m/z* 27,847 for the G5 PAMAM dendrimer) visible in Figs. 2 and 4 are indicative of the heterogeneous nature of these materials (see Note 3).

To investigate the degree of incorporation of drug into these structures (i.e., the drug-loading), MALDI-TOF analysis was also carried out in the low mass region where the molecular ion of the small molecule drug, in this case, MTX, would be visible. As can be seen in Fig. 3 (the low mass region of the dendrimer/drug complex shown in Fig. 1a), only a small peak occurs at *m/z* 455.01, which would correspond to the $[M+H]^+$ ion of the intact MTX drug, MW = 454. However, it should also be noted that in the case of this dendrimer/drug complex, the MTX was covalently attached via a linker and the linker-MTX molecular weight is 583 and the pseudomolecular ion for this species is absent.

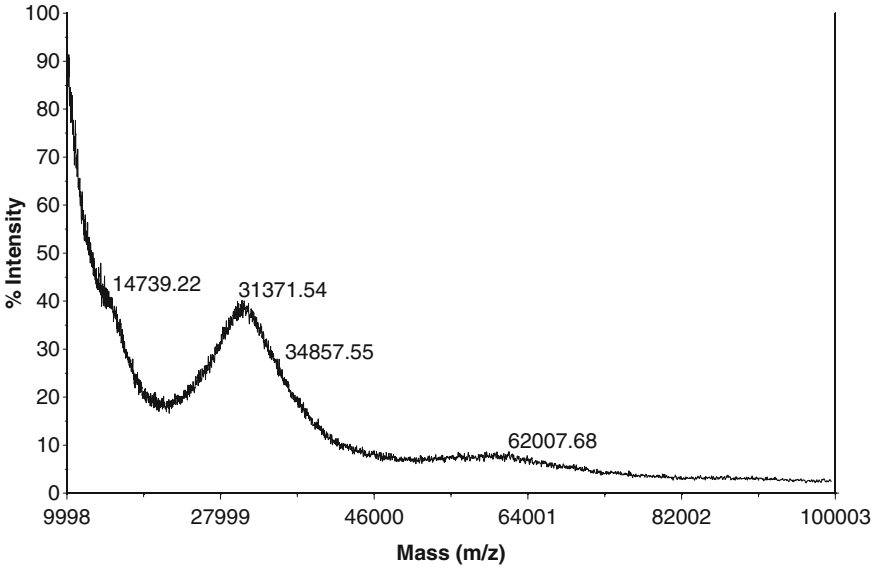

Fig. 2. MALDI-TOF mass spectrum of the dendrimer with covalently attached MTX (shown schematically in Fig. 1a), acquisition mass range: 1,000–100,000 amu. This dendrimer–MTX conjugate was synthesized using a 30-fold excess of the drug-linker unit (MTX-linker), so the theoretical molecular weight of this dendrimer–MTX complex is 28,854–46,344 amu (with *n* ranging from 0 to 30, where *n* is the number of conjugated drug-linker units) depending on the efficiency of the conjugation reaction. The theoretical mass of the drug-linker unit alone is 583 amu. The 31,371.54 amu labeled on the spectrum corresponds to approximately four conjugated drug-linker units, but the distribution clearly ranges from no attached drug to nearly the theoretical maximum.

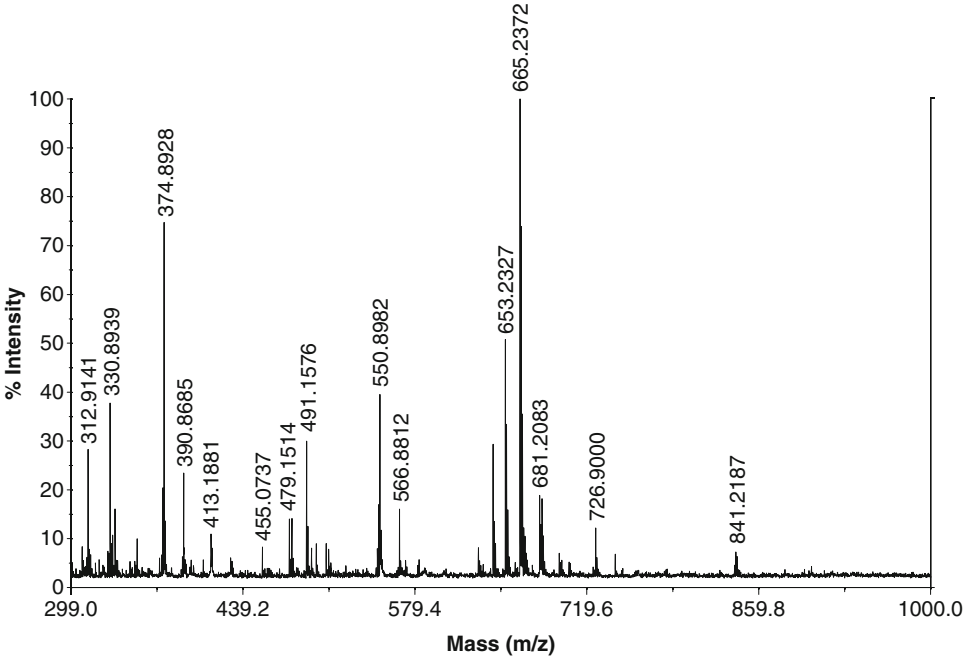

Fig. 3. MALDI-TOF mass spectrum of the dendrimer with covalently attached MTX (shown schematically in Fig. 1a), acquisition mass range: 300–1,000 amu. Methotrexate (MTX) is covalently attached to the dendrimer backbone. The molecular weight of MTX alone is 454.44 g/mol.

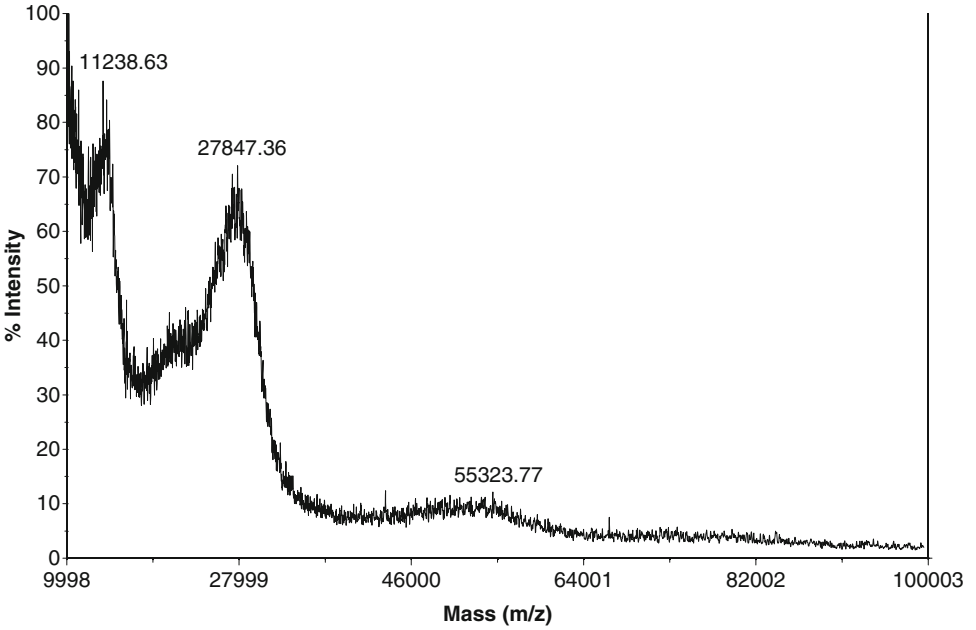

Fig. 4. MALDI-TOF mass spectrum the dendrimer MTX inclusion complex (shown schematically in Fig. 1b), acquisition mass range: 100–100,000 amu. The theoretical molecular weight for this complex ranges from 28,854 (no encapsulated MTX) to some maximum when the dendrimer is completely saturated with MTX molecules. Under MALDI-TOF conditions, the weak forces that stabilize the MTX interaction with the dendrimer matrix are destroyed and what is detected are the individual components: G5 PAMAM dendrimer at 27,847 (theoretical MW 28,854 – it is quite common in dendrimer synthesis that the end product is missing branches, etc. and deviates from the "perfect" theoretical structure) shown here and MTX $[M+H]^+$ peak at 455 amu (molecular weight of MTX 454.44 g/mol) in Fig. 5.

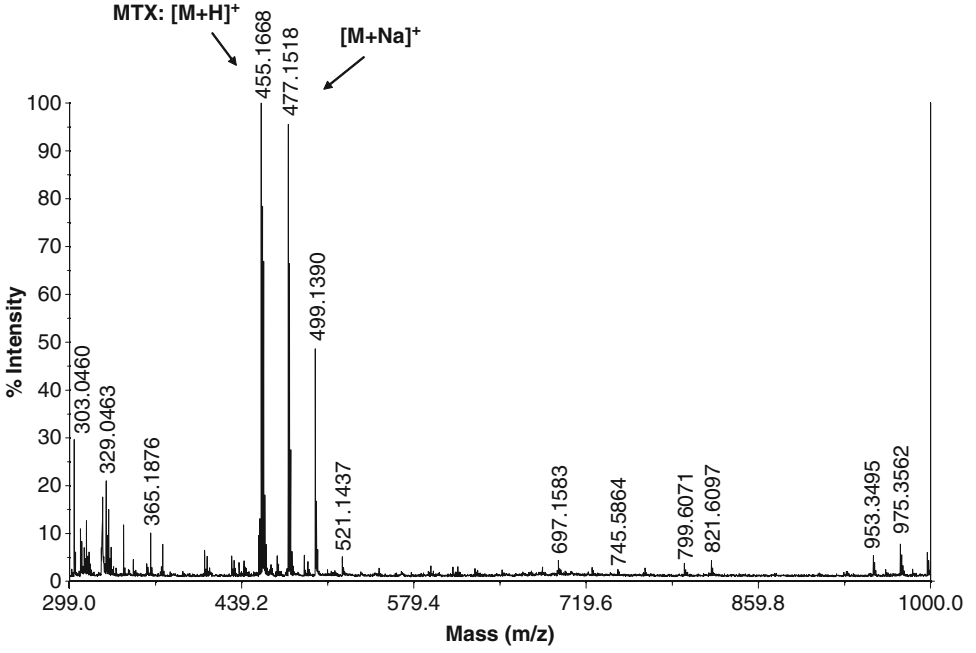

Fig. 5. MALDI-TOF mass spectrum of the dendrimer MTX inclusion complex (shown schematically in Fig. 1b), acquisition mass range: 300–1,000 amu. Methotrexate (MTX) as part of cage dendrimer structure. MTX molecular weight: 454.44 g/mol. One advantage of the use of 2,5-dihydroxybenzoic acid (DHB) as the matrix for MALDI-TOF MS of dendrimers is its relatively clean low molecular weight spectrum. It can therefore be used to track the drug inside the vehicle structure as part of the same experiment as analyzed for the dendrimer.

In contrast, Fig. 5 shows the MALDI-TOF mass spectrum in the low mass region for the encapsulated MTX-dendrimer sample (Fig. 1b). A clear pseudomolecular ion for MTX occurs at *m/z* 455.2 $[M+H]^+$ along with the sodiated analog at *m/z* 477.2 $[M+Na]^+$. This analysis also indicates the advantage of the use of DHB as the matrix, as there are relatively few matrix ions in the mass range of interest for small molecule analysis. The use of DHB as the MALDI matrix allows for the interrogation of both the dendrimer/vehicle molecular ion region (20–40 kDa) as well as drug (usually <1,000 amu).

4. Notes

1. Sample buffer. Many samples produced from biological sources or for use in biological systems will contain various salts or other materials that will interfere with analysis by mass spectrometry. Among the most common are nonvolatile salts such as sodium chloride and sodium phosphate (e.g., in PBS) or "preservatives" such as glycerol. When possible, dilution or reconstitution of the sample in these buffers should be avoided. MALDI mass spectrometry has a better tolerance to these types of contaminants due to the ionization mechanism (solid phase laser desorption) versus ESI (solution phase ionization). However, signal suppression can be significant if the molar amounts of contaminants are sufficiently high. Good references on the maximum recommended concentrations for common buffers can be found in Mock et al. (11), mass spectrometry instrument manuals, and the internet (12).
2. Concentration. While many claims in the literature can lead one to assume that very low concentrations of materials can be detected by mass spectrometry, there is a practical limit in the case of initial studies. In general, for multiple runs of the MALDI-TOF analysis presented here, 5–10 µL of a 10–20 µM solution is more than sufficient, with the same holding true for ESI, although more volume may be necessary. This amount of material will afford the mass spectrometrist with enough material that dilution and/or purification can be done if contaminating salts, etc., are present. A higher concentration is of particular importance if the expected molecular weight of the species of interest is >10 kDa. This concentration range is a best case scenario from the analytical viewpoint but should not be the determining factor to attempt the experiment.
3. Spectral interpretation. In general, the MALDI process produces a base peak (100%) that is the pseudomolecular ion, $[M+H]^+$, in many cases. Depending on the nature of the molecule being analyzed, doubly-charged, $[M+2H]^{2+}$, and

perhaps triply charged ions can be seen in the spectrum, occurring at 1/2 or 1/3, etc., the mass of the molecular ion. If the instrument being used has sufficient resolution, determination of the charge state of the ion can be determined by the spacing of the carbon isotope peaks. In some instances, a dimer, $[2M+H]^+$ may also be seen in the spectrum. This is usually due to a concentration effect rather than intramolecular interactions from the solution phase species. Simple dilution of the sample will lead to elimination of the dimer peak if it is due to the MALDI process.

4. MALDI matrix selection. The selection of the appropriate matrix for MALDI-TOF analysis is still rather empirical. While the choice of alpha-cyano-4-hydroxycinnamic acid (CHCA) for peptides and 3,5-dimethoxy-4-hydroxycinnamic acid (sinapinic acid) for proteins are generally accepted (13), the choice of matrix for novel materials, such as nanomaterials, requires both structural inspection and empirical investigation. Our choice of DHB for the matrix in these studies resulted from a review of the literature as well as comparisons with other common matrices including CHCA, sinapinic acid, and others. The best signal-to-noise ratio was achieved with the DHB recipe given.
5. Ionization mode. Choice of ionization mode (positive ion or negative ion) is dependant largely on the structures of the analytes of interest. In the case of the dendrimers presented here, the dominant presence of primary and tertiary amines indicates that positive ion analysis would be the most sensitive owing to the basic nature of the amines to form stable positive ions ($[M+H]^+$). In the case of structures with stabilized anions, negative ion analysis would likely be the best choice, assuming this mode of operation is available on the instrumentation being used.

Acknowledgments

This project has been funded in whole or in part with federal funds from the National Cancer Institute, National Institutes of Health, under contract N01-CO-12400. The content of this publication does not necessarily reflect the views or policies of the Department of Health and Human Services, nor does mention of trade names, commercial products, or organizations imply endorsement by the U.S. Government.

Jennifer Hall, Ph.D., Nanotechnology Characterization Laboratory, ATP, SAIC-Frederick, NCI-Frederick, provided useful comments and critical reading of the manuscript.

References

1. Matthews, O.A., Shipway, A.N., and Stoddart, J.F. (1998) Dendrimers – Branching out from Curiosities into New Technologies. *Prog Polym Sci.* **23**, 1–56.
2. Dykes, G.M. (2001) Dendrimers: A Review of Their Appeal and Applications. *J Chem Technol Biotechnol.* **76**, 903–918.
3. Rameshwer, S., Thomas, T.P., Peters, J.L., Desai, A.M., Kukowska-Latallo, J., Patri, A.K., Kotlyar, A., and Baker, J.R. Jr. (2006) HER2 Specific Tumor Targeting with Dendrimer Conjugated Anti-HER2 mAb. *Bioconjug. Chem.* **17**, 1109–1115.
4. Kukowska-Latallo, J.F., Candido, K.A., Cao, Z., Nigavekar, S.S., Majoros, I.J., Thomas, T.P., Balogh, L.P., Khan, M.K., and Baker, J.R. Jr. (2005) Nanoparticle Targeting of Anticancer Drug Improves Therapeutic Response in Animal Model of Human Epithelial Cancer. *Cancer Res.* **65**, 5317–5324.
5. Lee, C.C., Gillies, E.R., Fox, M.E., Guillaudeu, S.J., Frechet, J.M.J., Dy, E.E., and Szoka, F.C. (2006) A Single Dose of Doxorubicin-Functionalized Bow-Tie Dendrimer Cures Mice Bearing C-26 Colon Carcinomas. *Proc Natl Acad Sci USA.* **103**, 16649–16654.
6. Jensen, A.W., Maru, B.S., Zhang, X., Mohanty, D.K., Fahlman, B.D., Swanson, D.R., and Tomalia, D.A. (2005) Preparation of Fullerene-Shell Dendrimer–Core Nanoconjugates. *Nano Lett.* **5**, 1171–1173.
7. Peterson, J., Allikmaa, V., Subbi, J., Pehk, T., and Lopp, M. (2003) Structural Deviations in poly(amidoamine) Dendrimers: A MALDI-TOF MS Analysis. *Eur Polym J.* **39**, 33–42.
8. Shi, X., Banyai, I., Rodriguez, K., Islam, M.T., Lesniak, W., Balogh, P., Balogh, L.P., and Baker, J.R. Jr. (2006) Electrophoretic Mobility and Molecular Distribution Studies of poly(amidoamine) Dendrimers of Defined Charges. *Electrophoresis.* **27**, 1758–1767.
9. Karas, M. and Hillenkamp, F. (1998) Laser Desorption Ionization of Proteins with Molecular Masses Exceeding 10000 Daltons. *Anal Chem.* **60**, 2299–2301.
10. Kono, K., Liu, M., and Frechet, J.M.J. (1999) Design of Dendritic Macromolecules Containing Folate or Methotrexate Residues. *Bioconjug Chem.* **10**, 1115–1121.
11. Mock, K.K., Sutton, C.W., and Cottrell, J.S. (1992) Sample Immobilization Protocols for Matrix-Assisted Laser-Desorption Mass Spectrometry. *Rapid Commun Mass Spectrom.* **6**, 233–238.
12. http://www.masspec.scripps.edu/services/proteomics/saltol.php.
13. Lewis, K.J., Wei, J. and Siuzdak, G. (2000) Matrix-assisted Laser Desorption/Ionization Mass Spectrometry in Peptide and Protein Analysis, in *Encyclopedia of Analytical Chemistry* (Meyers, R.A., ed.) John Wiley & Sons, Chichester, UK, pp. 5880–5894.

Chapter 6

Zeta Potential Measurement

Jeffrey D. Clogston and Anil K. Patri

Abstract

This chapter describes a method for the measurement of the electrostatic potential at the electrical double layer surrounding a nanoparticle in solution. This is referred to as the zeta potential. Nanoparticles with a zeta potential between −10 and +10 mV are considered approximately neutral, while nanoparticles with zeta potentials of greater than +30 mV or less than −30 mV are considered strongly cationic and strongly anionic, respectively. Since most cellular membranes are negatively charged, zeta potential can affect a nanoparticle's tendency to permeate membranes, with cationic particles generally displaying more toxicity associated with cell wall disruption. This technique is demonstrated for two types of nanoparticles commonly used in biological applications: colloidal gold (strongly anionic) and amine-terminated PAMAM dendrimer (strongly cationic).

Key words: Zeta potential, surface charge, nanoparticles

1. Introduction

In an ionic solution, nanoparticles with a net charge will have a layer of ions (of opposite charge) strongly bound to their surface; this is referred to as the Stern layer. A second diffuse outer layer is comprised of loosely associated ions. These two layers are collectively called the electrical double layer. As the particle moves (due to Brownian diffusion or applied force), a distinction is created between ions in the diffuse layer that move with the nanoparticle and ions that remain with the bulk dispersant. The electrostatic potential at this "slipping plane" boundary is called the zeta potential and is related to the surface charge of the nanoparticle.

In zeta potential measurements, an electrical field is applied across the sample and the movement of the nanoparticles (electrophoretic mobility) is measured by laser doppler velocimetry (LDV). The Henry equation is then used to calculate the zeta potential, *z*:

$$U_e = \frac{2\varepsilon z f(\kappa a)}{3\eta},$$

Scott E. McNeil (ed.), *Characterization of Nanoparticles Intended for Drug Delivery*, Methods in Molecular Biology, vol. 697, DOI:10.1007/978-1-60327-198-1_6,

where U_e is the electrophoretic mobility, ε is the dielectric constant, η is the absolute zero-shear viscosity of the medium, $f(\kappa a)$ is the Henry function, and κa is a measure of the ratio of the particle radius to the Debye length. Nanoparticles with a zeta potential between −10 and +10 mV are considered approximately neutral, while nanoparticles with zeta potentials of greater than +30 mV or less than −30 mV are considered strongly cationic and anionic, respectively.

This chapter outlines the procedure for sample preparation for a zeta potential measurement and for determination of the zeta potential of nanoparticle in aqueous solutions. Guidelines for making successful zeta potential measurements are also provided, along with a discussion of relevant standards and data analysis. Finally, examples of the results of this measurement are illustrated for two types of nanoparticles: 30 nm nominal-diameter colloidal gold and fifth-generation (G5) polyamidoamine (PAMAM) amine-terminated dendrimers.

2. Materials

1. Instrument for measuring laser doppler velocimetry – phase analysis light scattering (LDV-PALS) or zeta potential.
2. Folded capillary cell (also called zeta cells). These are polycarbonate cells with gold-plated electrodes (e.g. DTS1060C, Malvern Instruments).
3. Caps for zeta cells (two per cell).
4. Zeta potential transfer standard (e.g. Malvern Instruments, DTS0050). This is carboxylated polystyrene latex dispersed in pH 9.22 buffer.
5. 10 mM NaCl (or similar low ionic strength solution).
6. Analyte nanoparticle solution (see Note 1).

3. Methods

3.1. Cleaning and Handling of Zeta Cells

1. Zeta cells should be rinsed thoroughly before use. This involves rinsing the zeta cells with water, followed by ethanol, and finally water again. As the zeta cells have two ports, it is recommended to flush a minimum of 1 mL of each rinsing solvent through each port to thoroughly rinse each electrode. This can be achieved by either using a 1 mL disposable syringe or a wash bottle filled with the corresponding rinsing solvent.
2. The zeta cells, after rinsing, should be dried using nitrogen to remove any remaining solvent. The nitrogen line/tube should have a filter to minimize dust during drying. The zeta cells should be capped until use to prevent any dust contamination.

3. Take care not to touch the measuring window of the zeta cells as well as the electrodes. Use of gloves is highly recommended to avoid any residual skin oil deposits.
4. After the zeta cells are rinsed, visually check the electrodes both inside and outside of the cell and the measuring window for any manufacturing defects such as scratches or nontransparent measuring windows, dirty or nonhomogenous surface coating of electrodes (electrodes are gold-plated), or any residual polycarbonate (from manufacturing process) in the cell or on the electrodes. New zeta cells should be used if any of these defects are found.
5. Zeta cells are to be used once per sample and then disposed. It is highly advised to not reuse or reclean the zeta cells for future measurements.

3.2. Nanoparticle Sample Preparation

1. Samples should be prepared in a low ionic strength medium (see Note 2). 10 mM NaCl is recommended. Suspending medium should be filtered *prior* to sample preparation using a 0.1 μm or smaller pore size membrane.
2. Sample concentration is particle-dependent (see Note 2). Ideal sample concentration is determined by the light scattering properties of the nanoparticles under analysis. For example, metallic nanoparticles (such as gold colloid) scatter light more strongly than similar sized carbon-based nanoparticles (such as dendrimers). As a result, the zeta potential must be measured at different concentrations for both of these types of particles. Representative data are shown at the end of this chapter (see Figs. 1 and 2).
3. Zeta potential is dependent on pH and therefore the sample pH should be measured before and after the zeta potential readings (see Note 3).

3.3. Loading Sample into the Zeta Cells

1. The zeta cell can accommodate a minimum of 750 μL of sample. Transfer the sample to a 1-mL disposable syringe, dislodge any air bubbles, and insert the syringe to one of the ports on the zeta cell. Fill the zeta cell with sample by gently depressing the syringe plunger. Remove the syringe from the zeta cell after the entire sample has been transferred.
2. Check for any air bubbles in the zeta cell or on the electrodes; gently tap the zeta cell to dislodge them. Visually check that both electrodes are submerged. Add more sample to the zeta cell if necessary by using a 1-mL disposable syringe; add sample in a drop-wise manner to one port and gently tap the zeta cell until the sample drop clears the port.
3. Cap both ports simultaneously to ensure even sample levels on both sides of the zeta cell.

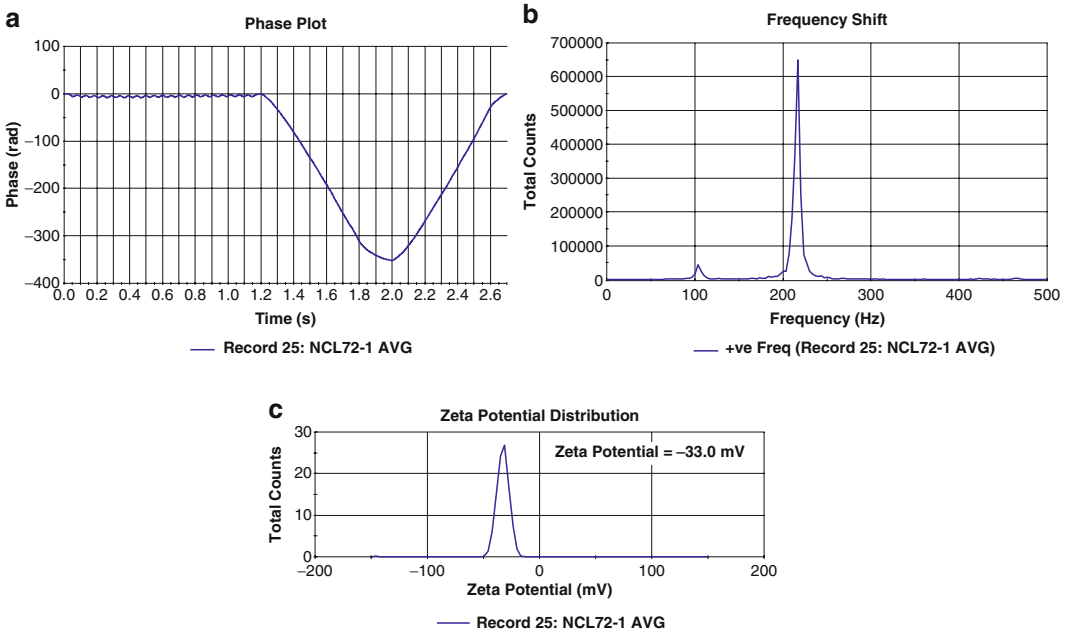

Fig. 1. The averaged (over five measurements) (**a**) phase plot, (**b**) frequency plot, and (**c**) zeta potential distribution for 30 nm colloidal gold. Sample concentration was 1.3 μg/mL in 10 mM NaCl with a pH value of 6.5. The sample was transferred to a zeta cell (DTS1060C, Malvern Instruments) and measured at 25°C using a Malvern ZetaSizer Nano ZS and an applied voltage of 150 V. The zeta potential was –33.0 ± 0.5 mV (n = 5). A viscosity of 0.891 centiPoise (cP), a dielectric constant of 78.6, and Henry function of 1.5 were used for the calculations.

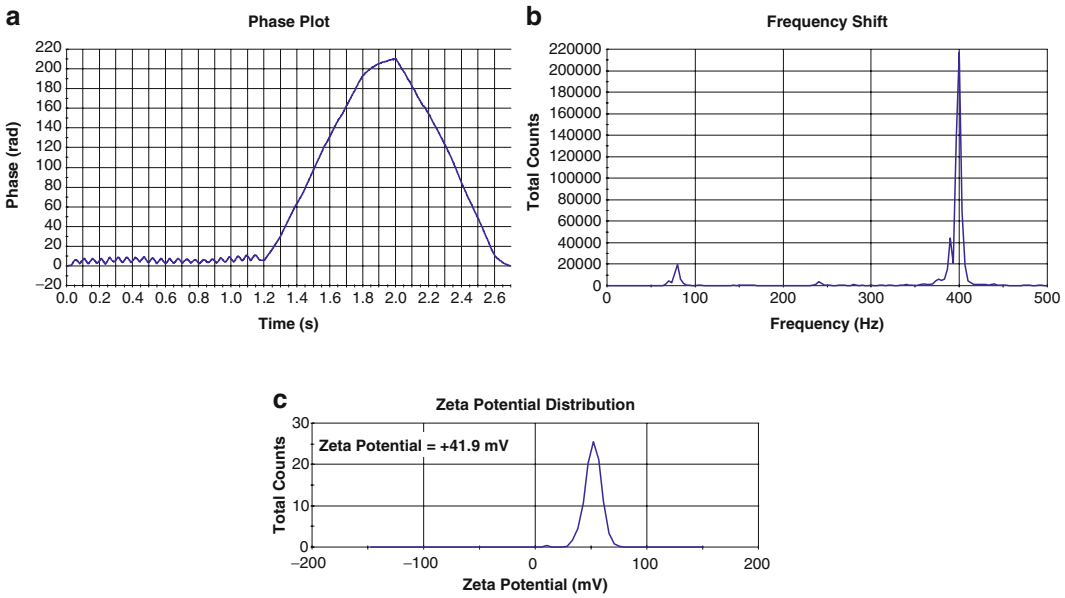

Fig. 2. The averaged (over four measurements) (**a**) phase plot, (**b**) frequency plot, and (**c**) zeta potential distribution for a fifth-generation (G5) polyamidoamine (PAMAM) amine-terminated dendrimer. Sample concentration was 2 mg/mL in 10 mM NaCl with a pH value of 7.4. The sample was transferred to a zeta cell (DTS1060C, Malvern Instruments) and measured at 25°C using a Malvern ZetaSizer Nano ZS and an applied voltage of 120 V. The zeta potential was +41.9 ± 5.5 mV (n = 4). A viscosity of 0.891 cP, a dielectric constant of 78.6, and Henry function of 1.5 were used for the calculations.

3.4. Measurement Procedure

1. The zeta cell (Malvern) contains a weld line (a small notch along the top of the cell) on one side; this is the front of the zeta cell and should be facing the front of the instrument. Before loading the zeta cell into the instrument, carefully wipe the measuring windows with lens paper. Once the zeta cell is placed in the instrument, check that the electrodes on the zeta cell are in contact with the leads in the instrument.
2. The temperature should be controlled and measured with an accuracy and precision of 0.3°C or better. An equilibration time of 2 min is recommended prior to starting measurements.
3. Perform a minimum of three runs per sample to establish measurement repeatability (see Note 4). Measurement duration (i.e., number of subruns per run) should be set according to instrument manufacturer's recommendations and will differ depending on particle size and scattering characteristics.
4. The applied voltage can be set to automatic or manual mode. In automatic mode, the best voltage is determined by the software. However, it is recommended to run in manual mode and start at a low voltage, typically 80 V, and increase the voltage gradually for optimal results (maximum voltage is 150 V for this instrument).

3.5. Data Analysis

A detailed description of the data analysis will not be given here. It is left for the reader to check the instrument's user manual to identify the data analysis algorithm. However, regardless of the instrument used, the electrophoretic mobility is determined experimentally and used to calculate the zeta potential from the Henry equation. The remaining terms in the equation (dielectric constant, viscosity, and Henry function) must be measured separately or based on reference values. Table 1 lists the viscosities at three different temperatures for 10 mM NaCl and the dielectric constant (1) at 25°C. The Henry function can be approximated as 1.5 (Smoluchowski model) for measurements made in aqueous medium with salt concentrations ≥10 mM (see Note 5).

1. The zeta potential, at a minimum, is reported with its standard deviation and the number of runs along with the measurement temperature, the pH, and concentration of the sample, and the dispersion medium composition. Additional

Table 1
Absolute viscosity of 10 mM NaCl at several temperatures

Aqueous medium	Absolute viscosity (mPa · s)			Dielectric constant
	20°C	25°C	37°C	
10 mM NaCl	1.003	0.891	0.693	78.6

information should be reported and include: Henry function approximation employed, viscosity of dispersing medium, dielectric constant, applied voltage, instrument make and model, and type of zeta cell used. Examples of zeta potential results are shown for 30 nm colloidal gold and a G5 amine-terminated dendrimer in Figs. 1 and 2, respectively.

2. Zeta potential values in the range of $-10 < 0 < 10$ mV are considered neutral (see Note 6).

4. Notes

1. Always wear appropriate personal protective equipment and take appropriate precautions when handling your nanomaterial. Many occupational health and safety practitioners recommend wearing two layers of gloves when handling nanomaterials. Also, be sure to follow your facility's recommended disposal procedure for your specific nanomaterial.
2. Zeta potential is dependent on pH, and the conductivity of the dispersing medium. Different values for zeta potentials are obtained depending on these factors and thus it is important to accurately measure and report them.
3. The pH of the sample should always be reported along with the zeta potential. Sometimes it is useful to adjust the native sample pH to a more relevant pH (e.g., closer to physiological pH for nanoparticles intended for biomedical applications). Close attention should be paid to the process of adjusting the pH. Rapid addition of strong acid or base may compromise the sample's integrity and result in a polydispersed sample (see Fig. 3). In this case, the zeta potential distribution may contain multiple peaks arising from the presence of differently charged species. It is recommended to titrate with 0.1 M HCl or 0.1 M NaOH in a drop-wise (~1–3 μL) manner and monitor the pH throughout. Alternatively, an autotitrator can be used to adjust the sample pH. Sample instability may be an issue for some samples due to pH adjustment and should be monitored carefully through other methods.
4. The quality of data can be assessed by examining several parameters. Check that the scattering intensity count rate is acceptable based on the instrument manufacturer's specifications. The phase plots should have alternating slopes with time followed by either a smooth positive or negative peak (see Figs. 1a and 2a). Review the frequency and phase plots; the baseline in the frequency plots should not be noisy but rather smooth (see Figs. 1b and 2b). The zeta potential should not change with measurement duration (i.e., number of runs) or with different applied voltages.

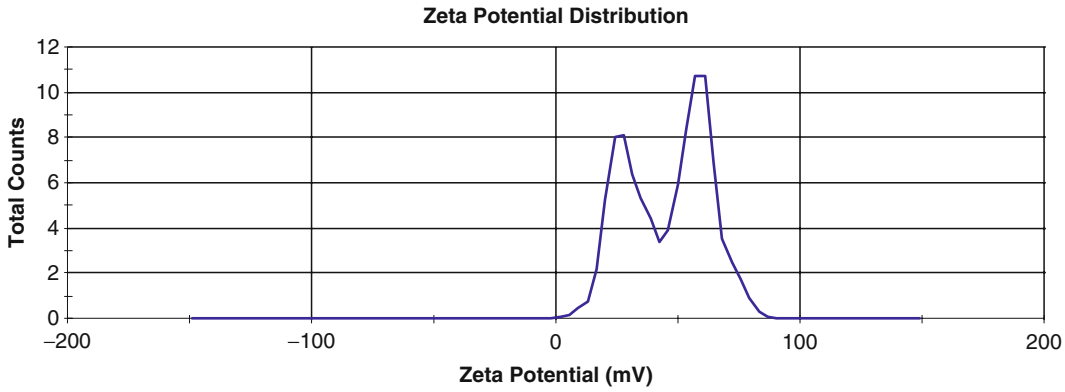

Fig. 3. The averaged (over four measurements) zeta potential distribution for a fifth-generation (G5) polyamidoamine (PAMAM) amine-terminated dendrimer. Experimental conditions were the same as in Fig. 2, except that the pH was lowered rapidly using 0.1 M HCl. This compromised the dendrimers' integrity leading to the appearance of two distinctly charged species.

Unreliable results can be caused by several factors. Periodically check that air bubbles do not form on the electrode surface as a result of the applied voltage. Gently tap the zeta cell to dislodge them before proceeding with the measurement. Check that the zeta cell is placed in the correct orientation and that the measuring window is clean. Samples should be optically clear and not turbid. Inconsistent zeta potential values with time can be a result of sample or electrode degradation. Blackening of the electrode surface or visual evidence of precipitate formation or change of sample color verifies such degradation. Lower applied voltages are recommended in these cases. Blackening of the electrodes also occurs if the dispersing medium has a high salt concentration (high conductivity). The authors highly recommend using 10 mM NaCl as the dispersing medium. Poor phase plots can be often remedied by increasing the number of subruns. Sample concentration is particle-specific and depends on the particle's scattering properties. Low concentrations may seriously degrade the signal-to-noise ratio and will result in noisy and inconsistent results. High concentrations can lead to multiple scattering effects and particle interactions, both of which can produce changes in the measured zeta potential. Typically, zeta potential measurements are made after dynamic light scattering (DLS) has been performed. If this is the case, normally the optimal concentration for DLS works well for zeta potential measurements.

5. Zeta potential measurements are based on first principles and hence no calibration is required. However, the instrument can be validated by running an appropriate standard. It is recommended to run such a standard along with the samples.

Such a standard is readily available from Malvern Instruments (zeta potential transfer standard, DTS0050).

6. The zeta potential value obtained from the measurement is an average value. Thus, if the sample is monodispersed, this value corresponds to the zeta potential of the single component in the sample. However, if the sample is polydispersed (i.e., contains several different species with variation in charge densities) the zeta potential distribution plot will contain multiple peaks corresponding to the multiple components. The zeta potential in this case can be reported as either an average across all charged species or (if the instrument software allows) the zeta potential for each peak. In the former case, it should be noted that the sample is polydispersed.

Acknowledgment

This project has been funded in whole or in part with federal funds from the National Cancer Institute, National Institutes of Health, under contract N01-CO-12400. The content of this publication does not necessarily reflect the views or policies of the Department of Health and Human Services, nor does mention of trade names, commercial products, or organizations imply endorsement by the U.S. Government.

Reference

1. Dukhovich, F.S., Darkhovskii, M.B., Gorbatova, E.N., Kurochkin, V.K. (2003) Molecular Recognition: Pharmacological Aspects. Nova Science Publishers, New York, NY.

Chapter 7

Size Measurement of Nanoparticles Using Atomic Force Microscopy

Jaroslaw Grobelny, Frank W. DelRio, Namboodiri Pradeep, Doo-In Kim, Vincent A. Hackley, and Robert F. Cook

Abstract

This chapter outlines procedures for sample preparation and the determination of nanoparticle size using atomic force microscopy (AFM). Several procedures for dispersing gold nanoparticles on various surfaces such that they are suitable for imaging and height measurement via intermittent contact mode, or tapping mode, AFM are first described. The methods for AFM calibration and operation to make such measurements are then discussed. Finally, the techniques for data analysis and reporting are provided. The nanoparticles cited are National Institute of Standards and Technology (NIST) Au nanoparticle Reference Materials RM 8011 (nominally 10 nm particles), RM 8012 (nominally 30 nm), and RM 8013 (nominally 60 nm).

Key words: Nanoparticles, atomic force microscopy

1. Introduction

This chapter outlines procedures for sample preparation and the determination of nanoparticle size using atomic force microscopy (AFM). An AFM typically utilizes a cantilever with a sharp probe to scan a specimen surface (1, 2). The cantilever beam is built-in at one end of a piezoelectric displacement actuator controlled by the AFM. At the other end of the cantilever is a probe tip that interacts with the surface. At close proximity to the surface, the probe experiences a force (attractive or repulsive) due to surface interactions, which imposes a bending moment on the cantilever. In response to this moment, the cantilever deflects, and this deflection is measured using a laser beam that is reflected from a mirrored surface on the back side of the cantilever onto a split photodiode. A schematic diagram of the system is shown in Fig. 1.

Scott E. McNeil (ed.), *Characterization of Nanoparticles Intended for Drug Delivery*, Methods in Molecular Biology, vol. 697,
DOI 10.1007/978-1-60327-198-1_7,

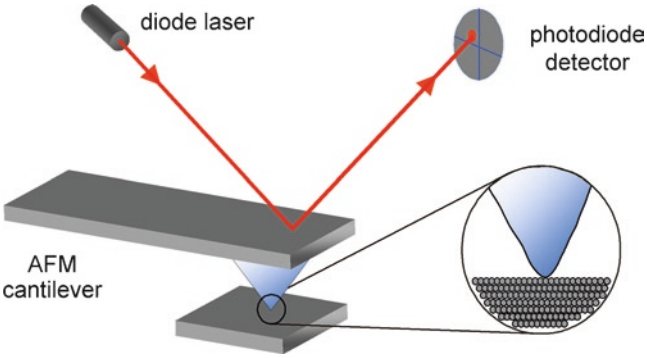

Fig. 1. Schematic diagram of an AFM. A laser beam is focused on the back of a cantilever that has a tip that interacts with a surface; the beam reflects into a four-quadrant photodetector. Normal forces between the tip and surface deflect the cantilever up or down; lateral forces twist the cantilever left and right. These deflections are measured by monitoring the deflection of the reflected laser.

The cantilever deflection is measured by the differential output (difference in responses of the upper and lower sections) of the split photodiode. The deflections are very small relative to the cantilever thickness and length and hence the probe displacement is linearly related to the deflection. The cantilever is typically silicon or silicon nitride with a tip radius of curvature on the order of nanometers.

Based on the nature of the probe–surface interaction (attractive or repulsive), an AFM can be selected to operate in various modes, namely contact mode, intermittent contact mode, or noncontact mode. In contact mode, the interaction between the tip and surface is repulsive, and the tip literally contacts the surface. At the opposite extreme, the tip interacts with the surface via long-range surface force interactions, and this is called noncontact mode. In intermittent contact mode, or tapping mode, the cantilever is oscillated close to its resonance frequency perpendicular to the specimen surface, at separations closer to the sample than in noncontact mode. As the oscillating probe is brought into proximity with the surface, the probe–surface interactions vary from long-range attraction to weak repulsion and, as a consequence, the amplitude (and phase) of the cantilever oscillation varies. During a typical imposed 100 nm amplitude oscillation, for a short duration of time, the tip extends into the repulsive region close to the surface, intermittently touching the surface and thereby reducing the amplitude. Intermittent contact mode has the advantage of being able to image soft surfaces or particles weakly adhered to a surface and is hence preferred for nanoparticle size measurements.

A microscope feedback mechanism can be employed to maintain a user-defined AFM set point; amplitude in the case of intermittent contact mode. When such feedback is operational, consistent

vibration amplitude can be maintained by displacing the built-in end of the cantilever up and down by means of a piezo-actuator (operation of an AFM with feedback off enables the interactions to be measured and this is known as force spectroscopy). This displacement directly corresponds to the height of the sample. A topographic image of the surface can be generated by rastering the probe over the specimen surface and recording the displacement of the piezo-actuator as a function of position.

Unlike electron microscopes, which provide a two-dimensional projection or a two-dimensional image of a sample, AFM provides a three-dimensional surface profile. Although the lateral dimensions are influenced by the shape of the probe, the height measurements can provide the height of nanoparticles with unprecedented accuracy and precision. If the particles are assumed to be spherical, the height measurement corresponds to the diameter or size of the particle. In this chapter, procedures for dispersing gold nanoparticles on various surfaces such that they are suitable for imaging and height measurement via intermittent contact mode AFM are described. The procedures for AFM calibration and operation to make such measurements are then discussed. Finally, the procedures for data analysis and reporting are provided. The nanoparticles cited are National Institute of Standards and Technology (NIST) Au nanoparticle Reference Materials RM 8011 (nominally 10 nm particles), RM 8012 (nominally 30 nm), and RM 8013 (nominally 60 nm).

2. Materials

1. Atomic force microscope.
2. AFM intermittent contact mode cantilevers.
3. AFM calibration grating.
4. Disc of substrate material (mica or silicon).
5. 0.1% poly-L-lysine (PLL, if using mica substrate).
6. 3-aminopropyldimethylethoxysilane (APDMES, if using silicon substrate).
7. Analyte nanoparticle solution (e.g., NIST Au nanoparticle Reference Materials: RM8011, RM8012, and RM8013, see Notes 1 and 2).
8. Ethanol and deionized (DI) water for cleaning and rinsing surfaces.
9. Optical microscope for initial sample inspection.
10. Image analysis software.

3. Methods

3.1. Nanoparticle Deposition Procedure (See Notes 3 and 4)

3.1.1. Mica Substrate

1. Mica is a layered mineral that can readily be cleaved along alkali-rich basal planes to form clean, atomically flat surfaces extending over several square cm. To prepare the substrate, a mica disc must be cleaved to produce a clean surface. Place the disc on a clean, lint-free cloth or directly on an AFM puck. Press a piece of adhesive tape against the surface of the disc and then smoothly remove the tape from the mica. The top layer of the mica should appear on the tape. Continue to cleave the mica until a full layer is removed and the exposed surface is smooth. Typically, this step needs to be repeated several times.
2. After cleaving, the mica disc is ready to be activated so as to promote adhesion between the substrate and the nanoparticles. The NIST Au nanoparticle RMs are dispersed in solution and stabilized by citrate ions that give the particles a negative charge. The mica substrate can be activated to have a positive charge that electrostatically binds the particles to the surface. The substrate is activated using dilute 0.1% PLL solution. To create the solution, dilute 0.1% PLL solution 1:10 with filtered DI water (e.g., add 0.5 mL PLL to 4.5 mL DI water). Use clean glassware for dilution and coating. Keep the diluted PLL solution refrigerated at 2–8°C until needed. Fully immerse the mica disc in the diluted PLL solution for 30 min at room temperature. To minimize evaporation, cover the solution with a glass dish. After the time has elapsed, remove the mica from the solution and blow dry with nitrogen.
3. After drying, apply ≈25 μL of undiluted nanoparticle solution onto the PLL-modified mica substrate using a micropipette. The gold solution should spread evenly across the surface. Incubate at room temperature using the following schedule:
   - 60 nm particles: 10 min
   - 30 nm particles: 5 min
   - 10 nm particles: 30 s

   The incubation time can be varied to modify the particle density on the surface as needed.
4. Rinse the substrate with filtered DI water and gently dry with nitrogen. The sample is now ready to image.

3.1.2. Silicon Substrate

1. The gold deposition procedure can also be conducted using silicon as the substrate material. Cleave a small sample (5 mm × 5 mm) from a silicon wafer. Clean the sample using the following procedure: 5 min in a plasma cleaner, 10 min in a glass container with ethanol placed in an ultrasonic cleaner, and 5 min in a plasma cleaner. At this time, the untreated

wafer supports a thin, native oxide layer. Place a drop of APDMES on the Si surface. Allow the APDMES to react with the underlying substrate for 2 h inside a closed vial. Rinse the excess APDMES off with ethanol followed by DI water.

2. After drying, apply ≈25 µL of undiluted nanoparticle solution onto the APDMES-modified silicon substrate using a micropipette. The gold solution should spread evenly across the surface. Incubate at room temperature using the following schedule:
   - 60 nm particles: 60 min
   - 30 nm particles: 30 min
   - 10 nm particles: 15 min

   The incubation time can be varied to modify the particle density on the surface as needed.
3. To prevent evaporation, the substrate with nanoparticle solution droplet should be closed inside a humidity chamber (closed container with DI water reservoir). Rinse the sample with ethanol followed by DI water, and dry with dry nitrogen prior to analysis.

3.2. Optical Microscope Inspection

Inspect each sample using an optical microscope before AFM imaging to find possible areas where one can expect a reasonably good dispersion of the particles. In most cases, the exterior of the dried droplet includes excess citrate, while the interior is citrate free with suitable particle distributions.

3.3. AFM Imaging and Size Measurement

3.3.1. Height Calibration

In order to obtain accurate measurements, the axial (z)-displacement of the piezoelectric stage needs to be calibrated using the traceable standards available. In Fig. 2, we show a schematic diagram and AFM image of a calibration grating, which in this case consists of a one-dimensional array of rectangular SiO_2 steps on a Si wafer. For this particular grating, the step height was certified to be 19.5 nm ± 0.8 nm. The step height is measured with an AFM calibrated using step height reference standards. The reference

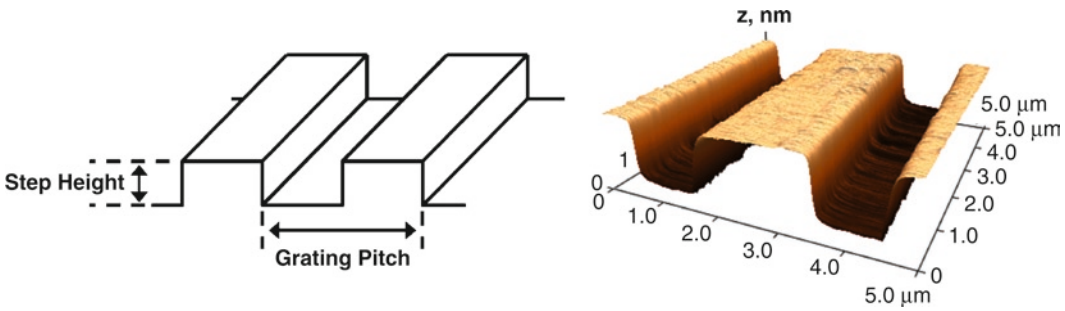

Fig. 2. Schematic diagram and AFM image of a calibration grating consisting of an array of rectangular SiO_2 steps on a Si wafer. For this particular grating, the step height was certified to be 19.5 nm ± 0.8 nm.

standards are three calibration gratings that were measured and certified by NIST (NIST Reports 821/261141-99 and 821/265166-01). After choosing a suitable grating (the step height of the grating should be similar to the characteristic height of the nanoparticles), measure the calibration grating in several locations using a sharp AFM tip and compare the average measured value to the certified step height. If the values are markedly different, consult the AFM manufacturer on how to recalibrate the z-displacement of the piezoelectric stage.

3.3.2. Operate in Imaging Mode

1. Intermittent contact mode in air

   Nanoparticles are fixed to the substrate via weak physical forces (e.g., electrostatic and van der Waals forces) (3, 4). As a result, intermittent contact mode is a suitable imaging mode in which the cantilever is driven to oscillate up and down at near its resonance frequency by a small piezoelectric element mounted in the AFM tip holder. The amplitude of this oscillation is greater than 10 nm, typically 100–200 nm.

2. Intermittent contact mode in fluid

   Though for these samples PLL or APDMES provided enough affinity for gold to be completely immobilized on the mica and silicon surface, other conditions might present the possibility that nanoparticles could be rolled or swept away by the AFM tip due to the shear force generated by intermittent contact mode in air. Also, residual excipients or salt could affect the height measurement. An alternative is to image nanoparticles with intermittent mode in fluid conditions. The PLL-coated mica or APDMES-covered silicon can be directly adopted as a substrate for intermittent mode AFM imaging under fluid conditions (see Note 5).

3.3.3. Consider Cantilever Properties (Tip Radius, Geometry, and Tilt)

Probes consist of a cantilever integrated with a sharp tip on the end. The properties and dimensions of the cantilever and sharp tip play an important role in determining the sensitivity and resolution of the AFM. Several of the key features that should be considered when choosing an AFM cantilever are listed and discussed below:

- Tip radius and geometry: A topographic AFM image is actually a convolution of the tip and sample geometry. While this does not affect height measurements, it does affect the overall representation of surface features. To minimize the convolution, it is best to use tips with radii <10 nm.
- Cantilever stiffness: Stable cantilever oscillations are required to successfully image a surface in intermittent contact mode and are only possible when the cantilever has enough energy to overcome adhesive forces (e.g., those arising from capillary menisci, van der Waals, and electrostatic forces) between the

tip and sample. To overcome these forces, cantilevers with stiffness ≈40 N/m are recommended.

- Cantilever tilt: In most AFM instruments, the cantilever itself is tilted by ≈10–20° relative to the surface. This is to ensure that the tip makes contact with the sample before any other component, such as the nearby sides of the cantilever chip. While this does not affect height measurements, it does result in an asymmetric representation of the features. In cases where this may be a problem, some cantilever manufacturers offer "on scan angle" symmetric tips, which compensate for the cantilever tilt via the tip geometry.

3.3.4. Determine Scan Size and Parameters

AFM images have a lateral (x, y) resolution and a vertical (z) resolution. The radius of curvature of the end of the tip will determine the highest lateral resolution obtainable with a specific tip. However, another factor that needs to be considered during image analysis is the number of data points, or pixels, present in an image in the x and y scan-direction. For example, in acquiring a 10 μm × 10 μm image with 512 pixels, the pixel size is ≈19.5 nm (10 μm/512 pixels ≈19.5 nm/pixel). In this case, it is not possible to resolve features smaller than 19.5 nm at a 10 μm scan size. Thus, it is important to consider the particle size when choosing the scan size. The following scan parameters can be used as starting points:

- 60 nm particles: scan size 2.0 μm × 2.0 μm, scan rate 1 Hz (per scan line)
- 30 nm particles: scan size 1.0 μm × 1.0 μm, scan rate 1 Hz
- 10 nm particles: scan size 0.5 μm × 0.5 μm, scan rate 1 Hz

3.3.5. Acquire Images

After completing the general setup for the AFM (e.g., calibrating the z-displacement of the piezoelectric stage, choosing and mounting the appropriate cantilever, tuning the cantilever, and so on), the instrument is now ready to begin the nanoparticle measurement process. At first, use a large scan size to identify a region with a homogeneous nanoparticle distribution. Once a suitable region has been identified, start taking the nanoparticle images, using the scan parameters above as a starting point. Adjust the oscillation amplitude feedback gains (proportional and integral) to ensure that the forward and backward line scans (profiles) look identical. Store the images on the computer with incremental filenames for postimaging analysis.

3.4. Image Analysis and Reporting Particle Size (See Note 6)

3.4.1. Flatten Images

Usually, the first step in AFM image processing is a line-wise flattening to remove artifacts of the image acquisition process. For instance, samples are not always mounted perfectly perpendicular to the AFM tip, resulting in some tilt that is not actually present on the sample surface. Other sources of artifacts include thermal drift and nonlinearity in the scanner. The flattening technique will correct these nonidealities by fitting each scan line with a polynomial

and subtracting it from the data. A first order (linear) correction is normally enough to remove any artifacts (see Note 7).

3.4.2. Draw Cross-Sectional Line Profiles

Another common feature included in most AFM software packages is the cross-section tool. A cross-sectional line can be drawn across any part of the image, and the vertical profile along that line is displayed. The cursors can be moved to make horizontal, vertical, and angular measurements. By making several cross-sectional line profiles through a nanoparticle, it is not only possible to calculate the particle height, but also to determine if the particle is isolated and sitting on a flat region (e.g., not on a step edge).

3.4.3. Height Measurement Procedure

Draw a fixed, moving, or averaged cross-section through each particle as shown in Fig. 3. Use the cursors to find both the average value for the baseline (on both sides of the nanoparticle) and the peak height. If the flattening procedure was done properly (i.e., the nanoparticles were excluded from the flattening process), the baseline should be relatively flat over the line scan. Subtract the average baseline height from the peak height to find the nanoparticle height. Repeat this procedure for at least 100 nanoparticles for statistical analysis.

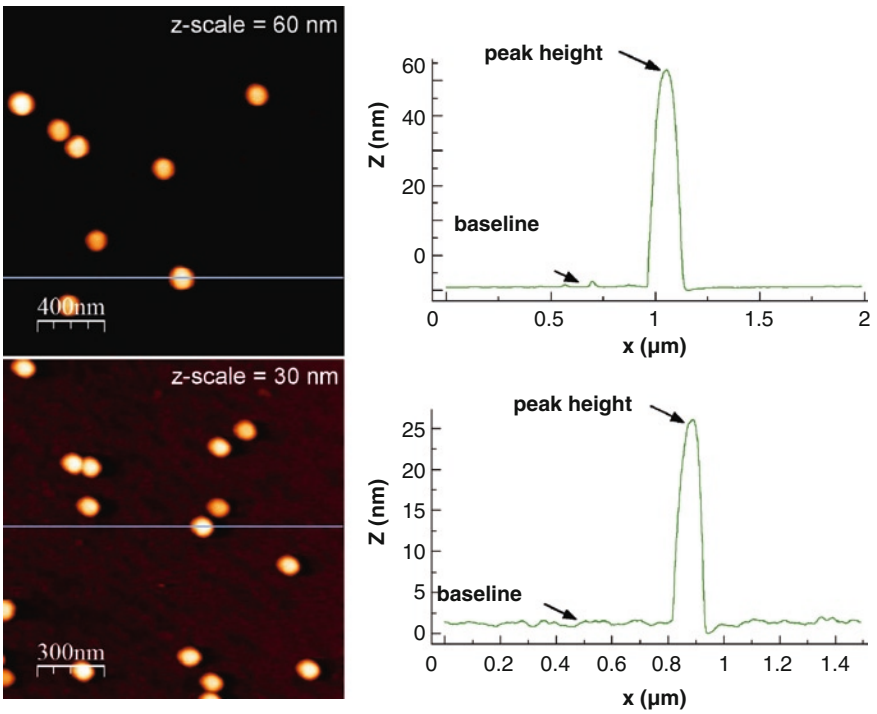

Fig. 3. AFM images and cross-sections for 60 and 30 nm nanoparticles (nominal). The difference between the peak height and the average baseline (from both sides of the nanoparticle) is the particle height.

3.4.4. Reporting Particle Size

Calculate the mean and the expanded uncertainty for the particle height distributions according to the following procedure (5, 6). The average, or arithmetic mean, particle height $\bar{X}$ is given by

$$\bar{X} = \frac{1}{n}\sum_{i=1}^{i=n} X_i,$$

where n is the number of measurements and X_i is the height of each particle. The most common method for describing the variation about the mean value is the standard deviation, or, more simply, the square root of the variance:

$$u_X = \sqrt{\frac{1}{n-1}\sum_{i=1}^{i=n}\left(X_i - \bar{X}\right)^2}.$$

However, the uncertainty associated with $\bar{X}$ is not defined by the standard deviation u_X, but by the standard deviation of the mean, or the standard error, $u_{\bar{X}}$. The standard error is related to the standard deviation via $u_{\bar{X}} = u_X/\sqrt{n}$, which yields

$$u_{\bar{X}} = \sqrt{\frac{1}{n(n-1)}\sum_{i=1}^{i=n}\left(X_i - \bar{X}\right)^2}.$$

It is important to consider not just the uncertainty associated with the mean particle height, but other sources of experimental uncertainty. In particular, it is necessary to include the uncertainty associated with the step height grating used to calibrate the AFM. In the case here, the calibration grating had a mean height G of 19.5 nm, with a standard uncertainty u_G of 0.35 nm (not to be confused with the *expanded* uncertainty of 0.8 nm). The combined standard uncertainty u_c is obtained by combining the individual standard uncertainties, $u_{\bar{X}}$ and u_G, using the following expression

$$u_c = \sqrt{{u_{\bar{X}}}^2 + {u_G}^2}.$$

The corresponding effective degrees of freedom ν_{eff} is obtained from the Welch–Satterthwaite equation

$$\frac{{u_c}^4}{\nu_{\text{eff}}} = \frac{{u_{\bar{X}}}^4}{\nu_{\bar{X}}} + \frac{{u_G}^4}{\nu_G},$$

where $\nu_{\bar{X}}$ and ν_G are the degrees of freedom for the height measurements and the calibration grating measurements, respectively. The *expanded* uncertainty U_p, or the uncertainty that defines an interval having a level of confidence p, is then given by

$$U_p = k_p u_c,$$

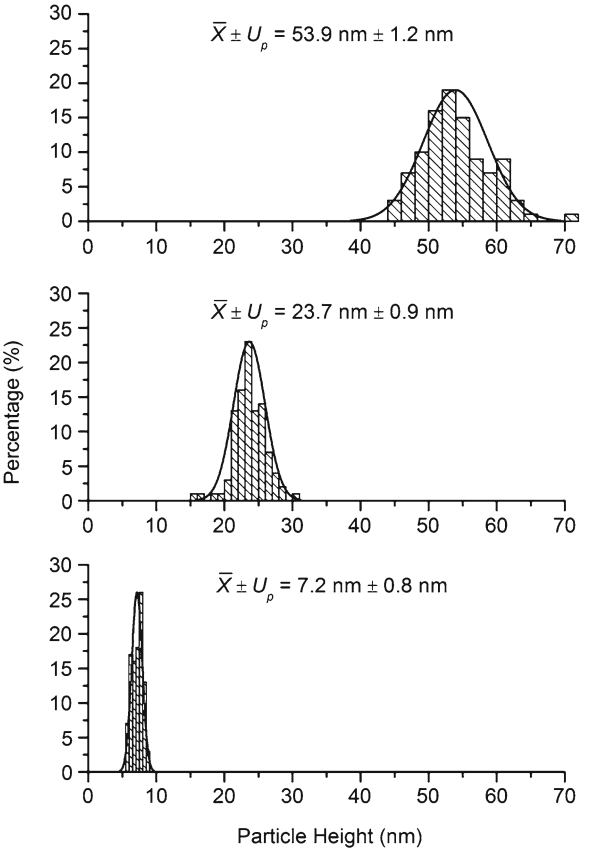

Fig. 4. Histograms for 60, 30, and 10 nm nanoparticles (nominal). For each data set, the mean and expanded uncertainty were calculated with a 95% confidence level. In all cases, the uncertainty in the mean is much less than the characteristic width of the fitted Gaussian distribution (*solid curves*).

where k_p is the coverage factor. The coverage factor is selected to achieve a desired level of confidence p using t-distribution tables (assuming ν_{eff} degrees of freedom). This yields a mean and expanded uncertainty for each data set that can be described by $\bar{X} \pm U_p$.

The height distributions for 60, 30, and 10 nm nanoparticles (deposited using procedure 1 on a mica substrate) are shown in Fig. 4. For each data set, the mean and expanded uncertainty were calculated with a 95% confidence level. Note that the uncertainty in the mean is a lot less than the characteristic width of the distribution.

4. Notes

1. Always wear appropriate personal protective equipment and take appropriate precautions when handling your nanomaterial.

Many occupational health and safety practitioners recommend wearing two layers of gloves when handling nanomaterials. Also, be sure to follow your facility's recommended disposal procedure for your specific nanomaterial.

2. The gold nanoparticle RM solutions should be stored at room temperature in their original package until opened for use and not exposed to intense direct light or ultraviolet radiation. Containers are best stored in the horizontal position. A color change from red to purple, or the appearance of black precipitate, indicates that the sample has been compromised. Prior to opening, gently invert the container several times to insure homogeneity and resuspension of any settled particles.
3. Nanoparticle samples need to be dispersed on flat surfaces for AFM measurements. The roughness of the surface should be much less than the nominal sizes of the nanoparticles in order to provide a consistent baseline for height measurements. High-quality mica, atomically flat polycrystalline gold (111) (deposited on mica), or single crystal silicon can all be used as substrates to minimize the effect of the surface roughness on nanoparticle measurements.
4. Gold nanoparticle suspensions typically contain free soluble species, such as citrate ions, which may interfere with either the deposition process or the subsequent AFM imaging. If this is the case, the user may want to adopt the following procedure, which utilizes a centrifuge to remove the additional free soluble species from the solution, prior to the surface activation and nanoparticle deposition techniques. For each nanoparticle size (60, 30, and 10 nm), place approximately 1 mL aliquots of native suspension from selected ampoules into 1.5 mL microtubes and centrifuge at the rotation speed and time listed below. Remove a portion of the supernatant from each microtube and replace it with DI water to obtain the proper dilution of the native suspension. No change in the stability of the suspension should be observed during this process.
    - 60 nm particles: dilution ratio 1:3, speed 2,040 *g*, time 5 min, volume of the suspension between 0.8 and 1 mL
    - 30 nm particles: dilution ratio 1:5, speed 5,220 *g*, time 6 min, volume of the suspension between 0.8 and 1 mL
    - 10 nm particles: dilution ratio 1:8, speed 16,000 *g*, time 20 min, volume of the suspension between 0.8 and 1 mL
5. For intermittent contact mode under fluid conditions: after preparing the substrate, mount it on the AFM stage by using double-sided tape. Place the fluid cell onto the substrate. Load an appropriate AFM probe and align the laser to make the deflected laser beam fall into the photodiode detector.

Then dilute the nanoparticles 10× with DI water and add the appropriate amount of sample to the fluid cell. When used for the gold RMs, the gold solution should immobilize evenly across the surface. Be sure to realign the laser and optimize the oscillation amplitude prior to scanning.

6. Once images are captured during real-time operation, they can be viewed, modified, and analyzed offline using the software supplied by the AFM manufacturer. Some of the more useful data visualization and processing features for nanoparticle measurements will be discussed here.
7. In the presence of nanoparticles, the flattening procedure becomes a bit more difficult. The software attempts to fit the polynomial to both the substrate and the nanoparticles, instead of just fitting to the substrate. To "eliminate" certain features during the flattening process, most AFM software packages include an "exclude points" function. Basically, this function will exclude all selected points during the flattening process, effectively ignoring the nanoparticles while flattening the underlying substrate.

Acknowledgment

The authors would like to thank Wolfgang Haller, Bin Ming, Jim Kelly, and John Dagata from the National Institute of Standards and Technology, in addition to Jiwen Zheng and Anil Patri from the Nanotechnology Characterization Laboratory, for their assistance with developing and documenting the nanoparticle deposition, measurement, and analysis techniques.

References

1. Meyer, E., Hug, H. J. and Bennewitz, R. (2004) *Scanning Probe Microscopy: The Lab on a Tip*. Springer-Verlag, Berlin.
2. Morris, V. J., Kirby, A. R. and Gunning, A. P. (1999) *Atomic Force Microscopy for Biologists*. Imperial College Press, London.
3. Schmid, G. (ed.) (2003) *Nanoparticles: From Theory to Application*. Wiley-VCH, Weinheim.
4. Kotov, N. A. (ed.). (2006). *Nanoparticle Assemblies and Superstructures*. CRC Press, Boca Raton, FL.
5. Taylor, B. N. and Kuyatt, C. E. (1993) *Guidelines for Evaluating and Expressing the Uncertainty of NIST Measurement Results*, NIST Technical Note 1297. National Institute of Standards and Technology, Gaithersburg, MD.
6. International Organization for Standardization (ISO) (1993) *Guide to the Expression of Uncertainty in Measurements*. Geneva, Switzerland.

Chapter 8

Biological Tissue and Cell Culture Specimen Preparation for TEM Nanoparticle Characterization

Kunio Nagashima, Jiwen Zheng, David Parmiter, and Anil K. Patri

Abstract

This chapter outlines the procedures for ex vivo TEM preparation of nanoparticle-containing tissue or cell culture samples using an epoxy resin embedding method. The purpose of this procedure is to preserve the structure of tissue in a hardened epoxy block with minimal disruption of cellular structures, to aid in the meaningful analysis of in vivo or cell culture experiments. The process begins with hydrated tissue and ends with tissue that is virtually water-free and preserved in a static state within a plastic resin matrix. The resin mixture permeates the dehydrated tissue, making the sample firm enough to cut. Procedures are also given for fixing nanoparticle-containing cell culture samples.

Key words: Nanoparticles, electron microscopy, transmission electron microscopy (TEM)

1. Introduction

Electron microscopy (EM) has long been used for ultrastructural analysis of both biological and nonbiological samples. There are basically two types of EM, transmission and scanning electron microscopy (TEM and SEM). TEM can visualize internal subcellular structures from thin sliced cells, while SEM yields more life-like cell surface images. TEM is of high resolution; it is one of only a few available instruments capable of resolving the structural features of nanoscale particles. When used in conjunction with detectors such as a backscattering detector (BSD) or energy dispersive X-ray spectroscopy (EDX) detector, SEM and TEM can be used to perform element analysis (see also Chapter 2.6).

In TEM, electrons emitted from a source are accelerated at high voltage potential and passed through a series of electromagnetic fields (conventionally called a "lens"). Some electrons pass

Scott E. McNeil (ed.), *Characterization of Nanoparticles Intended for Drug Delivery*, Methods in Molecular Biology, vol. 697,
DOI 10.1007/978-1-60327-198-1_8,

through the thinly sliced (70–90 nm) TEM sections under study, while other electrons are scattered or diffracted by the sample. The electrons that pass through the sample move through another set of magnetic fields (called the objective, intermediate, and projection lens) and finally collide with a fluorescent screen. During this collision, their kinetic energy is converted to visible light energy and exposes a photographic film or excites a CCD camera for digital imaging. This gives rise to a "shadow image" of the sample with different areas displayed with different darkness according to their density. Very thin slices of samples are required for TEM characterization so that the electrons can pass through the sample.

Modern TEM has a resolution (the ability to distinguish two closely located points) of about 1 Å (Angstrom, or 1×10^{-10} m). However, this does not mean one can always see biological molecules in TEM micrographs, since many biological molecules may not have a rigid structure or density capable of scattering high-velocity electrons. The electrons simply pass through the molecules and are therefore not visible in the resulting images. Techniques like embedding in epoxy resin (plastics) and flash freezing (cryo-TEM) can be used to render some biological molecules sufficiently structured to scatter electrons and be visible in TEM micrographs.

TEM allows detection of nanoparticles in biological materials (tissue specimens or cell culture samples) and visualization of fine cellular structures (details of subcellular organelles such as mitochondria, endoplasmic reticula, Golgi, centrioles, microtubules, endosomes, and ribosomes, all of which may not be resolved with a light microscope). Biological samples, however, always contain a large quantity of water. Conventional TEM requires that this water be removed, though new techniques such as variable-pressure or environmental TEM can be conducted on "wet" samples. The water removal for conventional TEM must be conducted without disrupting any of the fine cellular structures of the samples under study.

This chapter serves as an overview of sample preparation for TEM characterization of nanoparticles in tissue or cultured cell but is not an exhaustive review of this technique. The authors recommend the books cited in references (1) and (2).

2. Materials

1. 55°C Laboratory oven.
2. Ultramicrotome (Leica Microsystems, Wetzlar, Germany).
3. Color scale reference sheet (Leica Microsystems, Wetzlar, Germany).
4. Vacuum evaporator.
5. Resin embedding capsules.
6. Cell culture plates.

7. Inverted phase-contrast microscope (Nikon or similar).
8. TEM grids (EMS, 100–400 mesh).
9. Precision EM-grade tweezers.
10. Micropipettes (0.5–10 and 10–100 μL).
11. 0.1 M cacodylate buffer made from EMS sodium cacodylate powder.
12. 0.1 N sodium acetate buffer made from EMS sodium acetate powder.
13. Dulbecco's phosphate-buffered saline diluted to 1× (1× PBS).
14. EM-grade 4% formaldehyde + 2% glutaraldehyde in 0.1 M cacodylate buffer, pH 7.4 (see Note 1).
15. EM-grade 1% osmium tetroxide in 0.1 M sodium cacodylate buffer (OsO_4) (see Note 1).
16. Propylene oxide.
17. 0.5% uranyl acetate in 0.1 N acetate buffer.
18. 0.5% uranyl acetate in distilled water.
19. Ultrastain lead citrate (Leica Microsystems, Wetzlar, Germany).
20. 35, 50, 70, 95, and 100% EtOH.
21. Epoxy resin base (Electron Microscopy Sciences, Hatfield, PA) for tissue embedding and (Polysciences, Warrington, PA) for cell culture embedding.
22. Dodecenyl succinic anhydride (DDSA).
23. Nadic methyl anhydride (NMA).
24. Benzyldimethylamine (BDMA) or Dimethylaminomethylphenol (DMP-30).
25. Analyte nanoparticle-exposed tissue or cell culture sample (see Note 2).

3. Methods

3.1. Tissue Sample Preparation (See Fig. 1)

1. The tissue specimens should be stored in a vial containing primary fixative solution, 4% formaldehyde, and 2% glutaraldehyde in 0.1 M cacodylate buffer (see Note 3).
2. Transfer the tissue specimens to wax paper and immerse under fixatives. Dice tissue into small pieces (less than 3 mm). Place cut tissue into a labeled vial containing fresh 4% formaldehyde and 2% glutaraldehyde in 0.1 M cacodylate buffer (see Note 4). Let stand in the fixative at room temperature (RT) for at least 2 h with occasional agitation. At this point, the tissue may be stored overnight or for several days at 4°C.

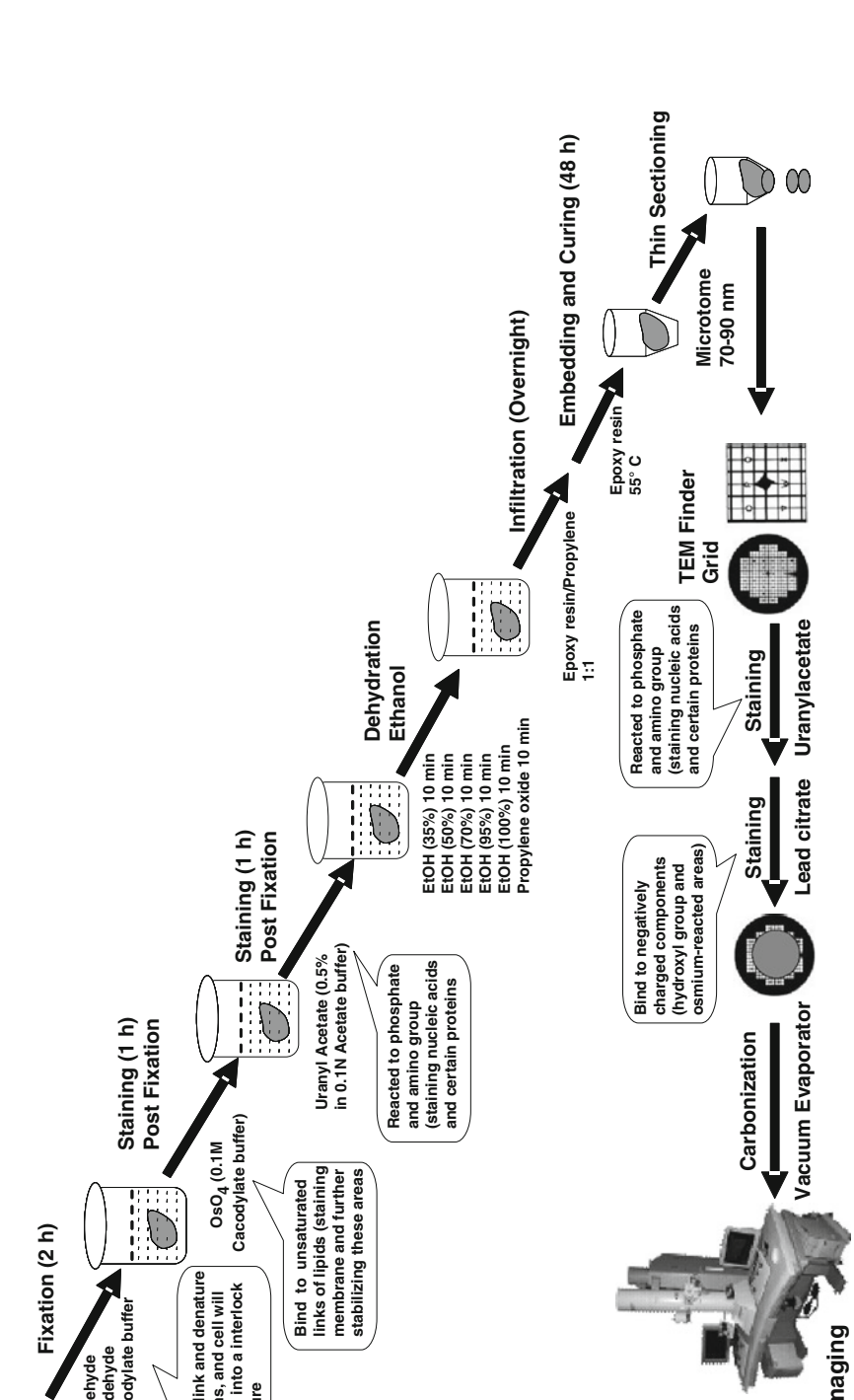

Fig. 1. Schematic illustration of TEM tissue sample preparation procedure. The tissue specimens were fixed in TEM fixative (formaldehyde and glutaraldehyde), postfixed in osmium tetroxide and uranyl acetate, dehydrated, infiltrated and embedded in an epoxy resin, sliced into 70–90 nm thin sections, and finally stained with uranyl acetate and lead citrate.

3. Wash tissue with three changes of 0.1 M cacodylate buffer at room temperature for 10 min for each wash (see Note 4).
4. Postfix and *en bloc* stain tissues by replacing the buffer with 1% OsO_4 in 0.1 M cacodylate. Cover the vial to protect the samples from exposure to light and allow standing for 1 h.
5. Rinse tissue specimen with two changes of 0.1 M cacodylate buffer for 10 min each and then with cold sodium (0.1 N) acetate buffer.
6. Stain *en bloc* with 0.5% uranyl acetate in 0.1 N acetate buffer for 1 h. While staining, cover the samples to protect them from light.
7. Rinse tissue specimen in two changes of acetate buffer for 10 min each.
8. Dehydrate stepwise in the following concentrations of ethanol, 10 min/change at room temperature: two changes in 36, 50, 70, 95 and three changes in 100% (see Note 5).
9. Rinse tissue with three changes of 100% propylene oxide for 10 min each at room temperature (see Note 6).
10. Infiltrate tissue specimen in 50/50 mixture (1:1 epoxy resin and propylene oxide mixture) overnight on a rotor in a chemical fume hood at room temperature (see Note 7).
11. Mix epoxy resin in the following proportions: Epoxy resin (4.9 g), DDSA (2.8 g), NMA (2.3 g), and then add DMP-30 (0.14 mL) (see Note 8).
12. Embed tissue in plastic capsules (i.e., BEEM capsule) and cure the resin in an oven (55°C) for 48 h.
13. Cured blocks are trimmed and sections with a thickness from 70 to 90 nm are cut using an ultramicrotome mounted with a diamond knife. The thickness of the section can be estimated by examining the interference color of the floating sections using a light microscope and a color scale reference sheet.
14. The thin sections afloat in a diamond knife boat are transferred onto copper mesh grids.
15. The grids are stained in 0.5% uranyl acetate in glass distilled water for 2 min. The excess stain is then washed off with five changes of glass distilled water for 2 min each. The grids are then secondarily stained with lead citrate for 90 s and the five washes with distilled water are repeated.
16. The thin sections on the grids are stabilized by carbon evaporation in a vacuum evaporator.
17. The grids are ready to be examined and imaged in the TEM (see Note 9).

3.2. Cell Culture Sample Preparation

Two methods are outlined here, for *in situ* and cell pellet fixation and embedding. The *in situ* method is suitable for those cells that need to be examined with minimal physical manipulations (e.g., scraping and centrifuge), while the pellet method is used for non-adherent cells (e.g., lymphoid, yeast, and bacteria cells).

3.2.1. In Situ Method

1. Grow cells in the cell culture plates.
2. Rinse cells for 1 min with serum-free media at the incubation temperature.
3. Pipette off the serum-free media.
4. Immediately add 2% glutaraldehyde in 0.1 M cacodylate buffer from the edge of the dish (see Note 3) at room temperature. Allow samples stand in the fixative at room temperature for at least 1 h. At this point, the samples may be stored overnight or for days at 4°C.
5. Wash samples with three changes of 0.1 M cacodylate buffer at room temperature for 10 min each (see Note 4).
6. Postfix sample by adding 1% OsO_4 in 0.1 M cacodylate to the wells. Cover the plate to protect samples from exposure to light and allow standing for 1 h.
7. Rinse samples with two changes of 0.1 M cacodylate buffer followed by one change of 0.1 N cold acetate buffer for 10 min/change.
8. Stain *en bloc* with 0.5% uranyl acetate in 0.1 N acetate buffer for 1 h. While staining, cover the samples to protect them from light.
9. Rinse samples in two changes of acetate buffer for 10 min each.
10. Dehydrate samples stepwise in the following concentrations of ethanol, 10 min/change at room temperature: two changes in 36, 50, 70, 95 and three changes in 100% (see Note 5).
11. Mix epoxy resin (see Note 8) in the following proportions: Epoxy resin (4.9 g), DDSA (2.8 g), NMA (2.3 g), and then add DMP-30 (0.14 mL).
12. Add epoxy resin to wells and incubate samples in a 55°C oven for 10 min. Then, remove the old resin and replace it with fresh. Repeat this "heat-and-replace" step three times.
13. Add a final amount of resin and incubate in the 55°C oven for 48 h.
14. Cured blocks are separated from the plate and examined with the inverted phase-contrast microscope to locate areas of good cell distribution.
15. Selected areas are cut from the resin block and glued to a blank block.

16. Samples are sliced into 70–90 nm thin sections using an ultramicrotome mounted with a diamond knife. The thickness of the section can be estimated from the interference color of the floating sections using a light microscope and a color scale reference sheet.
17. The thin sections afloat in a diamond knife boat are transferred onto copper mesh grids.
18. The grids are stained with 0.5% uranyl acetate in glass distilled water and lead citrate.
19. The thin sections on the grids are stabilized by carbon evaporation in a vacuum evaporator.
20. The grids are ready to be examined and imaged in the TEM.

3.2.2. Pellet Method

1. Grow cells in the 6-well cell culture plates.
2. Decant or aspirate culture medium.
3. Add 1-mL PBS (room temperature) and scrape cells with a disposable scraper.
4. Transfer the samples into a polypropylene microtube (1.5 mL).
5. Centrifuge samples at 100 × g or 1,000 rpm for 5 min.
6. Decant or aspirate PBS and gently add the EM fixative containing fresh 2% glutaraldehyde in 0.1 M cacodylate buffer (see Note 3). Let stand in the fixative at room temperature for at least 2 h with occasional agitation. At this point, the samples may be stored overnight or for days at 4°C.
7. Follow steps 5–17 in Subheading 3.1.

4. Notes

1. Use EM-grade reagents with appropriate buffer osmolarity (physiologic osmolarity is approximately 320 mmoles). Certain fixative buffers are toxic, volatile lung irritants and may be carcinogenic. Exercise care when handling these buffers; avoid breathing fumes or contact with skin. Handle these reagents in a well-ventilated chemical fume hood.
2. Always wear appropriate personal protective equipment, and take appropriate precautions when handling your tissue and cell culture specimen. Many occupational health and safety practitioners recommend wearing two layers of gloves when handling nanomaterials. Also, be sure to follow your facility's recommended disposal procedure for your specific biological samples and nanomaterial.

3. It is important to use fresh EM-grade aldehyde (formaldehyde and glutaraldehyde) for primary fixation. Use within 4 weeks of opening the formaldehyde ampoule.
4. After glutaraldehyde and formaldehyde fixation, a thorough wash with cacodylate buffer is required. We recommend three 10 min washes. Otherwise, the residual glutaraldehyde may generate a "peppery" background, upon combination with osmium tetroxide.
5. Dehydration is a step in which the water within the tissue is gradually replaced by ethanol. It is important to keep absolute ethanol (100%) tightly sealed.
6. Propylene oxide cannot be used for dehydration of cell cultures on polystyrene or polycarbonate plastic cell culture plates. Propylene oxide will dissolve many types of culture dishes and plastic test tubes. Polypropylene or glass containers are safe to use. Some resins will also interact adversely with cell culture plates.
7. Longer processing times are recommended for specimens with high connective tissue content such as skin, tendon, plant tissue, etc. The processing times should be increased for all steps and especially for the infiltration of the 50/50 epoxy resin and propylene oxide mixture in step 10 of Subheading 3.1. Failure to use longer time periods may cause an inhomogeneous and uneven resin infiltration, resulting in a poor TEM image.
8. The complete resin mixture for embedding should be freshly prepared for each embedding rather than stored as a mixture in a freezer for more than several days. After combining the components and stirring for 30 min, the mixture is maintained at room temperature for the embedding.
9. The modern EM is computer-controlled to improve image quality and for high throughput. Multisample holders by Gatan enable one to load many samples simultaneously, which are then automatically inserted one by one into the TEM. There are also various technological improvements to allow one to examine predefined areas, capture images, archive the image, and move on to another field of view.

Acknowledgment

This project has been funded in whole or in part by federal funds from the National Cancer Institute, National Institutes of Health, under contract N01-CO-12400. The content of this publication does not necessarily reflect the views or policies of the Department

of Health and Human Services, nor does the mention of trade names, commercial products, or organizations imply endorsement by the US Government.

References

1. Hayat, M.A. (1970) *Principles and techniques of electron microscopy*. Van Nostrand Reinhold Company, New York.
2. Bozzola, J.J. and Russell, L.D. (1999) *Electron microscopy: Principles and techniques for biologists*. Jones and Bartlett Publishers, New York.

Chapter 9

SEM X-Ray Microanalysis of Nanoparticles Present in Tissue or Cultured Cell Thin Sections

Jiwen Zheng, Kunio Nagashima, David Parmiter, Jason de la Cruz, and Anil K. Patri

Abstract

Energy Dispersive X-ray (EDX) microanalysis is a technique used for identification of the elemental composition of a specimen. The detection of nanoparticles in tissue is a common problem of biodistribution and toxicity studies. High-resolution transmission electron microscopy (TEM) can be employed to detect nanoparticles based on morphology; however, TEM alone cannot conclusively identify nanoparticles. Indeed, micrographs are often ambiguous due to particle aggregation, contamination, or morphology change after cellular uptake. EDX can be used to confirm the composition and distribution of the nanoparticles through spectrum and elemental mapping.

This protocol outlines the procedures for compositional identification of nanoparticles using an EDX spectrometer incorporated into a scanning electron microscopy (SEM) system. This protocol outlines sample preparation, EDX spectrum acquisition, elemental peak analysis and spectral mapping acquisition.

Key words: Nanoparticles, electron microscopy, energy dispersive X-ray spectroscopy (EDX)

1. Introduction

Energy Dispersive X-ray (EDX) microanalysis is a technique used for identification of the elemental composition of a specimen. During EDX analysis, a specimen is bombarded with an electron beam inside a scanning electron microscope. The bombarding electrons collide with the electrons of the specimen and displace them from their energy levels. A position vacated by an ejected inner shell electron is eventually occupied by a higher-energy electron from an outer shell. The electron transfer is accompanied by the release of energy through X-ray emission. The amount of energy released by the transferring electron depends on the energies of the initial and final shells. Atoms of each element release

Scott E. McNeil (ed.), *Characterization of Nanoparticles Intended for Drug Delivery*, Methods in Molecular Biology, vol. 697,
DOI 10.1007/978-1-60327-198-1_9,

X-rays with unique amounts of energy during the transfer process. The "fingerprint" energies of the emitted X-rays can then be used to identify an element (see Figs. 1 and 2). Also, EDX microanalysis is capable of generating a map of one or more chemical elements of interest. This map is obtained by running the acquisition of X-ray spectra in scanning mode and letting the

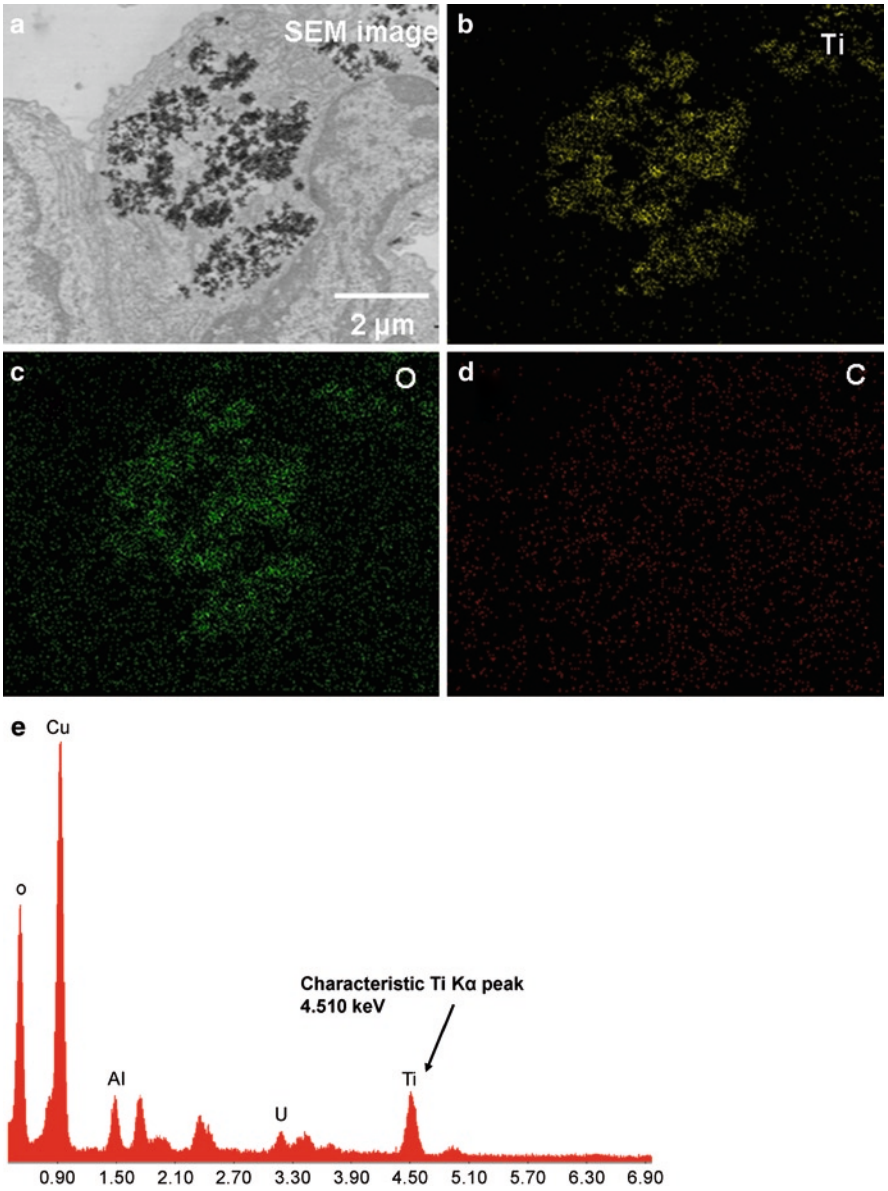

Fig. 1. SEM image (**a**) of a rodent lung thin-section containing TiO_2 particles and element X-ray spectral mapping of titanium (**b**) oxygen (**c**) and carbon (**d**) and the 2D spectrum (**e**) at the same survey area. The *yellow* in panel (**b**) represents titanium, the *green* in panel (**c**) represents oxygen and the *red* in panel (**d**) represents carbon. The *black* and *white* SEM image in panel (**a**) shows what are presumably TiO_2 particles (*black* grains in the center of image) accumulating in the lung thin-section. The characteristic titanium peak at 4.510 keV, indicated by the *arrow* in panel (**e**) confirms the presence of titanium. The X-ray mappings of titanium and oxygen (**b**, **c**) confirm that the particles in (**a**) are TiO_2 particles. [AU1]

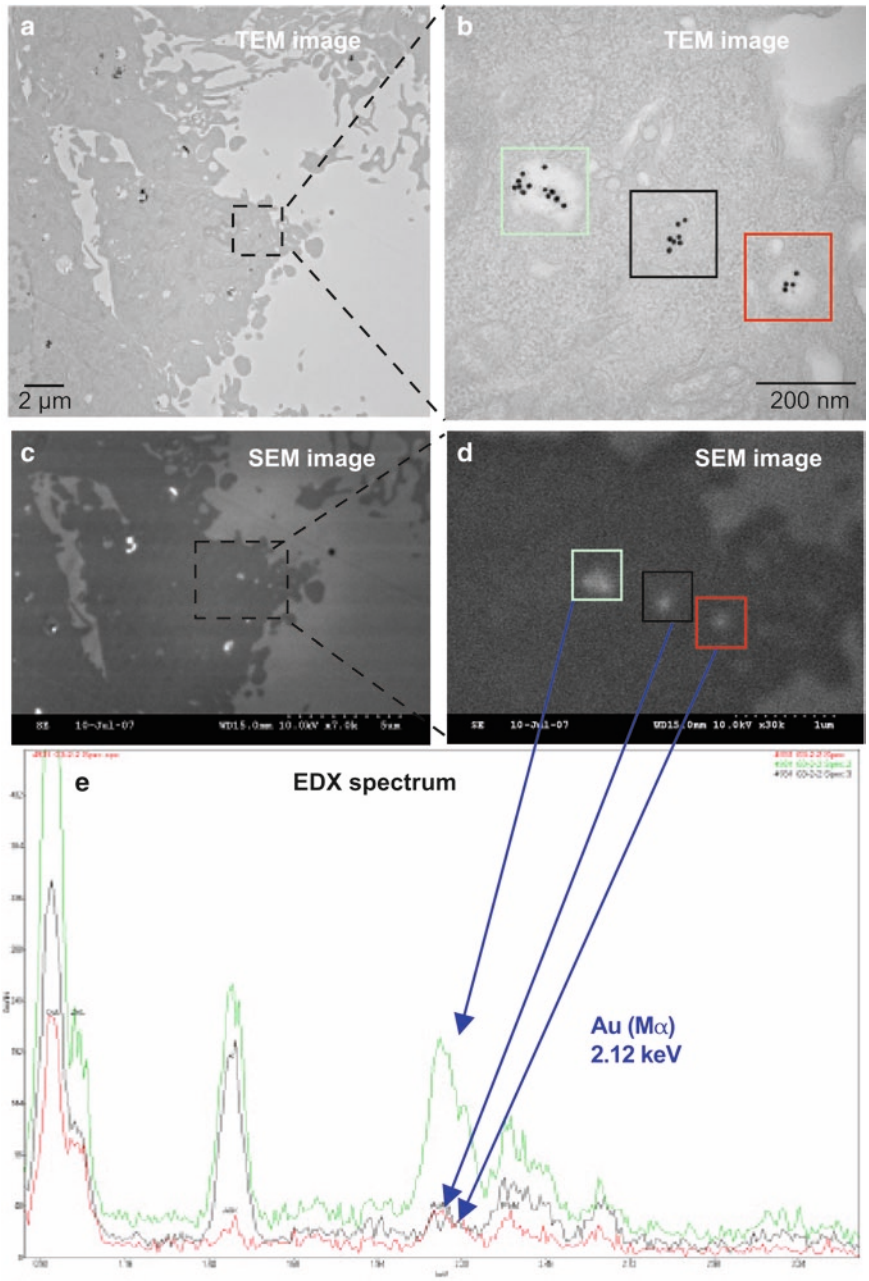

Fig. 2. TEM images (**a**, **b**), SEM images (**c**, **d**) and EDX spectra of gold nanoparticle uptake by macrophages. Panel (**a**) TEM image and (**c**) SEM image show the same region of cell culture where gold nanoparticles were taken up by macrophage cells. Panel (**b**) and (**d**) are higher magnification images of Panel (**a**) and (**c**), respectively. Panel (**e**) shows the spectra overlay confirming that the particles located in the selected areas (indicated in *green*, *black*, and *blue*) all contain gold.

software determine the concentration of the element of interest at each point while imaging. The color can be coded in order to indicate the absolute or relative concentration of the element of interest, thus giving a 2D image of the abundance of a particular element. This map can be combined with transmission electron

microscopy (TEM) or scanning electron microscopy (SEM) micrographs of the specimen in order to get information about the relative distribution of complementary or correlating elements. The spatial resolution of the elemental mapping is dependent upon various factors, including the accelerating voltage, beam concentration, detector limits, take-off angle, and noise-to-signal ratio.

It is very important to develop a standardized technique that is capable of detecting the presence and distribution of nanoparticles in tissue to confirm such properties as targeting and specificity. High-resolution TEM can be employed to detect nanoparticles based on their morphology. The identification of these nanoparticles, however, may still remain ambiguous due to the possible aggregation, contamination or morphology change after cellular uptake. So EDX can be used to confirm the composition and distribution of the nanoparticles through spectrum analysis and elemental mapping.

2. Materials

1. Epoxy-embedded analyte nanoparticle-exposed tissue or cell culture sample thin section (70–90 nm) prepared for EM analysis (see Chapter 8 of this volume).
2. Electron microscope (e.g., Hitachi SEM) equipped with Energy dispersive X-ray spectrometer (EDAX, compact detector unit (CDU)).
3. TEM grids (EMS).
4. Precision EM-grade tweezers.
5. STEM holder (EMS).

3. Methods

3.1. EDX Spectral Data Collection and Mapping Acquisition

1. Add liquid nitrogen to the EDX spectrometer dewar.
2. Load TEM grid (thin section on the TEM grid) to the STEM holder and place the holder on the EM stage.
3. Set the microscope to imaging.
4. Select the most appropriate voltage that yields the best peak-to-background ratios while minimizing beam damage to the tissue under study. Note that for thin specimens, higher energy generally produces less damage.
5. Set the beam current to the desired intensity. The smaller the current, the smaller the spot size, and the lower the noise it will generate. It is recommended to adjust the current based on magnification. Follow the user manual for your specific

SEM scope (for a Hitachi S3000 SEM, >90kx = 10, 50kx = 25, 25kx = 40, 10kx = <50, 5kx = <65, <5kx = up to 85).

6. Survey the specimen and select areas of interest (see Note 3).
7. Set the objective aperture to maximize sample exposure but minimize beam damage. (For Hatachi S3000, it does not require aperture in at magnification of 5×-1000×. Magnification of 1000×–2000× needs aperture 1 (0.15 μm), 2000×–4000× needs aperture 2 (0.08 μm), 4000×–8000× needs aperture 3 (0.05 μm) and >8000× magnification needs aperture 4 (0.03 μm)).
8. Optimize the detector-specimen geometry, by adjusting the detector-to-specimen distance (take care not to approach the specimen holder too closely), and by adjusting the specimen tilt angle. Make sure that X-ray path from specimen to the detector is not obstructed by the edge of the STEM holder or the grid bar. The optimum working distance depends upon the model of SEM and EDX detector, and where the detector is inserted into the SEM chamber. It is recommended to use working distance of 15.0 mm for Hitachi S3000.
9. Try to keep the measured X-ray count rates at about 800–1,000 counts per second (CPS) by adjusting the beam current. Though high beam current improves the count rate, it can cause organic mass loss from the specimen and specimen instability (an important factor for quantitative X-ray mapping with total acquisition times of several hours).
10. Adjust the dead time to 20–40%, and check the shape of the spectrum. Reduce excessive extraneous continuum X-ray signals and stray signals.
11. Acquire spectral data for at least 30 s for nanoparticles. The higher your CPS, the lower the time required to obtain good data.
12. Select the elements of interest and collect a map for at least 150 frames. Instruction for acquiring elemental maps is software-specific and usually straightforward. Elemental mapping is typically a time consuming procedure. For better mapping resolution, the optimum collection time is several hours or overnight with drift correction on.

3.2. Spectral Data Analysis

1. During or after spectrum collection, peak identification can be automatically carried out with the software provided by the EDX spectrometer manufacturer and does not generally present special problems. Some software provide a holographic peak deconvolution (HPD) function, which is a theoretical spectrum based on the peak identification list and spectrum parameters that are overlaid on the spectrum for comparison. This can make peak identification much simpler. For automatic peak identification, the longer the spectrum has been collected, the more accurate the identification will be. Keep in mind that only peaks that are significant, where

the counts in the peak (P) are more than three times the standard deviation of the counts in the background (B) under the peak, should be identified. It should also be noted that before a peak can be identified as a minor peak for an element (e.g., a $K\beta$ peak), the major peak for this element (i.e., the $K\alpha$ peak) should also be present in the spectrum. If a peak is identified as an L or M peak for a particular element, the corresponding K or L peaks should also be present.

2. In principle, for those samples which are smooth and flat, infinitely thick to the electron beam and homogenous within the interaction volume, the quantitative analysis will be accurate and simple. A standard that matches the types of samples to be analyzed should be tested after spectrum collection. The comparison with a standard of known composition is carried out, and a correction is made for the difference in atomic number (Z) factor, absorption (A) factor, and secondary fluorescence (F) factor between the specimen and standard. The ZAF correction was developed for metallurgical specimens, but is less well-developed for biological specimens. It can be difficult to quantitate element concentrations in a thin section (70–90 nm in thickness) specimen supported by a TEM grid since the electron beam excites the substrate (grid bar). However, an alternative P/B ratio method has been developed for thick biological specimens. Please refer to ref. (2) for the details of P/B ratio method.

4. Notes

1. Always wear appropriate personal protective equipment and take appropriate precautions when handling your nanomaterial. Many occupational health and safety practitioners recommend wearing two layers of gloves when handling nanomaterials. Also, be sure to follow your facility's recommended disposal procedure for your specific nanomaterial.
2. Tissue or cell culture thin sections prepared for TEM characterization can be directly used for SEM–EDX analysis. A scanning transmission electron microscopy (STEM) mode adaptor is needed to acquire TEM-like images and locate potential nanoparticles in tissue or cell culture. The EDX signal from the area near the edge of the adaptor may be blocked by the adaptor. It is recommended that the sample be rotated to improve the signal/noise ratio.
3. It is important to ensure that the chemical regents used to process the tissue or cell culture samples do not interfere with the elemental composition of the nanoparticles under study and that there is good separation between EDX peaks from these reagents and the nanoparticles. For example,

osmium tetroxide, uranyl acetate, and lead citrate are often used for secondary fixative and staining to help highlight subcellular structures during TEM tissue sample processing. However, the X-ray energy peak of Os (Mα 1.910 keV) and Pb (Mα 2.342 keV) fall in an area of the EDX spectrum which is adjacent to some elements of interest, for example, gold (Mα 2.120 keV). This can make it difficult to identify gold nanoparticles in tissue samples treated with osmium or lead.

Acknowledgment

This project has been funded in whole or in part with federal funds from the National Cancer Institute, National Institutes of Health, under contract N01-CO-12400. The content of this publication does not necessarily reflect the views or policies of the Department of Health and Human Services, nor does mention of trade names, commercial products, or organizations imply endorsement by the U.S. Government.

References

1. Hayat, M.A. (1970) *Principles and techniques of electron microscopy*. Van Nostrand Reinhold Company, New York, NY.
2. Bozzola, J.J. and Russell, L.D. (1999) *Electron microscopy, Principles and techniques for biologists*. Jones and Bartlett Publishers, New York, NY.
3. Goldstein, J., Newbury, D.E., Joy, D.C., Lyman, C.E., Echlin, P., Lifshin, E., Sawyer, L.C., Michael, J.R. (2003) *Scanning electron microscopy and X-ray microanalysis, 3rd Edition*, Springer Science+Business Media, New York, NY.
4. Roomans, G.M. (1981) Quantitative electron probe X-ray microanalysis of biological bulk specimens. *Scanning Electron Microscopy*. **2**, 344–356.

Chapter 10

Detecting and Measuring Free Gadolinium in Nanoparticles for MRI Imaging

Jeffrey D. Clogston and Anil K. Patri

Abstract

This chapter describes a method for the measurement of free gadolinium in nanoparticle samples. Conjugation of a gadolinium-chelate to a nanoparticle allows the particle's distribution to be imaged via magnetic resonance imaging (MRI). Free (unchelated) gadolinium is a known toxin, being a heavy metal, and may contribute towards total gadolinium concentration. Determining the amount of free gadolinium is therefore an important aspect of the preclinical characterization of gadolinium-chelate MRI imaging agent nanoparticles.

Key words: gadolinium, chelate, magnetic resonance imaging (MRI), Arsenazo, contrast agents

1. Introduction

This chapter describes a method for measuring free gadolinium in nanoparticle samples. Gadolinium-chelates are often used as magnetic resonance imaging (MRI) contrast agents and are frequently incorporated into nanoparticle formulations so that the distribution of the nanoparticle can be imaged using MRI. There is always the possibility that unchelated ("free") gadolinium may be present in the suspending solution of such nanomaterial, due to instability of chelate, poor synthesis or inefficient purification procedures. Free gadolinium is a known toxicant. For this reason, it is important to be able to quantitate any free gadolinium present in gadolinium-chelate containing nanoparticle formulations.

Arsenazo III binds to metal ions forming an Arsenazo–metal ion complex which can be quantified colorimetrically. It does not bind to complexed metal ions (1). The method described here utilizes colorimetry as an alternative to the more elaborate, accurate, sensitive, and expensive hyphenated techniques (LC coupled) with inductively coupled plasma-mass spectrometry

Scott E. McNeil (ed.), *Characterization of Nanoparticles Intended for Drug Delivery*, Methods in Molecular Biology, vol. 697,
DOI 10.1007/978-1-60327-198-1_10,

(ICP-MS) or inductively coupled plasma optical emission spectroscopy (ICP-OES). As this is a colorimetric assay, samples should be transparent so as not to interfere with detection of the gadolinium. However, a procedure employing dialysis is presented to extend the general applicability of this protocol to all nanoparticles regardless of their transparency. This procedure can be used to detect free soluble gadolinium in turbid and colored (interfering) nanoparticle samples. One limitation of this method is that it does not account for non-chelated insoluble Gd species/precipitates.

2. Materials

1. Ultraviolet–visible (UV–Vis) Spectrometer.
2. Disposable polystyrene cuvettes.
3. Mini dialysis unit with a 3.5 kDa molecular weight cut off (MWCO) membrane (e.g., Pierce, Slide-A-Lyzer, 3500 MWCO).
4. 1.8 mL cryo-vials.
5. Gadolinium (III) chloride hexahydrate ($GdCl_3 \cdot 6H_2O$).
6. Arsenazo III reagent is prepared by making an approximately 0.2 mM solution in water. For example, 78.25 mg of Arsenazo (molecular weight 776.37 g/mol, Sigma cat no. A92775) is dissolved in a 500-mL volumetric flask filled with Milli-Q water. Store at 4°C.
7. Analyte nanoparticle sample (see Notes 1 and 2).

3. Methods

3.1. Calibration Curve

A calibration curve is constructed to determine the concentration of free gadolinium. Gadolinium (III) chloride hexahydrate can be used as a source of free gadolinium and is recommended. Standards of gadolinium (III) chloride hexahydrate are prepared in water at several concentrations (typically 7) spanning 0–50 μg/mL Gd^{3+}. Note that the concentration range is based on Gd^{3+} and not gadolinium (III) chloride hexahydrate:

1. An approximately 20 mg/mL gadolinium (III) chloride hexahydrate stock is prepared. For example, a 21.8 mg/mL is prepared by weighing 21.8 mg and adding 1 mL Milli-Q water.
2. The stock solution (~20 mg/mL) is diluted ten-fold with Milli-Q water to give the ~2 mg/mL *dilution stock*. For example, 100 μL stock (here 21.8 mg/mL) and 900 μL Milli-Q water are mixed in a 2-mL centrifuge tube, yielding a *dilution stock* concentration of 2.18 mg/mL. This is used as the stock for all dilutions.

Table 1
Calibration standard preparation from an approximately 2 mg/mL dilution stock

No.	Volume dilution stock (μL)	Volume Milli-Q water (μL)	Total volume (μL)	[$GdCl_3 \cdot 6H_2O$] (μg/mL)	[Gd^{3+}] (μg/mL)
1	0	1,000	1,000	0	0
2	2	998	1,000	5.5	2.3
3	5	995	1,000	10.9	4.6
4	10	990	1,000	21.8	9.2
5	20	980	1,000	43.6	18.4
6	30	970	1,000	65.4	27.7
7	40	960	1,000	87.2	36.9
8	50	950	1,000	109.1	46.1

3. Calibration standards are prepared by diluting the *dilution stock* with Milli-Q water according to the Table 1. Note Gd^{3+} was calculated by multiplying the gadolinium (III) chloride hexahydrate concentration by the ratio (0.423) of gadolinium's molecular weight (157.25 g/mol) to the molecular weight of gadolinium (III) chloride hexahydrate (371.7 g/mol).
4. Measurement samples are prepared by mixing 100 μL 0.2 mM Arsenazo III, 50 μL calibration standard, and 850 μL water. In addition, a "Blank" is prepared by mixing 100 μL 0.2 mM Arsenazo III and 900 μL water.
5. The UV–Vis spectra (see Fig. 1a) are recorded for the "Blank" and measurement samples with water as the reference cell (for double-beam instruments). Absorbance values at 652 nm are noted.
6. To correct for background absorbance due to Arsenazo III, the absorbance at 652 nm for the "Blank" is subtracted from each standard absorbance reading.
7. A Beer's Law plot is constructed by plotting the absorbance at 652 nm versus Gd^{3+} concentration. A linear fit is performed which passes through the origin, with the slope being the extinction coefficient (see Fig. 1b).

3.2. Measurement Procedure

The presence and the amount of free gadolinium are quantified by using Arsenazo III. The procedure is first described for transparent nanoparticles; an additional step is necessary when dealing with turbid or colored nanoparticles (see Note 3).

For transparent or noninterfering nanoparticles:

1. Free gadolinium in the nanoparticle solution is determined by mixing 100 μL 0.2 mM Arsenazo III, 50 μL nanoparticle

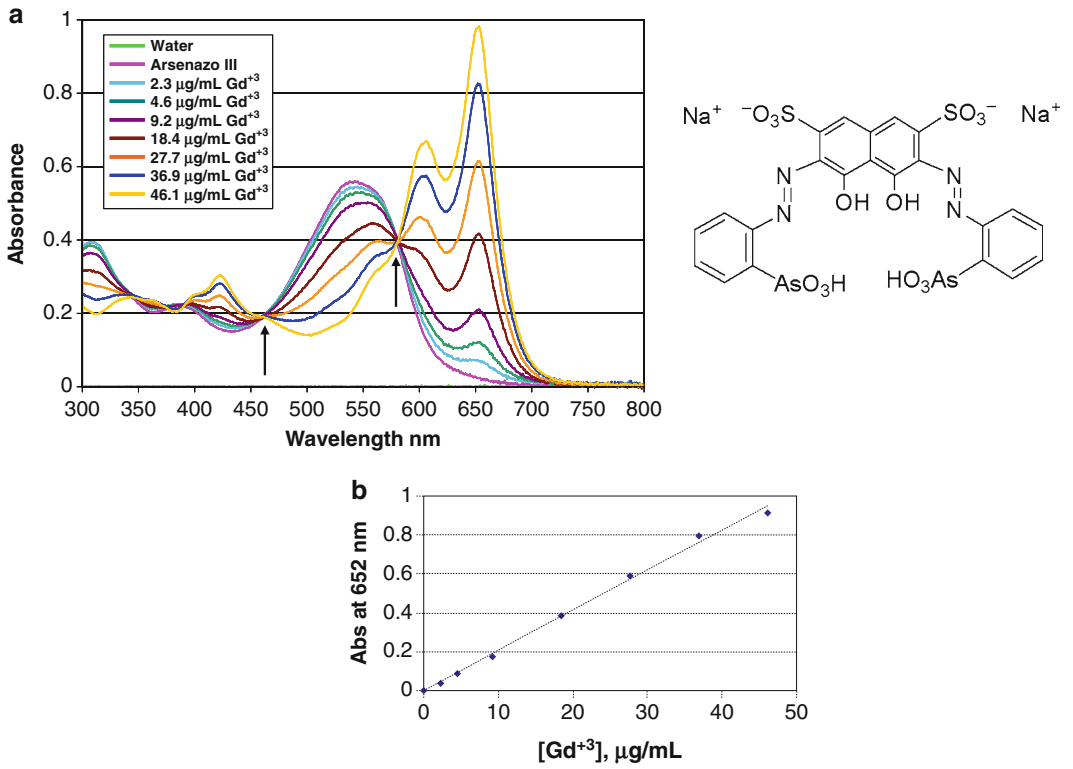

Fig. 1. Determination of free gadolinium using Arsenazo III assay. The UV–Vis spectra for each calibration standard (100 µL 0.2 mM Arsenazo III, 50 µL standard, and 850 µL water) is shown in (**a**). The isosbestic points have been labeled with *arrows*. A Beer's Law plot is constructed at 652 nm (**b**) and used to determine the extinction coefficient. The chemical structure of Arsenazo is shown to the *right* of the graph.

sample, and 850 µL water and recording its UV–Vis spectra at room temperature. Absorbance at 652 nm is noted.

2. The Beer's Law plot is used to determine the gadolinium concentration using the nanoparticle's absorbance at 652 nm (absorbance/extinction coefficient).

For turbid, nontransparent or interfering nanoparticles:

Nanoparticles that absorb at 652 nm will interfere with the colorimetric assay. Some examples of such nanoparticles include oil-in-water emulsions, liposomes, and metal-containing colloids (i.e., gold). As the sample will interfere with the assay, it cannot be added directly with Arsenazo III. To get around this, an additional step prior to gadolinium determination is performed (see Note 4).

3. Samples are dialyzed against water and assayed for free gadolinium. Briefly, 100 µL of sample ("Source" in Fig. 2) was dispensed into a mini dialysis unit and placed into a cryo-vial filled with 1.8 mL water ("Sink" in Fig. 2). A stirring bar is placed in the cryo-vial to effect mixing.
4. The contents in the cryo-vial were stirred with a magnetic bar placed on a stir plate at room temperature.

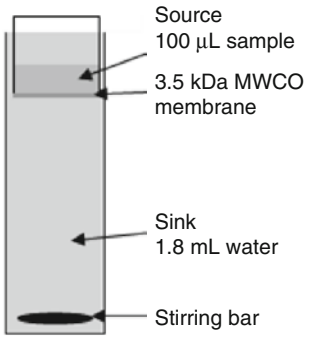

Fig. 2. Dialysis setup for the determination of free gadolinium for nontransparent or interfering nanoparticles. Sample (100 μL) is placed in a mini dialysis unit (3.5 kDa MWCO) and dialyzed against water with constant stirring at room temperature. The water is replaced daily and measured for free gadolinium as outlined in the text.

5. The water ("Sink") is collected and replaced daily with fresh water.
6. Free gadolinium concentration is determined for each daily "Sink" content as described in step 1 for "Transparent or noninterfering Nanoparticles." A "Blank" (i.e., Arsenazo only sample, see Subheading 3.2, step 4) absorbance at 652 nm is subtracted from the sample's absorbance and the Beer's Law plot is used to determine the free gadolinium concentration.
7. Dialysis continued until free gadolinium was no longer detected in the sink (typically 3 days).
8. Total free gadolinium is determined by summing each daily measurement.

3.3. Data Analysis

1. The determination of free gadolinium relies on the calibration curve. A Beer's Law plot is constructed by plotting the absorbance at 652 nm versus known (standards) gadolinium concentrations (i.e., gadolinium (III) chloride hexahydrate). The "Blank" Arsenazo (in essence, 0 μg/mL Gd^{3+}) should be subtracted from each standard. The slope of the line, forced through the origin, is the extinction coefficient and is used to convert unknown sample's absorbance to free gadolinium concentration. Sample "blanks" should also be prepared, measured, and their absorbance subtracted from the sample. The total amount of free gadolinium in the sample is calculated by using the calibration curve to determine its concentration, and then multiplied by the sample volume (see Note 5).
2. In the case of interfering nanoparticles, dialysis is performed. The free gadolinium concentration in the sink volume is determined as described above. The amount of free gadolinium is calculated by multiplying its concentration by the sink volume.

The total free gadolinium is determined by summing the amount of free gadolinium from each daily measurement until free gadolinium is no longer detected (see Note 6).

4. Notes

1. Always wear appropriate personal protective equipment and take appropriate precautions when handling your nanomaterial. Many occupational health and safety practitioners recommend wearing two layers of gloves when handling nanomaterials. Also, be sure to follow your facility's recommended disposal procedure for your specific nanomaterial.
2. The protocol describes a method for the determination of free gadolinium in nanoparticle solutions. The nanoparticles analyzed fall into two categories, noninterfering and interfering. As a general rule of thumb, if the sample is turbid it is likely to interfere with a colorimetric assay. Take a UV–Vis measurement of your nanoparticle to double-check if your sample absorbs at 652 nm to determine if it will interfere with the Arsenazo assay.
3. In terms of running calibration standards, it is important to first measure the Arsenazo blank not only to correct for its background absorbance, but to also run a nanoparticle/sample blank. This would correspond to mixing 50 μL sample and 950 μL water. The purpose of this blank is to see if your sample contributes to the absorbance at 652 nm, and is very important when your sample interferes with the assay. Of course, dialysis should prevent any nanoparticles from diffusing into the sink contents, but should be performed to ensure that any possible impurities in your sample do not interfere with the assay. To further check the Arsenazo assay, it is highly recommended to scan from 300 to 800 nm as opposed to recording a single wavelength (652 nm). Once standardized, a single wavelength reading in a multiwell plate reader would simplify the measurement and increase throughput. This is important because one can check to see if the assay is working properly by looking at two isosbestic points. The isosbestic point is the wavelength where two species (complexed and uncomplexed Arsenazo) have the same extinction coefficient ($\varepsilon = 0$). Arsenazo has two isosbestic points, at 462 and 581 nm (see Fig. 1a), therefore all samples whether standards, blanks or nanoparticle samples should pass through this point. This can be used as a diagnostic for the assay.
4. The protocol described for interfering nanoparticles makes use of dialysis. The sample is dialyzed against water using a

mini dialysis unit with a 3.5 kDa MWCO membrane. The mini dialysis unit should be capped and sealed to prevent solvent evaporation. Constant stirring should be performed to ensure there is no buildup of diffusing species at the membrane interface which would otherwise hinder free diffusion. Samples were dialyzed against water, but can be dialyzed against any buffer to provide ionic strength to screen any charge–charge interactions. Finally, a 3.5 kDa MWCO membrane was used. Higher MWCO membranes can be used to speed up dialysis but must still retain the nanoparticle.

5. A final note on the Arsenazo assay and its detection limit is noteworthy. The lowest measured standard in the calibration curve represents the assay's detection limit, which in this protocol was 2 μg/mL. Thus if the sample contains less than this amount, it will not be detected. The upper limit is, based on the calibration curve, is ~50 μg/mL. Samples with gadolinium concentrations exceeding this concentration should be diluted accordingly to fall within the calibration curve range. Remember to take this dilution into account when calculating the gadolinium concentration for that sample.
6. In the case of dialysis, consideration should be made when deciding the sample volume and concentration. Based on the sample's total loading of gadolinium, the minimum percent of free gadolinium that is detectable can be calculated based on the sink volume and the detection limit (i.e., (sink volume × detection limit)/total gadolinium loaded). To increase the concentration of free gadolinium detected in the sink, the sink volume or frequency of measurements can be reduced. Both will allow the free gadolinium in the sink to increase (less sink volume equates to higher concentration; replenishing the sink volume less allows free gadolinium to accumulate). Alternatively, the dialysis setup can be scaled up to allow for more sample volume and hence higher total gadolinium.

Acknowledgment

This project has been funded in whole or in part with federal funds from the National Cancer Institute, National Institutes of Health, under contract N01-CO-12400. The content of this publication does not necessarily reflect the views or policies of the Department of Health and Human Services, nor does mention of trade names, commercial products, or organizations imply endorsement by the U.S. Government.

Reference

1. Gouin, S. and Winnik, F.M. (2001) Quantitative Assays of the Amount of Diethylenetriaminepentaacetic Acid Conjugated to Water-Soluble Polymers Using Isothermal Titration Calorimetry and Colorimetry. *Bioconjug. Chem.* **12**, 372–377.

Chapter 11

Lipid Component Quantitation by Thin Layer Chromatography

Jeffrey D. Clogston and Anil K. Patri

Abstract

This chapter describes a thin layer chromatography (TLC) method for the quantitation of various lipids (such as phospholipids, sphingolipids, acylglycerols, and fatty acids) in lipid-based nanoparticle formulations such as liposomes and nanoemulsions. We illustrate this technique to quantify C6-ceramide (*N*-hexanoyl-d-erythro-sphingosine) in a nanoemulsion formulation. C6-ceramide is a powerful chemotherapeutic that is poorly soluble in aqueous buffers.

Key words: TLC, lipids, nanoemulsions, liposomes, ceramide

1. Introduction

This chapter presents a protocol for lipid component quantitation in lipid-based nanoparticle formulations such as liposomes and nanoemulsions utilizing thin layer chromatography (TLC). TLC provides a quick and inexpensive technique for the separation and identification of components in a mixture of lipids. TLC is usually cheaper and faster than high-pressure liquid chromatography (HPLC) or gas chromatography (GC)/mass spectrometry (MS) for the same purpose (1). As TLC is a chromatographic technique, it consists of a stationary phase, a thin layer of adsorbent (typically silica) coated on a glass support/plate, and a mobile phase, typically consisting of two or more organic solvents. Samples are spotted near the bottom of the TLC plate (designated as the "origin") which is then placed in a developing chamber containing a shallow layer of solvent. The solvent (the mobile phase) moves up the TLC plate due to capillary action. The components of the sample migrate up the TLC plate according to their strength of interaction

Scott E. McNeil (ed.), *Characterization of Nanoparticles Intended for Drug Delivery*, Methods in Molecular Biology, vol. 697,
DOI 10.1007/978-1-60327-198-1_11,

with the mobile and stationary phases. Once the solvent has reached the top of the plate (referred to as the "solvent front"), the plate is removed from the developing chamber and allowed to dry. The spots (i.e., the separated components of the sample) are then visualized by oxidation and thermal charring. Quantitation is then performed by image analysis of the charred sample in comparison to calibration standards.

This method is illustrated for determining the amount of C6-ceramide present in a nanoemulsion formulation. However, this method can be applied to quantitate other lipid components. Different solvent systems may need to be tested as well as different visualization techniques (fluorescent reagents and nonspecific stains) for optimized separation and detection of other lipid components. In addition, standards of the component of interest will be needed for quantitation purposes.

2. Materials

1. Lyophilizer.
2. Uniplates silica gel G 250 μm 5 × 20 cm.
3. Wiretrol disposable micropipettes 1–5 μL and plunger.
4. Hot plate (>200°C).
5. Cylindrical developing TLC tank for 5 × 10 cm and 4 × 8 cm TLC plates.
6. Polypropylene TLC spray stand.
7. Sprayer (nebulizer) 10 mL w/screw cap.
8. Wire rack for TLC plates.
9. TLC glass cutter.
10. 1.8 mL Cryo-vials.
11. 2 mL Glass vials with caps (use amber glass if working with light-sensitive lipids).
12. Image manipulation/quantitation software [similar capabilities to, e.g., ImageJ software (http://rsb.info.nih.gov/ij/)].
13. 4.2 M H_2SO_4.
14. Chloroform.
15. Methanol.
16. Isopropanol.
17. Analyte lipid-based nanoparticle sample (see Note 1) and lipid component standard (e.g., a known amount of purified lipid; a variety of these can be purchased from Avanti Polar Lipids, Inc., Alabaster, AL, USA).

3. Methods

3.1. Sample Preparation

Sample preparation for TLC involves dissolving the sample in an organic solvent, typically chloroform. As all lipid-based formulations contain some amount of water, samples must be lyophilized to remove water (water is nonvolatile and will remain at the origin after spotting). The removal of water also disrupts the integrity of the nanoparticle and allows for separation of the individual components as well as quantitation on a mass basis (i.e., %weight of the component per total dry weight of the sample).

3.1.1. Preparation of Nanoparticle Sample

1. Weigh an empty cryo-vial.
2. Aliquot 100 μL of nanoemulsion sample into preweighed cryo-vial.
3. Freeze sample by submerging into an isopropanol (IPA)/dry ice slurry.
4. Once frozen, lyophilize sample overnight to remove water.
5. Weigh the lyophilized sample the next day and subtract the empty cryo-vial weight (step 1) from this to give the sample amount.
6. Dissolve the lyophilized sample with an appropriate amount of chloroform to give a sample concentration of 50 μg/μL. Once dissolved, transfer to an amber glass vial and cap and seal with parafilm until ready for use. Store samples at 4°C to minimize solvent evaporation.

3.1.2. Preparation of Calibration Standards

1. Tare an empty glass vial (use amber glass if working with light-sensitive lipids).
2. Weigh accurately a minimum of 2 mg lipid standard.
3. Dissolve the lipid standard with an appropriate amount of chloroform to give a sample concentration of 0.5 μg/μL. Cap and seal the glass vial with parafilm and store at 4°C to minimize solvent evaporation.

3.1.3. Preparation of Rinsing and Solvent Systems

1. *Rinsing solvent*: Prepare a 10:1 (by volume) chloroform/MeOH (methanol) solution in a glass jar. Briefly, combine 100 mL chloroform and 10 mL MeOH using a graduated cylinder. Store in a solvent cabinet until ready to use.
2. *Solvent system*: The solvent depends on the lipid component under investigation. Some typical solvent systems include: chloroform/methanol (10:1 by volume), chloroform/acetone (94:4), chloroform/acetone/methanol/acetic acid (73.5:25:1:0.5), and hexane/toluene/acetic acid (70:30:1) by volume. The volume

ratios determine the polarity of the solvent system and can be adjusted depending on the separation required for a particular lipid component being quantified. For example, for C6-ceramide, we prepared a 50:3 (by volume) chloroform/IPA (isopropyl alcohol) solution in a glass jar. Briefly, combine 100 mL chloroform and 6 mL IPA using a graduated cylinder. Store in a solvent cabinet until ready to use.

3.1.4. Preparation of TLC Plates

TLC plates should be rinsed with the rinsing solvent (chloroform/MeOH) before running samples to remove any impurities on the plates which will affect the background to sample contrast. Note, steps 2 and 3 described below should be performed in a hood, and gloves should be worn when handling the TLC plates to prevent contamination (see Note 2).

1. The TLC plates used are 5 × 20 cm in dimensions. For the specified developing chambers, these plates are too long. Place the TLC plate silica side down on a kimwipe. Measure the midpoint of the TLC plate (10 cm) with a ruler. Using the straight edge of the ruler, score the glass using the TLC glass cutter. Gently snap the TLC plate into two. This will yield two 5 × 10 cm plates.
2. Prerinse the developing chamber by pouring the rinsing solvent (chloroform/MeOH) into the chamber to give a solvent height of ~1 cm. Seal the developing chamber with the appropriate lid and swirl the rinsing solvent within the developing chamber. Discard the rinsing solvent. Repeat two times.
3. To the prerinsed developing chamber, add enough rinsing solvent to give a solvent height of 0.5 cm. Place the TLC plate slightly at an angle in the developing chamber (silica side facing toward the top of the chamber) and seal. The rinsing solvent will move up the TLC plate due to capillary action (see Fig. 1). Allow the rinsing solvent to migrate up to about

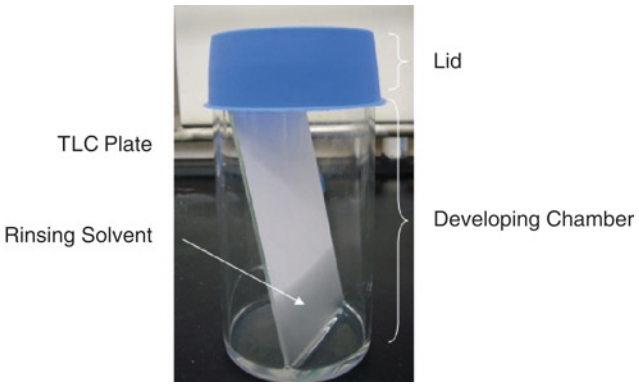

Fig. 1. Photograph of TLC plate in developing chamber. Note the rinsing solvent height and the angle of the TLC plate. The silica side is facing toward the *top* of the chamber.

0.5 cm below the top of the plate. Remove the lid and quickly place the TLC plate on the wire rack, silica side up. Allow the TLC plate to air dry (rinsing solvent is volatile) before repeating this step again. Keep the prerinsed TLC plates on the wire rack (silica side up) in the hood until ready to use. Discard the rinsing solvent.

3.2. Measurement Procedure

The measurement procedure, namely, the volume spotted and the sample and standard concentrations, is based on prior knowledge of the amount of component (C6-ceramide in this case) that should theoretically be present. The amounts spotted for the sample and the calibration standards may need to be changed depending on the actual amount.

1. Prerinse the developing chamber by pouring the solvent system (chloroform/IPA in this case) into the chamber to give a solvent height of ~1 cm. Seal the developing chamber with the appropriate lid and swirl the rinsing solvent within the developing chamber. Discard the solvent. Repeat twice.
2. To the prerinsed developing chamber, add enough solvent system to give a solvent height of 0.5 cm. Seal the developing chamber with the appropriate lid.
3. Mark on the prerinsed TLC plate a line 1 cm from the bottom of the TLC plate. This represents the origin, or where the samples will be spotted.
4. Along the origin line, four samples will be spotted using the disposable micropipettes. The lane order should be as follows: lipid component, lipid component, nanoformulation, lipid component at corresponding spotting volumes of 1, 2, 3, and 3 μL, respectively. When spotting, care should be taken to avoid touching the silica gel with the micropipettes or plunger. If spotting more than 1 μL, it is advisable not to dispense the complete sample at once, but rather dispense slowly (i.e., 0.5 μL) and then apply air gently to evaporate the chloroform before continuing spotting the remainder of the sample (this will keep the sample in one tight spot rather than have a large diffuse spot). Care should be taken to spot in the same location. The four samples should be spotted evenly across the origin line (see Note 3).
5. After the samples are spotted, the TLC plate is placed slightly at an angle (bottom of plate flush with the developing chamber bottom) in the developing chamber (silica side facing toward the top of the chamber) and sealed. Allow the solvent to migrate up to about 0.5 cm below the top of the plate (30–45 min for our setup). Remove the lid and quickly place the TLC plate on the wire rack, silica side up. Allow the TLC plate to air dry (solvent is volatile).

6. This next step involves spraying 4.2 M sulfuric acid (H_2SO_4). This step is done in the hood, wearing protective equipment. The sprayer is filled with sulfuric acid and connected to an air source. With one hand, hold the TLC plate (silica gel facing you) near the bottom (origin side) and with the other hand, operate the sprayer. A gentle mist is needed; reduce the air flow and increase the distance from the TLC plate to sprayer if necessary if the spray is too strong. Do not drench the plate with sulfuric acid.
7. Place the TLC plate on the hot plate and turn the hot plate on and to the setting which gives a temperature of ≥200°C. Thermal charring is complete when the spots can be visualized (black spots) and no more fumes are produced from the heating of the plate. An example of TLC plate after these steps is shown in Fig. 3 (see Note 4).

3.3. Data Analysis

Lipid component quantitation is based on image analysis. A picture of the TLC plate can be taken with a camera or with a scanner. It is recommended to run the sample and the calibration standards on the same plate to reduce the error in image acquisition. Once a ".tif" file of the TLC plate is obtained, open it using ImageJ (free software, v1.37). Invert the picture by selecting the "Edit" menu and then select "Invert." Using the "line" tool (on toolbar), draw a line across the spot of interest. Select "Analyze" followed by "Plot Profile" to obtain the intensity versus position plot. Copy the list and import it into suitable peak-fitting software. Fit the peak using an appropriate baseline and peak function (Gaussian) to obtain the intensity of that spot. Repeat for the remaining spots on the plate.

Once the spot intensities are obtained, construct a calibration curve by plotting the lipid component spot intensity versus amount spotted [i.e., concentration (0.5 μg/μL in this case) times volume spotted (1, 2, and 3 μL)]. Linear regression is performed using these three points to give a slope and *y*-intercept. Figure 2 shows the calibration curve based on the TLC plate shown in Fig. 3. Use the slope and *y*-intercept values to convert the sample spot intensity to lipid component amount [i.e., (spot intensity – *y*-intercept)/slope]. Make sure the sample spot intensity falls within the three calibration standards (see Note 5). The %weight of lipid component present in the sample is then calculated by dividing the weight of lipid component by the total weight spotted.

4. Notes

1. Always wear appropriate personal protective equipment and take appropriate precautions when handling your nanomaterial. Many occupational health and safety practitioners recommend

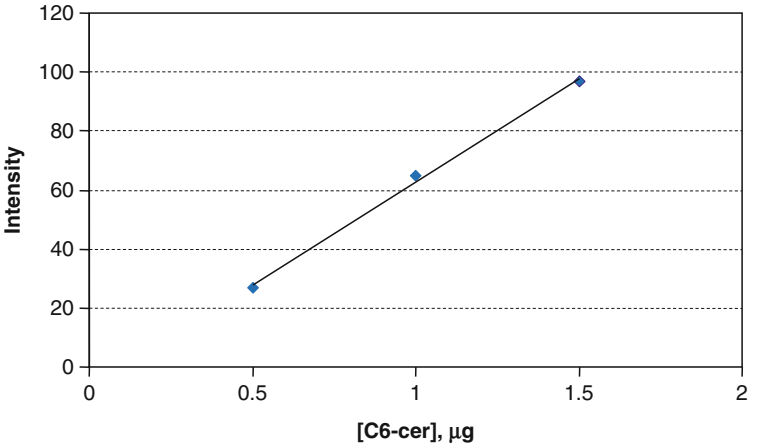

Fig. 2. Calibration curve for C6-ceramide based on the TLC results. *Spot intensities* were obtained using ImageJ software.

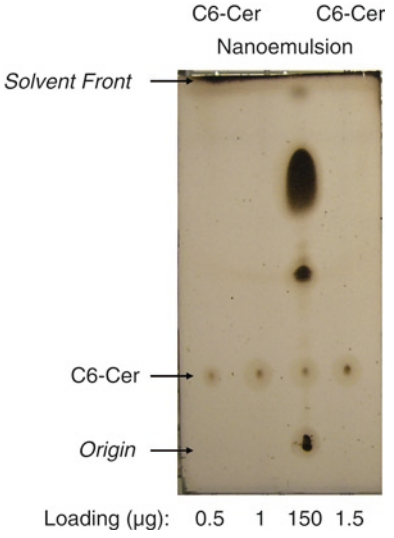

Fig. 3. Representative TLC plate after charring. The origin, solvent front, and loading per lane are labeled.

wearing two layers of gloves when handling nanomaterials. Also, be sure to follow your facility's recommended disposal procedure for your specific nanomaterial.

2. In general, gloves should be worn when handling TLC plates. Grease on your skin will show up when running TLC. Care should be taken to not touch or disturb the silica gel. Extra protective gear is recommended when spraying the TLC plates with sulfuric acid. TLC should be performed in a hood with adequate ventilation, especially during the charring process.
3. Spotting of sample should give a small tight spot. When spotting several microliters of sample, do so in small volume

increments and dry with air stream between each increment to reduce spreading.

4. Several TLC troubleshooting tips are given below:
   (a) Observation of a streak rather than a spot implies that the sample loading is too high. It can also mean that the solvent system is not adequate for the separation desired, or your sample contains highly polar (strongly acidic or basic) groups. The polarity of the solvent system should be adjusted accordingly.
   (b) If the solvent front runs at an angle, it implies that the TLC plate was not placed uniformly flat at the bottom of the developing chamber. This will result in incorrect migration rates for each of the lanes. The same result occurs if the sides of the TLC plate are not flat and uniform. In this case, the sides of the TLC plates should be trimmed to produce a uniform straight edge.
   (c) If the sample appears U-shaped, it implies that the silica gel was disturbed. Rerun with a fresh plate.
   (d) Too many spots observed on the plate implies contamination. Perform TLC in the hood to reduce any debris or accidental chemical contamination and wear gloves to prevent oil contamination from your skin.
   (e) If no spots are observed, make sure the concentration is high enough and that the solvent level in the developing chamber is not higher than the origin (sample will dissolve into the solvent rather than migrate up the TLC plate).
   (f) The vapor pressure of the developing solvent has to be maintained. For this purpose, equilibrate the sealed developing chamber several minutes before running samples. Alternatively, placing a strip of filter paper (with the same dimensions of the TLC plate) parallel to the TLC plate and shaking the solvent gently will achieve this.
5. This protocol outlines lipid component quantitation in a nanoemulsion formulation based on prior knowledge of its loading. After running TLC, check first to see that the spot for the lipid component standard (here, C6-ceramide was purchased from Avanti Polar Lipids, Inc., Alabaster, AL) comigrates with a spot in your sample. Second, check by visual inspection that the spot intensity for the lipid component in your sample falls between the low (1 μL) and high (3 μL) lipid component calibration standard spot intensities. If the sample spot intensity is lower, increase the sample loading (more volume spotted). If it is higher, then increase the calibration standard loading (more volume spotted).

Acknowledgments

This project has been funded in whole or in part with federal funds from the National Cancer Institute, National Institutes of Health, under contract N01-CO-12400. The content of this publication does not necessarily reflect the views or policies of the Department of Health and Human Services, nor does mention of trade names, commercial products, or organizations imply endorsement by the US Government.

Reference

1. Hamilton, R.J. and Hamilton, S. (1992) *Lipid Analysis: A Practical Approach*, Oxford University Press, Oxford, UK.

Part III

Assays for Sterility

Chapter 12

Detection and Quantitative Evaluation of Endotoxin Contamination in Nanoparticle Formulations by LAL-Based Assays

Barry W. Neun and Marina A. Dobrovolskaia

Abstract

Bacterial endotoxin or lipopolysaccharide (LPS) is a membrane component of all Gram-negative bacteria. The administration of products contaminated with bacterial endotoxin can cause fever, shock, and even death. Accordingly, the FDA sets limits on the number of endotoxin units (EU) that may be present in a drug or device product. Limulus amoebocyte lysate (LAL) is the extract from amoebocytes of the horseshoe crab *Limulus polyphemus*, which reacts with bacterial endotoxin. Detection of the products of this reaction is an effective means of quantifying the EU present in a drug formulation. However, nanoparticles frequently interfere with the reactivity of endotoxin, the LAL reaction, or the detection of the reaction products. This interference can be manifested as either an enhancement or an inhibition, causing a respective overestimation or underestimation of the EU in the sample. Here, we present two methods for the detection and quantification of endotoxin in nanoparticle preparations: one is based on an end-point chromogenic LAL assay, and the second approach is based on measuring the turbidity of the LAL extract.

Key words: endotoxin, lipopolysaccharide, Limulus amoebocyte lysate (LAL)

1. Introduction

The intravenous administration of a product containing endotoxin can cause a wide variety of physiological reactions, including endotoxin shock, fever, and even death. Endotoxins are potent inducers of inflammatory responses (1–3). When exposed to endotoxin, cells of the immune system (such as monocytes and macrophages) release mediators [such as tumor necrosis factor (TNF), interleukins, prostaglandins, platelet-activating factor] and produce free radicals. These mediators then cause the physiological effects associated with endotoxin exposure. Overwhelming

Scott E. McNeil (ed.), *Characterization of Nanoparticles Intended for Drug Delivery*, Methods in Molecular Biology, vol. 697,
DOI 10.1007/978-1-60327-198-1_12,

immune responses initiated by high concentration of endotoxins may lead to a systemic condition known as septic shock (4, 5).

Limulus amoebocyte lysate (LAL), a derivative of the blood of the horseshoe crab, *Limulus polyphemus*, clots when exposed to endotoxin. Minute amounts of endotoxin cause LAL to initially become turbid, and larger amounts eventually result in gelation. The tendency of LAL to form a gel clot in the presence of endotoxin has a long history in pharmaceutical and clinical fields for detection and rough quantification of bacterial endotoxin (6). The turbidity test presented here is considered to be more sensitive than the traditional gel-clot test. LAL clotting enzyme has also been shown to cleave certain synthetic amino acids that are carriers of a chromogenic *p*-nitroanilide group, and the color generated by this reaction is proportional to the quantity of endotoxin in the sample. The amount of endotoxin can, therefore, be measured through measurement of the yellow-colored product of this cleavage reaction (released *p*-nitroaniline), which has maximum absorbance at 405 nm. This principle is utilized in the endpoint chromogenic assay described in this chapter.

The turbidity test presented here makes direct use of the turbidity of the LAL reaction mixture after exposure to endotoxin. The turbidity is proportional to the amount of endotoxin present and can be measured against the turbidity in samples containing a known amount of endotoxin standard. In a kinetic turbidimetric assay, turbidity of a test sample is monitored continuously until a point in time when it reaches that of a standard curve.

Nanoparticles frequently interfere with the reactivity of endotoxin, the LAL reaction, or the colorimetric detection of the reaction products. For example, nanoparticles with absorbance at or close to 405 nm (e.g., some derivatized fullerenes), will most likely interfere with the chromogenic format of the LAL assay. Nanoparticle formulations with intrinsically high optical density (e.g., nanoliposomes and nanoemulsions) interfere with turbidity LAL assays. These interferences can manifest as enhancements, causing a respective overestimation of the endotoxin units in the sample. Alternatively, the presence of detergents in nanoparticle formulations may cause inhibition of the enzymatic reaction and thus result in endotoxin underestimation. Many non-nano products also interfere with the LAL reaction, and the 1987 US FDA guideline document, "Validation of the LAL test as an end-product endotoxin test for human and animal parenteral drugs, biological products, and medical devices" (7), has established criteria for a variety of parameters involved in chromogenic assays for endotoxin detection (including the range of tested concentrations, the linearity of the standard curve, and criteria for inhibition and enhancement controls). Assays described herein comply with the FDA's criteria, and Subheading 4 of this chapter outlines the specific measures that should be taken for nanoparticle samples.

2. Materials

2.1. Chromogenic End-Point Assay

1. Analyte nanoparticle sample (NS; see Notes 1 and 2) reconstituted in either pyrogen-free water or sterile pyrogen-free PBS to a final concentration of 1.0 mg/mL (requires approximately 1.0 mg of nanomaterial).
2. *p*-nitroanilide solution.
3. Plate reader capable of detecting absorbance at 405 nm.
4. Disposable endotoxin-free glass dilution tubes (13 mm × 100 mm).
5. Sterile 96-well plates.
6. Sodium hydroxide solution (0.1 N) made from dilution into pyrogen-free water.
7. Hydrochloric acid solution (0.1 N) made from dilution into pyrogen-free water.
8. Endotoxin stock solution made from *Escherichia coli* lipopolysaccharide (LPS) (see Note 3). This should be a United States Pharmacopeial Convention, Inc. (USP)-certified reference standard endotoxin (RSE).
9. LAL reagent: LAL reagent is supplied as lyophilized powder. Contents of each vial should be reconstituted per manufacturer's recommendations.
10. LAL reaction stop solution prepared as 25% volume/volume glacial acetic acid or 10% sodium dodecyl sulfate (SDS) in water.
11. Preparation of four calibration standard samples is shown in Table 1.
12. Preparation of one quality control sample is shown in Table 2.
13. Preparation of two inhibition/enhancement controls is shown in Table 3.

2.2. Kinetic Turbidity Assay

1. Sodium hydroxide solution (0.1 N) made from dilution into pyrogen-free water.
2. Hydrochloric acid solution (0.1 N) made from dilution into pyrogen-free water.
3. Endotoxin stock solution made from *E. coli* LPS (see Note 3). This should be a United States Pharmacopeial Convention, Inc. (USP)-certified RSE.
4. Pyrogen-free water.
5. Spectrophotometer capable of similar sensitivity of e.g., ACC's PyrosKinetix Instrument.

Table 1
Calibration samples for chromogenic assay

Calibration samples for chromogenic assay	Nominal concentration (EU/mL)	Preparation procedure
Cal 1	1.0	100 µL of stock + (*X*–1)/10 mL of pyrogen-free water[a]
Cal 2	0.50	500 µL of Cal 1 + 500 µL of pyrogen-free water
Cal 3	0.25	500 µL of Cal 2 + 500 µL of pyrogen-free water
Cal 4	0.10	100 µL of Cal 1 + 900 µL of pyrogen-free water

[a]*X* is concentration of the stock, e.g., if stock concentration is 23 EU/mL, then 100 µL of this stock should be diluted with 2.2 mL [(23–1)/10] of pyrogen-free water

Table 2
Quality control samples for chromogenic assay

Quality controls for chromogenic assay	Nominal concentration (EU/mL)	Preparation procedure
Int A[a]	1.0	10 µL of stock + (*X*–1)/100 mL of pyrogen-free water
QC1	0.4	100 µL of Cal 1 + 150 µL of pyrogen-free water

[a]Intermediate solution A is prepared to make QC1 and is not used further in the assay

Table 3
Inhibition enhancement control samples for chromogenic assay

IEC controls for chromogenic assay	Nominal concentration (EU/mL)	Preparation procedure
Int B[a]	1.0	10 µL of stock + (*X*–1)/100 mL of NS[b]
IEC	0.4	100 µL of Int B + 150 µL of NS[b]

[a]Intermediate solution B is prepared only to make IEC and is not used further in the assay
[b]*X* is the concentration of the stock, e.g., if stock concentration is 23 EU/mL, then 10 µL of this stock should be diluted with 0.22 mL [(23–1)/100] of NP solution/suspension (NS in the table)

6. LAL reagent: LAL reagent is supplied as a lyophilized powder. Contents of each vial should be reconstituted per manufacturer's recommendations.
7. Preparation of four calibration samples is shown in Table 4.
8. Preparation of one quality control sample is shown in Table 5.

Table 4
Calibration samples for turbidity assay

Calibration standards for turbidity assay	Nominal concentration (EU/mL)	Preparation procedure
Int C[a]	160[a]	100 µL of stock + 900 µL of pyrogen-free water[b]
Int D[a]	16[a]	100 µL of Int A + 900 µL of pyrogen-free water[b]
Cal 1	1.0	100 µL of Int B + 1500 µL of pyrogen-free water[b]
Cal 2	0.1	100 µL of Cal 1 + 900 µL of pyrogen-free reagent water
Cal 3	0.01	100 µL of Cal 2 + 900 µL of pyrogen-free water
Cal 4	0.001	100 µL of Cal 3 + 900 µL of pyrogen-free water

Numbers shown in the table above are calculated based on stock concentration of 1,600 EU/mL
[a] Intermediate solutions C and D are prepared to make the calibration samples and are not used further in the assay
[b] This is an example dilution of the RSE to make the first calibration standard, and intermediate solutions depend on the concentration of RSE stock

Table 5
Quality control samples for turbidity assay

Quality controls for turbidity assay	Nominal concentration (EU/mL)	Preparation procedure
Int A[a]	1.0	10 µL of stock + (X–1)/100 mL of pyrogen-free water
QC1	0.05	50 µL of Cal 1 + 950 µL of pyrogen-free water

[a] Intermediate solution A is prepared to make QC1 and is not used further in the assay

Table 6
Inhibition enhancement control samples for turbidity assay

Inhibition enhancement controls for turbidity assay	Nominal concentration (EU/mL)	Preparation procedure
IEC	0.05	25 µL of Cal 1 + 475 µL of NS

9. Preparation of one inhibition/enhancement controls is shown in Table 6.

3. Methods

3.1. End-Point Chromogenic Assay

1. Prepare calibration standard and quality control samples, inhibition/enhancement controls, and analyte nanomaterial sample (study sample) as described above.
2. Create a run template for the plate reader.
3. Carefully dispense 50 µL of pyrogen-free water blanks (four wells), calibration standards (two wells/each), controls (two wells/each), and unknown samples (two wells/each) into the appropriate wells of the microplate, prewarmed to 37°C.
4. Using a multichannel pipette, add 50 µL of LAL reagent to all wells containing blanks, calibration standards, controls, and unknown samples.
5. Incubate for 10 min at 37°C.
6. Add 100 µL of prewarmed *p*-nitroanilide solution to each well.
7. Incubate at a temperature of 37°C for another 6 min.
8. Using a multichannel pipette, add 100 µL of the LAL reaction stop solution to the samples in the microplate, and read and record absorbance at 405 nm.
9. Create a calibration curve from a linear regression algorithm to the absorbance of the calibration samples.
10. Calculate the endotoxin units (EU) contained in each well from their absorbance extrapolated to the calibration curve.
11. Calculate the percent coefficient of variation (%CV) and percent difference from theoretical (PDFT) of the calculated endotoxin concentrations from each calibration standard and quality control sample. %CV is the percentage of the mean of the standard deviation (SD) or $\%CV = 100 \times SD/\overline{EU}$ and $PDFT = 100 \times \left(\frac{\overline{EU} - EU_{theory}}{EU_{theory}} \right)$. Both the %CV and PDFT for

each well should be within 25%. If the values for the %CV and PDFT of the quality control sample are not within this range, all samples must be reprepared and the plate reread. The %CV and PDFT of at least three calibration standards should be within 25%, for the assay to be considered acceptable (8, 9).

12. Fit the calculated EU values from the eight wells containing calibration standards to a line, using a least-squares linear regression. The fitted line is your standard curve. The correlation coefficient of the standard curve must be at least 0.980, or else the assay should be repeated.
13. Precision of the nanoparticle sample should be within 25% (8, 9).
14. Precision and accuracy of inhibition/enhancement control should be within 25% if no endotoxin is detected in the nanoparticle sample and within 50% if endotoxin is detected in the nanoparticle sample (8, 9). If the accuracy of the inhibition/enhancement controls is outside of the range specified above, then the nanoparticles are interfering with the assay. If nanoparticle interference is detected, then analysis of diluted sample should be performed. Dilution of the nanoparticle sample should not exceed maximum valid dilution (MVD, see below).
15. If the maximum human (or rabbit) dose is not available for a nanoparticle formulation, the MVD can be calculated according to the following formula (8, 9):

$$\mathrm{MVD} = \frac{\mathrm{EU}_{\mathrm{lim}} \times [\mathrm{NS}]}{\mathrm{Sensitivity}}$$

where $\mathrm{EU}_{\mathrm{lim}}$ is the allowable limit of endotoxin in a product, [NS] is the concentration of the nanoparticle sample, and *Sensitivity* is the assay sensitivity (i.e., the assay's lower limit of detection). For example, if the nanoparticle concentration is 1 mg/mL and if assay sensitivity is 0.1 EU/mL, in this device (devices have allowable endotoxin limits of 0.5 EU/mL), then using this method, the MVD is 5 (0.5 EU/mL × 1.0 mg/mL/0.1 EU/mL).

16. Guideline acceptance criteria (8, 9) are shown in Table 7 (see Notes 4 and 5).

3.2. Kinetic Turbidity Assay

1. Create new experiment template for the plate reader.
2. Add 100 µL of negative control (water), calibration standards, quality control, IEC, and test nanoparticles into prelabeled glass tubes. Prepare duplicate tubes for each sample.
3. Using repeater pipette, add 100 µL of LAL reagent to the first test vial, vortex it briefly, and insert it into the test slot in the instrument carousel. Repeat this procedure for other

Table 7
FDA guidelines for endotoxin levels for drugs and devices

Devices not in contact with CSF	0.5 EU/mL
Devices in contact with CSF	0.06 EU/mL
Parenteral drugs not administered intrathecally	K/M, i.e., 5.0 EU/kg/maximum human (rabbit) dose/kg administered in a single 1-h period
Parenteral drugs administered intrathecally	K/M, i.e., 0.2 EU/kg/maximum human dose/kg administered in a single 1-h period

Nanoparticle formulations should be treated as devices for acceptance/rejection, unless data for K/M formula are available

samples, processing one sample at a time. Allow the instrument to run each point for no less than 2 h, to allow for samples with low amounts of endotoxin to develop. If no detectable endotoxin is present in the sample, the software will mark this sample as "not detected by 7,200 s" (see Notes 4 and 5).

4. Notes

1. Always wear appropriate personal protective equipment and take appropriate precautions when handling your nanomaterial. Many occupational health and safety practitioners recommend wearing two layers of gloves when handling nanomaterials. Also, be sure to follow your facility's recommended disposal procedure for your specific nanomaterial.
2. The pH of the analyte nanoparticle sample (study sample) should be checked using a pH meter microelectrode and adjusted if necessary with sterile NaOH or HCl to within 6.0–8.0 (assuming the suspension/solution has some buffering capacity). To avoid sample contamination from the microelectrode, always collect a small aliquot of the sample and use it to measure the pH.
3. For example, United States Pharmacopeial Convention, Inc. (USP)-certified RSE is supplied as part of LAL test kits (such as QCL-100 LAL test kit from Lonza, Basel, Switzerland or equivalent) as a lyophilized powder. The contents of the vial containing RSE should be reconstituted with 1.0 mL of pyrogen-free LAL reagent water to a final concentration of 15–40 EU/mL. The specific concentration is determined by

the value stated on the enclosed certificate of quality, which accompanies each RSE. During reconstitution and prior to use, the stock solution should be vortexed vigorously and allowed to equilibrate to room temperature. If RSE from other sources is used, follow supplier's instructions for reconstitution.

4. Catalytic nanoparticles, such as dendrimers, may cause false positives with the LAL test if they activate the LAL proteolytic cascade and generate a colorimetric product. Other nanoparticles may quench absorbance at the assay wavelength or adsorb endotoxin on their surfaces (e.g., gold colloids), leading to a false-negative pyrogenicity determination in this LAL assay. In our experience, most nanoparticles have the potential to interfere with the LAL assay, and only a few particle types do not interfere with this standard test (unpublished data).
5. When IEC control indicates particle interference with the assay, the test should be repeated with a diluted sample. As the sensitivity of this method is very high, the MVD appropriate for this test is 1:500. IEC control should be repeated for the diluted sample as well. One milliliter (1 mL) of the sample at each dilution is required. NCL standard practice includes analysis of the sample at three dilutions: 1:5, 1:50, and 1:500.

Acknowledgments

This project has been funded in whole or in part by federal funds from the National Cancer Institute, National Institutes of Health, under contract N01-CO-12400. The content of this publication does not necessarily reflect the views or policies of the Department of Health and Human Services, nor does the mention of trade names, commercial products, or organizations imply endorsement by the US Government.

References

1. Uribe, R.M., Lee, S., and Rivier, C. (1999) Endotoxin stimulates nitric oxide production in the paraventricular nucleaos of hypothalamus through nitric oxide synthase: correlation with hypothalamic-pituitary-adrenal axis activation. *Endocrinology* **140**(12), 5971–5981.
2. Chan, E. and Murphy, J.T. (2003) Reactive oxygen species mediate endotoxin-induced human dermal endothelial NF-kB activation. *J. Surg. Res.* **111**, 120–126.
3. Henricson, B.E., Benjamin, W.R., and Vogel, S.N. (1990) Differential cytokine induction by doses of lipopolysaccharide and monophosphoryl lipid A that result in equivalent early endotoxin tolerance. *Infect. Immun.* **58**(8), 2429–2437.
4. Ilkka, L. and Takala, J. (1996) Plasma endotoxin levels in the early phase of septic shock. *J. Intensive Care Med.* **22**, 1–9.
5. Shapira, L., Soskolne, W.A., Houri, Y., Barak, V., Halabi, A., and Stabholz, A. (1996) Protection

against endotoxic shock and lipopolysaccharide induced local inflammation by tetracycline: correlation with inhibition of cytokine secretion. *Infect. Immun.* **64**(3), 825–828.

6. Roth, R.I. and Levin, J. (1992) Purification of Limulus polyphemus proclotting enzyme. *J. Biol. Chem.* **267**, 24097–24102.
7. FDA (1987) Guideline on validation of the Limulus Amebocyte Lysate test as an end-product endotoxin test for human and animal parenteral drugs, biological products, and medical devices. December 1987.
8. http://www.iccvam.niehs.nih.gov/methods/pyrogen/pyrogen.htm
9. USP-NF (2007) Bacterial Endotoxins Test, volume 1. United States Pharmacopeia, Rockville, pp. 109–113.

Chapter 13

Analysis of Microbial Contamination in Nanoparticle Formulations

Timothy M. Potter and Marina A. Dobrovolskaia

Abstract

This chapter describes a procedure for quantitative determination of microbial contamination of a nanoparticle formulation. The protocol includes tests for yeast, mold, and bacteria using Millipore sampler devices. This approach is primarily intended to avoid contamination of cell cultures and transmitting potential microbial contaminants to animals in preclinical studies of efficacy, biodistribution, and toxicity. Other methods common to microbiology will likely work equally well.

Key words: Nanoparticles, contamination, bacteria, yeast, mold

1. Introduction

This protocol describes a procedure for quantitative determination of microbial contamination of a nanoparticle formulation. This assay requires 1.0 mL of test nanomaterials at concentration of 1 mg/mL or as reasonably achievable. The protocol includes tests for yeast, mold, and bacteria using Millipore sampler devices and makes use of Millipore samplers, dilution kits, and swab test kits. This approach is primarily intended to avoid contamination of cell cultures or transmitting microbial contaminants to animals in preclinical studies of efficacy, biodistribution, and toxicity. This method is not applicable to test nanoparticle antimicrobial activity, microbial resistance, and validation of the sterilization procedure or lot release. If this is your aim, more in depth analysis of sterility parameters can be performed according to the United States Pharmacopeia standards USP30-51, 30-61 and 30-71 (1–4).

Scott E. McNeil (ed.), *Characterization of Nanoparticles Intended for Drug Delivery*, Methods in Molecular Biology, vol. 697,
DOI 10.1007/978-1-60327-198-1_13,

2. Materials

1. Sterile PBS.
2. Yeast and mold sampler (Millipore, Billerica, MA).
3. Total count sampler (Millipore, Billerica, MA).
4. HPC count sampler (Millipore, Billerica, MA).
5. Test nanomaterial sample (see Notes 1 and 2).
6. Buffer used to reconstitute test nanomaterial.
7. Sodium hydroxide solution. Prepare from concentrated stock by dilution into sterile water to make solution with final concentration of 0.1 N.
8. Hydrochloric acid. Prepare from concentrated stock by dilution into sterile water to make solution with final concentration of 0.1 N.
9. Use sterile PBS or sterile water as negative control. Negative control is acceptable if no colony forming units (CFUs) are observed upon completion of the test.
10. For the positive control, use bacterial or yeast cell cultures (ATCC No. 25254 and MYA774, respectively) at dilution to allow at least 10 CFU/mL (see Note 3).
11. Preparation of nanoparticle samples. Nanoparticle samples should be reconstituted in sterile PBS to a final concentration of 1 mg/mL. The pH of the nanoparticle sample is checked using a pH microelectrode and should be adjusted as necessary to be within a pH range of 6–8 with sterile NaOH or HCl. If NaOH or HCL is not compatible with a given nanoparticle formulation, adjust the pH using a procedure approved by the nanoparticle manufacturer. To avoid sample contamination from the microelectrode, always collect a small aliquot of the sample and use it to measure pH.

3. Methods

1. Add 1 mL of nanoparticle formulation to 9 mL of complete cell culture media, mix well and incubate at 37°C 5% CO_2 for 7 days. At the end of incubation, document any change in media appearance such as change in color and/or turbidity.
2. Remove the sampler from its plastic bag and write the date and the sample reference number on the case with indelible marker.
3. Using sterile conditions remove a paddle from the Millipore case and apply 1 mL of control culture media or culture media

exposed to nanoparticles from step 1 onto the surface of a filter. Allow liquid to absorb, then recap the paddle. To prevent the paddle from drying out during incubation, it should be seated firmly in the case to form an air-tight seal.

4. Incubate for 72 h at a temperature of 35°C.
5. Remove the paddle from the case and examine for appearance of colonies (e.g., see Fig. 1). Perform colonies count.
6. Report results according to the following formula: No. of colonies × dilution = CFU/mL.
7. The assay is acceptable if the negative control and positive control indicate sterility and >10 CFU/mL, respectively.
8. The negative control is acceptable when it demonstrates no detectable bacterial, yeast or mold contamination.

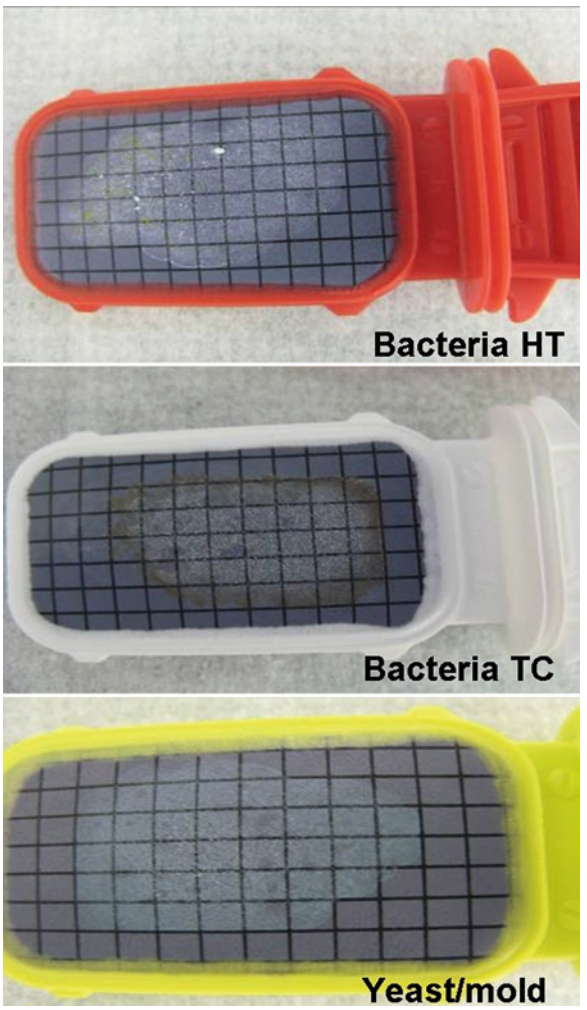

Fig. 1. Positive results from a test for microbial contamination of a polymer-based nanoparticle formulation.

9. The positive control is acceptable if at least 10 CFU of bacteria, yeast or mold are detected.
10. This test of the nanoparticle sample indicates negative result and is acceptable for use in further cell culture experiments if it shows no detectable bacteria, yeast, and mold contamination.

4. Notes

1. Always wear appropriate personal protective equipment and take appropriate precautions when handling your nanomaterial. Many occupational health and safety practitioners recommend wearing two layers of gloves when handling nanomaterials. Also, be sure to follow your facility's recommended disposal procedure for your specific nanomaterial.
2. If a nanoparticle formulation contains an active pharmaceutical ingredient which may inhibit microbial growth, we recommend testing the formulation at several concentrations/dilutions. Combining nanoparticle sample and positive control will give an idea about potential inhibition of the microbial growth by nanoparticle formulation.
3. If standard cultures are not available, a sample from another source known to contain bacteria and yeast/mold (e.g., rain water, floor swipe etc.) may be used. A positive control is acceptable if it allows identification of at least 10 CFU/mL.

Acknowledgments

This project has been funded in whole or in part with federal funds from the National Cancer Institute, National Institutes of Health, under contract N01-CO-12400. The content of this publication does not necessarily reflect the views or policies of the Department of Health and Human Services, nor does mention of trade names, commercial products, or organizations imply endorsement by the U.S. Government.

References

1. Samplers, dilution kits and swab test kits user guide. P15325, Rev. D., 8/99 Millipore Corp.
2. USP Standard 51 (2007) Antimicrobial effectiveness testing USP 30 NF 25 **1**.
3. USP Standard 61 (2007) Microbial limit tests USP 30 NF 25 **1**.
4. USP Standard 71 (2007) Sterility tests USP 30 NF 25 **1**.

Part IV

Assays for In Vitro Detection and Quantitation

Chapter 14

Gold Nanoparticle Quantitation via Fluorescence in Solution and Cell Culture

Parag Aggarwal and Marina A. Dobrovolskaia

Abstract

This chapter provides a protocol for quantitative analysis of gold in solution as well as gold uptake by macrophages. A 96-well fluorescence assay was developed to be able to determine gold concentrations for a given gold nanoparticle as well as quantify the degree of gold nanoparticle uptake by macrophages. This assay detects a decrease in the fluorescence of a dye upon forming a complex with gold and a ligand. The decrease in fluorescence is proportional to the amount of gold. This protocol provides a preliminary and qualitative first-step alternative for the determination of gold nanoparticle concentration without requiring expensive, time-consuming methods such as inductively coupled plasma mass spectroscopy. This protocol can be used to support the uptake studies by the light microscopy method described in Chapter 23. This assay requires 200 μL of each test nanoparticle at a concentration of the users choosing. Up to 32 variations of test nanoparticles can be evaluated in duplicate in one assay run.

Key words: fluorescence, gold, nanoparticles

1. Introduction

The classical method for elemental analysis on material such as gold has been the use of inductively coupled plasma mass spectroscopy (ICP-MS) (1). This method is very sensitive and reliable. However, ICP-MS is limited by expensive instrumentation, specialized training, and limited accessibility to an average user. In the absence of this instrument, a 96-well fluorescence assay described herein can be used to determine the concentration of gold in a given sample. This assay is based on a previous assay developed by Fujita et al. (2).

Previous spectrophotometric assays to determine gold concentrations were based on chromogenic agents that resulted in water-insoluble complexes that required an organic extraction before analysis (3). Sensitivity was also very low for these assays.

Scott E. McNeil (ed.), *Characterization of Nanoparticles Intended for Drug Delivery*, Methods in Molecular Biology, vol. 697,
DOI 10.1007/978-1-60327-198-1_14,

This procedure describes a fluorescence assay that is based on the principle of a complex formed among gold (III), a ligand, and an acidic dye, resulting in an aqueous complex (2). In this case, the ligand is thiamine and the dye is a fluorescent dye, Phloxine B. Upon the formation of this complex, the fluorescence of Phloxine B at 564 nm is quenched, proportional to the amount of gold present. Any gold in a form other than gold (III), such as colloidal gold, must first be dissolved/treated with aqua regia to obtain the proper oxidation state for the formation of the complex.

Various factors are involved in nanoparticle uptake into macrophages. To evaluate how gold colloids are taken up by RAW 264.7 cells and what factors influence this uptake, a method needs to be established to quantitate the amount of gold present in the cells. Two previous methods for this determination were the use of ICP-MS and transmission electron microscopy (TEM) imaging. Both are greatly expensive, and in the case of the TEM images, it provides only a qualitative answer as opposed to a quantitative analysis. Therefore, the fluorescence gold assay described above was employed for this analysis.

2. Materials

2.1. Reagents and Equipment

1. Phosphate-buffered saline (PBS), HyClone, cat#SH30256.
2. US-defined fetal bovine serum (FBS), HyClone, cat#SH30070.
3. Roswell Park Memorial Institute (RPMI)-1640 medium, HyClone, cat#SH30096.
4. Pen/Strep solution, HyClone, cat#SV30010.
5. Trypsin–ethylenediaminetetraacetic acid (EDTA), Gibco, cat#25200.
6. L-Glutamine, HyClone, cat#SH30034.
7. Trypan blue solution, Invitrogen, cat#15250-061.
8. Phloxine B, Acros Organics, cat#189470050.
9. Methylcellulose, Sigma, cat#M6385.
10. Thiamine hydrochloride, Sigma, cat#T4625.
11. Black 96-well clear-bottom plate, Costar, cat#3615.
12. Gold Chloride, Sigma, cat#520918.
13. Concentrated hydrochloric acid, Sigma, cat#258148.
14. Concentrated nitric acid, Fisher, cat#A200.
15. Sodium acetate, Sigma, cat#S8750.
16. Fluorescence plate reader.
17. TurboVap®.

Note: Equivalent reagents and equipment from other vendors can be used.

2.2. Cell Culture

1. An adherent RAW 264.7 Murine Macrophage Cell Line (ATCC®, cat#TIB-71) was used for these experiments. However, any adherent cell line of interest may be used. If a suspension cell line is used for the assay, cells can then be attached/fixed onto the cell culture plate (e.g., with Cyto-Spin) to allow for the removal of the supernatant for evaluation.

2.3. Equipment

1. Cell culture incubator with 5% CO_2 and 95% humidity.
2. 96-Well cell culture plate, Nunc, cat#161093.

3. Assay Preparation

3.1. Particles and Controls

1. Standard curve for Gold Chloride is prepared between 427 ng/mL and 30 μg/mL. Seven points on the calibration curve are used, see Fig. 1.
2. Three quality control points are chosen within the standard curve.
3. A diluted aqua regia is prepared by mixing one part of 6.32 N HNO_3 and three parts of 4.84 N HCl. This dilution is sufficiently enough to dissolve colloidal gold.

3.2. Cell Culture, Reagents, and Controls

1. Complete RPMI-1640 medium.
   The complete RPMI medium should contain the following reagents:
   10% FBS (heat inactivated).
   2 mM L-Glutamine.
   100 U/mL Penicillin.
   100 μg/mL Streptomycin sulfate.

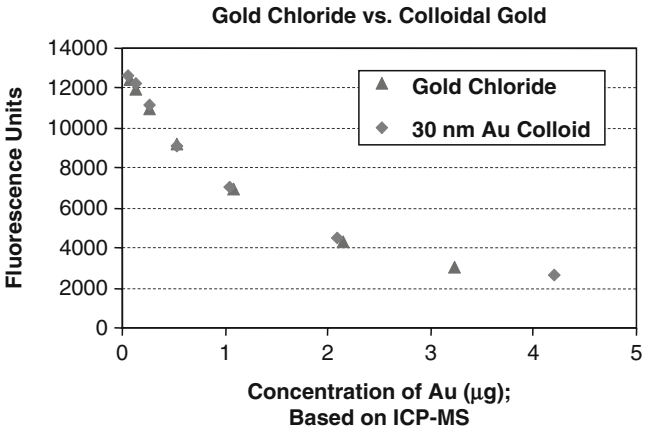

Fig. 1. Standard curve for gold assay. A solution of gold chloride ($AuCl_4$) and Ted Pella 30 nm gold colloids were used to determine the valid range of the assay. Both solutions gave similar results. The workable assay range was determined to be 42.7–3,000 ng Au or 134–8,570 ng/mL Au based on the 350 μL assay volume.

If desired, complete medium may be sterile filtered through a 0.22 μm polyethersulphone (PES) filter.
Store at 2–8°C. Before using, warm in a water bath.

2. Heat-inactivated fetal bovine serum.
   Thaw the FBS at room temperature or overnight at 2–8°C, and allow to equilibrate to room temperature. Incubate for 30 min at 56°C in a water bath, mixing at 5 min intervals. Single-use aliquots of FBS may be stored at 2–8°C for up to 1 month, or indefinitely at a nominal temperature of –20°C.

3.3. Cell Lines

1. Maintenance.
   Grow cells in complete medium. Subcultivate the cells by removing the medium, rinsing once with PBS, dislodging cells with 0.25% trypsin–EDTA solution, and resuspending in complete medium. A subcultivation ratio of 1:5–1:10 is recommended. Subcultivate every 2–3 days or when cells reach 75–80% confluency. A minimum of three subcultivations from the original stock should be performed prior to the uptake experiment.
2. Preparation for Experiment.
   One day prior to the experiment, dislodge the cells and resuspend in complete medium. Adjust the cell concentration to 1×10^5 cells per mL using complete medium. Plate 100 μL of cell suspension per well on a 96-well cell culture plate. Prepare duplicate wells for each sample and duplicate wells for each control. Incubate the plate overnight in a humidified 37°C, 5% CO_2 incubator.

3.4. Study Samples

1. Each control for this experiment is a sample of untreated cells (i.e., without nanoparticles).
2. Adjust nanoparticle concentration as desired. Nanoparticles can be manipulated (e.g., incubated with plasma, antibodies, chemical reagents, or other particles) depending on what is being evaluated for cell uptake. (For more information about nanoparticle concentration and manipulation, see Notes 1–5.)
3. Each final nanoparticle study sample should include 20 μL of the nanoparticle under study (after any desired manipulation) and 180 μL complete medium.

4. Experimental Procedure

4.1. Cell Culture

1. Using the 96-well plate prepared 1 day prior, remove the culture medium and add 200 μL of study sample (180 μL media and 20 μL nanoparticle solution) or control (medium only)

to the appropriate wells. Prepare duplicate wells of each sample and duplicate wells of each control.

2. Incubate the plate in a humidified 37°C, 5% CO_2 incubator for the time period of interest.
3. After the set time, remove 100 μL supernatant from the wells into separate tubes.
4. To remove protein interference from the cell culture medium (see Notes 1–5), wash the supernatant twice with 1 mL water and spin at 18,000 × *g* for 30 min between each wash. Reconstitute the resulting pellet in 100 μL water.
5. Mix the solution with 100 μL diluted aqua regia and store it at room temperature for at least 1 h or overnight.
6. Evaporate off the aqua regia by means of TurboVap or comparable instrumentation.
7. Reconstitute the resulting product in 100 μL of 1 M sodium acetate buffer.

4.2. Fluorescence Assay

Note: If no cell culture is preformed, analysis of gold can begin at this step. If gold is not in gold chloride form, start from Subheading 4, step 5 above.

1. In a black, clear-bottom 96-well plate, mix 100 μL of the test solution with acetate buffer pH 4.6, Phloxine B, methyl cellulose (used as a dye stabilizer), and thiamine at final concentrations of 225 mM, 0.2 mM, 0.1%, and 1 mM, respectively. The final assay volume is 350 μL.
2. Mix the plate for 5 min and incubate at 37°C for 1 h.
3. Mix the resulting plate for 5 min and place a 300 μL aliquot of each assay sample into a 96-well black-bottom plate.
4. The sample is excited at $\lambda = 350$ nm and the fluorescence measured at $\lambda = 564$ nm using a fluorescence plate reader.

5. Data Analysis/ Results

1. Analysis on various gold samples was performed by both an ICP-MS conducted by Agilent Technologies and the assay described above. The results were also compared with those stated by the vendor. Analysis revealed that concentrations determined by this fluorescence-based assay were comparable to those determined by the ICP-MS (Table 1).
2. The values obtained via the developed fluorescence-based assay were in very good agreement with values obtained from Agilent Technologies and their ICP-MS.

Table 1
Summary of comparison of results

Sample	ICP-MS (μg/mL)	Fluorescence-based assay (μg/mL)	Vendor's results (μg/mL)
30 nm Au colloids	45	45	50
50 nm Au colloids	42	45	50
Au chloride	258	250	240

6. Notes

1. Any gold in a form other than gold (III), such as colloidal gold, must first be dissolved/treated with aqua regia to obtain the proper oxidation state for the formation of the complex. We have established that a diluted form of aqua regia, a 2.5-fold dilution, is sufficient enough to dissolve the gold nanoparticles. The samples treated with aqua regia must be treated such that the aqua regia is removed before performing the fluorescence assay due to the high acidic nature of the aqua regia and the pH buffering required for the assay (see Fig. 2).
2. The major obstacle in analysis of biological samples is that proteins, such as those found in medium containing bovine serum, interfere with the assay. To overcome this issue, supernatant gold colloids in media were washed twice with water to remove excess proteins. The slight amount of proteins left after the washes did not interfere with the assay.
3. The assay was attempted on cell lysates of experimental cells. Unfortunately, the assay could not be used to analyze the cells themselves, but only the supernatant. It is possible that the assay is either not sensitive enough to detect the presence of minute amounts of gold inside the cells or that cellular debris that could not be removed was interfering with the assay.
4. If the original nanoparticle solution is too dilute for the desired assay, and the sample can be concentrated to be evaluated, care must be taken if concentrating via centrifugation. Not all nanoparticles can be concentrated via centrifugation. The limit is usually determined by the size and density of the nanoparticles. If centrifugation is possible, care must be taken to avoid the formation of aggregates during the concentration process.
5. As mentioned above, nanoparticles can be manipulated depending on what the end user is attempting to evaluate.

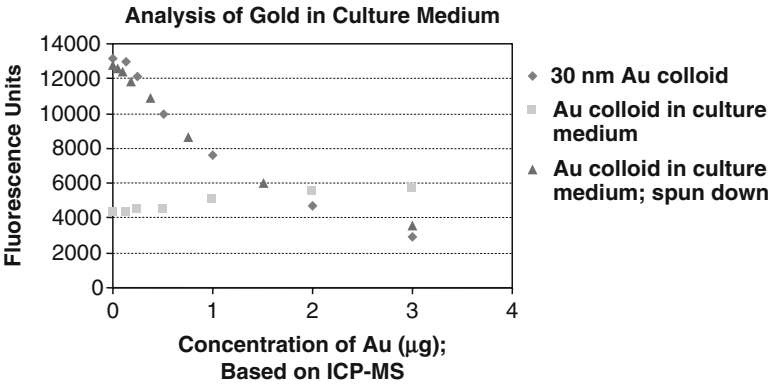

Fig. 2. Analysis of colloidal gold in cell culture media. A solution of Ted Pella 30 nm gold colloids in water was compared with a solution of Ted Pella 30 nm gold colloids in cell culture media (RPMI-1640 without Phenol Red). A second sample of gold colloid in media was spun down and reconstituted in water and tested. The interference resulting from the cell culture media was virtually eliminated after spinning and reconstituting.

Nanoparticles can be preincubated/pretreated with a variety of different substances, at the user's discretion. Care should be taken to purify samples before proceeding with the assay and to remove any extra preincubation/pretreatment substances which may artificially influence uptake. This can be accomplished through means such as centrifugation, dialysis, etc. Assay incubation time may also be manipulated to help determine a time relationship for phagocytosis.

Acknowledgments

This project has been funded in whole or in part with federal funds from the National Cancer Institute, National Institutes of Health, under contract N01-CO-12400. The content of this publication does not necessarily reflect the views or policies of the Department of Health and Human Services, nor does mention of trade names, commercial products, or organizations imply endorsement by the US Government.

References

1. Scheffer, A., Engelhard, C., Sperling, M., Buscher, W. (2008) ICP-MS as a new tool for the determination of gold nanoparticles in bioanalytical applications. *Analytical and Bioanalytical Chemistry* **390**(1), 249–52.
2. Fujita, Y., Mori, I., Matsuo, T. (1999) Spectrophotometric determination of gold(III) by an association complex formation between gold-thiamine and Phloxine. *Analytical Sciences* **15**(10), 1009–12.
3. Sandell, E. B. (1959) *Colorimetric determination of traces of metals.* 3rd ed. Interscience Publishers, New York.

Chapter 15

Quantitation of Nanoparticles in Serum Matrix by Capillary Electrophoresis

King C. Chan, Timothy D. Veenstra, and Haleem J. Issaq

Abstract

Sensitive and fast analytical techniques are needed to determine the concentration of nanoparticles in biological samples (e.g., blood and tissues) for biodistribution and toxicity studies. This chapter describes a method for the use of capillary zone electrophoresis (CZE) and micellar electrokinetic chromatography (MEKC) for the quantitation of fullerene nanoparticles in human serum matrix. Data on the fullerene-based nanoparticle carboxyfullerene (C3 fullerene) in human serum is presented as an example.

Key words: carboxyfullerene, nanoparticle, serum, capillary electrophoresis

1. Introduction

The detection and quantitation of nanoparticles in biological matrix is a common challenge for in vivo absorption, distribution, metabolism, and excretion (ADME), as well as for pharmacokinetic (PK) and toxicity studies. Carbon-based nanoparticles (e.g., liposomes, polymers, fullerenes, etc.) pose a particular challenge because techniques such as inductively coupled plasma-mass spectrometry (ICP-MS) and electron microscopy (EM) are not suitable for these particles.

High-performance capillary electrophoresis (CE) has become a powerful technique for separating ions and various types of molecules (1). CE can be performed in several modes, depending on the nature of the molecules under study. In capillary zone electrophoresis (CZE), the capillary is filled with buffer as the separation medium, and the technique is applicable to the separation of charged species that have different charge-to-mass ratios. Micellar electrokinetic chromatography (MEKC), in which micelles are

Scott E. McNeil (ed.), *Characterization of Nanoparticles Intended for Drug Delivery*, Methods in Molecular Biology, vol. 697,
DOI 10.1007/978-1-60327-198-1_15,

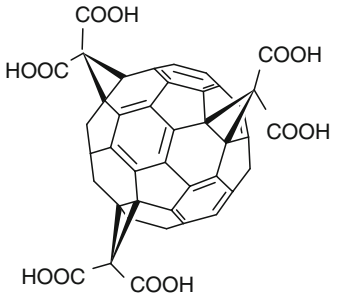

Fig. 1. Chemical structure of the carboxylated fullerene C3.

added to the separation buffer, extends CE's application to neutral molecules. The separation is based on the interaction between the hydrophobic moiety of the neutral molecules and the hydrophobic core of the micelle. MEKC was originally developed for the separation of neutral molecules, but it is also applicable to charged molecules with additional selectivity based on charge-to-mass ratio. UV absorption is the most common detection mode in CE.

Although CE has been demonstrated for several types of nanomaterials (2–12), limited work has been published for the quantitation of nanoparticles in biological matrices (13). In this chapter, methodologies based on CZE and MEKC are described for the quantitation of fullerene nanoparticles in a human serum matrix. Note that these methodologies (CZE and MEKC) are alternatives to each other and can be performed independently. The carboxylic acid derivative of fullerene (carboxyfullerene, C3 fullerene, Fig. 1) is used as an example. C3 fullerene is highly soluble and negatively charged due to the ionization of the carboxylic acid residue and has been studied extensively for its antioxidative and antimicrobial functions (14–20). The protocol may be modified for the quantitation of other nanoparticles in biological samples, e.g., by varying the micelle concentration and pH of the separation buffer or the sample treatment procedure.

2. Materials

1. C3 fullerene (C Sixty, Inc., Houston, TX).
2. Ultra Trol LN coating reagent (Target Discovery, Palo Alto, CA, see Note 1).
3. 10 mM Sodium tetraborate (pH 9.2).
4. 150 mM Sodium dodecyl sulfate (SDS).
5. 1 M Sodium hydroxide.
6. 40 mM Sodium phosphate (pH 7.4).
7. Human serum (Sigma, St Louis, MO).

8. CE apparatus with photodiode array detection (e.g., Beckman MDQ or comparable system, see Note 2). The detection wavelength should be set at 260 nm.
9. Fused-silica capillary, 50 μm i.d. (375 μm o.d.) × 40 cm long (TSP050375, Polymicro Technologies, Phoenix, AZ, see Note 3).
10. A detection window is created by removing the polyimide coating using the Window Maker (Microsolv Technology, Eatontown, NJ, see Note 4). The window should be cleaned carefully using a tissue paper soaked with methanol.

3. Methods

3.1. Preparation of Calibration Standards

1. Stock calibration standard of C3 fullerene in human serum is prepared by weighing ~0.5 mg of C3 fullerene in a 1-mL Eppendorf tube and adding an appropriate volume of human serum, to give a C3 fullerene concentration of 1 mg/mL.
2. C3 fullerene calibration standards are prepared by diluting the stock calibration standard with human serum to create calibration standards with C3 fullerene concentrations spanning 0–500 μg/mL. It is recommended to have a minimum of five calibration concentrations in this range. A minimum total volume of 100 μL per calibration standards should be prepared.
3. Calibration standards are stored at −20°C until ready for use. Allow the calibration standards to equilibrate to room temperature and gently vortex them before use.

3.2. Sample Preparation

1. For MEKC, samples are prepared by diluting the calibrations standards and the analyte sample fivefold, with water (e.g., 10 μL of serum sample + 40 μL of water, see Note 5).
2. For CZE, samples are prepared by diluting the calibrations standards and the analyte sample with 100 mM SDS (e.g., 10 μL of serum sample + 40 μL of 100 mM SDS in water, see Note 6).

3.3. Procedure

1. For MEKC separation (see Notes 7, 9–11), steps (a)–(e) below must be repeated for each calibration standard and the analyte sample. The steps below are input in the software (32 Karat v.7.0, Beckman Coulter in this case) used to run CE. The parameters given are specific for C3 fullerene but can serve as a good starting point if working with other fullerene-based nanoparticles.
   (a) Rinse the CE capillary with 1 M sodium hydroxide for 1 min at 50 psi.

(b) Rinse the CE capillary with water for 1 min at 50 psi.

(c) Rinse the CE capillary with 10 mM sodium tetraborate (pH 9.2) and 150 mM SDS for 1 min at 50 psi.

(d) Inject the sample for 20 s at 0.5 psi. Sample volume is dependent on the dimensions of the capillary; typically, the sample volume should not exceed 10% of the total capillary volume.

(e) Set the separation voltage to +14 kV.

2. For CZE separation (see Notes 8–11), steps (a)–(f) below must be repeated for each calibration standard and the analyte sample. The steps below are inputted in the software (32 Karat v.7.0, Beckman Coulter in this case) used to run CE. The parameters given are specific for C3 fullerene but can serve as a good starting point if working with other fullerene-based nanoparticles.

(a) Rinse the CE capillary with 1 M sodium hydroxide for 1 min at 50 psi.

(b) Rinse the CE capillary with water for 1 min at 50 psi.

(c) Rinse the CE capillary with Ultra Trol reagent for 1 min at 50 psi.

(d) Rinse the CE capillary with 40 mM, sodium phosphate buffer pH 7.4 for 1 min at 50 psi.

(e) Inject the sample for 20 s at 0.5 psi. Sample volume is dependent on the dimensions of the capillary; typically, the sample volume should not exceed 10% of the total capillary volume.

(f) Set the separation voltage to −14 kV.

3.4. Data Analysis

1. A calibration curve is constructed by plotting the corrected peak area (peak area divided by migration time) versus C3 fullerene concentration for each calibration standard. Most CE software programs will determine the baseline and hence report the migration time and peak area for each peak. It is important to note that the corrected peak area is used and not the peak area alone in the calibration curve. The calibration curve should be linear over the range from 0 to 500 μg/mL, with a correlation coefficient greater than 0.99 ($R^2 > 0.99$), as shown in Fig. 2 (MEKC) and Fig. 3 (CZE).

2. The corrected peak area (peak area divided by migration time) for the analyte sample is calculated. The calibration curve (in step 1 above) is used to relate the corrected peak area with C3 fullerene concentration.

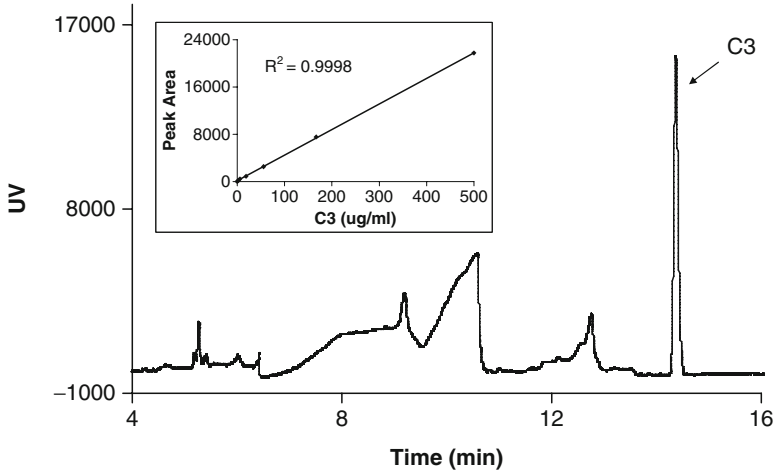

Fig. 2. A typical MEKC electropherogram using a 10 mM tetraborate buffer containing 150 mM SDS. The calibration curve is shown in the inset and is linear over the range from 0 to 500 μg/mL, with a correlation coefficient of 0.9998.

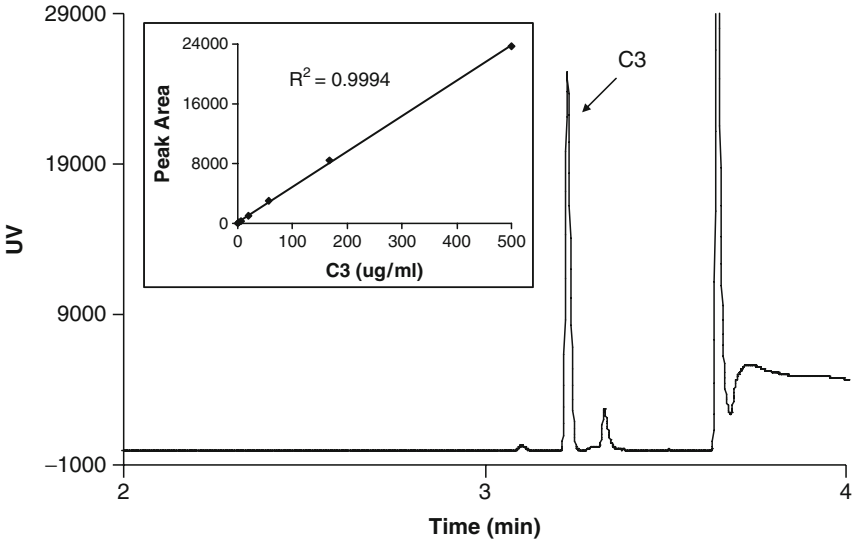

Fig. 3. A typical CZE electropherogram of a SDS-treated serum sample. The calibration curve is shown in the inset and is linear over the range from 0 to 500 μg/mL, with a correlation coefficient of 0.9994.

4. Notes

1. The fused-silica separation capillary is negatively charged due to the ionization of the surface silanol groups, resulting in strong electroosmotic (EO) flow, which pushes all neutral and charged analytes to the detector. The overall mobility of an analyte is the difference between the EO flow and its

intrinsic electrophoretic mobility. The Ultra Trol LN is a proprietary reagent used to coat the capillary wall for suppressing the EO flow. The overall mobility of an analyte in a coated capillary is thus close to its intrinsic electrophoretic mobility. The coating procedure (Subheading 3.3, step 2) takes several minutes to perform. An alternative approach for the assay without the dynamic coating step is to use a permanent coated capillary that has negligible EO flow (e.g., 04650-ZF Microsolv Technology Corporation). Do not rinse a coated capillary with NaOH as it will damage the surface coating. Only one buffer rinse is needed between runs.

2. A single-wavelength detector at 260 nm can be used for the assay. The peak identity is tentatively confirmed by matching the migration time of the sample spiked with standard. A photodiode-array detector allows additional confirmation of the peak by matching its absorption spectrum with that of standard.
3. CE is typically performed with capillaries of 20–100 μm internal diameter and several hundred volts/cm electric-field strength. The narrow-bore capillaries provide high surface-to-volume ratios that result in effective dissipation of Joule heating, permitting the use of high field strength for fast and efficient separation. Capillary clogging and reduced detection sensitivity can be a problem when the capillary is too narrow. In contrast, a large-bore capillary is needed for improving sensitivity, but a low electric field or low ionic strength buffer is required to avoid excessive Joule heating, resulting in long analysis time and broad peaks. Thus, factors such as capillary size, buffer type, detection sensitivity, speed of analysis, and resolution should be considered for other nanoparticle types.
4. The Window Maker is a convenient tool for making a detection window on the capillary. An alternative way is to cover a section of the capillary with two 1-cm long aluminum foils with about 2-mm gap between them. A detection window is created by burning off the polyimide coating in the gap using a flame. Wipe the window carefully with a tissue paper soaked with methanol to remove the coating residue.
5. Serum has a high salt content and needs to be diluted with water before analysis, to minimize injection artifacts such as current fluctuation and degraded peak shape.
6. The C3 fullerene binds to human serum albumin (21, 22), and its determination by CZE is only feasible after effective sample treatment that releases C3 fullerene from the protein complex. Common sample treatment procedures such as protein precipitation by organic solvent or protein denaturation by 6 M urea are not effective; but the addition of 80 mM SDS

(final concentration) to the sample is sufficient to disrupt the C3 fullerene–serum protein binding. The treatment is performed simply by diluting the serum sample 5× with 100 mM SDS solution. Further increases in the concentration of SDS beyond 80 mM did not improve the quantitation of C3 fullerene. Since the addition of SDS to the sample increases its ionic strength, the concentration of the separation buffer also needs to be increased to minimize sample injection artifacts such as current fluctuation and degraded peak shape.

7. MEKC is a useful method for analyzing drugs in biological samples with minimum sample treatment (23–25). The addition of SDS in the running buffer serves two purposes. First, it solubilizes the serum proteins by complexation followed by the release of C3 fullerene. Second, it facilitates C3 fullerene quantitation by separating it from the serum proteins and other endogenous components. A typical MEKC electropherogram using a 10 mM tetraborate buffer containing 150 mM SDS is shown in Fig. 2. The detection limit of the assay is 1.3 μg/mL (signal-to-noise ratio = 3). The recovery is 108%, which is calculated by comparing the peak area of 100 μg/mL C3 fullerene spiked in human serum to that in phosphate-buffered saline.
8. A negative separation voltage is applied as the intrinsic mobility of C3 fullerene is the driving force of the separation when the EO flow is suppressed by the dynamic coating. A typical CZE electropherogram of a SDS-treated serum sample is shown in Fig. 3. The detection limit of the assay is 0.5 μg/mL (S/N = 3). The recovery is approximately 104%, which is calculated by comparing the peak area of 100 μg/mL C3 fullerene spiked in human serum to that in phosphate-buffered saline.
9. Both CZE and MEKC are able to quantify C3 fullerene in human serum, but CZE has some advantages over MEKC. C3 fullerene migrates faster than the serum proteins with a coated capillary, resulting in a shorter run time on CZE, as the separation can be terminated as soon as the C3 fullerene peak is detected. In contrast, MEKC separation time is longer as C3 fullerene migrates slower than the serum proteins. The use of a permanently coated capillary can reduce the total analysis time even further as the dynamic coating steps are eliminated. In addition, CZE is more sensitive than MEKC as the baseline noise is higher with a SDS micellar buffer. Furthermore, the CZE migration time variation of C3 fullerene with dynamically coated capillaries is less than that of MEKC, due to the excellent reproducibility of the modified capillary surface.

10. The selection of CZE or MEKC for the assay in serum depends on the nature of the nanoparticles. For example, in contrast to C3 fullerene, the determination of the nanoparticle dendrofullerene (DF1) in serum is only feasible by CZE (13). Modification of the protocol for other nanoparticles may be necessary for their effective assay in human serum.
11. In addition to human serum matrix assays, CZE and MEKC are also efficient tools to determine the purity of C3 fullerene and DF1 nanoparticle standards for quality control applications (13).

Acknowledgments

This project has been funded in whole or in part by federal funds from the National Cancer Institute, National Institutes of Health, under contract N01-CO-12400. The content of this publication does not necessarily reflect the views or policies of the Department of Health and Human Services, nor does the mention of trade names, commercial products, or organizations imply endorsement by the US Government.

References

1. Landers, J.P. (2007) Handbook of Capillary and Microchip Electrophoresis and Associated Microtechniques, 3 ed. CRC Press, Boca Raton, FL.
2. Chang, T.H., Liu, F.K., Chang, Y.C., Chu, T.C. (2008) Rapidly characterizing the growth of au nanoparticles by CE. *Chromatographia*. **67**, 723–30.
3. Pyell, U. (2008) CE characterization of semiconductor nanocrystals encapsulated with amorphous silicium dioxide. *Electrophoresis*. **29**, 576–89.
4. Liu, F.K. (2007) A high-efficiency capillary electrophoresis-based method for characterizing the sizes of Au nanoparticles. *Journal of Chromatography A*. **1167**, 231–5.
5. Pereira, M., Lai, E.P.C., Hollebone, B. (2007) Characterization of quantum dots using capillary zone electrophoresis. *Electrophoresis*. **28**, 2874–81.
6. Sedlakova, P., Svobodova, J., Miksik, I., Tomas, H. (2006) Separation of poly(amidoamine) (PAMAM) dendrimer generations by dynamic coating capillary electrophoresis. *Journal of Chromatography B Analytical Technologies in the Biomedical and Life Sciences*. **841**, 135–9.
7. Shi, X., Majoros, I.J., Patri, A.K., et al. (2006) Molecular heterogeneity analysis of poly(amidoamine) dendrimer-based mono- and multifunctional nanodevices by capillary electrophoresis. *Analyst*. **131**, 374–81.
8. Shi, X., Banyai, I., Rodriguez, K., et al. (2006) Electrophoretic mobility and molecular distribution studies of poly(amidoamine) dendrimers of defined charges. *Electrophoresis*. **27**, 1758–67.
9. Shi, X., Banyai, I., Lesniak, W.G., et al. (2005) Capillary electrophoresis of polycationic poly(amidoamine) dendrimers. *Electrophoresis*. **26**, 2949–59.
10. Shi, X., Majoros, I.J., Baker, J.R. Jr. (2005) Capillary electrophoresis of poly(amidoamine) dendrimers: from simple derivatives to complex multifunctional medical nanodevices. *Molecular Pharmaceutics*. **2**, 278–94.
11. Shi, X., Patri, A.K., Lesniak, W., et al. (2005) Analysis of poly(amidoamine)-succinamic acid dendrimers by slab-gel electrophoresis and capillary zone electrophoresis. *Electrophoresis*. **26**, 2960–7.
12. Tamisier-Karolak, S.L., Pagliarusco, S., Herrenknecht, C., et al. (2001) Electrophoretic

behavior of a highly water-soluble dendro[60] fullerene. *Electrophoresis.* **22**, 4341–6.

13. Chan, K.C., Patri, A.K., Veenstra, T.D., McNeil, S.E., Issaq, H.J. (2007) Analysis of fullerene-based nanomaterial in serum matrix by CE. *Electrophoresis.* **28**, 1518–24.
14. Quick, K.L., Ali, S.S., Arch, R., Xiong, C., Wozniak, D., Dugan, L.L. (2008) A carboxyfullerene SOD mimetic improves cognition and extends the lifespan of mice. *Neurobiology of Aging.* **29**, 117–28.
15. Lin, A.M.Y., Yang, C.H., Ueng, Y.F., et al. (2004) Differential effects of carboxyfullerene on MPP+/MPTP-induced neurotoxicity. *Neurochemistry International.* **44**, 99–105.
16. Lin, A.M.Y., Fang, S.F., Lin, S.Z., Chou, C.K., Luh, T.Y., Ho, L.T. (2002) Local carboxyfullerene protects cortical infarction in rat brain. *Neuroscience Research.* **43**, 317–21.
17. Foley, S., Curtis, A.D.M., Hirsch, A., et al. (2002) Interaction of a water soluble fullerene derivative with reactive oxygen species and model enzymatic systems. *Fullerenes Nanotubes and Carbon Nanostructures.* **10**, 49–67.
18. Tsao, N., Luh, T.Y., Chou, C.K., et al. (2002) In vitro action of carboxyfullerene. *Journal of Antimicrobial Chemotherapy.* **49**, 641–9.
19. Lin, H.S., Lin, T.S., Lai, R.S., D'Rosario, T., Luh, T.Y. (2001) Fullerenes as a new class of radioprotectors. *International Journal of Radiation Biology.* **77**, 235–9.
20. Monti, D., Moretti, L., Salvioli, S., et al. (2000) C60 carboxyfullerene exerts a protective activity against oxidative stress-induced apoptosis in human peripheral blood mononuclear cells. *Biochemical and Biophysical Research Communications.* **277**, 711–7.
21. Benyamini, H., Shulman-Peleg, A., Wolfson, H.J., Belgorodsky, B., Fadeev, L., Gozin, M. (2006) Interaction of C-60-fullerene and carboxyfullerene with proteins: docking and binding site alignment. *Bioconjugate Chemistry.* **17**, 378–86.
22. Belgorodsky, B., Fadeev, L., Ittah, V., et al. (2005) Formation and characterization of stable human serum albumin-tris-malonic acid [C-60]fullerene complex. *Bioconjugate Chemistry.* **16**, 1058–62.
23. Holzgrabe, U., Brinz, D., Kopec, S., Weber, C., Bitar, Y. (2006) Why not using capillary electrophoresis in drug analysis? *Electrophoresis.* **27**, 2283–92.
24. Pappas, T.J., Gayton-Ely, M., Holland, L.A. (2005) Recent advances in micellar electrokinetic chromatography. *Electrophoresis.* **26**, 719–34.
25. Kunkel, A., Watzig, H. (1999) Micellar electrokinetic capillary chromatography as a powerful tool for pharmacological investigations without sample pretreatment: A precise technique providing cost advantages and limits of detection to the low nanomolar range. *Electrophoresis.* **20**, 2379–89.

Part V

In Vitro Assays for Toxicity

Chapter 16

Evaluation of Cytotoxicity of Nanoparticulate Materials in Porcine Kidney Cells and Human Hepatocarcinoma Cells

Timothy M. Potter and Stephan T. Stern

Abstract

This chapter describes method for evaluation of nanomaterial cytotoxicity by examining effects on porcine kidney (LLC-PK1) and human cancerous liver cells (Hep G2). Several studies indicate that many nanoparticles are cleared from the body through the kidney or liver, making these organs good choices for target organ toxicity evaluation. In this standard, two separate metrics (MTT and LDH) provide complementary data, that can be used to identify interference.

Key words: Nanoparticles, cytotoxicity, MTT, LDH

1. Introduction

This chapter describes a method for cytotoxicity testing of nanoparticle formulations in porcine proximal tubule cells (LLC-PK1) and human hepatocarcinoma cells (Hep G2). The method utilizes two metrics for cytotoxicity, 3-(4,5-dimethyl-2-thiazolyl)-2,5-diphenyl-2H-tetrazolium bromide (MTT) reduction and lactate dehydrogenase (LDH) release.

MTT is a yellow water-soluble tetrazolium dye, the tetrazolium ring of which is reduced by live cells to a water-insoluble purple formazan. The amount of formazan can be determined by solubilizing it in dimethyl sulfoxide (DMSO) and measuring it spectrophotometrically. Comparisons between the spectra of treated and untreated cells can give a relative estimation of cytotoxicity (1). MTT reduction mainly occurs in the mitochondria through the action of succinate dehydrogenase (2), though there are reports that indicate that reduction of MTT may also occur

Scott E. McNeil (ed.), *Characterization of Nanoparticles Intended for Drug Delivery*, Methods in Molecular Biology, vol. 697,
DOI 10.1007/978-1-60327-198-1_16,

outside the mitochondria in some systems (3–5). The MTT assay is commonly regarded as an assay for mitochondrial function.

LDH is a cytosolic enzyme that is released upon cell lysis. The LDH assay, therefore, is a measure of membrane integrity. The basis of the LDH assay is that LDH oxidizes lactate to pyruvate, pyruvate reacts with the tetrazolium salt INT (2-*p*-iodophenyl-3-*p*-nitrophenyl-5-phenyl tetrazolium chloride) to form formazan, and the water-soluble formazan dye is detected spectrophotometrically (6, 7).

These assays are intended to compare the cytotoxicity of a series of related nanomaterials. Meaningful comparison of unrelated nanomaterials is not possible without additional characterization of the physicochemical properties of each individual nanomaterial in the assay matrix. The nanoparticle samples should have undergone previous characterization to determine the physiochemical state to permit adequate data interpretation, and to allow prediction of biological responses. For example, lot-to-lot variations in particle size and surface characteristics could lead to different cytotoxicity results. The nanoparticles should not be contaminated with bacterial, yeast, or mold and the level of endotoxin should be known or determined, as all of these contaminants may cause cytotoxicity.

2. Materials

1. LLC-PK1 (porcine proximal tubule cells) cell line (ATCC No. CL-101).
2. Hep G2 (human hepatocarcinoma) cell line (ATCC No. HB-8065).
3. Coulter-type counter or hemocytometer.
4. Medium 199 (M199) cell culture medium with 2 mM L-glutamine and containing 3% fetal bovine serum (FBS).
5. RPMI 1640 cell culture media with 2 mM L-glutamine and containing 10% fetal bovine serum (FBS).
6. 96-well flat bottom cell culture plates.
7. Plate reader capable of detecting absorbance from 490 to 680 nm.
8. 96-well plate centrifuge set at 700–800 × *g*.
9. MTT reaction mixture: 5 mg/mL MTT (3-(4,5-dimethylthiazolyl-2)-2,5-diphenyltetrazolium bromide) in phosphate buffered saline (PBS). Store for up to 1 month at 4°C in the dark.
10. LDH reaction mixture (for one 96-well plate): Add 250 µL of catalyst from BioVision LDH-Cytotoxicity Assay Kit (BioVision, Mountain View, CA or similar, see Note 1)

reconstituted in 1 mL deionized H_2O for 10 min (vortexed) to 11.25 mL of dye solution from BioVision LDH-Cytotoxicity Assay Kit (BioVision, Mountain View, CA or similar see Note 1). Use immediately.

11. Glycine buffer: 0.1 M glycine and 0.1 M NaCl, pH 10.5. Store at room temperature.
12. Dimethyl sulfoxide (DMSO).
13. Positive control for MTT cytotoxicity in LLC-PK1 cells: 25 mM acetaminophen (APAP) in Medium 199 (M199) cell culture media.
14. Positive control for MTT cytotoxicity in hepatocytes: 20 mM acetaminophen (APAP) in RPMI 1640 cell culture media.
15. A positive control for LDH cytotoxicity: dilute Triton X-100 to 1% in cell culture medium.
16. Analyte nanoparticle sample (see Note 2).

3. Methods

3.1. Cell Preparation

3.1.1. LLC-PK1 Cells

1. Harvest cryopreserved cells according to the instructions from the supplier (limit passages to 20). An example of the appearance of the cells is given in Fig. 1.
2. Count the cell concentration using a coulter-type counter or hemocytometer.

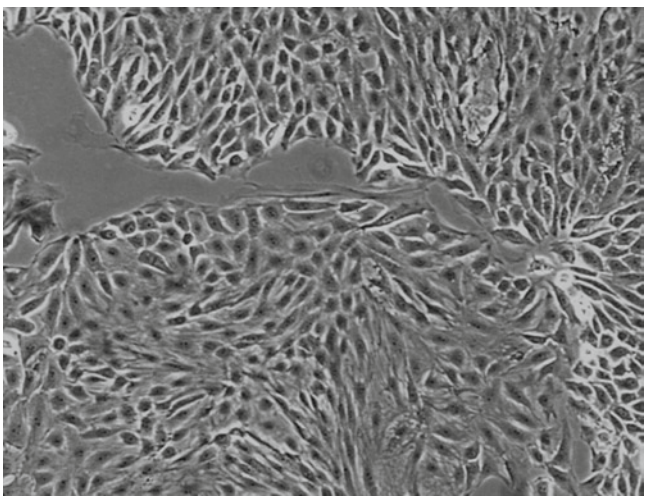

Fig. 1. Example of LLC-PK1 cell culture appearance. Image was taken with a phase-contrast microscope at ×225 magnification. LLC-PK1 cells are approximately 80% confluent at this stage.

	1	2	3	4	5	6	7	8	9	10	11	12
A	Cells Media	Cells Samp. 1 Dilution 9	Cells Samp. 1 Dilution 8	Cells Samp. 1 Dilution 7	Cells Samp. 1 Dilution 6	Cells Samp. 1 Dilution 5	Cells Samp. 1 Dilution 4	Cells Samp. 1 Dilution 3	Cells Samp. 1 Dilution 2	Cells Samp. 1 Dilution 1	Cells APAP	Cells TritonX 1 %
B	Cells Media	Cells Samp. 1 Dilution 9	Cells Samp. 1 Dilution 8	Cells Samp. 1 Dilution 7	Cells Samp. 1 Dilution 6	Cells Samp. 1 Dilution 5	Cells Samp. 1 Dilution 4	Cells Samp. 1 Dilution 3	Cells Samp. 1 Dilution 2	Cells Samp. 1 Dilution 1	Cells APAP	Cells TritonX 1 %
C	Cells Media	Cells Samp. 1 Dilution 9	Cells Samp. 1 Dilution 8	Cells Samp. 1 Dilution 7	Cells Samp. 1 Dilution 6	Cells Samp. 1 Dilution 5	Cells Samp. 1 Dilution 4	Cells Samp. 1 Dilution 3	Cells Samp. 1 Dilution 2	Cells Samp. 1 Dilution 1	Cells APAP	Cells TritonX 1 %
D	Media Media	Media Samp. 1 Dilution 9	Media Samp. 1 Dilution 8	Media Samp. 1 Dilution 7	Media Samp. 1 Dilution 6	Media Samp. 1 Dilution 5	Media Samp. 1 Dilution 4	Media Samp. 1 Dilution 3	Media Samp. 1 Dilution 2	Media Samp. 1 Dilution 1	Cells APAP	Media TritonX 1 %
E	Media Media	Media Samp. 2 Dilution 9	Media Samp. 2 Dilution 8	Media Samp. 2 Dilution 7	Media Samp. 2 Dilution 6	Media Samp. 2 Dilution 5	Media Samp. 2 Dilution 4	Media Samp. 2 Dilution 3	Media Samp. 2 Dilution 2	Media Samp. 2 Dilution 1	Cells APAP	Media TritonX 1 %
F	Cells Media	Cells Samp. 2 Dilution 9	Cells Samp. 2 Dilution 8	Cells Samp. 2 Dilution 7	Cells Samp. 2 Dilution 6	Cells Samp. 2 Dilution 5	Cells Samp. 2 Dilution 4	Cells Samp. 2 Dilution 3	Cells Samp. 2 Dilution 2	Cells Samp. 2 Dilution 1	Cells APAP	Cells TritonX 1 %
G	Cells Media	Cells Samp. 2 Dilution 9	Cells Samp. 2 Dilution 8	Cells Samp. 2 Dilution 7	Cells Samp. 2 Dilution 6	Cells Samp. 2 Dilution 5	Cells Samp. 2 Dilution 4	Cells Samp. 2 Dilution 3	Cells Samp. 2 Dilution 2	Cells Samp. 2 Dilution 1	Cells APAP	Cells TritonX 1 %
H	Cells Media	Cells Samp. 2 Dilution 9	Cells Samp. 2 Dilution 8	Cells Samp. 2 Dilution 7	Cells Samp. 2 Dilution 6	Cells Samp. 2 Dilution 5	Cells Samp. 2 Dilution 4	Cells Samp. 2 Dilution 3	Cells Samp. 2 Dilution 2	Cells Samp. 2 Dilution 1	Cells APAP	Cells TritonX 1 %

Fig. 2. Example of 96-well plate format.

3. Dilute cells to a density of 2.5×10^5 cells/mL in M199 (3% FBS) cell culture media.
4. Plate 100 µL cells/well as per plate format described in Fig. 2 for four plates (time zero 6 h sample exposure, 24 h sample exposure, 48 h sample exposure). The format indicates no cells in rows D and E, as they serve as particle blanks to be subtracted from cell treatment wells. Each plate accommodates two samples (Rows A–C and F–H). Each nanoparticle is tested at nine dilutions. Column 11 receives the APAP positive control and column 12 receives Triton X-100.
7. Incubate plates for 24 h at 5% CO_2, 37°C and 95% humidity. The cells should be approximately 80% confluent at this stage.

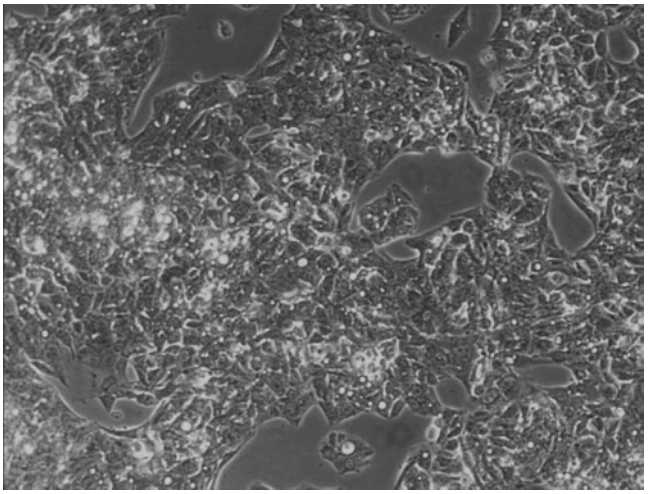

Fig. 3. Example of HEP G2 cell culture appearance. Image was taken with a phase-contrast microscope at ×225 magnification. Human hepatocarcinoma cells (Hep G2) are approximately 80% confluent at this stage.

3.1.2. Hep G2 Cells

1. Harvest cells from flasks prepared from cryopreserved cells according to the instructions from the supplier (limit passages to 20). An example of the appearance of the cells is shown in Fig. 3.
2. Count cell concentration using a coulter-type counter or hemocytometer.
3. Dilute cells to a density of 5.0×10^5 cells/mL in RPMI 1640 (2 mM L-glutamine, 10% FBS) cell culture media.
4. Plate 100 µL cells as per plate format described in Fig. 2 for four plates. The format indicates no cells in rows D and E and they serve as particle controls. Each plate accommodates two samples (Rows A–C and F–H). Each nanoparticulate material is tested at nine dilutions. Column 11 receives the APAP positive control and column 12 receives Triton X-100.
5. Incubate plates for 24 h at 5% CO_2, 37°C and 95% humidity. The cells should be approximately 70% confluent at this stage.

3.2. Time Zero Plate

1. Remove time zero plates from the incubator and replace media from Triton X-100 positive control wells (see plating format in Fig. 2) with 200 µL 1% Triton X-100. Add 100 µL of media to the remaining wells. Let the plate set for 10 min at room temperature. Spin at $700 \times g$ for 3 min.
2. For LLC-PK1 cells, remove 100 µL of media from each well and transfer to another plate on ice maintaining the plate format in Fig. 2. For Hep-G2 cells, remove 50 µL of media from

each well and transfer to another plate on ice maintaining the plate format in Fig. 2. Use this plate for the LDH assay upon completion of the incubation (see Subheading 3.4 below).

3. Continuing with what will be the MTT plate, remove remaining media from wells and discard.
4. Add 200 µL of fresh media to all wells.
5. Add 50 µL of MTT reaction mixture to all wells.
6. Cover in aluminum foil and incubate for 37°C for 4 h.
7. Remove plate from incubator and spin at 700 × *g* for 3 min.
8. Aspirate media and MTT reaction mixture.
9. Add 200 µL of DMSO to all wells.
10. Add 25 µL of glycine buffer to all wells.
11. Shake plate on an orbital shaker briefly.
12. Read at 570 nm on plate reader using a reference wavelength of 680 nm.

3.3. 6-, 24-, and 48-h Exposure Plates: Nanoparticle Sample and Positive Control Addition (See Note 3)

1. Dilute the nanoparticle sample in cell culture medium, making a total of nine 1:4 dilutions.
2. Add 100 µL of each nanoparticle sample dilution and positive control to 6-, 24-, and 48-h exposure plates as per the plate format shown in Fig. 2.
3. Following the 6-, 24-, and 48-h exposures, proceed with MTT assay as for time zero plate (proceed from Subheading 3.2, step 2) and LDH assay as described below.

3.4. LDH Assay

1. For LLC-PK1 cells, add 100 µL of the LDH reaction mixture to each well of transfer plate prepared in Subheading 3.2, step 2. For Hep-G2 cells, add 50 µL of the LDH reaction mixture to each well of transfer plate prepared in Subheading 3.3, step 2. Shake plate on an orbital shaker briefly.
2. Incubate at room temperature for up to 20 min in the dark.
3. Read the plate on plate reader at 490 nm using a reference wavelength of 680 nm.

3.5. Calculations and Analysis

1. For the LDH and MTT assays, rows D and E are used as sample blanks which are subtracted from the corresponding sample and control columns (see Fig. 2).
2. Columns 1 (rows A–C) and 12 (rows A–C) correspond to the media negative control and Triton X-100 positive control wells, respectively, for sample columns 2 (rows A–C)–11(rows A–C). Columns 1 (rows F–H) and 12 (rows F–H) are the media control and Triton X-100 positive control wells, respectively, for sample columns 2 (rows F–H)–11 (rows F–H) (see Fig. 2).

3. LDH Assay:

   Calculate the percentage LDH leakage as:

$$\%\text{Total LDH}_{\text{leakage}} = \frac{(\text{NS}_{\text{absorbance}} - \text{NC}_{\text{absorbance}})}{(\text{PC}_{\text{absorbance}} - \text{NC}_{\text{absorbance}})} \times 100$$

   where $\text{NS}_{\text{absorbance}}$ is the individual absorbance of the nanoparticle sample, $\text{NC}_{\text{absorbance}}$ is the mean absorbance of the negative control (cells with media only), and $\text{PC}_{\text{absorbance}}$ is the mean absorbance of the Triton X-100 positive control.

4. MTT Assay:

   Calculate the percentage cell viability as:

$$\%\text{Cell Viability} = \left(\frac{\text{NS}_{\text{absorbance}}}{\text{NC}_{\text{absorbance}}} \right) \times 100$$

   where $\text{NS}_{\text{absorbance}}$ is the individual absorbance of the nanoparticle sample, $\text{NC}_{\text{absorbance}}$ is the mean absorbance of the negative control (cells with media only).

5. The mean, standard deviation (SD) and percent coefficient of variation (% CV) should be calculated for each blank, positive control, negative control, and nanoparticle sample.
6. The 48 h % cell viability and % total LDH leakage for the APAP positive controls should be less than 75% and greater than 15%, respectively, for the kidney cytotoxicity assay, and less than 50% and greater than 50%, respectively, for hepatocyte cytotoxicity assay. If this condition is not met, the assay must be repeated (see Note 4).
7. The positive and sample replicate coefficient of variations should be within 50%. If this condition is not met, the assay must be repeated.
8. If the acceptance criteria are met, determine the highest concentration of the nanoparticulate material that does not interfere with the assay system indicated in rows D and E.
9. The concentration–response curves for the 48 h MTT and LDH data should be classified as having complete (two observed asymptotes) or incomplete (second asymptote not obtained) curves, single point activity (activity at the highest concentration only), or no activity. For all complete 48 h concentration–response curves, a nonlinear fit of the sigmoidal hill equation should be performed, and an estimate of potency (EC_{50}), efficacy ($E_{\max}$), minimum response (E_0), and hill slope (γ) from Hill equation (below) fit should be reported.

$$E = E_0 + \frac{(E_{\max} - E_0)C^{\gamma}}{\text{EC}_{50}^{\gamma} \cdot C^{\gamma}}$$

Any excluded points (excluded by outlier analysis) should also be reported.

4. Notes

1. Other LDH cytotoxicity assay kits can be used. For these, follow their instructions for dye and catalyst preparation.
2. Always wear appropriate personal protective equipment and take appropriate precautions when handling your nanomaterial. Many occupational health and safety practitioners recommend wearing two layers of nitrile gloves when handling nanomaterials, and perform work in an exhausted BSL II-B2 hood. Also, be sure to follow your facility's recommended disposal procedure for your specific nanomaterial.
3. This test method involves the use of a spectrophotometer with readings at 490, 570, and 680 nm. If the particle suspension interferes at these wavelengths, a method to eliminate the particles from the solution to be analyzed shall be used. If there is no method to eliminate the particles or correct the readings with an appropriate blank, this test method is not applicable and other methods must be explored.
4. Precision and bias have not been determined for this assay.

Acknowledgments

This project has been funded in whole or in part with federal funds from the National Cancer Institute, National Institutes of Health, under contract N01-CO-12400. The content of this publication does not necessarily reflect the views or policies of the Department of Health and Human Services, nor does mention of trade names, commercial products, or organizations imply endorsement by the U.S. Government.

References

1. Alley, M.C., Scudiero, D.A., Monks, A. et al. (1998) Feasibility of drug screening with panels of human tumor cell lines using a microculture tetrazolium assay. *Cancer Res.* **48**, 589–601.
2. Slater, T.F., Sawyer, B. and Struli, U. (1963) Studies on succinate-tetrazolium reductase systems III, points of coupling of four different tetrazolium salts. *Biochim. Biophys. Acta* **77**, 383–393.
3. Altman, F.P. (1976) Tetrazolium salts and formazans. *Prog. Histochem. Cytochem.* **9**, 1–56.
4. Burdon, R.H., Gill, V. and Rice-Evens, C. (1993) Reduction of a tetraxolium salt and superoxide generation in human tumor cells (HeLa). *Free Radic. Res. Commun.* **18**, 369–380.
5. Liu, Y., Peterson, D.A., Kimura, H. and Schubert, D. (1997) Mechanism of cellular

3-(4,5-dimethylthiazol-2-yl)-2,5-diphenyltetrazolium bromide (MTT) reduction. *J. Neurochem.* **69**, 581–593.

6. Decker, T. and Lohmann-Matthes, M.L. (1988) A quick and simple method for the quantitation of lactate dehydrogenase release in measurements of cellular cytotoxicity and tumor necrosis factor (TNF) activity. *J. Immunol. Methods* **115**, 61–69.
7. Korzeniewski, C. and Callewaert, D.M. (1983) An enzyme-release assay for natural cytotoxicity. *J. Immunol. Methods* **64**, 313–320.

Chapter 17

Monitoring Nanoparticle-Treated Hepatocarcinoma Cells for Apoptosis

Timothy M. Potter and Stephan T. Stern

Abstract

This chapter describes a method for monitoring nanoparticle treated human hepatocarcinoma cells (Hep G2) for apoptosis. The protocol utilizes a fluorescent method to determine the degree of caspase-3 activation.

Key words: Apoptosis, cell death, nanoparticles, hepatocarcinoma

1. Introduction

Apoptosis is a complex biological process for killing and removing unwanted cells. Apoptosis occurs both as part of normal development and during disease (1, 2). Many proteins are involved in apoptosis. In mammalian cells, apoptosis is initiated by activation of the caspase family of cysteine proteases (there are 14 identified caspases in humans). Of the caspases, caspase-3 is among the most frequently activated cell death proteases. However, caspase-3 is also important for survival, as caspase-3-knockout mice die at very young ages (3).

This assay quantifies caspase-3 activation in vitro by measuring the cleavage of DEVD-7-amino-4-trifluoromethyl coumarin (AFC) to free AFC, which emits yellow-green fluorescence ($\lambda_{max} = 505$ nm). Here, this free AFC is measured using a microtiter 96-well plate reader.

2. Materials

1. RPMI 1640 cell culture medium with 2 mM L-glutamine and containing 10% FBS.

Scott E. McNeil (ed.), *Characterization of Nanoparticles Intended for Drug Delivery*, Methods in Molecular Biology, vol. 697,
DOI 10.1007/978-1-60327-198-1_17,

2. Costar six-well flat bottom cell culture plates, (Costar, Cat. No. 3506).
3. Quick Start Bradford Dye Reagent, 1× (Bio-Rad Lab., Inc., Cat. No. 500-0205).
4. Nanoparticle solution (see Notes 1 and 2).
5. L-Glutamine (Hyclone No. SH30034.01).
6. Fetal bovine serum (Hyclone SH30070.03).
7. Cell line: Hep G2 (human hepatocarcinoma) (ATCC No. HB-8065).
8. Plate reader (Safire^2-Tecan).
9. Acetaminophen (APAP) positive control: Add 8 mg acetaminophen (Sigma Cat. No. A7085) to a total volume of 5 mL RPMI 1640 cell culture media to make a 10 mM solution. Sterile filter using a 0.2 μm filter.
10. Biovision Caspase-3 Fluormeteric Assay Kit (Biovision Cat. #K105-25).
11. Add 10 mL of the DTT solution (from Biovision kit) to 1 mL of the 2× reaction buffer.
12. Thaw the cell lysis buffer (from Biovision kit) and store at 4°C (see Note 3).
13. DEVD-AFC (from Biovision kit) (see Note 4).

3. Methods

3.1. Cell Preparation (or As Recommended by Supplier)

1. Harvest cryopreserved cells from prepared flasks (see Note 5).
2. Count cell concentration using a coulter counter or hemocytometer.
3. Dilute cells to a density of 7.5×10^5 cells/mL in RPMI 1640 cell culture media (2 mM L-glutamine, 10% FBS).
4. Plate 2 mL of diluted cells to each well of a six-well plate (1.5×10^6 cells/well). Test samples, media and positive controls are run in triplicate, 24 wells total (time zero media control, 6 h sample exposure + media control, 24 h sample exposure + media control + positive control, and 48 h sample exposure + media control).
5. Incubate plates for 24 h at 5% CO_2, 37°C and 95% humidity (see Note 6).
6. Replace cell culture media with 2 mL media containing test material or positive control (see Note 2).

3.2. Caspase Activation Assay

1. Wash well with 1 ml of room temperature PBS.
2. Add 200 μL ice cold lysis buffer to the well, scrape cells and collect in 0.6 mL Eppendorf tubes.

3. Incubate on ice for 10 min and centrifuge at 2,000×*g* for 5 min.
4. Transfer 50 µL of supernatant to a 96-well plate reader. Add 50 µL of 2× reaction buffer (with DTT) to each sample well. Retain remaining cell lysate for protein determination.
5. Add 5 µL of DEVD-AFC substrate (50 µM final concentration) and incubate at 37°C for 1–2 h.
6. Read fluorescence at ex. 415 nm and em. 505 nm on a microtiter plate reader.

3.3. Determining the Amount of Protein Via Bradford Assay

1. Dilute the 2 mg/mL BSA standard to make a standard curve from 0.125 to 1.0 mg/mL in 0.5 N NaOH.
2. Add 5 µL of standard, cell lysate supernatant, or water blank to each well of a microtiter plate in duplicate according the template in Fig. 1.
3. Add 250 µL of 1× Bradford dye reagent to each well of the plate.
4. Incubate at room temperature for at least 5 min and not longer than 1 h.
5. Read absorbance on a microtiter plate at 595 nm.

			Set A			Set B						
	1	2	3	4	5	6	7	8	9	10	11	12
A	1 mg/mL	1 mg/mL	Media 0 h #1	Media 0 h #2	Media 0 h #3	Media 0 h #1	Media 0 h #2	Media 0 h #3				
B	0.75 mg/mL	0.75 mg/mL	Media 6 h #1	Media 6 h #2	Media 6 h #3	Media 6 h #1	Media 6 h #2	Media 6 h #3				
C	0.5 mg/mL	0.5 mg/mL	Sample 6 h #1	Sample 6 h #2	Sample 6 h #3	Sample 63 h #1	Sample 6 h #2	Sample 6 h #3				
D	0.25 mg/mL	0.25 mg/mL	Media 24 h #1	Media 24 h #2	Media 24 h #3	Media 24 h #1	Media 24 h #2	Media 24 h #3				
E	0.125 mg/mL	0.125 mg/mL	Sample 24 h #1	Sample 24 h #2	Sample 24 h #3	Sample 24 h #1	Sample 24 h #2	Sample 24 h #3				
F			Positive Control 24 h #1	Positive Control 24 h #2	Positive Control 24 h #3	Positive Control 24 h #1	Positive Control 24 h #2	Positive Control 24 h #3				
G			Media 48 h #1	Media 48 h #2	Media 48 h #3	Media 48 h #1	Media 48 h #2	Media 48 h #3				
H			Sample 48 h #1	Sample 48 h #2	Sample 48 h #3	Sample 48 h #1	Sample 48 h #2	Sample 48 h #3			Blank	Blank

Fig. 1. 96-well plate template. *Columns 1 and 2* contain samples for making the BSA standard curve, *columns 3–5* contain the analyte samples media and positive controls, *columns 11 and 12* contain spectrophotometer blanks. Each sample is run in duplicate (*columns 6–8* are duplicates of *columns 3–5*).

3.4. Calculations and Acceptance Criteria

1. The total protein normalized caspase-3 activity as a percentage of the control is calculated as:

$$\%\text{Control activity} = \left(\frac{\text{Sample fluorescence}}{\text{Total sample lysate protein(mg)}} \div \frac{\text{Mean of media control fluorescence}}{\text{Mean of total media control lysate protein(mg)}}\right) \cdot 100$$

   Mean, SD and % CV should be calculated for each positive control and sample.

2. Protein concentration is determined from the BSA standard curve following linear regression analysis ($y = x$ (slope) $+ y$ intercept). Total protein (in milligrams) is determined from the equation:

$$\text{Total lysate protein(mg)} = [\text{protein(mg / mL)}] \cdot 0.05\text{mL sample volume}$$

   The mean, standard deviation (SD) and percent coefficient of variation (% CV) should be calculated for the positive control and each sample.

3. The fold change in caspase activity at 24 h for the APAP positive control versus media negative control should be at least three.

4. The positive and sample replicate coefficient of variations should be within 50%.

5. The assay is acceptable if the above two conditions are met. Otherwise, the assay should be repeated until acceptance criteria are met (see Note 7).

4. Notes

1. Always wear appropriate personal protective gear (e.g., gloves, lab coat, goggles, respirator, etc.) and take appropriate precautions when handling your nanomaterial. Many occupational health and safety practitioners recommend wearing two layers of gloves when handling nanomaterials. Also, be sure to follow your facility's recommended disposal procedure for your specific nanomaterial.

2. The appropriate test nanomaterial concentrations should be determined based on the results of an in vitro cytotoxicity assay (e.g., the same or similar to those described in Chapter 16).

3. These solutions should be made up in advance and can be kept stable for up to 6 months at 4°C.

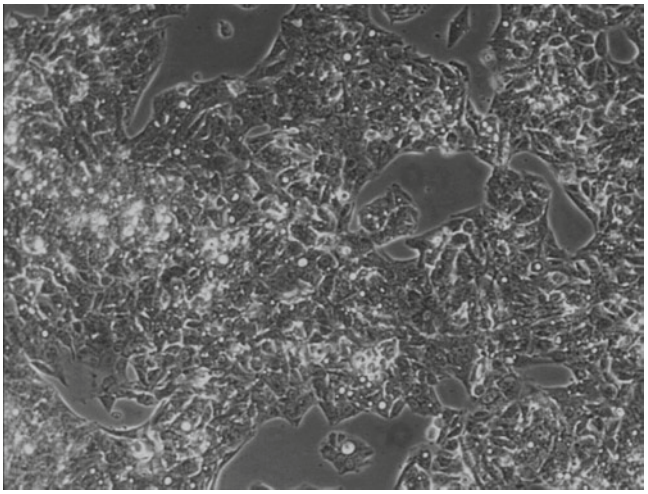

Fig. 2. Example of human hepatocarcinoma cells (HEP G2) cell culture appearance. Image was taken with a phase-contrast microscope at ×225 magnification. Human hepatocarcinoma cells (HEP G2) are approximately 80% confluent at this stage.

4. Work in the dark. The fluorescent solution used here (DEVD-AFC) is light sensitive and must be prepared and used in the dark. Prepare in a dark room and take all appropriate measures to protect the solution from light.
5. The cells should be limited to 20 passages.
6. The cells should be approximately 70% confluent at this stage. See also Fig. 2 (shown at approximately 80% confluence).
7. If statistical analysis determines that the total protein normalized control and treated fluorescence are significantly different from one another, then the fold change in fluorescence can be considered meaningful. This result would indicate that sample treatment significantly affected cell apoptosis.

Acknowledgments

This project has been funded in whole or in part with federal funds from the National Cancer Institute, National Institutes of Health, under contract N01-CO-12400. The content of this publication does not necessarily reflect the views or policies of the Department of Health and Human Services, nor does mention of trade names, commercial products, or organizations imply endorsement by the U.S. Government.

References

1. Thompson, C.B. (1995) Apoptosis in the pathogenesis and treatment of disease. *Science* **267**, 1456–1462.
2. Jacobson, M.D., Weil, M. and Raff, M.C. (1997) Programmed cell death in animal development. *Cell* **88**, 347–354.
3. Kuida, K., Zheng, T.S., Kuan C.Y., Yang, D., Karasuyama, H., Rakic, P. and Flavell, R.A. (1996) Decreased apoptosis in the brain and premature lethality in CPP32-deficient mice. *Nature* **384**, 368–372.

Chapter 18

Detecting Reactive Oxygen Species in Primary Hepatocytes Treated with Nanoparticles

Banu Zolnik, Timothy M. Potter, and Stephan T. Stern

Abstract

This chapter describes a protocol for testing nanoparticle formulations for reactive oxygen species generation in male Sprague-Dawley (SD) primary hepatocytes. The protocol utilizes the fluorescent redox active probe, dichlorofluorescein diacetate (DCFH-DA). Primary hepatocytes were chosen for this assay since they have greater metabolic activity than hepatocyte cell lines. This method extends previous standardized cytotoxicity methods for particulates by evaluating mechanisms of toxicity in potential target organ cells. Oxidative stress has been identified as a likely mechanism of nanoparticle toxicity, and cell-based in vitro systems for evaluation of nanoparticle-induced oxidative stress are widely considered an important component of biocompatibility screens.

Key words: Reactive oxygen species, oxidative stress, hepatocytes, nanoparticles

1. Introduction

Oxidative stress is a state of disequilibrium in which ROS (reactive oxygen species) production overwhelms cellular glutathione and antioxidant enzyme defenses. Particles can generate ROS by several potential surface-mediated mechanisms, involving active and photoactive electronic configurations, or surface contaminants, such as transition metals or redox cycling organics (1). Since smaller particles have a greater total surface area than larger particles for the same mass, surface-mediated ROS-generation may be of particular concern for nanoscale materials (2). ROS generation and the resulting oxidative stress have been suggested as a common mechanism by which certain ambient inhaled nanoparticles induce pulmonary toxicity (e.g. diesel exhaust particles) (3). Pulmonary toxicity has also been shown to correlate with the surface

Scott E. McNeil (ed.), *Characterization of Nanoparticles Intended for Drug Delivery*, Methods in Molecular Biology, vol. 697,
DOI 10.1007/978-1-60327-198-1_18,

area dose-metric for some engineered nanoparticles, such as polystyrene and titanium dioxide nanoparticles (4, 5). However, it remains unclear as to whether the oxidative stress paradigm can be extended to engineered nanoparticles in general. Although ROS generation has been observed in vitro for several engineered nanoparticles such as carbon black, fullerenes (6–8), preliminary in vivo studies have not shown these in vitro screens to be predictive (9).

ROS production can be evaluated with the redox active dye dichlorofluorescein (10). Dichlorofluorescein diacetate (DCFH-DA) is an acetylated analog that is ionized following acetate cleavage by intracellular esterases, trapping the dye in the cellular interior, and upon ROS-mediated oxidation fluoresces at, excitation 485 nm and emission 530 nm. In this method, a microplate spectrophotometer assay is used to monitor ROS generation in nanoparticle-treated primary hepatocytes by quantifying DCFH fluorescence.

2. Materials

1. 2′,7′-Dichlorodihydrofluorescein Diacetate (Molecular Probes Catalog # D399).
2. Dimethyl sulfoxide (Aldrich Catalog # 154938).
3. HyQ Phosphate Buffered Saline (PBS) (1×) (HyClone Catalog # SH30256.01).
4. Diethyl maleate (DEM), 97% (Aldrich Catalog # D97703-1006).
5. Williams Media E (Sigma Catalog # W1878).
6. L-glutamine (HyClone Catalog # SH30034.01).
7. Penicillin/Streptomycin [InVitrogen (Gibco) Catalog # 15140-122].
8. Fetal bovine serum (FBS) (HyClone Catalog # SH30070.03).
9. Insulin (Sigma Catalog # I-1882).
10. Dexamethasone (Sigma Catalog # D4902).
11. ITS+ Premix (insulin, human transferrin, and selenous acid) (BD Biosciences Catalog # 354352).
12. Black Costar 96-well plates, (Sigma Catalog. # CLS3603) (case of 48).
13. Cells: Cryopreserved Male Sprague-Dawley primary hepatocytes (Cellzdirect Cat. #RTCH-M).
14. Plate reader (Safire^2 – Tecan).
15. DEM Positive Control: prepare 5 mM DEM treatment solution in William's Medium E Maintenance Media (described below).

16. ROS Fluorescent Probe reagent (see Note 1)
    (a) DCFH-DA Stock (10 mM): 5 mg in 1 mL of DMSO.
    (b) DCFH-DA Working Stock (40 μM): *QS* 200 μL of 10 mM Stock to 50 mL in PBS buffer.

3. Methods

3.1. Cell Preparation (or as Recommended by Supplier)

Prepare the two required media for the hepatocytes, as follows:

1. Thaw Media:
   Add 100 μL of insulin stock (4 mg/mL) (stored in –20°C) and 10 μL of 10 mM dexamethasone stock (stored in –20°C) to 100 mL of William's Medium E with serum (2 mM L-glutamine, 50 U/mL penicillin, 50 μg/mL streptomycin and FBS 5%).
2. Maintenance Media:
   Add 1 mL of ITS+ (stored in TC fridge) and 1 μL dexamethasone to 100 mL of William's Medium E (2 mM L-glutamine, 50 U/mL penicillin, and 50 μg/mL streptomycin).
3. Warm the Thaw Media to 37°C in the water bath and thaw the vial containing hepatocytes as follows:
   1. Add a few milliliters of warm Thaw Media to a 50 mL conical tube, swirl the media and aspirate off supernatant.
   2. Wipe the vial with 70% EtOH, loosen and retighten the cap.
   3. Swirl the vial in the water bath until only a small ice pellet remains (about 1 min, 45 s).
   4. Wipe the vial with 70% EtOH and transfer the contents to the 50 mL conical tube.
4. Add Thaw media to the tube as follows:
   1. Add 1 mL by adding 200 μL at a time, swirling between additions.
   2. Add 5 mL by adding 500 μL at a time, swirling between additions.
   3. Add 5 mL by adding 1 mL at a time, swirling between additions.
   4. QS the tube to 50 mL.
   5. Spin the cells at room temperature for 4 min at 70×*g*.
   6. Carefully aspirate the supernatant and add 5 mL of Thaw media and gently resuspend by pipetting.
   7. Count viable cell density using a hemocytometer.

	1	2	3	4	5	6	7	8	9	10	11	12
A	Cells Media	Cells Samp. 1 Dilution 9	Cells Samp. 1 Dilution 8	Cells Samp. 1 Dilution 7	Cells Samp. 1 Dilution 6	Cells Samp. 1 Dilution 5	Cells Samp. 1 Dilution 4	Cells Samp. 1 Dilution 3	Cells Samp. 1 Dilution 2	Cells Samp. 1 Dilution 1	Cells DEM 0.5 mM	Cells Media
B	Cells Media	Cells Samp. 1 Dilution 9	Cells Samp. 1 Dilution 8	Cells Samp. 1 Dilution 7	Cells Samp. 1 Dilution 6	Cells Samp. 1 Dilution 5	Cells Samp. 1 Dilution 4	Cells Samp. 1 Dilution 3	Cells Samp. 1 Dilution 2	Cells Samp. 1 Dilution 1	Cells DEM 0.5 mM	Cells Media
C	Cells Media	Cells Samp. 1 Dilution 9	Cells Samp. 1 Dilution 8	Cells Samp. 1 Dilution 7	Cells Samp. 1 Dilution 6	Cells Samp. 1 Dilution 5	Cells Samp. 1 Dilution 4	Cells Samp. 1 Dilution 3	Cells Samp. 1 Dilution 2	Cells Samp. 1 Dilution 1	Cells DEM 0.5 mM	Cells Media
D	Media Media	Media Samp. 1 Dilution 9	Media Samp. 1 Dilution 8	Media Samp. 1 Dilution 7	Media Samp. 1 Dilution 6	Media Samp. 1 Dilution 5	Media Samp. 1 Dilution 4	Media Samp. 1 Dilution 3	Media Samp. 1 Dilution 2	Media Samp. 1 Dilution 1	Media DEM 0.5 mM	Media Media
E	Media Media	Media Samp. 2 Dilution 9	Media Samp. 2 Dilution 8	Media Samp. 2 Dilution 7	Media Samp. 2 Dilution 6	Media Samp. 2 Dilution 5	Media Samp. 2 Dilution 4	Media Samp. 2 Dilution 3	Media Samp. 2 Dilution 2	Media Samp. 2 Dilution 1	Media DEM 0.5 mM	Media Media
F	Cells Media	Cells Samp. 2 Dilution 9	Cells Samp. 2 Dilution 8	Cells Samp. 2 Dilution 7	Cells Samp. 2 Dilution 6	Cells Samp. 2 Dilution 5	Cells Samp. 2 Dilution 4	Cells Samp. 2 Dilution 3	Cells Samp. 2 Dilution 2	Cells Samp. 2 Dilution 1	Cells DEM 0.5 mM	Cells Media
G	Cells Media	Cells Samp. 2 Dilution 9	Cells Samp. 2 Dilution 8	Cells Samp. 2 Dilution 7	Cells Samp. 2 Dilution 6	Cells Samp. 2 Dilution 5	Cells Samp. 2 Dilution 4	Cells Samp. 2 Dilution 3	Cells Samp. 2 Dilution 2	Cells Samp. 2 Dilution 1	Cells DEM 0.5 mM	Cells Media
H	Cells Media	Cells Samp. 2 Dilution 9	Cells Samp. 2 Dilution 8	Cells Samp. 2 Dilution 7	Cells Samp. 2 Dilution 6	Cells Samp. 2 Dilution 5	Cells Samp. 2 Dilution 4	Cells Samp. 2 Dilution 3	Cells Samp. 2 Dilution 2	Cells Samp. 2 Dilution 1	Cells DEM 0.5 mM	Cells Media

Fig. 1. Example of 96-well plate format.

8. Dilute cells to a density of 7.5×10^5 cells/mL in Maintenance media.
9. Plate 150 µL cells/well as per plate format (see Fig. 1) for time zero, 0.5, 1, 1.5, 2, 2.5 and 3 h sample exposure.
10. Incubate plates for 4 h at 5% CO_2, 37°C and 95% humidity (see Fig. 2).

3.2. Addition of Nanomaterials to Hepatocytes

1. See Note 2. The highest concentration of nanomaterial tested should be at the limit of solubility. The test sample should be at physiological pH. Neutralization of acidic/basic test samples may be required.

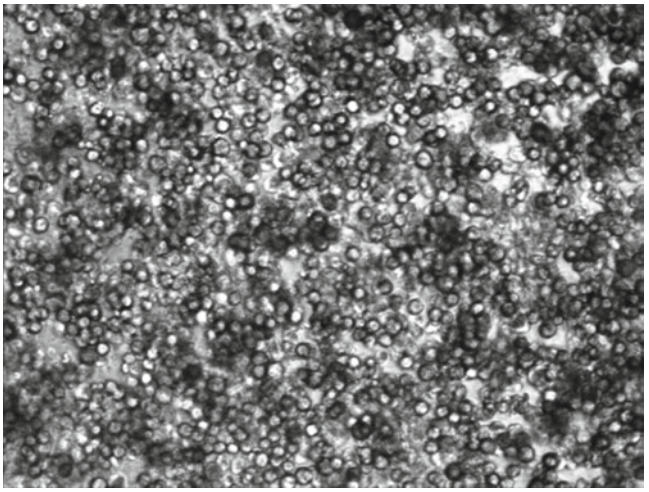

Fig. 2. Example of SD primary hepatocytes cell culture appearance. Image was taken with a phase contrast microscope at 250× magnification.

2. Dilute test compound in Maintenance media, making a total of nine 1:4 dilutions.
3. See Note 1. Add 150 µL of 40 µM DCFH-DA to test sample exposure plate containing 150 µL of Maintenance media (Final concentration of DCFH-DA is 20 µM) and incubate cells for 30 min under standard culture conditions. Centrifuge the plates at 70 × *g* for 4 min without applying the brake. Remove DCFH-DA and wash the plate with 200 µL of media at 70 × *g* for 4 min with no deceleration. Read time zero plate and add 200 µL of each dilution to each plate as per plate format (see Fig. 1).
4. Remove test plate at 0.5, 1, 2, and 3 h post exposure from the incubator and read at excitation wavelength 485 nm and emission wavelength 530 nm.

3.3. Calculations and Acceptance Criteria

1. In our 96-well plate format, rows D&E contain cell-free blanks, which are subtracted from the corresponding sample and control columns (see Fig. 1).
2. The wells labeled Cells 1(A–C, F–H) and 12(A–C, F–H) contain the media controls, and those labeled Cells 11 (A–C, F–H) contain the DEM positive controls for samples 2(A–C, F–H)–10(A–C, F–H) (see Fig. 1).

$$\%\,\text{Control Fluorescence} = \left(\frac{\text{Sample Fluorescence}}{\text{Media Control Fluorescence}}\right)\cdot 100$$

3. The mean, standard deviation (SD), and percent coefficient of variation (%CV) percent control fluorescence should be

calculated for each of the positive control and unknown sample.

4. The DCFH fluorescence for the DEM positive control should be at least 140% of the media control at 2 h.
5. The positive controls and sample replicate coefficient of variations should be within 50%.
6. The assay is acceptable if the conditions described above are met. Otherwise, the assay should be repeated until these acceptance criteria are met.

4. Notes

1. Work in the Dark. The fluorescent redox reactive probe used here (DCFH-DA) is light sensitive and must be prepared and used in the dark. Prepare in a dark room and take all appropriate measures to protect the solutions from light.
2. Always wear appropriate personal protective equipment and take appropriate precautions when handling your nanomaterial. Many occupational health and safety practitioners recommend wearing two layers of nitrile gloves when handling nanomaterials, and performing all work in an exhausted BSL II-B2 hood. Also, be sure to follow your facility's recommended disposal procedure for your specific nanomaterial.

Acknowledgments

This project has been funded in whole or in part with federal funds from the National Cancer Institute, National Institutes of Health, under contract N01-CO-12400. The content of this publication does not necessarily reflect the views or policies of the Department of Health and Human Services, nor does mention of trade names, commercial products, or organizations imply endorsement by the U.S. Government.

References

1. Nel, A., Xia, T., Mädler, L., Li, N. (2006) Toxic potential of materials at the nanolevel. *Science* **311**, 622–627.
2. Oberdörster, G., Oberdoster, E., Oberdorster, J. (2005) Nanotoxicology: an emerging discipline evolving from studies of ultrafine particles. *Environ. Health Perspect.* **113**, 823–839.
3. Donaldson, K., Stone, V., Clouter, A., Renwick, L., MacNee, W. (2001) Ultrafine particles. *Occup. Environ. Med.* **58**, 211–216.
4. Brown, D.M., Wilson, M.R., MacNee, W., Stone, V., Donaldson, K. (2001) Size dependent proinflammatory effects of ultrafine polystyrene particles: a role for surface area

and oxidative stress in the enhanced activity of ultrafines. *Toxicol. Appl. Pharmacol.* **175**, 191–199.

5. Oberdörster, G., Ferin, J., Lehnert, B.E. (1994) Correlation between particle size, in vivo particle persistence, and lung injury. *Environ. Health Perspect.* **102**(Suppl 5), 173–179.
6. Koike, E., Kobayashi, T. (2006). Chemical and biological oxidative effects of carbon black nanoparticles. *Chemosphere* **65**, 946–951.
7. Sayes, C., Fortner, J., Guo, W., Lyon, D., Boyd, A., Ausman, K., Tao, Y., Sitharaman, B., Wilson, L., Hughes, J., West, J., Colvin, V.L. (2004) The differential cytotoxicity of water-soluble fullerenes. *Nano Lett.* **4**, 1881–1887.
8. Yamakoshi, Y., Umezawa, N., Ryu, A., Arakane, K., Miyata, N., Goda, Y., Masumizu, T., Nagano, T. (2003) Active oxygen species generated from photoexcited fullerene (C60) as potential medicines: O2-* versus 1O2. *J. Am. Chem. Soc.* **125**, 12803–12809.
9. Sayes, C.M., Marchione, A.A., Reed, K.L., Warheit, D.B. (2007) Comparative pulmonary toxicity assessments of C60 water suspensions in rats: few differences in fullerene toxicity in vivo in contrast to in vitro profiles. *Nano Lett.* 7, 2399–2406.
10. Black, M.J., Brandt, R.B. (1974) Spectrofluorometric analysis of hydrogen peroxide. *Anal. Biochem.* **58**, 246.

Chapter 19

Assay to Detect Lipid Peroxidation upon Exposure to Nanoparticles

Timothy M. Potter, Barry W. Neun, and Stephan T. Stern

Abstract

This chapter describes a method for the analysis of human hepatocarcinoma cells (HEP G2) for lipid peroxidation products, such as malondialdehyde (MDA), following treatment with nanoparticle formulations. Oxidative stress has been identified as a likely mechanism of nanoparticle toxicity, and cell-based in vitro systems for evaluation of nanoparticle-induced oxidative stress are widely considered to be an important component of biocompatibility screens. The products of lipid peroxidation, lipid hydroperoxides, and aldehydes, such as MDA, can be measured via a thiobarbituric acid reactive substances (TBARS) assay. In this assay, which can be performed in cell culture or in cell lysate, MDA combines with thiobarbituric acid (TBA) to form a fluorescent adduct that can be detected at an excitation wavelength of 530 nm and an emission wavelength of 550 nm. The results are then expressed as MDA equivalents, normalized to total cellular protein (determined by Bradford assay).

Key words: Lipid peroxidation, oxidative stress, hepatocytes, nanoparticles

1. Introduction

One of the mechanisms by which oxidative stress from reactive oxygen species cause injury to cells is by lipid peroxidation. Lipid peroxidation can result in cellular membrane damage and formation of toxic reactive byproducts (1). In this method, the products of the lipid peroxidation cycle are used as markers of oxidative stress following 3, 6, and 24 h treatment with nanoparticle formulations. The reaction cycle for lipid peroxidation is displayed in Fig. 1.

The products of lipid peroxidation, lipid hydroperoxides, and aldehydes, such as malondialdehyde (MDA), can be measured via a thiobarbituric acid reactive substances (TBARS) assay. In this assay, which is performed in both cell culture media and cell lysate, MDA combines with thiobarbituric acid (TBA) in a 1:2

Scott E. McNeil (ed.), *Characterization of Nanoparticles Intended for Drug Delivery*, Methods in Molecular Biology, vol. 697,
DOI 10.1007/978-1-60327-198-1_19,

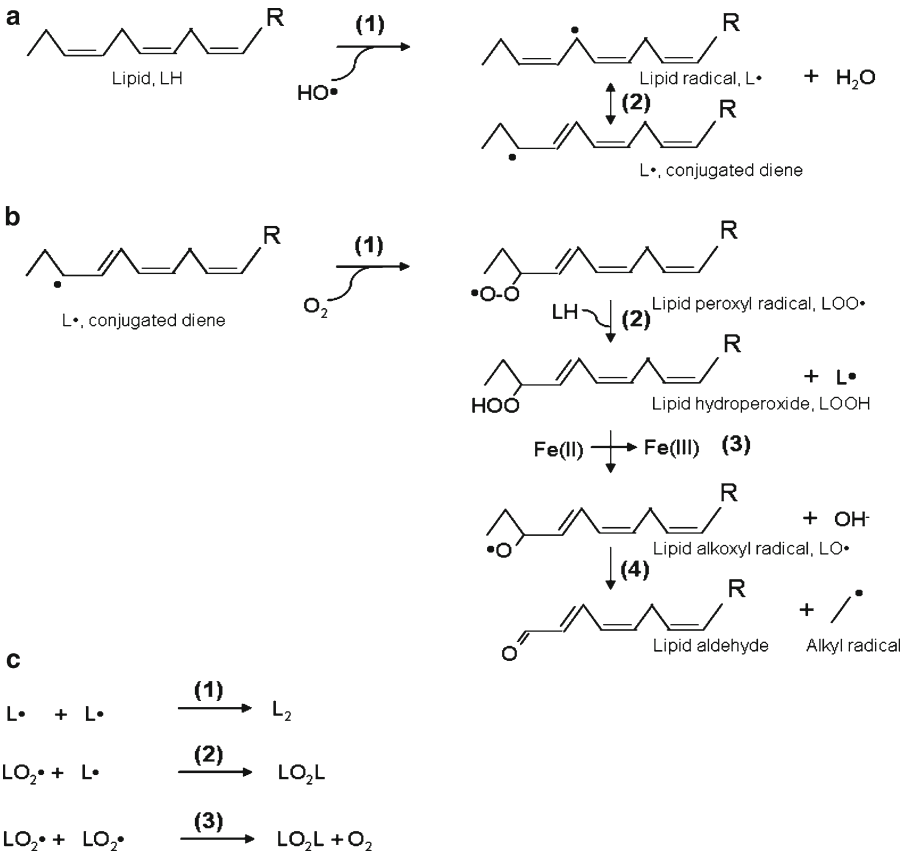

Fig. 1. Lipid peroxidation cycle. The lipid peroxidation cycle has three phases, (**a**) initiation, (**b**) propagation, and (**c**) termination. (**a**) The initiation phase begins with (1) hydrogen abstraction by a radical initiator, in this example the hydroxyl radical (HO·), resulting in formation of a lipid radical (L·). The lipid radical, L·, can then undergo (2) electron rearrangement to form a conjugated diene radical. (**b**) The lipid radical, in this case the conjugated diene, then enters the propagation phase, where (1) oxygen addition occurs, resulting in formation of the lipid peroxyl radical, LOO·. The lipid peroxyl radical, LOO·, can then initiate a second round of (2) hydrogen abstraction of another lipid, forming a lipid radical, L·, and lipid hydroperoxide, LOOH. The lipid hydroperoxide, LOOH, can undergo (3) homolysis by transition metal catalyzed fenton chemistry, to form a lipid alkoxyl radical, LO·. The lipid alkoxyl radical, LO·, can then undergo fragmentation (β-scission) to form a lipid aldehyde and alkyl radical (**c**) The final phase is termination, whereby radicals undergo radical addition to form stable products: (1) two lipid radicals, L·, can react to form a dimers, L_2; (2) a lipid radical and lipid peroxyl radical can react to form a ketone, LO_2L; (3) it is also possible for two lipid peroxyl radicals to react to form a ketone, LO_2L, and molecular oxygen, O_2 (adapted from (4), (5)).

stoichiometry to form a fluorescent adduct that can be measured at an excitation wavelength of 521 nm and an emission wavelength of 552 nm. TBARS are expressed as MDA equivalents, normalized to total cellular protein (2). The assay is performed in both cell culture media and lysate because the MDA levels are much higher in media, and the sensitivity is greater. It is important to note that while the TBARS assay results are expressed in MDA equivalents, the TBARS assay is not specific to MDA alone, as other TBA-reactive substances are present in the cultures (albeit at low concentrations) and can be generated during sample preparation (3).

2. Materials

1. Cryopreserved Hep G2 (human hepatocarcinoma, ATCC No. HB-8065) cells.
2. RPMI 1640 cell culture medium with 2 mM L-glutamine and containing 10% fetal bovine serum (FBS).
3. Six-well flat bottom cell culture plates.
4. 96-well cell culture plates.
5. Fluorescent spectrophotometer plate reader capable of measuring ex. 530 nm and em. 550 nm.
6. Phosphate buffered saline, pH 7.4 (PBS).
7. Analyte nanoparticle samples (see Notes 1 and 2).
8. Positive control: 5 mM solution of diethyl maleate (DEM) in RPMI 1640. Should be used within 24 h.
9. 15% w/v trichloroacetic acid (TCA) for cell media TBARS: add 7.5 mL TCA for a total volume of 50 mL in deionized distilled water. This can be prepared in advance. Store at 4°C.
10. 0.67% w/v thiobarbituric acid (TBA) with 0.01% w/v butylated hydroxytoluene (BHT): 0.335 g TBA and 0.01% BHT for a total volume of 50 mL in deionized distilled water. Should be used within 24 h and kept on ice.
11. Spectroscopic grade 1-butanol.
12. 2.5% w/v TCA for cell media TBARS: 1.25 g TCA for a total volume of 50 mL in deionized distilled water. This can be prepared in advance. Store at 4°C.
13. Bovine serum albumin (BSA) standard solution, 2 mg/mL. (Bio-Rad, Hercules, CA).
14. Bradford assay dye reagent (Bio-Rad, Hercules, CA).
15. 0.05 N Sodium hydroxide (NaOH).
16. MDA tetraethylacetal (1,1,3,3 Tetraethoxypropane) (MDA) standard samples for creating standard curve (see Note 3). The media and lysate MDA standards are used for determination of MDA equivalents in cell media and cell lysate samples, respectively:
    (a) 400 nmol/mL MDA standard sample: *QS* 50 µL of MDA to 500 mL with ice-cold distilled deionized water (or 2.5% TCA for cell lysate standard curve) and vortex.
    (b) 4 nmol/mL MDA standard sample: *QS* 1 mL of (a) to 100 mL with ice-cold distilled deionized water (or 2.5% TCA for cell lysate standard curve) and vortex.

(c) 2 nmol/mL MDA standard sample: 1 mL of (b) + 1 mL of distilled deionized water (or 2.5% TCA for cell lysate standard curve) and vortex.

(d) 1 nmol/mL MDA standard sample: 1 mL of (c) + 1 mL of distilled deionized water (or 2.5% TCA for cell lysate standard curve) vortex.

(e) 0.5 nmol/mL MDA standard sample: 1 mL of (d) + 1 mL distilled deionized water (or 2.5% TCA for cell lysate standard curve) vortex.

(f) 0.25 nmol/mL MDA standard sample: 1 mL of (e) + 1 mL distilled deionized water (or 2.5% TCA for cell lysate standard curve) vortex.

(g) 0.125 nmol/mL MDA standard sample: 1 mL of (f) + 1 mL distilled deionized water (or 2.5% TCA for cell lysate standard curve) vortex.

(h) 0.063 nmol/mL MDA standard sample: 1 mL of (g) + 1 mL distilled deionized water (or 2.5% TCA for cell lysate standard curve) vortex.

(i) 0.031 nmol/mL MDA standard sample: 1 mL of (h) + 1 mL distilled deionized water (or 2.5% TCA for cell lysate standard curve) vortex.

(j) 0.015 nmol/mL MDA standard sample: 1 mL of (i) + 1 mL distilled deionized water (2 or 0.5% TCA for cell lysate standard curve) vortex.

(k) 0.007 nmol/mL MDA standard sample: 1 mL of (j) + 1 mL distilled deionized water (or 2.5% TCA for cell lysate standard curve) vortex.

17. Quality control samples (see Note 4):

(a) Media QC: 0.8 nmol/mL: 1 mL of MDA standard sample (b) + 4 mL distilled deionized water vortex.

(b) Lysate QC: 0.025 nmol/mL: 1 mL of MDA standard sample (g) + 4 mL 2.5% TCA vortex.

3. Methods

3.1. Cell Preparation (or As Recommended by Cell Supplier)

1. Harvest cryopreserved cells (see Note 5) and count cell concentration using a coulter counter or hemocytometer.
2. Dilute cells to a density of 7.5×10^5 cells/mL in RPMI 1640 cell culture media with 2 mM L-glutamine and containing 10% FBS.
3. Plate 2 mL of diluted cells (approximately 1.5×10^6 cells) in each well of a six-well cell culture plate. Twenty-one wells (3.5 plates) containing cells will be needed (3 h media control,

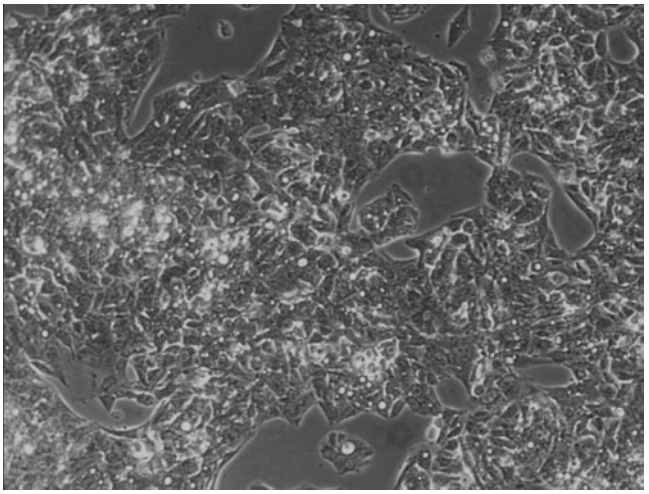

Fig. 2. Example Hep G2 cell culture appearance. Image was taken with a phase contrast microscope at ×200 magnification. Human hepatocarcinoma cells (HEP G2) are approximately 80% confluent at this stage.

3 h nanoparticle treated, 3 h DEM positive, 6 h media control, 6 h nanoparticle treated, 24 h media control, 24 h nanoparticle treated).

4. Incubate plates for 24 h at 5% CO_2, 37°C and 95% humidity (see Note 6 and Fig. 2).
5. Replace cell culture media with media containing test nanomaterial or DEM positive control. Incubate for 3, 6, or 24 h as indicated: triplicate samples of each of nanoparticle-treated, positive control DEM-treated, and negative control (untreated) samples should be incubated for 3, 6, and 24 h.

3.2. Cell Media Sample/MDA Standard Preparation

1. Collect cell media following treatment.
2. Add 400 µL 15% TCA and 800 µL of 0.67% TBA with 0.01% BHT, to 500 µL of media or media MDA standard in a 5 mL amber vial. Vortex and heat for 20 min in a 95°C water bath. Allow to cool, add 3 mL butanol, and gently mix phases. Transfer 200 µL of the butanol phase (top) to a 96-well plate, using the media sample columns 3–5 or media MDA standard and quality control columns 1 and 2, as per the plating format in Fig. 3.

3.3. Cell Lysate Sample/MDA Standard Preparation

1. Wash six well plates with ice-cold PBS.
2. Scrape cells into 1 mL 2.5% TCA.
3. Centrifuge cells at 13,000 × *g* for 2 min.
4. Retain pellet for protein quantitation by Bradford assay. The pellet can be frozen at –20°C until analysis.

	1	2	3	4	5	6	7	8	9	10	11	12
A	Std B 4.0 nmol/mL	Std B 4.0 nmol/mL	Media 3 h # 1	Media 3 h # 2	Media 3 h # 3	Std F 0.25 nmol/mL	Std F 0.25 nmol/mL	Media 3 h # 1	Media 3 h # 2	Media 3 h # 3		Blank Cell Media
B	Std C 2.0 nmol/mL	Std C 2.0 nmol/mL	Sample 3 h # 1	Sample 3 h # 2	Sample 3 h # 3	Std G 0.125 nmol/mL	Std G 0.125 nmol/mL	Sample 3 h # 1	Sample 3 h # 2	Sample 3 h # 3		Blank Cell Media
C	Std D 1.0 nmol/mL	Std D 1.0 nmol/mL	Positive Control 3 h # 1	Positive Control 3 h # 2	Positive Control 3 h # 3	Std H 0.063 nmol/mL	Std H 0.063 nmol/mL	Positive Control 3 h # 1	Positive Control 3 h # 2	Positive Control 3 h # 3		Blank Cell Media
D	Std E 0.5 nmol/mL	Std E 0.5 nmol/mL	Media 6 h # 1	Media 6 h # 2	Media 6 h # 3	Std I 0.031 nmol/mL	Std I 0.031 nmol/mL	Media 6 h # 1	Media 6 h # 2	Media 6 h # 3		Blank Cell Lysate
E	Std F 0.25 nmol/mL	Std F 0.25 nmol/mL	Sample 6 h # 1	Sample 6 h # 2	Sample 6 h # 3	Std J 0.015 nmol/mL	Std J 0.015 nmol/mL	Sample 6 h # 1	Sample 6 h # 2	Sample 6 h # 3		Blank Cell Lysate
F	Std G 0.125 nmol/mL	Std G 0.125 nmol/mL				Std K 0.007 nmol/mL	Std K 0.007 nmol/mL					Blank Cell Lysate
G	QC 1	QC 1				QC 2	QC 2					
H												

Fig. 3. Template for 96-well plate. *Columns 1 and 2* contain samples for cell media standard curve and media quality control samples, *columns 3–5* contain cell media samples, *columns 6 and 7* contain samples for cell lysate standard curve and lysate quality control samples, *columns 8–10* contain cell lysate samples, *column 12* contains spectrophotometer blanks. The 3 h and 6 h samples can be run on the same day (3 h samples sit on ice until ready for analysis). The 24 h samples will be set up the next day and run in an identical manner.

5. Add 400 µL 15% TCA and 800 µL of 0.67% TBA/0.01% BHT, to 500 µL of lysate supernatant or lysate MDA standard. Vortex and heat for 20 min in a 95°C water bath. Allow to cool, add 3 mL butanol, and gently mix. Transfer 200 µL of the butanol phase (top) to a 96-well plate, using the lysate sample columns 8–10 or lysate MDA standard and quality control columns 6 and 7, as per the plating format in Fig. 3.

3.4. Reading Media/ Lysate Plates

1. Read plate in fluorescence mode with an excitation wavelength of 530 nm and emission wavelength of 550 nm, and calculate MDA equivalents as explained Subheading 3.6.

3.5. Protein Determination Via Bradford Assay

1. Dilute the 2 mg/mL BSA standard to make a standard curve from 0.125 to 1.0 mg/mL in 0.05 N NaOH.
2. Resuspend pellets (from step 4 of Subheading 3.3) in 0.5 mL of 0.05 N NaOH.
3. Add 5 µL of BSA standard, resuspended protein pellets, or 0.05 N NaOH blank to each well of a 96-well plate according the template in Fig. 4 (each sample is examined in duplicate).
4. Add 250 µL of Bradford assay dye reagent to each well of the 96-well plate.

			Set A			Set B						
	1	2	3	4	5	6	7	8	9	10	11	12
A	**1 mg/mL**	**1 mg/mL**	Media 3 h # 1	Media 3 h # 2	Media 3 h # 3	Media 3 h # 1	Media 3 h # 2	Media 3 h # 3				
B	**0.75 mg/mL**	**0.75 mg/mL**	Sample 3 h # 1	Sample 3 h # 2	Sample 3 h # 3	Sample 3 h # 1	Sample 3 h # 2	Sample 3 h # 3				
C	**0.5 mg/mL**	**0.5 mg/mL**	Positive Control 3 h # 1	Positive Control 3 h # 2	Positive Control 3 h # 3	Positive Control 3 h # 1	Positive Control 3 h # 2	Positive Control 3 h # 3				
D	**0.25 mg/mL**	**0.25 mg/mL**	Media 6 h # 1	Media 6 h # 2	Media 6 h # 3	Media 6 h # 1	Media 6 h # 2	Media 6 h # 3				
E	**0.125 mg/mL**	**0.125 mg/mL**	Sample 6 h # 1	Sample 6 h # 2	Sample 6 h # 3	Sample 6 h # 1	Sample 6 h # 2	Sample 6 h # 3				
F			Media 24 h # 1	Media 24 h # 2	Media 24 h # 3	Media 24 h # 1	Media 24 h # 2	Media 24 h # 3				
G			Sample 24 h # 1	Sample 24 h # 2	Sample 24 h # 3	Sample 24 h # 1	Sample 24 h # 2	Sample 24 h # 3				
H											Blank	Blank

Fig. 4. Template for 96-well plate for Bradford assay. *Columns 1 and 2* contain samples for making the BSA standard curve, *columns 3–5* contain the analyte samples, *columns 6–8* contain duplicates of the analyte samples, *columns 11 and 12* contain spectrophotometer blanks.

5. Incubate at room temperature for at least 5 min and not longer than 1 h.
6. Read and record absorbance at 595 nm.

3.6. Calculations and Acceptance Criteria

1. TBARS assay concentrations are determined by interpolation of the MDA standard curves following linear regression, expressed as MDA equivalents, and normalized to the amount of total protein.
2. The protein concentration is determined from interpolation of the BSA standard curve following linear regression analysis. Total protein (in milligrams) is determined from the equation:

$$\text{Total protein(mg)} = [\text{protein(mg/mL)}] \cdot 0.5\text{mL}$$

3. Total lysate or medium MDA equivalents normalized to total protein are calculated as:

$$\text{MDA}_{\text{Protein normalized}} = [\text{MDA(ng/mL)}] \cdot \frac{1\text{mL}}{\text{Total protein(mg)}} = \frac{\text{MDA(ng)}}{\text{Total protein(mg)}}$$

4. The mean (μ), standard deviation (SD), and percent coefficient of variation $\left(\%\mathrm{CV} = \left(\frac{\mathrm{SD}}{\mu}\right) \times 100\right)$ protein-normalized total MDA equivalents should be calculated for each control and nanoparticle sample.
5. There should be at least a two-fold difference between the total protein-normalized medium and lysate DEM positive control compared to untreated negative control at 3 h. The quality control samples should be within 15% of their theoretical values.
6. The replicate samples of the DEM positive control, nanoparticle samples, and quality control samples should have coefficient of variations within 50%.
7. The assay is acceptable if these conditions are met. Otherwise, the assay should be repeated.
8. A statistical analysis should be conducted to determine if the protein-normalized MDA equivalents for the nanoparticle-treated and untreated cells are significantly different from one another. A statistically significant result would indicate that nanoparticle treatment significantly affected cellular lipid peroxidation.

4. Notes

1. Always wear appropriate personal protective equipment and take appropriate precautions when handling your nanomaterial. Many occupational health and safety practitioners recommend wearing two layers of nitrile gloves when handling nanomaterials, performing work in an exhausted BSL II-B2 hood. Also, be sure to follow your facility's recommended disposal procedure for your specific nanomaterial.
2. The appropriate test nanomaterial concentrations should be determined based on the results of an in vitro cytotoxicity assay (e.g., the same or similar to those described in Chapter 16).
3. The media MDA standard curve is diluted in deionized distilled water, while the cell lysate MDA standard curve samples are diluted in 2.5% TCA.
4. Large volumes of quality control samples can be made up in advance and retained for subsequent runs of the assay.
5. The cells should be limited to 20 passages.
6. The cells should be approximately 80% confluent at this stage. See also Fig. 2.

Acknowledgments

This project has been funded in whole or in part with federal funds from the National Cancer Institute, National Institutes of Health, under contract N01-CO-12400. The content of this publication does not necessarily reflect the views or policies of the Department of Health and Human Services, nor does mention of trade names, commercial products, or organizations imply endorsement by the U.S. Government.

References

1. Mylonas, C., Kouretas, D. (1999) Lipid peroxidation and tissue damage. *In Vivo* **13**(3), 295–309.
2. Dubuisson, M.L., de Wergifosse, B., Trouet, A., Baguet, F., Marchand-Brynaert, J. and Rees, J.F. (2000) Antioxidative properties of natural coelenterazine and synthetic methyl coelenterazine in rat hepatocytes subjected to tert-butyl hydroperoxide-induced oxidative stress. *Biochem. Pharmacol.* **60**, 471–478.
3. H. Esterbauer and K.H. Cheeseman (1990) Determination of aldehydic lipid peroxidation products: malonaldehyde and 4-hydroxynonenal, *Methods Enzymol.* **186**, 407–421.
4. Gregus and Klaassen (1996) Mechanisms of toxicity, in Klaassen (ed): Casarett & Doull's Toxicology: The Basic Science of poisons, Fifth Edition. New York: McGraw-Hill, pp. 45–46.
5. Mead (1984) Free Radical Mechanisms in Lipid Peroxidation and Prostaglandins, in Armstrong, Sohal, Cutler, Slater (eds.): New York: Raven Press, pp. 53–57.

Chapter 20

Monitoring Glutathione Homeostasis in Nanoparticle-Treated Hepatocytes

Timothy M. Potter, Barry W. Neun, and Stephan T. Stern

Abstract

This chapter describes a method for the analysis of human hepatocarcinoma cells (Hep G2 cells) for reduced and oxidized glutathione, following treatment with nanoparticle formulations. Glutathione is a tripeptide (L-γ-glutamyl-L-cysteinyl-glycine) present intracellularly in millimolar concentrations and one of the primary cellular antioxidant defenses against oxidative stress. An increase in the relative amount of oxidized to reduced glutathione may be indicative of oxidative stress, while a decrease in the overall glutathione pool may be indicative of conjugative metabolism or impaired synthesis. The method presented in this chapter utilizes a colorimetric method for detection of reduced and oxidized glutathione.

Key words: Glutathione, oxidative stress, hepatocarcinoma, nanoparticles

1. Introduction

Glutathione is one of the primary cellular antioxidant defenses against oxidative stress. Glutathione is a tripeptide (L-γ-glutamyl-L-cysteinyl-glycine) present intracellularly in millimolar concentrations. The cysteine amino acid in glutathione can function as a thiol reducing agent, thus buffering cellular oxidants. Glutathione homeostasis is predominantly regulated by a complex cycle of synthesis and catabolism that occurs in the liver, lung, and kidney. Under physiological conditions, glutathione reductase rapidly reduces any oxidized glutathione (GSSG) to its thiol form (GSH), so that under normal conditions more than 98% of intracellular glutathione is GSH (1).

Oxidative stress can result in depletion of GSH, and accumulation GSSG (2). Thus, this inversion of the GSH/GSSG ratio can be used as a marker of oxidative stress. Alternatively, a decrease

Scott E. McNeil (ed.), *Characterization of Nanoparticles Intended for Drug Delivery*, Methods in Molecular Biology, vol. 697,
DOI 10.1007/978-1-60327-198-1_20,

in the overall amount of GSH can be indicative of conjugative metabolism or impaired synthesis (1).

This chapter describes a method for the analysis of human hepatocarcinoma cells (Hep G2 cells) for reduced and oxidized glutathione, following 3, 6, and 24-h exposure to nanoparticle formulations. This method extends previous standardized cytotoxicity methods for particulates (3, 4), by evaluating mechanisms of toxicity in potential target organ cells. Oxidative stress has been identified as a likely mechanism of nanoparticle toxicity (5), and cell-based in vitro systems for evaluation of nanoparticle-induced oxidative stress are widely considered an important component of biocompatibility screens (6). This protocol utilizes a colorimetric method for detection of reduced and oxidized glutathione. In this assay, GSH interacts with 5-5′-dithiobis (2-nitrobenzoic acid) (DTNB) to form the colored product 2-nitro-5-thiobenzoic acid and GSSG, which is detected at 415 nm. Then, GSSG is reduced by glutathione reductase to form reduced glutathione GSH, which is again measured by the preceding method. Preincubation of the sample with the thiol masking agent 1-Methyl-4vinylpyridinium prevents measurement of GSH, allowing measurement of GSSG only (7).

2. Materials

1. Cryopreserved Hep G2 (human hepatocarcinoma, ATCC # HB-8065) cells.
2. RPMI 1640 cell culture medium with 2 mM L-glutamine and containing 10% Fetal Bovine Serum (FBS).
3. 96-well and 6-well flat bottom cell culture plates.
4. Plate reader capable of measuring absorbance at 415 and 595 nm.
5. Phosphate buffered saline, pH 7.4.
6. 5% SSA (5-Sulfosalicylic acid dihydrate) solution (see Note 1): Prepare a 10 mL solution of 500 mg SSA in deionized water.
7. 400 mM sodium carbonate solution (see Note 2): Prepare a 500 mL solution of 21 g of sodium carbonate in deionized water.
8. 200 mM sodium carbonate solution with 2.5% SSA: Dilute 400 mM solution 1:2 with 5% SSA solution.
9. Phosphate-EDTA (ethylenediaminetetraacetic acid tetrasodium salt dihydrate) dilution buffer (100 mM Na_3PO_4 –

1 mM EDTA, pH 7.4, see Note 2): prepare a solution of approximately 8.2 g sodium phosphate and 208 mg EDTA in 500 mL deionized water. Adjust pH to 7.4.

10. 0.5 mM M4VP (1-Methyl-4vinyl-pyridinium) masking reagent (OXIS International Inc., Foster City, CA, see Note 1): prepare a 5 mL solution of 7 mg M4VP in 5% SSA solution, then dilute 1:10 in 5% SSA solution.
11. Reaction mixture [1.9 units/mL glutathione reductase, 0.4 mM NADPH (β-nicotinamide adenine dinucleotide 2′-phosphate reduced tetrasodium salt)]: prepare a 20 mL solution of 38 units of glutathione reductase and 7 mg NADPH in phosphate-EDTA dilution buffer (see Note 1).
12. Diethyl maleate (DEM), positive control: Prepare 0.5 mM DEM treatment solution in RPMI 1640 cell culture medium.
13. 10 ng/μL GSSG standard stock solution: prepare a solution of 10 mg GSSG in 10 mL 5% SSA. Add 10 uL of this solution to 990 μL of 5% SSA.
14. GSH/GSSG standards (see Note 1)
    (a) Six GSH calibration samples (5, 4, 3, 2, 1, and 0.5 ng/μL GSH calibration samples): add 50, 40, 30, 20, 10, and 5 μL of the 10 ng/μL oxidized glutathione (GSSG) standard stock solution to micro eppendorf tubes and fill to a total volume of 100 μL with 200 mM sodium carbonate-2.5% SSA solution.
    (b) GSSG quality control sample (8 ng/mL GSSG+8 ng/mL GSH): prepare a solution of 10 mg GSH and 10 mg GSSG in 10 mL 5% SSA solution. Then dilute this solution 1:12.5 in 5% SSA, then 1:10 in 5% SSA (for a final concentration of 8 ng/μL).
    (c) Total GSH quality control sample (3 ng/mL GSSG): prepare a 10 mL solution with 10 mg GSSG in 200 mM sodium carbonate-2.5% SSA. Then dilute this solution 1:30 in 200 mM sodium carbonate-2.5% SSA, then 1:10 in 200 mM sodium carbonate-2.5% SSA (for a final concentration of 3 ng/μL).
15. 4.5 mM DTNB [5-5′-Dithiobis (2-nitrobenzoic acid)] substrate: prepare a 5 mL solution of 9 mg DTNB in phosphate-EDTA dilution buffer.
16. Bovine serum albumin (BSA) standard solution, 2 mg/mL (Bio-Rad, Hercules, CA).
17. Bradford assay dye reagent (Bio-Rad, Hercules, CA).
18. 0.05 N Sodium Hydroxide (NaOH).
19. Analyte nanomaterial sample (see Notes 3 and 4).

3. Methods

3.1. Cell Preparation (or as Recommended by Cell Supplier)

1. Harvest cryopreserved cells (see Note 5) and count cell concentration using a coulter counter or hemocytometer.
2. Dilute cells to a density of 7.5×10^5 cells/mL in RPMI 1640 cell culture media with 2 mM L-glutamine and containing 10% FBS.
3. Plate 2 mL of diluted cells (approximately 1.5×10^6 cells) in each well of a 6-well cell culture plate. Twenty-one wells (3.5 plates) containing cells will be needed (3 h media control, 3 h nanoparticle-treated, 6 h media control, 6 h nanoparticle-treated, 6 h DEM positive control, 24 h media control, 24 h nanoparticle-treated).
4. Incubate plates for 24 h at 5% CO_2, 37°C, and 95% humidity (see Note 6).
5. Replace cell culture media with media containing test nanomaterial. Incubate for 3, 6, and 24 h and include the DEM positive control at 6 h. All nanoparticle sample exposure timepoints and positive controls are run in triplicate.
6. Wash well with 1 mL of room temperature PBS.
7. Remove PBS, add 100 µL ice-cold 5% SSA solution to the plate and scrape cells. Transfer lysed cells to 0.6 mL eppendorf tubes and incubate for 10 min on ice. Centrifuge at 8,000 × *g* for 5 min. Prepare supernatants as described below. Retain pellet for determination of cellular protein by Bradford assay (Subheading 3.3). Pellet can be frozen at –20°C until analysis. The 3 h and 6 h samples can be run on the same day (3 h samples sit on ice until ready for analysis). The 24 h samples will be set up the next day and run in an identical manner.
8. Total GSH supernatants: dilute 5 µL of supernatant 1:2 with 5% SSA solution, then further dilute 1:2 with 400 mM sodium carbonate solution, then further dilute 1:8 with phosphate-EDTA dilution buffer (total dilution 1:32). Transfer supernatant to wells of 96-well plate as designated in the template in Fig. 1.
9. GSSG supernatants: dilute 5 µL of supernatant 1:2 with 5 µL of M4VP masking reagent in an eppendorf tube, then further dilute 1:2 with 400 mM sodium carbonate solution (total dilution 1:4). Incubate for 2 min at room temperature. Transfer supernatant to wells of 96-well plate as designated in the template in Fig. 1.

3.2. GSSG/GSH Measurement

1. Add 170 µL of reaction mixture (1.9 units/mL glutathione reductase, 0.4 mM NADPH) to each well of the 96-well plate as designated in Fig. 1. Incubate for 10 min at room temperature.

			GSH			GSSG						
	1	2	3	4	5	6	7	8	9	10	11	12
A	0.5 ng/μL	0.5 ng/μL	Media 3 h #1	Media 3 h #2	Media 3 h #3	Media 3 h #1	Media 3 h #2	Media 3 h #3				
B	1 ng/μL	1 ng/μL	Sample 3 h #1	Sample 3 h #2	Sample 3 h #3	Sample 3 h #1	Sample 3 h #2	Sample 3 h #3				
C	2 ng/μL	2 ng/μL	Positive Control 6 h #1	Positive Control 6 h #2	Positive Control 6 h #3	Positive Control 6 h #1	Positive Control 6 h #2	Positive Control 6 h #3				
D	3 ng/μL	3 ng/μL	Media 6 h #1	Media 6 h #2	Media 6 h #3	Media 6 h #1	Media 6 h #2	Media 6 h #3				
E	4 ng/μL	4 ng/μL	Sample 6 h #1	Sample 6 h #2	Sample 6 h #3	Sample 6 h #1	Sample 6 h #2	Sample 6 h #3				
F	5 ng/μL	5 ng/μL										
G	GSH QC	GSH QC										
H	GSSG QC+ M4VP	GSSG QC+ M4VP									Blank	Blank

Fig. 1. 96-well plate template for GSSG/GSH measurement. *Columns 1 and 2* contain samples for making the total GSSG standard curve and quality control samples, *columns 3–5* contain the analyte nanoparticle samples, media and positive controls for GSH measurement, *columns 6–8* contain the same analyte nanoparticle samples, media and positive controls for GSSG measurement, and *columns 11–12* contain spectrophotometer blanks.

2. Add 20 μL of GSH calibration samples, GSSG quality control samples, total GSH quality control samples, and diethyl maleate (DEM) positive control samples to each well as designated in Fig. 1. Mix and incubate for 10 min at room temperature.
3. Add 10 μL of DTNB substrate solution to each well. Mix and immediately read absorbance at 415 nm kinetically, with 5 cycles at 300 s intervals.

3.3. Protein Quantitation via Bradford Assay

1. Dilute the 2 mg/mL BSA standard to make a standard curve from 0.125 to 1.0 mg/mL in 0.05 N NaOH.
2. Resuspend pellets (from step 7 of Subheading 3.1) in 0.5 mL of 0.05 N NaOH.
3. Add 5 μL of BSA standard, resuspended protein pellets, or 0.05 N NaOH blank to each well of a microtiter plate according the template in Fig. 2 (each sample is examined in duplicate).
4. Add 250 μL of Bradford assay dye reagent to each well of the 96-well plate and mix.

			Set A			Set B						
	1	2	3	4	5	6	7	8	9	10	11	12
A	1 mg/mL	1 mg/mL	Media 3 h #1	Media 3 h #2	Media 3 h #3	Media 3 h #1	Media 3 h #2	Media 3 h #3				
B	0.75 mg/mL	0.75 mg/mL	Sample 3 h #1	Sample 3 h #2	Sample 3 h #3	Sample 3 h #1	Sample 3 h #2	Sample 3 h #3				
C	0.5 mg/mL	0.5 mg/mL	Positive Control 6 h #1	Positive Control 6 h #2	Positive Control 6 h #3	Positive Control 6 h #1	Positive Control 6 h #2	Positive Control 6 h #3				
D	0.25 mg/mL	0.25 mg/mL	Media 6 h #1	Media 6 h #2	Media 6 h #3	Media 6 h #1	Media 6 h #2	Media 6 h #3				
E	0.125 mg/mL	0.125 mg/mL	Sample 6 h #1	Sample 6 h #2	Sample 6 h #3	Sample 6 h #1	Sample 6 h #2	Sample 6 h #3				
F			Media 6 h #1	Media 6 h #2	Media 6 h #3	Media 6 h #1	Media 6 h #2	Media 6 h #3				
G			Sample 6 h #1	Sample 6 h #2	Sample 6 h #3	Sample 6 h #1	Sample 6 h #2	Sample 6 h #3				
H											Blank	Blank

Fig. 2. 96-well plate template. *Columns 1 and 2* contain samples for making the BSA standard curve, *columns 3–5* contain the analyte nanoparticle samples, media and positive controls for protein quantitation, *columns 6–8* contain a duplicate set of the same samples, and *columns 11–12* contain spectrophotometer blanks.

5. Incubate at room temperature for at least 5 min and not longer than 1 h.
6. Read on a microtiter plate at 595 nm.

3.4. Calculations and Acceptance Criteria

1. Assay total GSH and GSSG concentrations are determined from interpolation of the GSH standard curves following linear regression. These GSH concentrations should then be normalized to the amount of total protein.
2. The protein concentration is determined from interpolation of the BSA standard curve following linear regression analysis. Total protein (in milligrams) is determined from the equation:

$$\text{Total Protein (mg)} = \left[\text{protein}\left(\frac{\text{mg}}{\text{mL}}\right)\right]\cdot 0.5\text{mL}$$

3. The mean (μ), standard deviation (SD), and percent coefficient of variation ($\%\text{CV} = (\text{SD}/\mu)\times 100$) protein-normalized total GSH (or GSGG) concentration should be calculated for each control and nanoparticle sample.
4. The protein-normalized total GSH concentration of the DEM positive control should be at least 40% lower than the media negative control at 6 h.

5. The replicate samples of the DEM positive control and nanoparticle samples should have coefficient of variations within 50%.
6. The assay is acceptable if these conditions are met. Otherwise, the assay should be repeated.

4. Notes

1. These reagent solutions are not stable for long periods and should be used within 24 h.
2. These reagent solutions should be made up in advance and can be kept stable for up to 2 months at −20°C.
3. Always wear appropriate personal protective equipment and take appropriate precautions when handling your nanomaterial. Many occupational health and safety practitioners recommend wearing two layers of nitrile gloves when handling nanomaterials, and perform work in an exhausted BSL II-B2 hood. Also, be sure to follow your facility's recommended disposal procedure for your specific nanomaterial.
4. The appropriate test nanomaterial concentrations should be determined based on the results of an in vitro cytotoxicity assay (e.g. the same or similar to those described in Chapter 16).
5. The cells should be limited to 20 passages.
6. The cells should be approximately 80% confluent at this stage. See Fig. 3.

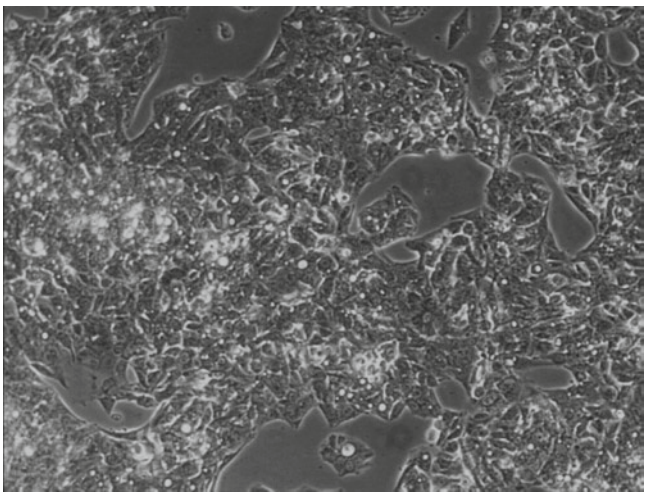

Fig. 3. Example of human hepatocarcinoma cells (HEP G2) cell culture appearance. Image was taken with a phase contrast microscope at 200× magnification. Human hepatocarcinoma cells (HEP G2) are approximately 80% confluent at this stage.

Acknowledgments

This project has been funded in whole or in part by federal funds from the National Cancer Institute, National Institutes of Health, under contract N01-CO-12400. The content of this publication does not necessarily reflect the views or policies of the Department of Health and Human Services, nor does the mention of trade names, commercial products, or organizations imply endorsement by the U.S. Government.

References

1. Deleve, L.D. and Kaplowitz, N. (1991) Glutathione metabolism and its role in hepatotoxicity. *Pharmacol. Ther.* **52**, 287–305.
2. Halliwell, B. and Gutteridge, J.M.C. (1999) *Free Radicals in Biology and Medicine*. Oxford University Press, Oxford.
3. ISO 10993-5 Biological evaluation of medical devices: Part 5 Tests for *in vitro* cytotoxicity.
4. F1903 – 98 Standard Practice for Testing for Biological Responses to Particles *In Vitro*.
5. Li, N., Xia, T. and Nel, A.E. (2008) The role of oxidative stress in ambient particulate matter-induced lung diseases and its implications in the toxicity of engineered nanoparticles. *Free Radic. Biol. Med.* **44**, 1689–1699.
6. Ayres, J.G., Borm, P., Cassee, F.R., Castranova, V., Donaldson, K., Ghio, A., Harrison, R.M., Hider, R., Kelly, F., Kooter, I.M., Marano, F., Maynard, R.L., Mudway, I., Nel, A., Sioutas, C., Smith, S., Baeza-Squiban, A., Cho, A., Duggan, S. and Froines, J. (2008) Evaluating the toxicity of airborne particulate matter and nanoparticles by measuring oxidative stress potential – a workshop report and consensus statement. *Inhal. Toxicol.* **20**, 75–99.
7. Shaik, I.H. and Mehvar, R. (2006) Rapid determination of reduced and oxidized glutathione levels using a new thiol-masking reagent and the enzymatic recycling method: application to the rat liver and bile samples. *Anal. Bioanal. Chem.* **385**, 105–113.

Chapter 21

Autophagy Monitoring Assay: Qualitative Analysis of MAP LC3-I to II Conversion by Immunoblot

Christopher B. McLeland, Jamie Rodriguez, and Stephan T. Stern

Abstract

Lysosomal dysfunction is a recognized toxic mechanism for xenobiotics, which can result in various pathological states. There is concern that nanoparticles, in particular, may cause lysosomal pathologies, since they are likely to accumulate within lysosomes. Dysregulation of the autophagy-lysosomal degradation pathway is an example of lysosomal dysfunction associated with exposure to some nanomaterials. Here, we present a method to monitor autophagy by measurement the autophagosome marker LC3-II, a phosphatidylethanolamine (PE)-conjugated form of microtubule-associated protein 1 light chain 3-I (MAP LC3-I). As other conditions could potentially result in LC3-II expression, treatment-related changes in expression should be further evaluated by morphological assessment, using techniques such as electron microscopy, to confirm autophagosome involvement.

Key Words: Autophagy, lysosomal dysfunction, nanoparticles

1. Introduction

Lysosomal dysfunction is recognized as a potential toxic mechanism for xenobiotics, which can result in various pathological states (1). There is concern that nanoparticles, in particular, may cause lysosomal pathologies as they are likely to accumulate within lysosome (2). Lysosomal dysfunction could potentially result from nanoparticle biopersistence or inhibition of lysosomal enzymes, such as inhibition of phospholipase, resulting in phospholipidosis, or inhibition of lysosomal protein degradation, resulting in lysosomal overload (1). Exposure to some nanomaterials has been associated with dysregulation of the autophagy-lysosomal degradation pathway and accumulation of autophagic vacuoles (3). This increase in autophagic vacuoles could result from increased autophagosome production, inhibition of autophagosome maturation,

Scott E. McNeil (ed.), *Characterization of Nanoparticles Intended for Drug Delivery*, Methods in Molecular Biology, vol. 697,
DOI 10.1007/978-1-60327-198-1_21,

or disruption of autolysosome breakdown. Common methods used to detect autophagy include microscopy and protein modification assays, such as assays to measure the microtubule-associated protein light chain 3-I (MAP LC3-I) lipidation product MAP LC3-II (4). MAP LC3-II is commonly used as a marker of autophagosome and, therefore, used to monitor autophagy.

This chapter presents a method to measure MAP LC3-I and the lipidated form MAP LC3-II by immunoblot. Although the molecular weight of LC3-II is greater than that of LC3-I, LC3-II migrates faster in electrophoresis due to its hydrophobicity. The amount of LC3-II subunit is used as a surrogate marker of autophagy (5). As other conditions could potentially result in formation of LC3-II, treatment-related changes in LC3-II levels should be further evaluated by morphological assessment, using techniques such as electron microscopy, to confirm autophagosome involvement.

2. Materials

1. Cell extraction buffer: add 17 μL of 0.3 M phenylmethanesulfonyl fluoride (PMSF) (Sigma, Cat #P7626) stock in dimethyl sulfoxide (DMSO) to 5 mL of cell extraction buffer (Invitrogen, Cat #FNN0011), to make 1 mM PMSF solution. Add 250 μL of reconstituted protease inhibitor cocktail (Sigma, Cat. #P-2714) to 5 mL of this solution. Use fresh.
2. TBST (Tris-buffered saline + 0.01% Tween 20) (Amresco, Cat. #J640-4L): dilute 25× stock of tris-buffered saline (TBS) in distilled water by mixing 40 mL of the stock with 960 mL of water. Then, add 100 μL of Tween 20 (Polysorbate 20) (Sigma, Cat. #P7949) and mix well. Unused buffer can be stored at room temperature (RT) overnight or up to 1 week at a nominal temperature of 4°C.
3. Blocking buffer: add 5 μL of Tween 20 to 50 mL of StartingBlock Blocking Buffer (Pierce, Cat. #37538) and mix well (to make a 0.01% solution). Use fresh.
4. Primary antibody solution: thaw an aliquot of mouse monoclonal antibody anti-LC3 antibody (e.g., NanoTools, cat no. 0231-100/LC3-5F10) and dilute 1:200 in 5 mL of the blocking buffer. Use freshly prepared (see Note 1).
5. Secondary antibody solution: Dilute peroxidase-conjugated donkey anti-mouse IgG(H + L) (e.g., Jackson Immuno Research Labs, cat no. 715-035-151) 1:50,000 in 50 mL of blocking buffer. Use freshly prepared solution. Discard after use (see Note 1).
6. 4–20% Tris–glycine gels (Invitrogen, Cat. #EC6025).

7. Running buffer: Tris-Glycine Running Buffer (Invitrogen, Cat. #LC2675): Prepare working solution by diluting 10x concentrated stock with distilled water. For example, mix 100 ml stock with 900 ml of water. Use Fresh.
8. NuPAGE LDS 4× sample buffer (Invitrogen, Cat. #NP0007) with reducing agent (10x) (Invitrogen, Cat. #NP0004).
9. Western S, polyvinylidene fluoride (PVDF) protein blotting membrane (Schlieicher&Schuell, Cat. #10 413 052).
10. India ink stain: Add 100 μL of Pelikan Fount India-17 Black drawing ink (Pelikan, Cat. #221143) to 100 mL of PBS that contains Tween 20 (0.3%). This can be stored at RT for several months.
11. Blotting paper (Schlieicher&Schuell, Cat. #CB-03).
12. Tris-Glycine Transfer Buffer (Invitrogen, Cat. #LC3675) with 20% Methanol: Prepare working buffer from 25X stock solution by diluting 40 ml of stock in 760 ml distilled water; then add 200 ml of methanol. Chill before use and use immediately.
13. Methanol (Sigma-Aldrich, Cat. #179337).
14. ECL Western Blotting Substrate (Pierce, Cat. #32106).
15. Hyperfilm ECL (Amersham Biosciences, RPN Cat. #2103K) (film for detection of chemiluminescent signal).
16. Protein standard/molecular weight marker.
17. BCA protein assay standard curve (e.g., Pierce BCA assay (Pierce, Cat. #23235)): Prepare reagents for BCA standard curve, using the dilution scheme in Table 1. The diluent

Table 1
BSA Standard Curve Preparation

Vial	Volume of diluent (μL)	Volume and source of BSA (μL)	Final BSA concentration (μg/mL)
A	900	100 stock	200
B	800	200 vial A	40
C	400	400 vial B	20
D	400	400 vial C	10
E	400	400 vial D	5
F	400	400 vial E	2.5
G	480	320 vial F	1
H	400	400 vial G	0.5
I	800	0	blank

Note: Diluent: Add an equivalent ratio of cell extraction buffer to H_2O to match the dilution buffer of the cell lysate samples

should be of the same ratio of cell extraction buffer to pyrogen-free H_2O as used to dilute samples.

18. Working reagent (WR): the formula for total volume of working reagent (WR_{tot}):

$$WR_{tot} = (s+u) \times r \times WR_{sample}$$

where s is the number of standards, u is the number of unknowns, r is the number of replicates, and WR_{sample} is the volume of working reagent per sample. One hundred and fifty microliters of WR is required for each sample if using a microplate procedure. Prepare the working reagent by mixing 25 parts of BCA reagent A and 24 parts reagent B with one part of reagent C (25:24:1; A,B, and C).

19. Hanks' balanced salt solution (with calcium and magnesium). (Invitrogen, Cat. #14025) Positive Control.
20. Hybridization bags.
21. Film cassette.
22. Analyte nanomaterial sample (see Notes 2 and 3).

3. Methods

3.1. Cell Lysate Preparation

1. Cells are treated in T-75 flasks with positive control starvation buffer, (HBSS) media negative control, or nanomaterial, for the desired time period based on previous in vitro characterization (see Note 3). Cells are washed three times with ice-cold PBS (1×) and scraped in 1 mL of ice-cold PBS (1×), transferred to a 15-mL conical tube, and centrifuged at $700 \times g$ for 3 min at 4°C.
2. Supernatant is discarded and cells are then lysed with 200 µL of cell extraction buffer containing protease inhibitors. Lysed cells are placed on ice for 30 min, and vortexed every 10 min. The lysate is centrifuged at 15,000g for 10 min at 4°C. The clear lysate is then aliquoted into clean microcentrifuge tubes.
3. Lysate samples can be used immediately, kept on ice, or stored at –80°C until use (see Note 4).
4. The protein content in cell lysate samples should be determined by the BCA protein assay outlined below.

3.2. BCA Protein Assay

1. Pipette 150 µl of each standard or unknown sample replicate into a microplate well.
2. Add 150 µl of the WR to each well and mix plate thoroughly on a plate shaker for 30 s.

3. Cover plate and incubate at 37°C for 2 h.
4. Cool plate to RT.
5. Measure the absorbance at or near 562 nm on a plate reader.
6. Blank correction: subtract the average 562 nm absorbance reading of the blank standard replicates from the 562 nm reading of all other individual standard and unknown sample replicates.
7. Prepare a standard curve by plotting the average (blank-corrected) 562 nm reading for each BSA standard vs. its concentration in microgram per milliliter. Use the standard curve to determine the protein concentration of each unknown sample.

3.3. Immunoblot

1. Dilute aliquots of all sample cell lysates to the lowest sample protein concentration determined by the BCA assay, to obtain equal protein loading and greatest assay sensitivity (e.g., if 0.8 μg protein/μL is the lowest cell lysate protein concentration, dilute all samples to 0.8 μg/uL in H2O.). Add 10 μL of 4× NuPAGE buffer and 4 uL of reducing agent to 30 μL of diluted sample. Vortex and heat at a temperature of 95°C for 5 min. Spin in a microcentrifuge at maximum speed for 30 min and carefully transfer supernatants to clean tubes (see Note 4).
2. Assemble gel running system. Prime wells with running buffer, then load 3 μL of the molecular weight protein standard, and 20–30 μL of test samples and controls in duplicate.
3. Run gel at 125 V for approximately 2 h or until dye reaches the bottom of the gel.
4. Rinse the gel with deionized water and assemble protein transfer sandwich using PVDF.
5. Perform protein transfer overnight at 30 mA at 4°C.
6. Wash PVDF membrane three times with 50–100 mL of TBST for approximately 15 min each, with rocking.
7. Block the membrane with 50 mL of blocking buffer containing 0.01% Tween-20 at RT for approximately 1 h, with rocking.
8. Incubate membrane with primary antibody solution for 2 h at RT, using hybridization bags cut to size, with rocking.
9. Wash the membrane twice with 50–100 mL of TBST, for 15 min each, with rocking.
10. Incubate the membrane with the secondary antibody solution for 1 h at RT, with rocking.
11. Wash the membrane twice with 50–100 mL of TBST, for 15 min each, with rocking.

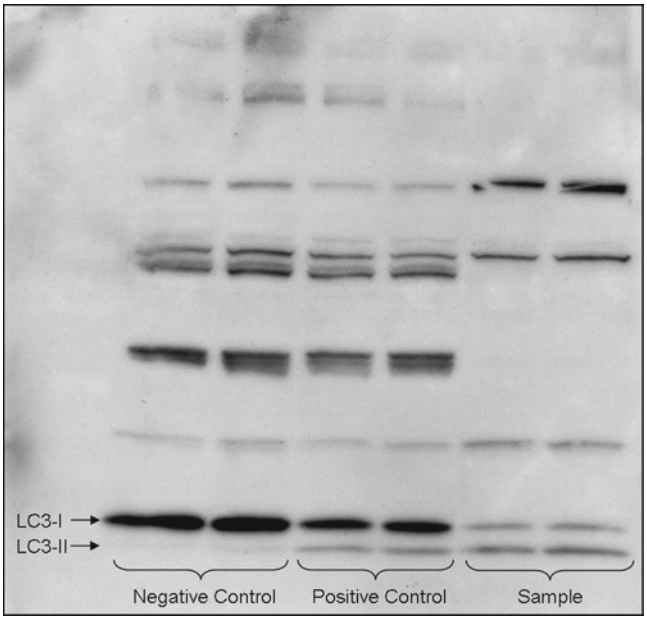

Fig. 1. LC3 immunoblot. LLC-PK1 cells were treated for 6 h with media, starvation buffer, and nanoparticle sample in duplicate. Cell lysate proteins were separated by SDS-PAGE, transferred to PVDF membrane, and probed for LC3 reactive proteins. LC3-I and II split products are labeled on the immunoblot.

12. Incubate membrane with 3 mL of peroxidase substrate solution (1:1 peroxidase substrate to luminol enhancer solution) for approximately 1 min and allow blot to develop for 5 and 8 min (see Fig. 1).

3.4. India Ink Staining

1. Wash blot in 100 mL of PBS/Tween 20 (0.3%), with two changes at 5 min each.
2. Place the blot in ~100 mL of India ink suspension 10 of materials.
3. Incubate at RT for 15 min–18 h. Longer incubations will increase sensitivity.
4. Destain by washing the blot in multiple changes of PBS.
5. Let blot air-dry and place in saran wrap to archive.

3.5. Assay Acceptance Criteria

1. Run is acceptable if both replicates of the positive control demonstrate acceptable performance, i.e., evident lipidation of LC3-I–LC3-II in comparison to negative media control.
2. If one of the replicates of the positive control fails to meet the acceptance criterion, the entire run should be repeated.
3. If both replicates of a study sample demonstrate evident conversion of LC3-I, or one replicate is positive and the other replicate demonstrates intermediate conversion, the sample is considered positive.

4. If one replicate of the nanoparticle sample is positive and the other replicate is negative, then this nanoparticle sample should be reanalyzed.
5. If both replicates of a nanoparticle sample demonstrate lipidation of LC3-I to LC3-II, then the sample is considered positive for autophagy interaction.
6. India ink staining of blot in section 3.4 can be used to insure comparable protein loading, as well as reprobing of initial blot with antibody to a housekeeping protein such as Beta-actin. If unequal protein loading is observed, the gel should be rerun.

4. Notes

1. If antibody from a source other than that tested in validation is used, the final dilution of this antibody can be adjusted to provide more optimal assay performance (i.e., minimum background, high signal-to-noise ratio).
2. Always wear appropriate personal protective equipment and take appropriate precautions when handling your nanomaterial. Many occupational health and safety practitioners recommend wearing two layers of gloves when handling nanomaterials. Also, be sure to follow your facility's recommended disposal procedure for your specific nanomaterial.
3. The appropriate test nanomaterial concentrations should be determined based on the results of an in vitro cytotoxicity assay (e.g., the same or similar to those described in Chapter 16).
4. At this stage, samples can be used for further analysis if frozen at a temperature of –80°C. If frozen, samples should be thawed at RT, vortexed, and briefly spun down before analysis.

Acknowledgments

This project has been funded in whole or in part by federal funds from the National Cancer Institute, National Institutes of Health, under contract N01-CO-12400. The content of this publication does not necessarily reflect the views or policies of the Department of Health and Human Services, nor does the mention of trade names, commercial products, or organizations imply endorsement by the U.S. Government.

References

1. Schneider, P., Korolenko, T.A., and Busch, U. (1997). A review of drug-induced lysosomal disorders of the liver in man and laboratory animals. *Microsc Res Tech.* **36**, 253–75.
2. Moore, M.N. (2006). Do nanoparticles present ecotoxicological risks for the health of the aquatic environment? *Environ Int.* **32**, 967–76.
3. Zabirnyk, O., Yezhelyev, M., and Seleverstov, O. (2007). Nanoparticles as a novel class of autophagy activators. *Autophagy.* **3**, 278–81.
4. Klionsky, D.J., Cuervo, A.M., and Seglen, P.O. (2007) Methods for monitoring autophagy from yeast to human. *Autophagy.* **3**, 181–206.
5. Mizushima, N., and Yoshimori, T. (2007) How to interpret LC3 immunoblotting. *Autophagy.* **3**, 542–5.

Chapter 22

Monitoring Lysosomal Activity in Nanoparticle-Treated Cells

Barry W. Neun and Stephan T. Stern

Abstract

Certain nanoparticles have been shown to accumulate within lysosome and hence may cause lysosomal pathologies such as phospholipidosis, lysosomal overload, and autophagy. This chapter describes a method for evaluation of lysosomal activity in porcine kidney cells (LLC-PK1) after exposure to nanoparticles. This method uses the accumulation of a cationic fluorescent dye (LysoTracker Red) in acidic cellular compartments as an indicator of total lysosome content. The lysotracker signal is normalized to the signal from a thiol-reactive dye which is proportional to the total number of viable cells.

Key words: Nanoparticles, lysosomal activity, lysosome, nanoparticle autophagy, lysotracker

1. Introduction

Lysosomal dysfunction is recognized as a potential toxic mechanism for xenobiotics that can result in various pathological states (1). There is concern that nanoparticles in particular may cause lysosomal pathologies, since they are likely to accumulate within lysosome (2). Lysosomal dysfunction could result from nanoparticle biopersistance or inhibition of lysosomal enzymes, such as inhibition of phospholipase resulting in phospholipidosis or inhibition of lysosomal protein degradation resulting in lysosomal overload (1). Nanoparticle exposure has also been shown to cause autophagic activation (3), resulting in increased lysosomal-mediated degradation of cellular organelles. Common methods used to characterize lysosomal activity include direct morphological assessment via light and electron microscopy, in both cell culture and tissue samples, as well as use of lysosomal dyes (4, 5). The method detailed in this chapter utilizes a lysosomal dye-staining method and is suited to high-throughput screening.

The method in this chapter is based on one previously developed by Rodriguez-Enriquez et al. (6). However, the method presented here uses LLC-PK1 cells rather than rat primary hepatocytes,

Scott E. McNeil (ed.), *Characterization of Nanoparticles Intended for Drug Delivery*, Methods in Molecular Biology, vol. 697,
DOI 10.1007/978-1-60327-198-1_22,

has different LysoTracker dye incubation conditions, and does not require a fixation step. Additionally, this method utilizes a CellTracker dye (in addition to the LysoTracker dye) for normalization of viable cell number. CellTracker green CMFDA is deacetylated within viable cells to a thiol-reactive dye that remains in the cytosol, and is used to normalize the LysoTracker signal to viable cells. LysoTracker Red is a cationic fluorescent dye that preferentially accumulates in the acidic lysosomal compartment. Therefore, the amount of dye taken up by cells in culture can be used as an indicator of lysosome content. Decreased dye uptake (relative to control) may indicate conditions such as decreased lysosomal stability, while increased dye uptake may be indicative of autophagic activation. As other conditions (such as changes in lysosomal pH) can also cause changes in dye uptake, treatment-related responses to dye uptake should be further evaluated by morphological assessment, using techniques such as electron microscopy, to confirm lysosomal involvement.

2. Materials

1. 50 nM LysoTracker Red stain (see Note 1): add 5 µL 1 mM LysoTracker Red (DND-99, Invitrogen, Cat. #L7528) to 95 µL phenol-free RPMI cell culture medium (HyClone, Cat. #SH3060501). Then, add 100 µL of this solution to 10 mL phenol-free RPMI to make a 50 nM Lysotracker Red stain working solution.
2. 10 µM CellTracker green co-stain (see Note 1): add 50 µL dimethylsulfoxide (DMSO) to 50 µg CellTracker green dye (CellTracker Green CMFDA, Invitrogen, Cat. #C2925). Add 50 µL of this solution to the 50 nM working solution to make the co-staining solution.
3. Nanoparticle sample (see Notes 2 and 3) diluted in M199 cell culture medium (Lonza, Allendale, NJ) with 3% Fetal Bovine Serum (FBS).
4. Costar 96-well flat-bottom cell culture plates.
5. Hank's Balanced Salt Solution (with calcium and magnesium) (Gibco, Cat. #24026).
6. LLC-PK1 Cells (ATTC #CL-101).

3. Methods

3.1. LLC-PK1 Cell Preparation

1. Harvest cells from cryopreserved cells according to the instructions from the supplier (limit passages to 20). An example of the appearance of the cells is in Fig. 1.

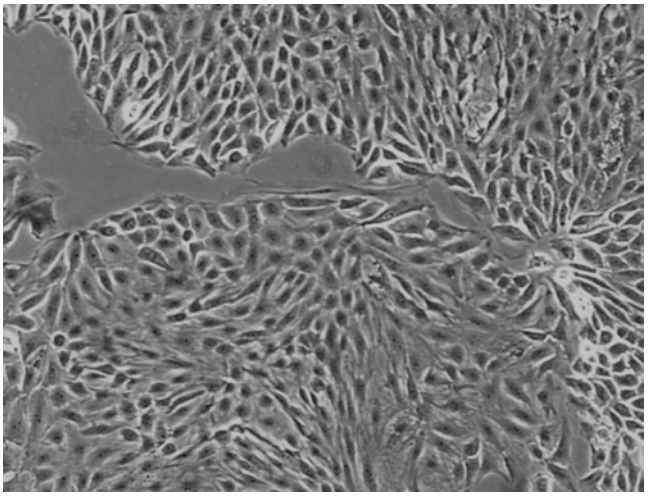

Fig. 1. Example of LLC-PK1 cell culture appearance. Image was taken with a phase-contrast microscope at 225× magnification. LLC-PK1 cells are approximately 80% confluent at this stage.

2. Count the cell concentration using a Coulter counter or hemocytometer.
3. Dilute cells to a density of 1×10^5 cells/mL in M199 (3% FBS) cell culture media.
4. Plate 100 µL of cells per well as per plate format for 96-well plate as outlined in Fig. 2. The format indicates no cells in rows D & E, and they serve as blanks. Three plastes are required, for time points 4, 24 and 48h. Incubate plates at 37C, 5% CO_2 and 95% humidity for 24h (cells should be approximately 80% confluent, see Fig. 1).
5. Remove media and add 100 µL of test samples and positive (HBSS) and media controls samples and positive HBSS starvation control to the plate as indicated in Fig. 1. Each plate accommodates only one sample. The top half of the plate (Row A-C) is stained, and the bottom half of the plate (Rows F-H) serves as unstained particle controls to identify assay interference. Each nanoparticle is tested at nine dilutions for a total of ten wells.
6. Incubate plates as designated in 5% CO_2, at 37°C and 95% humidity.

3.2. LysoTracker/ CellTracker Stain

1. Wash plate twice with 200 µL phenol-free RPMI medium/ well.
2. Add 100 µL of 50 nm LysoTracker Red and 10 µM CellTracker green co-stain to the top half of the plate and phenol-free RPMI medium to the bottom half of the plate, and incubate for 1 h.

	1	2	3	4	5	6	7	8	9	10	11	12
A	Cells Media Control	Cells Sample Dilution 10	Cells Sample Dilution 9	Cells Sample Dilution 8	Cells Sample Dilution 7	Cells Sample Dilution 6	Cells Sample Dilution 5	Cells Sample Dilution 4	Cells Sample Dilution 3	Cells Sample Dilution 2	Cells Sample Dilution 1	Cells **HBSS pos control**
B	Cells Media Control	Cells Sample Dilution 10	Cells Sample Dilution 9	Cells Sample Dilution 8	Cells Sample Dilution 7	Cells Sample Dilution 6	Cells Sample Dilution 5	Cells Sample Dilution 4	Cells Sample Dilution 3	Cells Sample Dilution 2	Cells Sample Dilution 1	Cells **HBSS pos control**
C	Cells Media Control	Cells Sample Dilution 10	Cells Sample Dilution 9	Cells Sample Dilution 8	Cells Sample Dilution 7	Cells Sample Dilution 6	Cells Sample Dilution 5	Cells Sample Dilution 4	Cells Sample Dilution 3	Cells Sample Dilution 2	Cells Sample Dilution 1	Cells **HBSS pos control**
D	Media Media Control Blank	Media Sample Dilution Blank 10	Media Sample Dilution Blank 9	Media Sample Dilution Blank 8	Media Sample Dilution Blank 7	Media Sample Dilution Blank 6	Media Sample Dilution Blank 5	Media Sample Dilution Blank 4	Media Sample Dilution Blank 3	Media Sample Dilution Blank 2	Media Sample Dilution Blank 1	Media HBSS pos control blank
E	Media Media Control Blank	Media Sample Dilution Blank 10	Media Sample Dilution Blank 9	Media Sample Dilution Blank 8	Media Sample Dilution Blank 7	Media Sample Dilution Blank 6	Media Sample Dilution Blank 5	Media Sample Dilution Blank 4	Media Sample Dilution Blank 3	Media Sample Dilution Blank 2	Media Sample Dilution Blank 1	Media HBSS pos control blank
F	Cells Media Control	Cells Sample Dilution 10	Cells Sample Dilution 9	Cells Sample Dilution 8	Cells Sample Dilution 7	Cells Sample Dilution 6	Cells Sample Dilution 5	Cells Sample Dilution 4	Cells Sample Dilution 3	Cells Sample Dilution 2	Cells Sample Dilution 1	Cells **HBSS pos control**
G	Cells Media Control	Cells Sample Dilution 10	Cells Sample Dilution 9	Cells Sample Dilution 8	Cells Sample Dilution 7	Cells Sample Dilution 6	Cells Sample Dilution 5	Cells Sample Dilution 4	Cells Sample Dilution 3	Cells Sample Dilution 2	Cells Sample Dilution 1	Cells **HBSS pos control**
H	Cells Media Control	Cells Sample Dilution 10	Cells Sample Dilution 9	Cells Sample Dilution 8	Cells Sample Dilution 7	Cells Sample Dilution 6	Cells Sample Dilution 5	Cells Sample Dilution 4	Cells Sample Dilution 3	Cells Sample Dilution 2	Cells Sample Dilution 1	Cells **HBSS pos control**

Fig. 2. Example of 96-well plate format. HBS stands for Hank's balanced salt solution (with calcium and magnesium) HBSS is sed as a positive control of lysosomal activation. HBSS starves cells and induces autophagy-related lysosomal activity.

3. Rinse plate twice with 200 µL of phenol-free RPMI/well and add 200 µL phenol-free RPMI to each well.
4. Read fluorescence at ex. 544 nm/em. 590 nm (Lysotracker Red), ex. 492 nm/em. 517 nm (Cell Tracker Green).

3.3. Calculations

1. The percent control LysoTracker Red fluorescence (%LRF) is calculated as:

$$\%\mathrm{LRF} = \frac{\mathrm{NE}_{590\mathrm{nm}} - \mathrm{CFNBE}_{590\mathrm{nm}}}{\mathrm{CE}_{590\mathrm{nm}} - \mathrm{CFMBE}_{590\mathrm{nm}}}$$

Where NE_{590nm} is the Lysotracker Red emission of the nanoparticle sample, $CFNBE_{590nm}$ is the Lysotracker Red emission of the cell-free nanoparticle blank, CFMBE is the Lysotracker Red emission of the cell-free media control blank, and CE_{590nm} is the Lysotracker Red emission of the media control.

2. Similarly, the percent control CellTracker green fluorescence (%CGF) is calculated as:

$$\%\mathrm{CGF} = \frac{\mathrm{NE}_{466nm} - \mathrm{CFNBE}_{466nm}}{\mathrm{CE}_{466nm} - \mathrm{CFMBE}_{466nm}}$$

Where NE_{466nm} is the Cell Tracker Green emission of the nanoparticle sample, $CFNBE_{466nm}$ is the Cell Tracker Green emission of the cell-free nanoparticle blank, CFMBE is the Cell Tracker Green emission of the cell-free media control blank, and CE_{466nm} is the Cell Tracker Green emission of the media control.

3. The mean (μ), standard deviation (SD), and %CV ($\%CV = (\mathrm{SD}/\mu) \times 100$) of the ratio of %LRF to %CGF should be calculated for each nanoparticle sample and positive control.
4. Fluorescence of the sample dilution wells in the bottom, unstained portion of the plate indicates that the test material may cause assay interference.
5. The starvation-positive control wells (HBSS cells wells) average should be 150% of control or greater at 24 h, and %CV should be less than 50%.
6. If the above acceptance criteria are not met, the assay should be repeated.
7. The %CV of the sample dilution wells should be less than 50%, or the assay should be repeated.
8. Significant differences between media and nanoparticle teated wells indicate a treatment-related effect on lysosomal activity. As other conditions (such as changes in lysosomal pH) can also cause changes in dye uptake, treatment-related responses to dye uptake should be further evaluated by morphological assessment, using techniques such as electron microscopy, to confirm lysosomal involvement.

4. Notes

1. Work in the Dark. The dyes used in this method are light-sensitive and must be prepared and used in the dark. Prepare in a dark room and take all appropriate measures to protect the solution from light.

2. Always wear appropriate personal protective equipment and take appropriate precautions when handling your nanomaterial. Many occupational health and safety practitioners recommend wearing two layers of nitrile gloves when handling nanomaterials, and performing all work in an exhausted BSL II-B2 hood. Also, be sure to follow your facility's recommended disposal procedure for your specific nanomaterial.
3. Test your nanoparticle at physiological pH at a highest concentration approaching the limit of solubility and then at nine 1:4 dilutions (for a total of ten nanoparticle test samples). It may be necessary to neutralize acidic/basic nanoparticle samples to achieve physiological pH.
4. This test method involves the use of a fluorescent spectrophotometer with readings at ex. 544 nm/em. 590 nm (Lysotracker Red), ex. 492 nm/em. 517 nm (Cell Tracker Green). If the particle suspension interferes at these wavelengths this test method may not be applicable, and other methods must be explored.
5. Precision and bias have not been determined for this assay.

Acknowledgments

This project has been funded in whole or in part by federal funds from the National Cancer Institute, National Institutes of Health, under contract N01-CO-12400. The content of this publication does not necessarily reflect the views or policies of the Department of Health and Human Services, nor does the mention of trade names, commercial products, or organizations imply endorsement by the U.S. Government.

References

1. Schneider, P., Korolenko, T.A., and Busch, U. (1997). A review of drug-induced lysosomal disorders of the liver in man and laboratory animals. *Microsc Res Tech.* **36**, 253–75.
2. Moore, M.N. (2006). Do nanoparticles present ecotoxicological risks for the health of the aquatic environment? *Environ Int.* **32**, 967–76.
3. Zabirnyk, O., Yezhelyev, M., and Seleverstov, O. (2007). Nanoparticles as a novel class of autophagy activators. *Autophagy* **3**, 278–81.
4. Monteith, D.K., Morgan, R.E., Halstead, B. (2006). In vitro assays and biomarkers for drug-induced phospholipidosis. *Expert Opin Drug Metab Toxicol.* **2**, 687–96.
5. Klionsky, D.J., Cuervo, A.M., Seglen, P.O. (2007). Methods for monitoring autophagy from yeast to human. *Autophagy* **3**, 181–206.
6. Rodriguez-Enriquez, S., Kim, I., Currin, R.T., and Lemasters, J.J. (2006). Tracker dyes to probe mitochondrial autophagy (mitophagy) in rat hepatocytes. *Autophagy* **2**, 39–46.

Part VI

In Vitro Immunological Assays

Chapter 23

Method for Analysis of Nanoparticle Hemolytic Properties In Vitro

Barry W. Neun and Marina A. Dobrovolskaia

Abstract

Hemolysis is damage to red blood cells (RBCs), which results in the release of the iron-containing protein hemoglobin into plasma. Here we describe an in vitro assay specifically developed for the analysis of nanoparticle hemolytic properties (see Fig. 1). In this assay, analyte nanoparticles are incubated in blood, and hemoglobin is released by damaged cells and converted to red-colored cyanmethemoglobin by reagents. The nanoparticles and undamaged RBCs are then removed by centrifugation, and the amount of cyanmethemoglobin in the supernatant is measured by spectrophotometry. This measured absorbance is compared to a standard curve to determine the concentration of hemoglobin in the supernatant. This hemoglobin concentration is then compared to that in the supernatant of a blood sample treated with a negative control to obtain the percentage of nanoparticle-induced hemolysis.

Key words: nanoparticles, hemolysis, hemoglobin, red blood cells (RBC)

1. Introduction

Hemolysis is a potentially life-threatening condition, as it may result in anemia and jaundice. Certain natural and engineered nanoparticles have been shown to be hemolytic, and preclinical characterization of the blood contact properties of newly developed nanomedicines includes a screen for hemolytic potential. The small size and unique physicochemical properties of nanoparticles may cause their interactions with RBCs to differ from those of conventional pharmaceuticals, and standard pharmacological screens for hemolysis must be modified for application to nanoparticles.

Here we describe an in vitro assay developed specifically for the analysis of nanoparticle hemolytic properties. This is a colorimetric assay to determine the percentage of nanoparticle-induced hemolysis from the concentration of released hemoglobin when blood is exposed to nanoparticles. Red-colored cyanmethemoglobin (CMH)

Scott E. McNeil (ed.), *Characterization of Nanoparticles Intended for Drug Delivery*, Methods in Molecular Biology, vol. 697,
DOI 10.1007/978-1-60327-198-1_23,

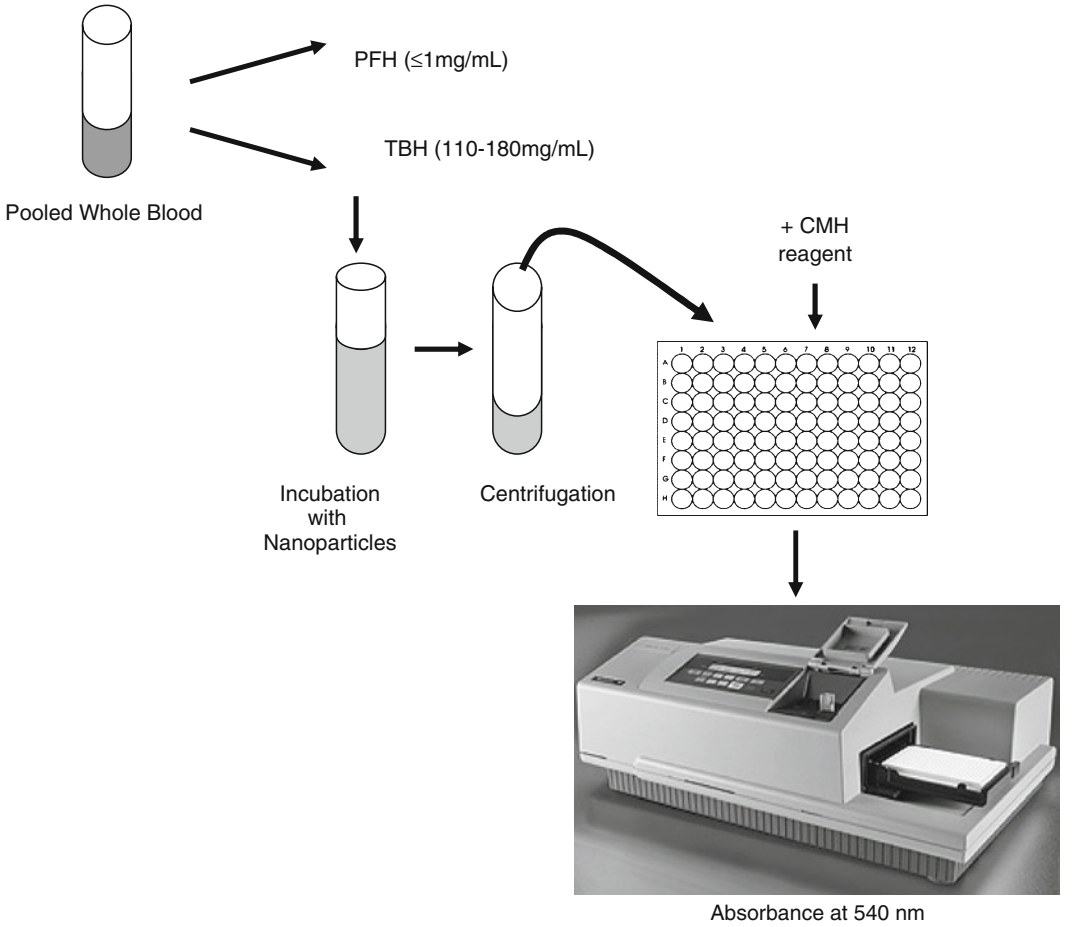

Fig. 1. Schematic illustration of the steps in this in vitro assay to evaluate nanoparticle hemolytic properties. PFH is plasma-free hemoglobin. CMH is cyanmethemoglobin. TBH is total blood hemoglobin.

(a derivative of hemoglobin formed by reaction with ferricyanide in the presence of bicarbonate) is detected by spectrophotometry of hemoglobin standard samples and the supernatants of nanoparticle samples incubated with blood after undamaged red blood cells (RBCs) have been removed by centrifugation. This method is developed based on existing international standard ASTMF 756-00 (1). The method is optimized for nanoparticle partial acceptance criteria are based on recommendations for bioanalytical method validation below (2, 3).

One of the biggest challenges in using this test for analysis of nanoparticles is particle interference with the assay. This interference may be due to particle absorbance near the wavelength used to detect CMH or to nanoparticle adsorption of hemoglobin making it unavailable for the detection. Alternatively, nanoparticle pro-coagulant properties may cause blood clots that effectively prevent erythrocytes from coming into contact with the nanoparticles (protection by the clots). Here, we provide a few examples of these types of interferences and suggest approaches to identify and overcome them.

2. Materials

1. Cyanmethemoglobin (CMH) reagent (StanBio Laboratory, Boerne, TX).
2. Hemoglobin Standard (StanBio Laboratory, Boerne, TX).
3. Ca^{2+}/Mg^{2+}-free PBS. Store at room temperature.
4. Pooled normal human whole blood anti-coagulated with lithium–heparin.
5. Polyethylene glycol, MW 8,000: Polyethylene glycol is supplied as 40% stock solution in water. Use this solution as the negative control. Store the stock solution at a temperature of +4°C.
6. Triton X-100: Dilute concentrated stock solution of Triton X-100 to a final concentration of 1% in sterile distilled water. Prepare single-use aliquots and store at a temperature of +4°C. This solution will serve as the positive control.
7. Distilled water.
8. 96-Well plates.
9. Analyte nanoparticle sample (see Note 1).

3. Methods

3.1. Sample Preparation

1. Preparation of calibration samples. Prepare calibration samples following the scheme in Table 1.
2. Preparation of quality controls. Prepare quality control samples following the scheme in Table 2.

Table 1
Preparation of calibration samples

Calibration sample	Nominal Conc. (mg/mL)	Preparation procedure
Cal 1	0.80	2 mL of Stock solution (hemoglobin standard in CMH reagent)
Cal 2	0.40	1 mL Cal 1 + 1 mL CMH reagent
Cal 3	0.20	1 mL Cal 2 + 1 mL CMH reagent
Cal 4	0.10	1 mL Cal 3 + 1 mL CMH reagent
Cal 5	0.05	1 mL Cal 4 + 1 mL CMH reagent
Cal 6	0.025	1 mL Cal 5 + 1 mL CMH reagent

Table 2
Preparation of quality control samples

Quality control samples	Nominal Conc. (mg/mL)	Preparation procedure
QC 1	0.625	1.5 mL of Stock hemoglobin standard + 0.42 mL CMH reagent
QC 2	0.125	200 µL QC 1 + 800 µL CMH reagent
QC 3	0.125	200 µL QC 1 + 800 µL CMH reagent

3. Preparation of analyte nanoparticle samples. The nanoparticle formulation will be tested at four concentrations: high concentration (determined by expected therapeutic dose or as reasonably achievable) and three serial 1:5 dilutions of the high concentration. The assay requires 300 µL of test nanomaterial.

3.2. Qualification of Blood (Steps 1–9) and Hemolysis Test (Steps 10–23)

1. Collect whole blood from at least three donors in tubes containing Li–heparin as anti-coagulant. The blood can be stored at 4°C for up to 48 h. On the day of assay prepare pooled blood by mixing equal proportions of blood from each donor.
2. Take a 2–3 mL aliquot of the pooled blood and centrifuge for 15 min at 800 × *g*.
3. Collect supernatant. Keep at room temperature. The collected sample is used to determine the amount of plasma-free hemoglobin (PFH).
4. Add 200 µL of each calibration standard (CAL), quality control (QC), and blank (B0) CMH reagent to each designated well on 96-well plate. Follow the plate 1 map scheme shown in Fig. 2. Position nanoparticle samples so they are bracketed by quality control samples.
5. Add 200 µL of total blood hemoglobin (TBH) sample prepared by combining 20 µL of the pooled whole blood and 5.0 mL of CMH reagent to the designated wells. Follow plate 1 map scheme shown in Fig. 2.
6. Add 100 µL of plasma (PFH) per designated well on 96-well plate. Follow plate 1 map scheme shown in Fig. 2.

Fig. 2. Plate map for 96-well plate. B0 stands for blank. CAL stands for calibration sample. QC for quality control sample. PFH is plasma-free hemoglobin. TBH is total blood hemoglobin. TBHd is total blood hemoglobin after dilution to theoretical value of 10 mg/mL. NP stands for nanoparticle sample.

Plate 1 - used to determine amount of total blood hemoglobin and plasma free hemoglobin

	1	2	3	4	5	6	7	8	9	10	11	12
A	B0	CAL1	CAL2	CAL3	CAL4	CAL5	CAL6	QC1	QC2	QC3	TBH	TBH
B	B0	CAL1	CAL2	CAL3	CAL4	CAL5	CAL6	QC1	QC2	QC3	TBH	TBH
C	TBH	PFH	PFH	PFH	B0	QC1	QC2	QC3				
D	TBH	PFH	PFH	PFH	B0	QC1	QC2	QC3				
E												
F												
G												
H												

Plate 2 or any subsequent plates - used to determine hemolysis in nanoparticle samples

	1	2	3	4	5	6	7	8	9	10	11	12
A	B0	CAL1	CAL2	CAL3	CAL4	CAL5	CAL6	QC1	QC2	QC3	TBHd	TBHd
B	B0	CAL1	CAL2	CAL3	CAL4	CAL5	CAL6	QC1	QC2	QC3	TBHd	TBHd
C	TBHd	NP w/Blood	NP w/Blood	NP w/Blood	NP w/Blood	NP w/Blood	NP w/Blood	NP w/Blood	NP w/Blood	NP w/Blood	NP w/Blood	NP w/Blood
D	TBHd	NP w/Blood	NP w/Blood	NP w/Blood	NP w/Blood	NP w/Blood	NP w/Blood	NP w/Blood	NP w/Blood	NP w/Blood	NP w/Blood	NP w/Blood
E	NP w/Blood	NP w/o Blood	NP w/o Blood	NP w/o Blood	NP w/o Blood	NP w/o Blood	NP w/o Blood	NP w/o Blood	NP w/o Blood	NP w/o Blood	NP w/o Blood	NP w/o Blood
F	NP w/Blood	NP w/o Blood	NP w/o Blood	NP w/o Blood	NP w/o Blood	NP w/o Blood	NP w/o Blood	NP w/o Blood	NP w/o Blood	NP w/o Blood	NP w/o Blood	NP w/o Blood
G	NP w/o Blood	PC	PC	NC	NC	B0	QC1	QC2	QC3			
H	NP w/o Blood	PC	PC	NC	NC	B0	QC1	QC2	QC3			

7. Add 100 µL of CMH reagent to each well containing sample (see Note 2).
8. Cover plate with plate sealer and gently shake on a plate shaker for 1–2 min (shaker speed settings should be vigorous enough to allow mixing the reagent, but avoid spillage and cross-well contamination, e.g., LabLine shaker setting no. 2).
9. Read the absorbance of all wells at 540 nm. Create a calibration curve from a linear regression algorithm to the absorbance of the calibration samples. Calculate and record the amount of hemoglobin contained in each well from their absorbance extrapolated to the calibration curve. Use a dilution factor of 2 for the PFH samples and a dilution factor of 251 for the TBH samples (see Note 3). The calculated PFH concentration should be below 1 mg/mL.
10. Dilute pooled whole blood with Ca^{2+}/Mg^{2+}-free PBS to adjust total hemoglobin concentration to approximately 10 mg/mL.
11. In an Eppendorf tube, add 100 µL of nanoparticle sample, blank (i.e., buffer used to reconstitute nanoparticle sample), positive, and negative control. Prepare six tubes for each nanoparticle sample, three tubes for the blank, two tubes for the positive control, and two tubes for the negative control.
12. Add 700 µL of Ca^{2+}/Mg^{2+}-free PBS to each tube.
13. Add 100 µL of the whole blood prepared in step 10 to each tube, except for three tubes of each nanoparticle sample. To these tubes, add 100 µL of Ca^{2+}/Mg^{2+}-free PBS. These samples represent a "without blood" control and are used to evaluate potential interference of the nanomaterial with the assay (e.g., absorbance at or close to 540 nm, reactivity with CMH reagent, etc. see Note 4).
14. Cover tubes and gently rotate to mix (see Note 5).
15. Place the tubes in a water bath set at 37°C and incubate for 3 h mixing the samples every 30 min. Alternatively, tubes may be incubated for 3 h on a tube rotator in an incubator set at 37°C.
16. Remove the tubes from the water bath or incubator. If the water bath was used, remove water from the exterior of the tubes.
17. Centrifuge the tubes for 15 min at 800×*g* (see Note 6). Examine each tube for the presence of potential interference.
18. Prepare a fresh set of calibration samples and quality controls.
19. To the fresh 96-well plate add 200 µL of blank reagent, calibration samples, quality controls, or total blood hemoglobin sample (TBHd) prepared by combining 400 µL of blood

from step 10 with 5.0 mL of CMH reagent. Follow the plate 2 scheme shown in Fig. 2.

20. Add 100 μL of nanoparticle samples, positive and negative controls per well. Fill 12 wells for each sample (two wells for each of the six nanoparticle sample tubes prepared in step 11) and four wells for each control. Follow the plate 2 scheme in Fig. 2.
21. Add 100 μL of CMH reagent to each well containing sample and controls (see Note 2).
22. Cover plate with plate sealer and gently shake on a plate shaker (e.g., LabLine shaker speed setting no. 2).
23. Read the absorbance of each well at 540 nm. Create a second calibration curve from a linear regression algorithm to the absorbance of the calibration samples. Calculate and record the amount of hemoglobin contained in each well from their absorbance extrapolated to the calibration curve. Use dilution factor 18 for samples and controls (where blood is diluted 1:9) and dilution factor 13.5 for TBHd.

3.3. Calculations and Criteria for Assay Acceptance

1. A linear regression algorithm is used to build two calibration curves. The following parameters should be calculated for each calibrator and quality control sample.
   The percent coefficient of variation (%CV) is calculated as:

$$\%\mathrm{CV} = \left(\frac{\mathrm{SD}}{\mu}\right) \times 100,$$

   where SD is the standard deviation and μ is the mean.
   The percent difference from theoretical (PDFT) is calculated as:

$$\mathrm{PDFT} = \frac{\left(\mathrm{Conc}_{\mathrm{calculated}} - \mathrm{Conc}_{\mathrm{Theoretical}}\right)}{\mathrm{Conc}_{\mathrm{Theoretical}}} \times 100.$$

   %CV and PDFT should be calculated for each blank, positive control, negative control, and unknown sample.
2. %CV and PDFT for each calibration standard and quality control should be within 20%. The exception is Cal 6, for which 30% is acceptable. An entire plate is acceptable if 2/3 of all quality control sample levels and at least one of each calibration sample level have %CV and PDFT <20%.
3. % CV for each positive control, negative control, and unknown sample should be within 20%. If both replicates of positive control or negative control fail to meet this acceptance criterion, the run should be repeated.

4. Within an acceptable run, if two of three replicates of an unknown sample fail to meet the acceptance criterion, the unknown sample should be reanalyzed.

4. Notes

1. Always wear appropriate personal protective equipment and take appropriate precautions when handling your nanomaterial. Many occupational health and safety practitioners recommend wearing two layers of gloves when handling nanomaterials. Also, be sure to follow your facility's recommended disposal procedure for your specific nanomaterial.
2. *Do not* add CMH reagent to wells containing calibration standards, quality controls, TBH, or TBHd. These samples were prepared in CMH reagent and do not require further dilution.
3. Calibration standards and quality control samples are prepared twice, and separate calibration curves are generated with each set of calibration standards. The first set is used to qualify the blood (i.e., to determine the total blood hemoglobin and plasma-free hemoglobin in steps 1–9 of Subheading 3.2) and the second set is used to evaluate hemolysis in test samples (steps 10–23 of Subheading 3.2).
4. If nanoparticles have absorbance at or close to 540 nm, it is necessary to remove the particles from the supernatant before proceeding to the next step. For example, 10–50 nm colloidal gold nanoparticles have absorbance at 535 nm. For these nanoparticles, after step 17, the supernatants should be transferred to fresh tubes and centrifuged 30 min at 18,000 × *g*. The most effective method for removing nanoparticles from the supernatant will vary with the type of nanoparticles (e.g., small superparamagnetic iron oxide nanoparticles can be removed from supernatants by magnetic separation, see Fig. 3), and when applied, appropriate validation experiments should be conducted to ensure that a given separation procedure does not affect assay performance. In certain cases, removing the nanoparticles from the supernatant without disturbing hemoglobin is not feasible. In these instances, the result from the "without blood" control can be subtracted from the nanoparticle sample (see step 13 of Subheading 3.2 above).
5. Vortexing may damage erythrocytes and should be avoided.
6. When centrifugation is complete, examine the tubes and record any unusual appearance. See example in Fig. 4.

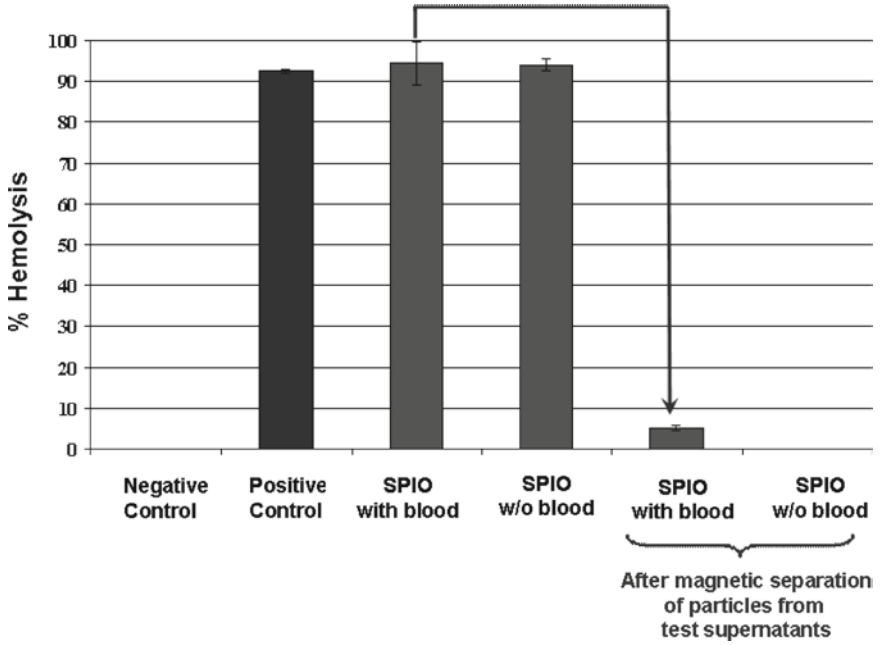

Fig. 3. Example of false-positive interference. In this example, superparamagnetic iron oxide nanoparticles were tested in the hemolysis assay. When the optical density (OD) of the nanoparticles is evaluated against the hemoglobin standard curve, it results in 100% hemolysis. When a control sample containing all reaction components except the blood (without blood control) is evaluated against the same standard curve, the calculated percent hemolysis is also very high and approaching 100%. Before testing on the 96-well plate, the tube containing cell-free supernatant was incubated on a magnet for 16 h. At the end of the incubation, iron oxide nanoparticles accumulated near the magnet, which allowed for the collection of the nanoparticle-free supernatant. When this supernatant was evaluated against the standard curve, no percent hemolysis was calculated in the without blood control and nanoparticle hemolysis was below 2%.

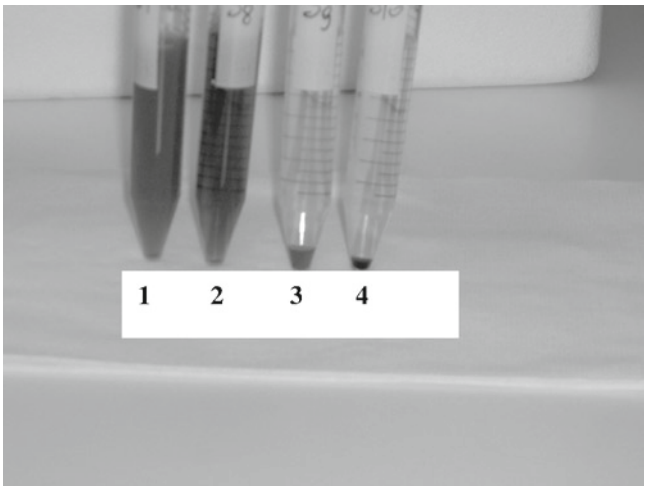

Fig. 4. Example of false-negative interference. This example demonstrates the importance of recording sample appearance after centrifugation to avoid false-negative results. Polystyrene nanoparticles with size 20 nm (tube 1) and polystyrene nanoparticles with size 50 nm (tube 2) demonstrated hemolytic activity, which can be observed by the shade of supernatant. Polystyrene nanoparticles with size 80 nm were also hemolytic; however, they absorbed hemoglobin which is evident from the pellet size and shade. Sample no. 4 is the negative control. No hemolytic activity was observed in the supernatant, and intact red blood cells formed tight dark pellet on the *bottom* of the tube.

Acknowledgments

This project has been funded in whole or in part with federal funds from the National Cancer Institute, National Institutes of Health, under contract N01-CO-12400. The content of this publication does not necessarily reflect the views or policies of the Department of Health and Human Services, nor does mention of trade names, commercial products, or organizations imply endorsement by the US Government.

References

1. ASTM standard practice F 756-00. Assessment of hemolytic properties of materials.
2. DeSilva, B., Smith, W., Weiner, R., Kelley, M., Smolec, J., Lee, B., Khan, M., Tacey, R., Hill, H., and Celniker, A. (2003) Recommendations for the bioanalytical method validation of ligand-binding assays to support pharmacokinetic assessments of macromolecules. *Pharm Res.* **11**, 1885–900.
3. Bioanalytical method validation. Guidance for industry. FDA/CDER/CVM. May 2001. BP.

Chapter 24

Method for In Vitro Analysis of Nanoparticle Thrombogenic Properties

Barry W. Neun and Marina A. Dobrovolskaia

Abstract

Thrombus formation is complex process involving both cellular and molecular (protein) components. Platelets are responsible for maintaining hemostasis and for preventing excessive bleeding. These cells aggregate along with other plasma components and blood cells to form blood clots. Undesirable platelet aggregation may lead to life-threatening conditions such as stroke. Thrombogenicity is the property of a material to induce the formation of a thrombus, which results in partial or complete occlusion of a blood vessel. The tendency to cause platelet aggregation and perturb plasma coagulation can serve as an in vitro measure of a nanomaterial's likelihood to be thrombogenic in vivo. This chapter describes a procedure for in vitro analyses of platelet aggregation and plasma coagulation time. Platelet-rich plasma (PRP) is obtained from freshly derived human whole blood and incubated with nanoparticles. Then the plasma is examined using a particle count and size analyzer to determine the number of active platelets. The percent aggregation is calculated by comparing the number of active platelets in the nanoparticle-exposed sample to control plasma. To measure the plasma coagulation time, platelet-poor plasma from human whole blood is exposed to nanoparticles in vitro and analyzed in prothrombin (PT), activated partial thromboplastin (APTT), and thrombin time assays.

Key words: Nanoparticles, thrombogenicity, platelet aggregation, platelet, blood, plasma coagulation

1. Introduction

Thrombogenicity is the property of a material to induce the formation of a thrombus, which results in partial or complete occlusion of a blood vessel. Formation of a thrombus is a natural mechanism to prevent blood loss upon blood vessel damage. However, when a thrombus is caused by other conditions (e.g., thrombocytosis or a foreign material or drug), it may lead to a life-threatening condition such as stroke. Many blood components are involved in the formation of a thrombus. Platelets are small (~2 μm in size) cells, which originate from megakaryocytes

Scott E. McNeil (ed.), *Characterization of Nanoparticles Intended for Drug Delivery*, Methods in Molecular Biology, vol. 697,
DOI 10.1007/978-1-60327-198-1_24,

in the bone marrow. Platelets represent a key cellular component in the initiation of a thrombus. Platelet activation and aggregation are often used as surrogate marker for material/drug-mediated thrombogenicity. Previous studies have demonstrated that some nanomaterials can cause platelet aggregation and that this property largely depends on particle surface characteristic (1).

In this chapter, we describe a method for analysis of a nanoparticle's propensity to induce platelet aggregation or to interfere with collagen-induced platelet aggregation in vitro. Platelet-rich plasma (PRP) is obtained from freshly derived human whole blood and incubated with nanoparticles for 15 min at a temperature of 37°C. Afterwards, the PRP is analyzed using a particle count and size analyzer to determine the number of active platelets (2) (Fig. 1). The percent aggregation is calculated by comparing the number of active platelets counted in the nanoparticle-exposed sample to the one in an untreated PRP sample. Collagen is used in this test as a positive control. To evaluate potential nanoparticle interference (either enhancement or inhibition) with collagen-induced platelet aggregation, an additional series of test PRP samples are prepared and analyzed. The second part of the assay is evaluation of plasma coagulation time (Fig. 2) and How nanoparticles affect this part of homestasis control system (4). Both methods were developed to meet industry requirements to Bioanalytical procedures (3).

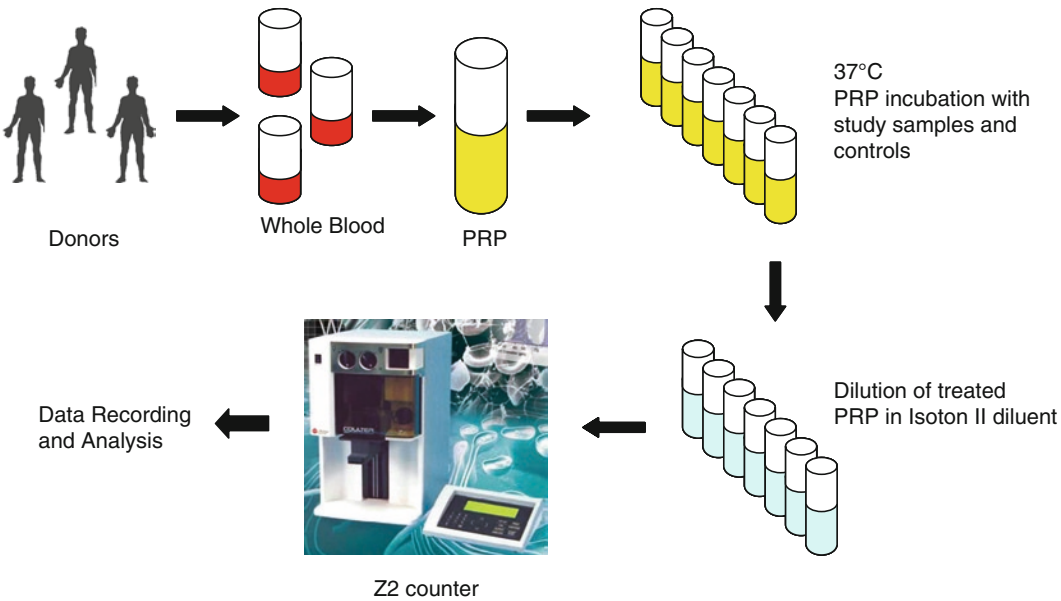

Fig. 1. Schematic diagram of platelet aggregation assay.

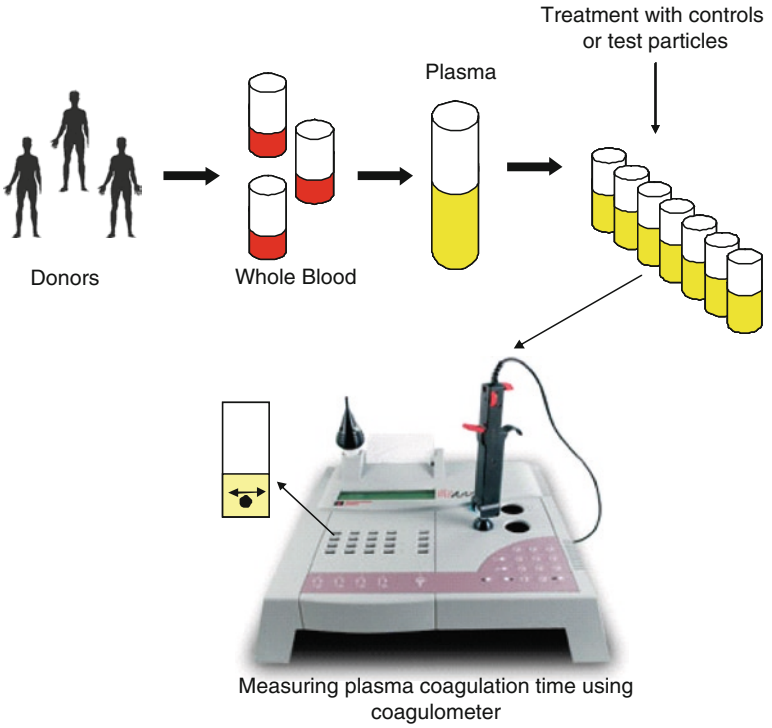

Fig. 2. Schematic diagram of coagulation time measurement.

2. Materials

The materials listed below are required for platelet aggregation study:

1. Calibration standards, 5 μm.
2. RPMI cell culture medium for use as a negative control (phosphate-buffered saline (PBS) may also be used for this purpose).
3. Sheath fluid appropriate for the instrument (e.g., Isoton II diluent or equivalent).
4. Buffer for cleaning and maintaining aperture tube (e.g., Coulter Clense or equivalent).
5. Freshly drawn human whole blood anti-coagulated with sodium citrate and obtained from at least three healthy donors known to be off any anti-inflammatory and anti-histamine medications, blood thinning agents and birth control pills (see Note 1).
6. Collagen (5–20 μg/mL).
7. Particle count and size analyzer (Beckman Coulter or equivalent).

8. Analyte nanoparticle samples (see Notes 2 and 3).

The materials listed below are required for plasma coagulation study:

9. Neoplastine Cl reagent.
10. Thrombin.
11. $CaCl^{2+}$ M.
12. Owren-Koller reagent.
13. PTT-A reagent.
14. Standard plasma samples known to be normal and abnormal in terms of coagulation time (e.g., CoagControlN+ABN from Diagnostica Stago or equivalent).
15. Coagulometer.

3. Methods

3.1. Platelet Aggregation

1. Prepare your particle count and size analyzer instrument as described in its user manual. For reference, see ref. 2.
2. Obtain PRP by spinning freshly drawn whole blood for 8 min at 200 × *g*. Pool the PRP from at least three donors before proceeding to next step (see Note 4).
3. (a) In three microcentrifuge tubes, combine 100 μL of PRP and 25 μL of either (1) the nanoparticles or (2) positive control (collagen) or (3) negative control (RPMI medium).

Prepare three replicates of each sample (nine samples in total). These samples will provide data on tendency of the test nanomaterial to induce platelet aggregation.

(b) In a separate set of three tubes, combine 100 μL of PRP with

- 25 μL of negative control (RPMI medium) and 25 μL of positive control (collagen).
- 25 μL of test nanomaterial and 25 μL of positive control (collagen).

Prepare three replicates for each combination (six samples in total). These samples will provide data on the tendency of the test nanomaterial to interfere with platelet aggregation caused by collagen.

(c) Prepare one control tube, in which combine 100 μL of RPMI and 25 μL of nanoparticles. This control will be used to determine any potential particle interference with instrument counting procedure.

4. Vortex briefly to mix ingredients and incubate for 15 min at 37°C.

5. Add 10 mL of sheath fluid (e.g., Isoton II diluent) into blood cell counter vials. Prepare two vials for each sample replicate.
6. Add 20 μL of PRP treated with positive control, negative control, or test nanomaterial. Cover vials and gently invert them to mix diluted samples (see Note 5). Proceed with platelet count determination using particle count and size analyzer immediately.
7. The following parameters should be calculated for each control and test sample:

   Platelet count:

$$\frac{5 \times \mathrm{RC}}{100} = \text{No. of platelets} \times 10^{9}\,\mathrm{L}^{-1},$$

   where RC is the readout of the particle count and size analyzer.

   Percent platelet aggregation (% Agg):

$$\%\mathrm{Agg} = \frac{(\text{No. of platelets}_{\text{control}} - \text{No. of platelets}_{\text{nanoparticles}})}{\text{No. of platelets}_{\text{control}}} \times 100.$$

   Percent coefficient of variation (% CV) in % Aggregation:

$$\%\mathrm{CV} = \left(\frac{\mathrm{SD}}{\mu_{\%\mathrm{Agg}}} \right) \times 100,$$

   where $\mu_{\%\mathrm{Agg}}$ is the mean value of the % Aggregation from all replicate samples.
7. % CV for each control and test sample should be within 25%.
8. If both replicates of positive control or negative control fail to meet acceptance criterion described above, the run should be repeated.
9. Within an acceptable run (by above criteria), if two of three replicates of the unknown sample fail to meet acceptance criterion described above, the unknown sample should be reanalyzed.
10. Some nanoparticles do not induce platelet aggregation in this assay (e.g., particles tested to generate Fig. 1). Other nanoparticles are very potent in inducing platelet aggregation (e.g., particles tested to generate Fig. 4b).

3.2. Plasma Coagulation Time

Spin the blood 10 min at 2,500 × *g* at 20–22°C; collect plasma and pool (see Note 6). Analyze two duplicates of test-plasma in each of coagulation assays, run one duplicate before nanoparticles treated plasma samples and second duplicate at the end of each run (Fig. 2).

3.3. Preparation of Nanoparticle-Treated Test-Plasma

1. In a microcentrifuge tube, combine 90 µL of nanoparticles preparation and 900 µL of test plasma, mix well and incubate 30 min at 37°C. Prepare three tubes for each nanoparticle preparation.
2. Set-up the instrument test parameters for each of four assays. Refer to Table 1 for a quick list of instrument settings and reagent volumes, and let the instrument to warm up to 5–10 min prior to use (see Note 7).

Table 1
Plasma coagulation assays at glance

Assay	Instrument settings/time/volumes
PT (Neoplastine)	*Control* CoagControlN+ABN *Settings* Max time: 60 s Incubation time: 120 s Single/duplicate: duplicate Precision: 5% *Volumes* Plasma: 100 µL Neoplastine reagent: 100 µL (PIP position 4) *Normal coagulation time* ≤13.4 s
APTT	*Control* CoagControlN+ABN *Settings* Max time: 120 s Incubation time: 180 s Single/duplicate: duplicate Precision: 5% *Volumes* Plasma+PTT-A reagent: 50 + 50 µL $CaCl_2$: 50 µL (PIP position 2) *Normal coagulation time* ≤34.1 s
Thrombin	*Control* CoagControlN+ABN *Settings* Max time: 60 s Incubation time: 60 s Single/duplicate: duplicate Precision: 5% *Volumes* Plasma: 100 µL Thrombine: 100 µL (PIP position 4) *Normal coagulation time* ≤21 s

3. Prepare all reagents and warm them up to 37°C prior to use (see Note 8).
4. Place test cuvettes on coagulometer (see Note 9).
5. Add one metal ball into each cuvette and let cuvette with ball warm for at least 3 min before use.
6. Add 100 μL of control or test plasma to a cuvette when test PT and thrombine time, and 50 μL when test APTT and reptilase (refer Table 1 for a reference). Prepare duplicate cuvettes for each plasma sample.
7. Only APTT and Reptilase test – add 50 μL of PTT-A reagent (APTT test) or Owren–Koller reagent (reptilase test) to plasma samples in cuvettes.
8. Start timer for each of the test rows by pressing A, B, C, or D buttons. Ten seconds before time is up timer starts beeping. When this happens, immediately transfer cuvettes to PIP row and press PIP button to activate pipettor.
9. When time is up, add coagulation activation reagent to each cuvette and record coagulation time. Refer to "Appendix" for the time of coagulation activation reagent and volume for each of four assays.
10. A percent coefficient of variation should be calculated for each control or test according to the following formula: % CV = SD/Mean × 100%.
11. % CV for each control and test sample should be within 5%.
12. If two duplicates of the same study sample demonstrated results different more than 5%, this sample should be reanalyzed.

4. Notes

1. During the blood collection procedure, the first 2 mL of blood should be discarded. Exposure of either blood or PRP to cold temperatures (<20°C) should be avoided, as it will induce platelet aggregation (Fig. 3).
2. Always wear appropriate personal protective equipment and take appropriate precautions when handling your nanomaterial. Many occupational health and safety practitioners recommend wearing two layers of gloves when handling nanomaterials. Also, be sure to follow your facility's recommended disposal procedure for your specific nanomaterial.
3. Nanoparticle formulations should be reconstituted in RPMI or another cell culture medium, which does not interfere with

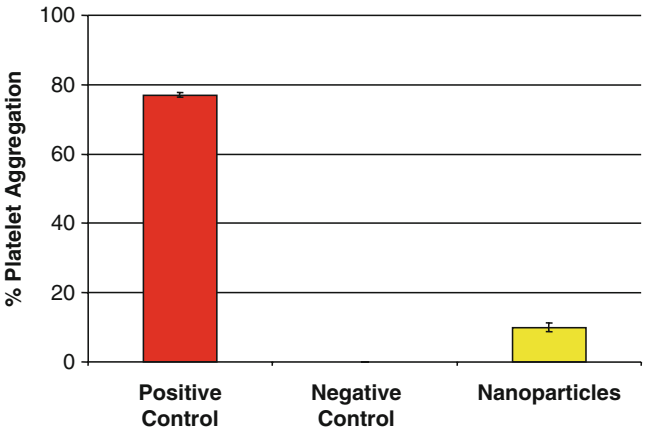

Fig. 3. Example of data generated using in vitro platelet aggregation assay.

platelet aggregation. The following parameters have to be considered when selecting the nanoparticle concentration to test in this assay: solubility, pH within physiological range, and stability in plasma. Nanoparticle formulations are tested at four concentrations: a high concentration (determined from either the expected therapeutic dose of the formulation or based on the results of an in vitro cytotoxicity assay similar to those described in Chapter 16) and three serial 1:5 dilutions of the high concentration. The assay requires 150 µL of test nanomaterial formulation.

4. PRP must be prepared as soon as possible and no longer than 1 h after blood collection. PRP must be kept at room temperature and should be used within 4 h.
5. Dilutions of tested samples and controls should be performed *ex tempore*, process one sample at a time. Counts should be performed within 2 h of removal from the incubator.
6. Use freshly collected whole blood within 1 h after collection. Pooled plasma is stable for 8 h at room temperature. Do not refrigerate or freeze.
7. A coagulometer is necessary to measure coagulation times. The assay described in this chapter was developed using a Start4 coagulometer (Diagnostica Stago, Parsippany, NJ). Other coagulometers can be used but may require slight modification of the method. Please follow the manufacturer's instructions
8. Lyophilized reagents should be reconstituted at least 30 min prior to use.
9. This assay measures a delay in coagulation time relative to a threshold. The threshold varies for each coagulation test.

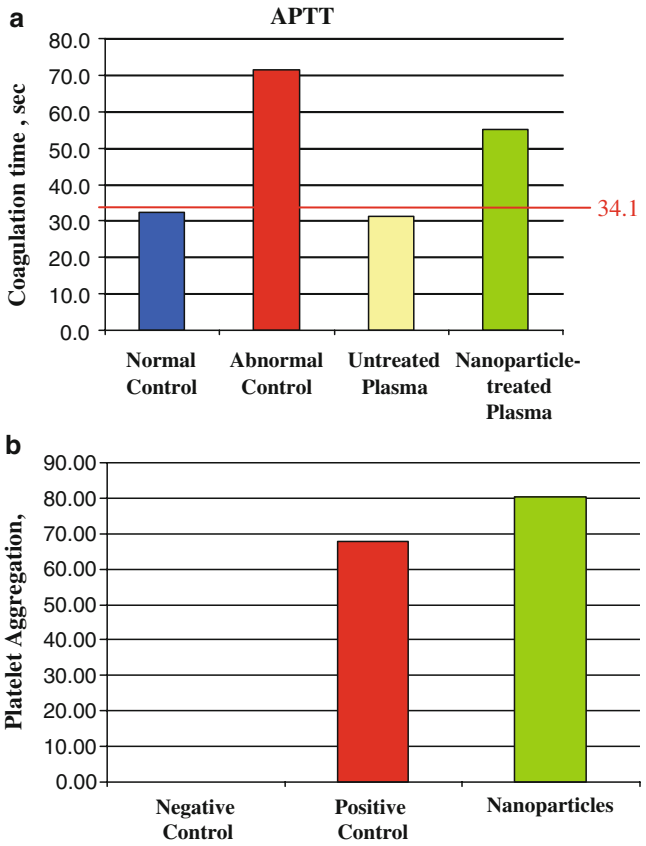

Fig. 4. Example of data generated using in vitro APTT test. (**a**) In coagulation test, a delay in APTT coagulation time was observed. *Red line* indicates limit for the coagulation time (34.1 s) in APTT test which is considered normal. These data agree with platelet aggregation result for the same nanoparticle showing positive test result (**b**).

Figure 4 shows an example of delayed APTT time following exposure to a nanoparticle formulation.

Acknowledgments

This project has been funded in whole or in part with federal funds from the National Cancer Institute, National Institutes of Health, under contract N01-CO-12400. The content of this publication does not necessarily reflect the views or policies of the Department of Health and Human Services, nor does mention of trade names, commercial products, or organizations imply endorsement by the US Government.

Appendix: Instrument Settings, Times, and Volumes

		Settings				Volumes		Normal coagulation time (s)
Assay	Control	Max time (s)	Incubation time (s)	Single/ duplicate	Precision (%)	Plasma	Reagent	
PT (neoplastine)	CoagControlN+ABN	60	120	Duplicate	5	100 µL Plasma	Neoplastine reagent: 100 µL (PIP Position 4)	≤13.4
APTT	CoagControlN+ABN	120	180	Duplicate	5	50 µL Plasma + 50 µL PTT-A Reagent	$CaCl_2$: 50 µL (PIP Position 2)	≤34.1
Thrombine	CoagControlN+ABN	60	60	Duplicate	5	100 µL Plasma	Thrombine: 100 µL (PIP Position 4)	≤21
Reptilase	System Control N+P	60	120	Duplicate	5	50 µL Plasma + 50 µL Owren-Koller Reagent	Reptilase: 100 µL (PIP Position 4)	≤20

References

1. Koziara, J. M., Oh, J. J., Akers, W. S., Ferraris, S. P., Mumper, R. J. (2005) *Blood Compatibility of Cetyl Alcohol/Polysorbate-Based Nanoparticles.* Pharm. Res. **22**, 11, 1821–8.
2. Beckman Coulter Z series User manual # 991 4591-D, section A8.4.2.
3. Bioanalytical method validation. Guidance for industry. FDA/CDER/CVM. May 2001. BP.
4. STArt4 Standard Operating procedure and Training manual. Diagnostica Stago, cat#26987, June 2002.

Chapter 25

Qualitative Analysis of Total Complement Activation by Nanoparticles

Barry W. Neun and Marina A. Dobrovolskaia

Abstract

This chapter describes a method for qualitative detection of complement activation by western blot. This method uses the cleavage product of the C3 component as a marker for complement activation by any pathway. In this protocol, human plasma is exposed to nanoparticles and then analyzed by polyacrylamide gel electrophoresis (PAGE) followed by western blot with anti-C3-specific antibodies. These antibodies recognize both the native C3 component of complement and its cleavage products. The amounts of C3 and the C3 cleavage products are compared to the amounts in control (untreated) plasma and to plasma treated with a positive control to provide a quick and inexpensive qualitative assessment of complement activation.

Key words: Nanoparticles, complement, anaphylaxis, C3, western blot

1. Introduction

The complement system is a biochemical cascade that serves as one arm of the overall immune defense system, which clears pathogens from the body. It is composed of several components (C1, C2,…, C9) and factors (B, D, H, I, and P) and is called the complement system because it "complements" the antibody-mediated immune response. There are three major pathways leading to complement activation (Fig. 1). They are the classical complement pathway, the alternative complement pathway, and the lectin pathway. The classical complement pathway is activated by immune (i.e., antigen–antibody) complexes. Activation of the alternative pathway is antibody independent. The lectin pathway is initiated when the plasma protein mannose binds to lectin. Activation of *any* of these three pathways results in cleavage of the C3 component.

Scott E. McNeil (ed.), *Characterization of Nanoparticles Intended for Drug Delivery*, Methods in Molecular Biology, vol. 697,
DOI 10.1007/978-1-60327-198-1_25,

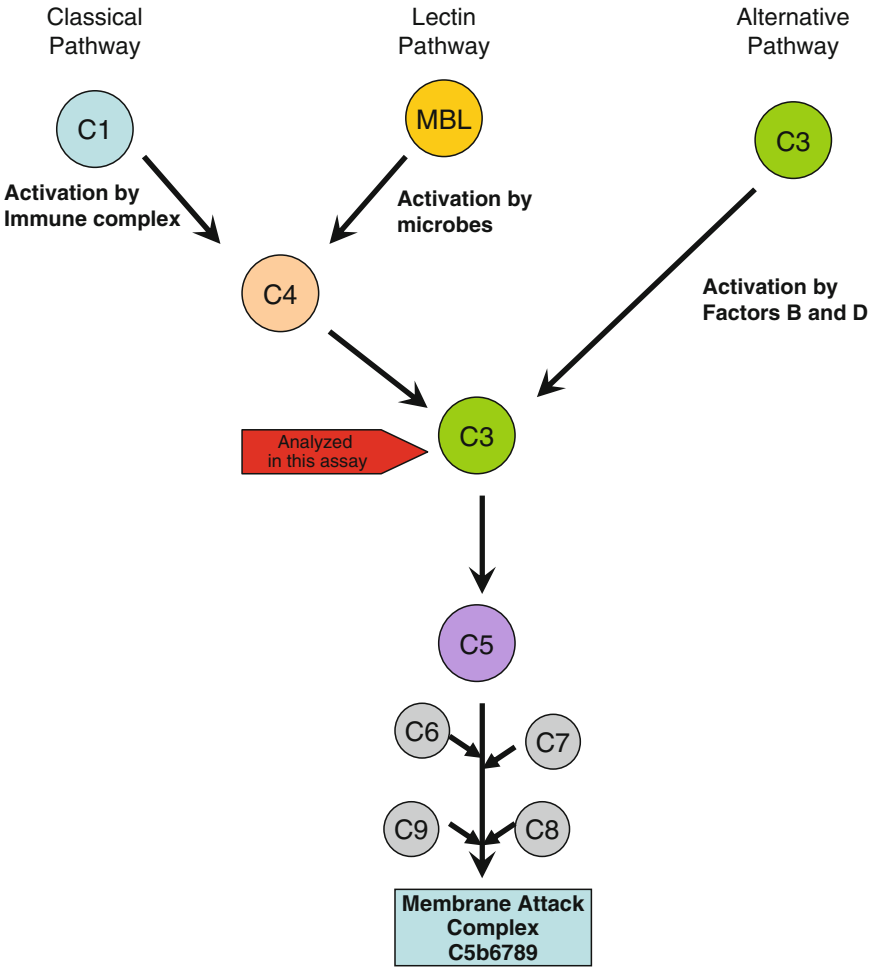

Fig. 1. Complement activation pathways. The antibodies used in this assay detect both full C3 protein and any C3 cleavage products.

Some degree of local complement activation is desirable for vaccines, since complement activation enhances antigen presentation. However, for most systemically administered drugs, complement activation is undesirable and can cause hypersensitivity (allergic) reactions and even anaphylaxis, a life-threatening condition. As such, nanoparticles intended for systemic administration should be tested for their tendency to activate the complement system. An example of a nanotech drug inducing undesirable complement activation was provided by Chanan-Khan et al. (1) who followed up clinical studies reporting hypersensitivity reactions to the nanoliposome doxorubicin formulation, Doxil®, and found that complement activation was causing hypersensitivity. Another recent study on a different nanotech formulation (2) demonstrated that local complement activation was essential to that drug's efficacy as a vaccine delivery system, causing uptake by

dendritic cells, activation of T-cells, and complementing the antigen-specific immune response.

Why certain nanoparticles cause activation of the complement system has not been definitively determined; however, it is generally recognized that surface charge plays an important role. Charged nanoparticles activated complement more than their neutral counterparts in studies investigating polypropylene sulfide nanoparticles (2), lipid nanocapsules (3), cyclodextrin-containing polycation-based nanoparticles (4), and polystyrene nanospheres (5). Polymer coatings (such as polyethylene glycol (PEG) and poloxamine 908), which partially neutralize surface charge, have been shown to reduce nanoparticle-mediated complement activation (3, 6). However, similar studies using dextran and chitosan (7) showed that the degree of complement activation was influenced by the size and conformation of the polymer, not determined by charge effects alone.

In the method presented here, we detect the C3 component of complement as a marker of complement activation (8). Human plasma is exposed to nanoparticles and then analyzed by polyacrylamide gel electrophoresis (PAGE) followed by western blot with anti-C3-specific antibodies. These antibodies recognize both the native C3 component of complement and its cleavage products. The amounts of C3 and the C3 cleavage products are then compared to the amounts in control (untreated) plasma and to plasma treated with a positive control (cobra venom factor). The antibody used in this method is generated using purified human C3 component of the complement. Since cross reactivity with C3 of other species was unknown for this antibody, and complement protein is conserved between mammalians, we have tested it in plasma samples obtained from mouse, rat, guinea pig, mini pig, and monkey, and we have found that it works well with all these species and is more sensitive to monkey and human C3 protein.

This "yes or no" protocol was designed to provide a quick and inexpensive qualitative assessment of complement activation. Nanoparticles which are determined to cause complement activation using this assay should be further investigated to delineate the pathway associated with the complement activation.

2. Materials

1. Concentrated 4× sample buffer containing SDS and reducing agent (either 50 mM DTT or 10% β-mercaptoethanol), e.g., laemmli buffer or equivalent.
2. 10% Tris–glycine polyacrylamide–SDS gel (see Note 1).

3. Tris–glycine running buffer: prepare working solution by diluting 10× concentrated stock with distilled water. For example, mix 100 mL of stock with 900 mL of water. Use within 24 h (see Note 1).
4. Tris–glycine transfer buffer with 20% methanol: prepare working buffer from 25× stock solution. For example, prepare 1 L of buffer diluting 40 mL of stock in 800 mL of distilled water, then add 200 mL of methanol. Mix well. Chill before use. Use within 24 h.
5. TBST (Tris-buffered saline + 0.01% Tween 20): dilute 25× stock of tris-buffered saline (TBS) in distilled water by mixing 40 mL of the stock with 960 mL of water. Then add 100 μL of Tween 20 (Polysorbate 20) and mix well. Unused buffer can be stored at room temperature overnight or up to 1 week at 4°C.
6. Blocking buffer (5% milk in TBST): dissolve 5 g of non-fat dry milk in 100 mL of TBST. Use within 24 h.
7. Ponceau S stain solution: dilute stock solution with distilled water by mixing 10 mL of the stock solution with 40 mL of water. Mix well. Store at room temperature for up to 2 weeks.
8. Primary antibody solution (see Note 2): thaw an aliquot of goat polyclonal anti-C3 antibody (e.g., Calbiochem) and dilute 1:2,000 in the blocking buffer. Use within 24 h.
9. Secondary antibody solution (see Note 2): dilute donkey anti-goat IgG (H+L) conjugated to HRP (Jackson ImmunoResearch Labs, West Grove, PA). HRP conjugate 1:50,000 in blocking buffer. Use within 24 h. Discard after use.
10. Positive control (cobra venom factor): cobra venom factor (CVF, Quidel Corporation, San Diego, CA) is usually supplied as a lyophilized powder. Reconstitute the powder with water using volumes as recommended by the manufacturer. Prepare daily use aliquots and store at −80°C. Use 10 μL (1.1–50 U) of CVF solution. Avoid subjecting the CVF to more than two freeze/thaw cycles.
11. Negative Control (Ca^{2+}/Mg^{2+}-free phosphate-buffered saline): sterile Ca^{2+}/Mg^{2+}-free PBS is used as a negative control. Store at room temperature for up to 6 months.
12. Analyte nanoparticle samples (see Notes 3 and 4).
13. Veronal buffer.
14. 10% Tris–glycine gels.
15. NuPAGE lithium dodecyl sulfate (LDS) 4× sample buffer.
16. Reducing agent such as dithiothreitol (DTT) or β-mercaptoethanol.
17. Pooled human plasma anticoagulated with Na-citrate.

18. Polyvinylidene difluoride (PVDF) protein blotting membrane.
19. Blotting paper.
20. Methanol.
21. Chemiluminescent peroxidase western blotting substrate.
22. Film for the detection of chemiluminescent signals from protein blots.
23. Protein molecular weight ruler/standard.
24. Film cassette.
25. An imaging system sensitive to chemiluminescence can be used as alternative to the film.

3. Methods

1. In a microcentrifuge tube, combine equal volumes (10 μL of each) of veronal buffer, human plasma, and a test sample (i.e., positive control, negative control, nanoparticle study sample or buffer used to reconstitute nanoparticles if different than PBS, see Note 5).
2. Vortex tubes to mix all reaction components, pulse spin in a microcentrifuge to bring any drops down and incubate in an incubator at 37°C for 1 h.
3. To each tube, add 10 μL of 4× sample buffer supplemented with reducing agent; vortex and heat at 95°C for 5 min. Spin in a microcentrifuge at a maximum speed for 30 min and carefully transfer supernatants to clean tubes (see Note 6).
4. Assemble gel running system. Prime wells with running buffer, then load protein marker and 3 μL of test samples and controls prepared in step 3.
5. Run gel at 125 V for approximately 2 h or until dye reaches the bottom of the gel.
6. Rinse the gel with deionized water and assemble protein transfer system by aligning gel onto PVDF membrane surrounded by two layers of blotting paper presoaked in transfer buffer.
7. Perform protein transfer either overnight at 25–30 mA or 1–2 h at 100 mA.
8. Rinse membrane with deionized water.
9. Add 40 mL of Ponceau S solution and incubate on a rocking platform for approximately 5 min.
10. Wash the membrane with deionized water twice for approximately 10 min to remove excess of Ponceau stain. If staining

reveals no problem with protein transfer (e.g., air bubbles, smears, or variable protein loads) proceed to next step.

11. Wash membrane with 50 mL of TBST for approximately 15 min.
12. Block the membrane with blocking buffer at room temperature for approximately 1 h.
13. Incubate membrane with primary antibody solution for 90 min at room temperature. The antibody concentration is selected according to the manufacturer's recommendations.
14. Wash the membrane twice with 50 mL of TBST. Each wash step is 15–20 min at room temperature.
15. Incubate the membrane with the secondary antibody solution for 90 min at room temperature. The antibody concentration is selected according to the manufacturer's recommendations.
16. Wash the membrane twice with 50 mL of TBST. Each wash step is 15–20 min.
17. Incubate membrane with peroxidase substrate for approximately 1 min and proceed with blot development immediately. If film is used, the exposure time is approximately 2–5 min. When imaging system is used, the optimal exposure time should be selected empirically for a given system. An example of western blot is shown in Fig. 1.

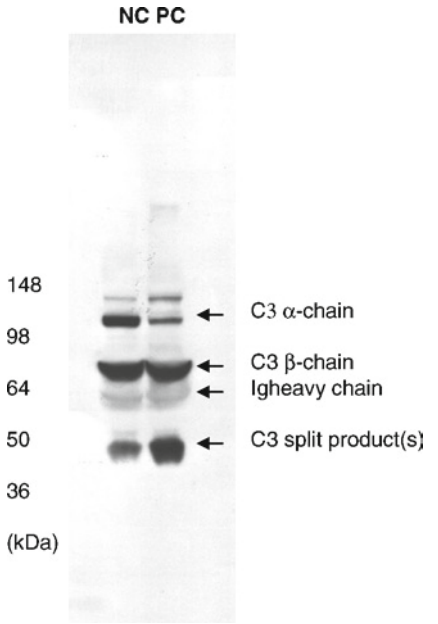

Fig. 2. Example western blot for complement activation. On the image above, NC stands for the negative control sample, PC is the positive control sample (cobra venom factor), and MW stands for molecular weight of the protein marker. C3 (α chain) size is ~115 kDa, C3-cleavage product(s) (C3c, iC3b[C3α']) are ~43 kDa.

18. See Fig. 2 and Note 7 for an example western blot run. Run is acceptable if both replicates of the positive and negative controls demonstrate acceptable performance, i.e., evident cleavage of C3 component of complement in former and no or minor amount of cleaved C3 in latter. If one of the replicates of the positive or the negative control fails to meet acceptance criterion, the entire run should be repeated. If both replicates of a nanoparticle sample demonstrate evident cleavage of the C3 component of complement, or one replicate is positive and the other replicate demonstrate intermediate cleavage, the nanoparticle sample is considered positive and should be analyzed further using a quantitative assay. If one replicate of a nanoparticle sample demonstrates positive response and the second replicate is negative, then this nanoparticle sample should be reanalyzed. If both replicates of a nanoparticle sample demonstrate no obvious cleavage of the C3 component of complement, the sample is considered negative and no further in vitro analysis is necessary. If both replicates of a nanoparticle sample demonstrate intermediate cleavage of the C3 component of complement, the sample is considered positive and should be further analyzed.

4. Notes

1. 10% Tricine gels and 10% bis–tris gels can also be used. If tricine gels are used, the running buffer should be tricine–SDS. If bis–tris gels are used, the running buffer should be MES (2-(*N*-morpholino)ethanesulfonic acid) SDS. The advantage of bis–tris gels is their longer shelf-life compared to tris–glycine and tricine gels. The method described in this chapter will provide good resolution and detection of C3 split product in any of these electrophoresis systems.
2. If using an antibody from a different source is used, the final dilution should be adjusted to minimize the background signal and maximize the signal-to-noise ratio.
3. Always wear appropriate personal protective equipment and take appropriate precautions when handling your nanomaterial. Many occupational health and safety practitioners recommend wearing two layers of gloves when handling nanomaterials. Also, be sure to follow your facility's recommended disposal procedure for your specific nanomaterial.
4. This assay requires 20 μL of nanoparticles. The following parameters have to be considered when selecting the concentration: solubility, pH within physiological range, and stability in plasma. For the initial run, a concentration of 1 mg/mL or approaching the limit of solubility should be used.

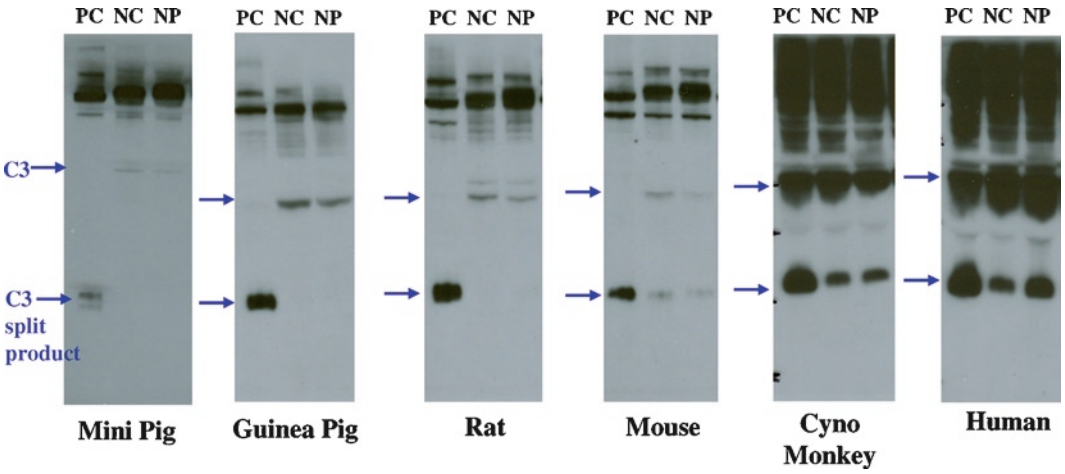

Fig. 3. Analysis of complement activation by nanoparticle formulation in plasma from various species. Plasma samples derived from various species were collected on day 1 and stored at 4°C for 48 h before the experiment. The plasma samples were treated with either PBS (negative control, NC) or nanoparticle formulation in PBS (nanoparticle, NP). Cobra venom factor was used as a positive control (PC). Samples were prepared and analyzed as described in the protocol. The polyclonal antibodies used in this assay recognized both full C3 and C3 cleavage products. This study demonstrates that these antibodies can cross-react with C3 protein from mini pig, guinea pig, mouse, rat, and cyno monkey as evident by the appearance of the C3 split product in PC sample of each matrix. Of interest, activation of the complement system by this particular nanoparticle formulation was detectable only in human plasma.

5. Each sample is prepared in duplicate.
6. At this point, samples can be frozen at –20°C and stored for later use. Samples should be thawed at room temperature, vortexed, and pulse centrifuged before analysis.
7. The antibody used in this assay is generated using the purified human C3 component of complement. Figure 3 shows that this antibody cross-reacts with C3 protein from mouse, rat, mini pig, guinea pig, and monkey plasma. Rodents (especially mice and rats) are commonly used in toxicological studies. One limitation of such studies is that a negative result for nanoparticle-induced complement activation in these species may not be relevant to humans (see Fig. 3).

Acknowledgments

This project has been funded in whole or in part with federal funds from the National Cancer Institute, National Institutes of Health, under contract N01-CO-12400. The content of this publication does not necessarily reflect the views or policies of the Department of Health and Human Services, nor does mention of trade names, commercial products, or organizations imply endorsement by the U.S. Government.

References

1. Chanan-Khan, A. Szebeni, J., Savay, S., Liebes, L., Rafique, N. M., Alving, C. R., Muggia, F. M. (2003) Complement activation following first exposure to pegylated liposomal doxorubicin (Doxil®): possible role in hypersensitivity reactions. *Ann Oncol* **14**, 1430–37.
2. Reddy, S. T., van der Vlies, A. J., Simeoni, E., Angeli, V., Randolph, G. J., O'Neil, C. P., Lee, L. K., Swartz, M. A., Hubbell, J. A., (2007) Exploiting lymphatic transport and complement activation in nanoparticle vaccines. *Nat Biotechnol* **25** (10), 1159–64.
3. Vonarbourg, A., Passirani, C., Saulnier, P., Simard, P., Leroux, J. C., Benoit, J. P. (2006) Evaluation of pegylated lipid nanocapsules versus complement system activation and macrophage uptake. *J Biomed Mater Res A* **78** (3), 620–8.
4. Bartlett, D. W., Davis, M. E. (2007) Physicochemical and biological characterization of targeted, nucleic acid-containing nanoparticles. *Bioconjug Chem* **18** (2), 456–68.
5. Nagayama, S., Ogawara, K., Fukuoka, Y., Higaki, K., Kimura, T. (2007) Time-dependent changes in opsonin amount associated on nanoparticles alter their hepatic uptake characteristics. *Int J Pharm* **342** (1–2), 215–21.
6. Al-Hanbali, O., Rutt, K. J., Sarker, D. K., Hunter, A. C., Moghimi, S. M. (2006) Concentration dependent structural ordering of poloxamine 908 on polystyrene nanoparticles and their modulatory role on complement consumption. *J Nanosci Nanotechnol* **6** (9–10), 3126–33.
7. Bertholon, I., Vauthier, C., Labarre, D. (2006) Complement activation by core-shell poly (isobutylcyanoacrylate)-polysaccharide nanoparticles: influences of surface morphology, length, and type of polysaccharide. *Pharm Res* **23** (6), 1313–23.
8. Xu, Y., Ma, M., Ippolito, G. C., Schroeder, H. W., Carrol, M. C., Volanakis, J. E. (2001) Complement activation in factor D-deficient mice. *Proc Natl Acad Sci USA* **98**, 14577–82.

Chapter 26

Method for Analysis of Nanoparticle Effects on Cellular Chemotaxis

Sarah L. Skoczen, Timothy M. Potter, and Marina A. Dobrovolskaia

Abstract

Chemotaxis is the phenomenon in which cells direct their movements in the presence of certain chemicals (chemoattractants or chemorepellents). Leukocyte recruitment (via chemotaxis) is an important component of the inflammatory response, both in physiological host defense and in a range of prevalent disorders that include an inflammatory component. Circulating leukocytes in the bloodstream migrate towards the site of inflammation in response to a complex network of proinflammatory signaling molecules (including cytokines, chemokines and prostaglandins). This chapter describes a method for rapid measure of the chemoattractant capacity of nanoparticulate materials. This method is an in vitro model for chemotaxis, in which promyelocytic leukemia cell migration through a filter is monitored using a fluorescent dye.

Key words: Nanoparticles, chemotaxis, chemoattractant, immune response

1. Introduction

Cell migration is an important part of many biological processes, including development and the immune response. Altered cell motility has been implicated in a variety of diseases, including cancer. For example, tumor metastasis occurs because of the increased motility of tumor cells. Many motility-altering molecules are also targets for cancer therapies, including tyrosine kinases (1) and components of the actin cytoskeleton (2). Methods for studying cell motility are particularly useful as part of the nanoparticle-based drug discovery process, since inflammatory cell recruitment by nanoparticle-based drugs may affect the degree to which these compounds are internalized by immune cells and the biodistribution and bioavailability of the drug.

Motile stimuli can be characterized as chemotactic or chemokinetic, with chemotactic stimuli producing cellular movement in a

Scott E. McNeil (ed.), *Characterization of Nanoparticles Intended for Drug Delivery*, Methods in Molecular Biology, vol. 697,
DOI 10.1007/978-1-60327-198-1_26,

specific direction and chemokinesis producing random movement. Chemotactic stimuli can be further divided into chemoattractant or chemorepellent, producing motion either towards (attractant) or away (repellent) from the stimuli. In this chapter, we describe an in vitro method to measure chemotaxis based on an earlier method by Boyden (3). This method uses a two-part 96-well plate, separated by an 8 μm filter, with the lower chamber containing the nanoparticles and the upper chamber containing promyelocytic leukemia cells HL-60. Following a 4 h incubation period, the top filter plate is removed, and chemotaxis is directly quantified by staining the migrated cells in the bottom plate with a fluorescent dye (Calcein AM). An increase in fluorescence serves as a measure of chemotaxis. Detection of fluorescence in this assay requires metabolism of Calcein AM by active live cells. Cytotoxic nanoparticles may interfere with this assay by killing chemotactic cells which may not be detected (4).

2. Materials

1. Heat inactivated fetal bovine serum (FBS): thaw a bottle of FBS at room temperature (or overnight at 2–8°C and allow to equilibrate to room temperature). Incubate for 30 min at 56°C in a water bath, mixing every 5 min. Single use aliquots may be stored at 2–8°C for up to 1 month or at −20°C for several months.
2. Complete RPMI: complete RPMI medium should contain the following reagents: 20% FBS (heat inactivated), 4 mM L-glutamine, 1.5 g/L sodium bicarbonate, 100 U/mL penicillin, and 100 μg/mL streptomycin sulfate (see Note 1).
3. Starving medium (SM): low serum medium should contain the following reagents: 0.2% Bovine serum albumin (BSA), 4 mM L-glutamine, 1.5 g/L sodium bicarbonate, 100 U/mL penicillin, and 100 μg/mL streptomycin sulfate (see Note 1).
4. Positive control. On the day of experiment, dilute heat-inactivated FBS in serum-free medium supplemented with 0.2% BSA to a final concentration of 20%.
5. Negative control. Phosphate buffered saline (PBS) pH 7.4 serves as the negative control.
6. Calcein AM dye working solution: Dilute stock solution of Calcein AM (e.g. from Molecular Probes) in PBS prewarmed at 37°C to a final concentration of 4 μM (e.g. add 10 μL of stock Calcein AM to 2.503 mL of 1× PBS). The working dilution should be prepared *ex tempore*. Calcein AM has excitation/emission maxima of 577/595 nm. For detection on a plate reader, excitation/emission of 485/535 nm is recommended by the manufacturer.

7. Analyte nanoparticle samples (see Notes 2 and 3): this assay requires 1.4 mL of nanoparticles dissolved/resuspended in starving medium (i.e. three 150 µL triplicates per sample).
8. Cells: HL-60 (ATCC#CCL-240) is a promyelocytic cell line derived by S.J. Collins, et al. from a patient with acute promyelocytic leukemia. Cultures can be maintained by the addition of fresh medium or replacement of medium. Alternatively, cultures can be centrifuged and subsequently resuspended at 1×10^5 viable cells/mL. Do not allow cell concentration to exceed 1×10^6 cells/mL. Maintain cell density between 1×10^5 and 1×10^6 viable cells/mL.
9. Trypan Blue solution pH 7.1–7.4: 0.4% in 0.81% sodium chloride and 0.06% potassium phosphate dibasic.
10. Cell culture-certified β-mercaptoethanol.
11. 96-well filter plates with 3 µm membrane.
12. 96-well culture tray.
13. 96-well optical bottom plates.
14. Cell culture incubator with 5% CO_2 and 95% relative humidity.
16. Inverted microscope.
17. Hemacytometer.
18. Plate reader capable of fluorescence detection.

3. Methods

3.1. Cell Preparation

1. Expand cells in T75 flasks until they are about 80–90% confluent (~3–5 days before performing the steps given in Subheading 3.2). Two days before performing the steps outlined in Subheading 3.2, feed the cells following a regular maintenance procedure.
2. One day before cell treatment, count cells using trypan blue exclusion method and hemacytometer. Cell viability should be 95–100%. Pellet cells for 8 min at $120 \times g$ in a 15 mL tube.
3. Resuspend cells in starving medium (SM) and incubate overnight at 37°C in a humidified incubator (95% relative humidity, 5% CO_2).
4. On the day you will start cell treatment, count cells using trypan blue exclusion method and adjust concentration to 1×10^6 viable cells per mL in the starving medium. Cell viability should be at least 90%.

3.2. Cell Treatment

1. Insert fresh filter plate into feeding tray and set it aside.
2. Add 150 μL of positive control, negative control, and test-nanomaterial in starving medium to feeding tray (see Fig. 1 also see Note 4).
3. Add 50 μL of cell suspension prepared in step 4 in subheading 3.1 per well of multiscreen filter plate (50,000 cells per well, see Fig. 1 also see Note 4).
4. Gently assemble multiscreen filter plate and feeding tray containing the controls and test particles. Henceforth, we will refer to this as the "Assay Plate". Avoid shaking or tilting plates as it will disturb concentration gradient.
5. Cover the plate and incubate for 4 h at 37°C in a humidified incubator (5% CO_2, 95% relative humidity). During incubation, prewarm PBS to 37°C and equilibrate Calcein AM to room temperature.
6. After the incubation, remove the chemotaxis assay plate from the incubator. As before, avoid shaking or tilting the plates. Gently remove filter plate and discard it.
7. Add 50 μL of PBS and 50 μL of Calcein AM working solution to the appropriate wells and 150 μL of 1× PBS plus 50 μL of Calcein AM working solution to the reagent background control wells on the feeding tray as shown in Fig. 2. Henceforth, we will refer to this as the "Calcein Plate". Incubate this plate for at least 1 h at 37°C.
8. Transfer 180 μL of the solutions from the Calcein Plate to the corresponding wells on the optical-bottom plate and read the optical-bottom plate on a fluorescent plate reader at 485/535 nm.

SM	SM	SM	SM	SM	SM	NC	NC	NC	PC	PC	PC
SM	SM	SM	SM	SM	SM	NC	NC	NC	PC	PC	PC
SM	SM	SM	SM	SM	SM	NC	NC	NC	PC	PC	PC
NS1	NS1	NS1	NS2	NS2	NS2	NS3	NS3	NS3	NS4	NS4	NS4
NS1	NS1	NS1	NS2	NS2	NS2	NS3	NS3	NS3	NS4	NS4	NS4
NS1	NS1	NS1	NS2	NS2	NS2	NS3	NS3	NS3	NS4	NS4	NS4

Fig. 1. This shows an example layout for the filter plate (the filter is at the bottom of the wells of this plate). The wells in the filter plate receive 50,000 cells in 50 μL. The wells are labeled as follows: SM for starving medium, NC for negative control (PBS), PC for positive control, and NS for nanoparticle sample.

PBS	PBS	PBS	CAM	CAM	CAM	CAM	CAM	CAM	CAM	CAM	CAM
PBS	PBS	PBS	CAM	CAM	CAM	CAM	CAM	CAM	CAM	CAM	CAM
PBS	PBS	PBS	CAM	CAM	CAM	CAM	CAM	CAM	CAM	CAM	CAM
CAM	CAM	CAM	CAM	CAM	CAM	CAM	CAM	CAM	CAM	CAM	CAM
CAM	CAM	CAM	CAM	CAM	CAM	CAM	CAM	CAM	CAM	CAM	CAM
CAM	CAM	CAM	CAM	CAM	CAM	CAM	CAM	CAM	CAM	CAM	CAM
RBC	RBC	RBC	RBC	RBC	RBC	RBC	RBC	RBC	RBC	RBC	RBC

Fig. 2. This is a diagram of an example layout for the lower plate (calcein AM Plate). The wells are labeled as follows: PBS for the wells containing 50 μL PBS, CAM for wells containing 50 μL calcein AM, RBC for reagent background control (these wells contain 150 μL PBS and 50 μL calcein AM).

3.3. Calculations

1. Background chemotaxis (BC) is calculated as:

$$BC = MF_{CAM} - MF_{PBS} - MF_{BG}$$

where MF_{CAM} is the mean fluorescence of the Calcein AM-containing wells, MF_{PBS} is the mean fluorescence of the PBS wells, and MF_{BG} is the mean fluorescence of the background reagent wells.

2. Nanoparticle chemotaxis (NC) is calculated as:

$$NC = MF_{NS} - MF_{PBS} - MF_{BG}$$

Where MF_{NS} is the mean fluorescence of the nanoparticle sample wells, MF_{PBS} is the mean fluorescence of the PBS wells, and MF_{BG} is the mean fluorescence of the background reagent wells.

3. Fold chemotaxis is then calculated as NC/BC. For nanoparticle samples, twofold induction with respect to background is considered significant (see Fig. 3).

4. Percent coefficient of variation (%CV) in the fold chemotaxis is calculated as:

$$\%CV = \left(\frac{SD}{\mu_{FC}}\right) \times 100,$$

where μ_{FC} is the mean value of the fold chemotaxis from all replicate samples.

5. Percent Coefficient of Variation (%CV) for each control and test sample should less than 30%.

6. If two of the three replicates of the positive or negative control fail to meet the %CV acceptance criterion described above, the assay should be repeated.

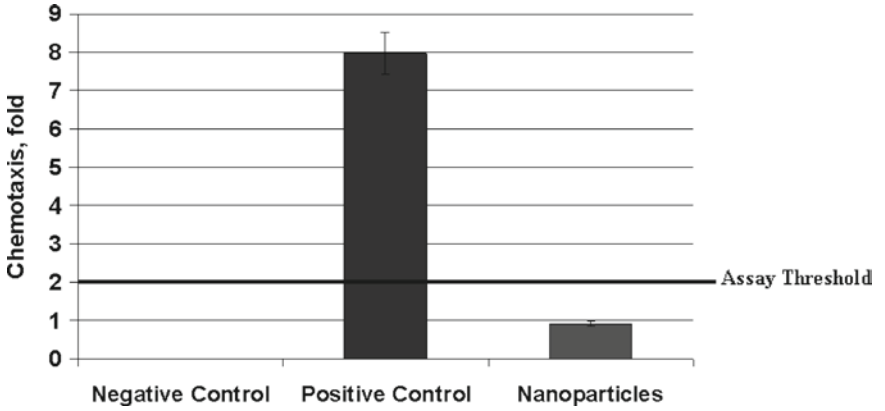

Fig. 3. Example data for the chemotaxis assay. Assay was performed as described in the protocol using negative control, positive control, and one nanoparticle formulation. Fold chemotaxis induction was calculated according to the formula NC/BC for all samples. No detectable chemotaxis was observed in the negative control, an eightfold increase in chemotaxis was observed in the positive control, and a weak approximately onefold increase was observed for the nanoparticle sample. Though some cells migrated through the filter in the quantity above background chemotaxis, this response is not qualified as significant because it below the assay threshold. Chemotaxis in nanoparticle samples is considered positive if the fold induction is at least two compared to background chemotaxis.

7. If two of the three replicates of the nanoparticle samples fail to meet the %CV acceptance criterion described above, the nanoparticle sample should be reanalyzed.

4. Notes

1. Store at 4°C protected from light for no longer than 1 month. Before use, warm the medium in a water bath.
2. Always wear appropriate personal protective equipment and take appropriate precautions when handling your nanomaterial. Many occupational health and safety practitioners recommend wearing two layers of gloves when handling nanomaterials. Also, be sure to follow your facility's recommended disposal procedure for your specific nanomaterial.
3. The following questions have to be considered when selecting the concentration: solubility, pH within physiological range, stability in plasma, and potential cytotoxicity. In general, nanoparticles are tested at four concentrations. The highest concentration is approximately 1 mg/mL, but could be higher or lower depending on the nanoparticle's solubility and cytotoxicity. Three serial 1:5 dilutions of the highest concentration are also included in the analysis.
4. Avoid generating bubbles while adding solutions to wells.

Acknowledgments

This project has been funded in whole or in part by federal funds from the National Cancer Institute, National Institutes of Health, under contract N01-CO-12400. The content of this publication does not necessarily reflect the views or policies of the Department of Health and Human Services, nor does the mention of trade names, commercial products, or organizations imply endorsement by the U.S. Government.

References

1. Brunelleschi, S., Penengo, L., Santoro, M.M. and Gaudino, G. (2002) Receptor tyrosine kinases as targets for anti-cancer therapy. *Curr. Pharm. Des.* **8**, 1959–1972.
2. Giganti, A., Friederich, E. (2003) The actin cytoskeleton as a therapeutic target: state of the art and future directions. *Prog. Cell Cycle Res.* **5**, 511–525.
3. Gallagher, R., Collins, S., Trujillo, J., McCredie, K., Ahearn, M., Tsai, S., Metzgar, R., Aulakh, G., Ting, R., Ruscetti, R. and Gallo, R. (1979) Characterization of the continuous, differentiating myeloid cell line (HL-60) from a patient with acute promyelocytic leukemia. *Blood* **54**, 713–733.
4. Kamath, L. (2003) Multi-Screen-MIC Application Note. Lit# AN1060EN00. Millipore Life Science Division, Millipore, USA, April 14.

Chapter 27

In Vitro Analysis of Nanoparticle Uptake by Macrophages Using Chemiluminescence

Sarah L. Skoczen, Timothy M. Potter, and Marina A. Dobrovolskaia

Abstract

This chapter provides a protocol for qualitative evaluation of nanoparticle internalization by phagocytic cells such as macrophages. This protocol uses luminol chemiluminescence to detect nanoparticle uptake. This protocol provides a preliminary qualitative look at phagocytosis which should be confirmed by other techniques such as electron microscopy, confocal microscopy, or as applicable to a given nanoparticle sample.

Key words: Nanoparticles, phagocytosis, macrophage uptake

1. Introduction

This chapter describes a protocol for evaluation of nanoparticle internalization by phagocytic cells such as macrophages. Such internalization is an important criterion to evaluate as part of a thorough assessment of the biodistribution and bioavailability of nanoparticles for medical purposes. The route of cellular uptake of nanoparticles is still a subject of study, and is most-likely dependent on a range of influencing factors, including the size and constituent material of the nanoparticle, as well as which type of cell is being investigated. For macrophages, the route of nanoparticle uptake is most likely some form of phagocytosis (1, 2, 6–8).

This protocol uses luminol chemiluminescence (see Fig. 1) to detect nanoparticle uptake and may not be applicable to certain types of nanomaterials (see Fig. 2). Modification(s) of the current procedure, and or change in detection dye may be required for formulations which demonstrate interference with luminol-dependent chemiluminescence. For example, luminol-dependent chemiluminescence is known to be influenced by the presence of red blood cells, by phenol red, and HEPES buffer (5).

Scott E. McNeil (ed.), *Characterization of Nanoparticles Intended for Drug Delivery*, Methods in Molecular Biology, vol. 697,
DOI 10.1007/978-1-60327-198-1_27,

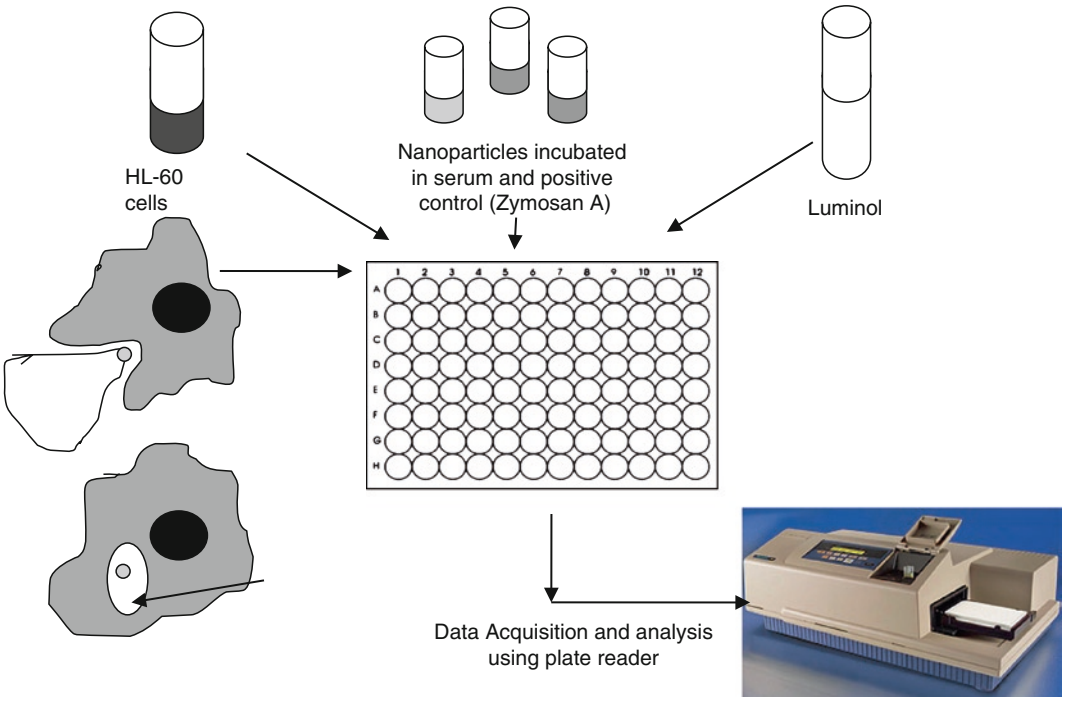

Fig. 1. Schematic illustration of the method described in this chapter.

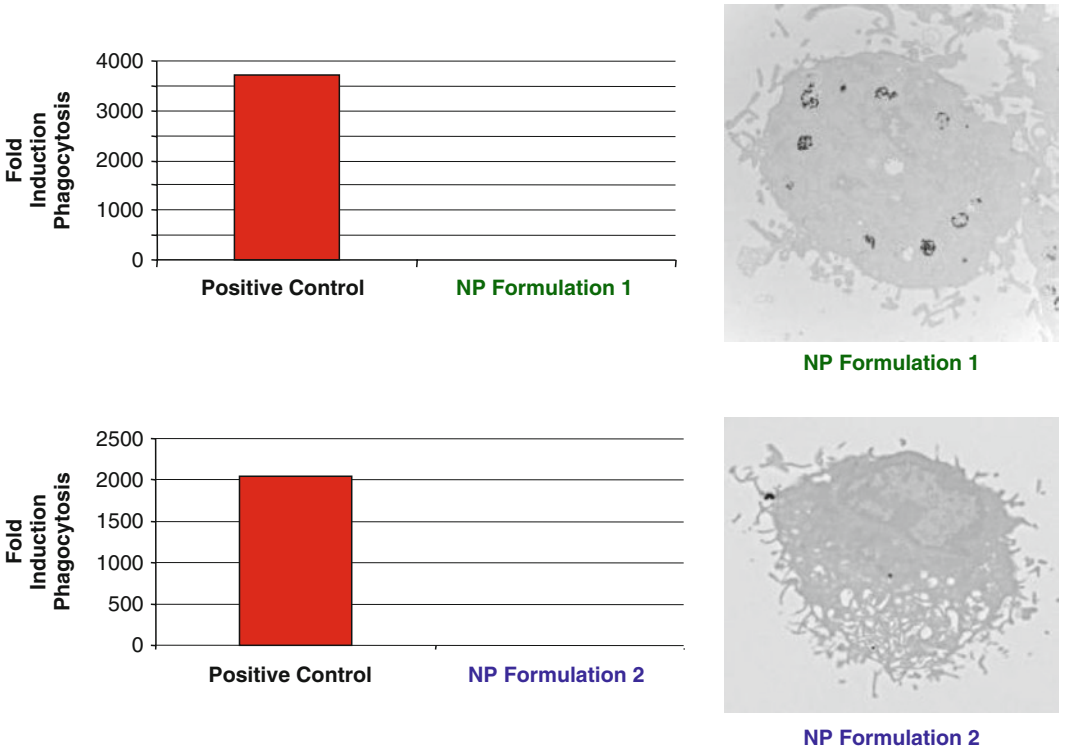

Fig. 2. As explained in the introduction, this protocol uses luminol chemiluminescence to detect nanoparticle uptake and may not be applicable for certain types of nanomaterials. Modification(s) of the current procedure, and or change in detection dye may be required for formulations which demonstrate interference with luminol-dependent chemiluminescence. Here we show the results of this method for two nanoparticle formulations in comparison with direct observation by TEM microscopy. The luminol assay described here was not sensitive to discern a difference in uptake between the two formulations, though this was clearly evident by TEM (nanoparticles indicated with *arrows*).

This assay is limited by the sensitivity at which luminol can be detected inside cells. Certain types of nanoparticles (e.g. fluorescent nanoparticles such as quantum dots) may be detected more easily and with higher sensitivity using direct detection via confocal microscopy or flow cytometry. Many electron-dense nanomaterials can be visualized inside of cellular compartments by electron microscopy (EM), and transmission electron microscopy (TEM) is the technique-of-choice to evaluate the uptake of such particles (2–4).

2. Materials

1. Phosphate Buffered Saline (PBS) will be used as a negative control and for preparing other solutions.
2. Zymosan A Stock solution. Prepare Zymosan A stock at final concentration of 2 mg/mL in PBS. Use freshly prepared solution.
3. Heat-inactivated fetal bovine serum (FBS). Thaw a bottle with FBS at room temperature or overnight at 4°C, and allow to equilibrate to room temperature. Incubate for 30 min at 56°C in a water bath, mixing every 5 min (see Note 1).
3. Complete RPMI-1640 medium should contain the following reagents: 10% FBS-heat inactivated, 2 mM L-glutamine, 100 U/mL penicillin, and 100 µg/mL streptomycin sulfate (see Note 2).
4. Trypan blue solution (0.4% in 0.81% sodium chloride and 0.06% potassium phosphate dibasic, pH 7.1–7.4).
5. Human serum or plasma pooled from at least three donors.
6. Positive control. Combine Zymosan A stock and human serum or plasma. Use 1 mL of serum/plasma per each 0.5 mL of zymosan A stock. Incubate Zymosan A with serum/plasma for 30 min at 37°C. Wash Zymosan A particles two times with PBS (use 1 mL of PBS per each 0.5 mL of original zymosan stock and a centrifuge setting of 2,000 × *g* for 2 min) and resuspend in PBS to a final concentration of 2 mg/mL (see Note 3).
7. Luminol Stock (10 mM in DMSO). Dissolve luminol in DMSO to a final concentration of 10 mM, e.g. dissolve 17.7 mg of luminol in 10 mL of DMSO. Prepare daily use aliquots and store at −20°C, protected from light.
8. Luminol Working solution (250 µM in PBS). On the day of the experiment thaw an aliquot of the luminol stock solution and dilute with PBS to a final concentration of 250 µM (e.g. spike 250 µL of 10 mM stock into 10 mL of PBS). Protect from light.

9. Flat-bottom 96-well white luminescence plates.
10. Cell culture incubator with 5% CO_2 and 95% relative humidity.
11. Inverted microscope.
12. Hemacytometer.
13. Plate reader capable of working in luminescence mode.
14. Analyte nanoparticle sample, 600 μL dissolved/resuspended in PBS (see Notes 4 and 5).
15. Cells

    HL-60 (ATCC#CCL-240) is a promyelocytic cell line derived by S.J. Collins, et al. from a patient with acute promyelocytic leukemia. Cultures can be maintained by the addition of fresh medium or replacement of medium. Alternatively, cultures can be centrifuged and subsequently resuspended at 1×10^5 viable cells/mL. Do not allow cell concentration to exceed 1×10^6 cells/mL. Maintain cell density between 1×10^5 and 1×10^6 viable cells/mL. On the day of the experiment, count cells using trypan blue. The cell viability should be ≥90%.

3. Methods

1. Turn on plate reader, warm it up to 37°C, place empty white 96-well test-plate inside the reader chamber to warm the plate up and set-up assay template.
2. Adjust cell concentration to 1×10^7 per mL by spinning cell suspension down and reconstituting in complete medium. Maintain at room temperature.
3. Add 100 μL of analyte nanoparticles in PBS and controls to designated wells (follow plate map scheme in Fig. 3). Prepare three duplicate wells for each sample and two duplicate wells for positive and negative control. Always leave duplicate wells for each of the following controls: (1) luminol-only control (no cells), (2) nanoparticles-only, and (3) nanoparticles with luminol (no cells).
4. Add 100 μL working luminol solution in PBS to each well containing sample. Do not forget to add luminol to two "luminol only" control wells (see Note 6).
5. Plate 100 μL of cell suspension per well on 96-well white plate.

Blank	PC	NC	NS1	NS1	NS1	NS2	NS2	NS2	Blank	PC	NC
Blank	PC	NC	NS1	NS1	NS1	NS2	NS2	NS2	Blank	PC	NC
LML	NS1 LML	NS2 LML	NS1	NS2							
LML	NS1 LML	NS2 LML	NS1	NS2							

Cells No cells

Fig. 3. This shows an example layout for the plate reader. The wells are labeled as follows: NC for negative control (PBS), PC for positive control, LML for luminol, and NS for nanoparticle sample.

6. Start kinetic reading on a luminescence plate reader immediately.
7. The plate reader will calculate the mean luminescence for each well. A percent coefficient of variation (%CV) is used to control precision and calculated for each control or test sample according to the following formula:

$$\%\mathrm{CV} = \left(\frac{\mathrm{SD}}{\mu_{\mathrm{F}}}\right) \times 100,$$

where μ_{F} is the mean value of the fluorescence from all replicate samples.

8. The percent coefficient of variation (%CV) for each control and test sample should be less than 30%.
9. If two of the three replicates of the positive or negative control fail to meet the %CV acceptance criterion described above, the assay should be repeated.
10. If two of the three replicates of the nanoparticle samples fail to meet the %CV acceptance criterion as described above, the nanoparticle sample should be reanalyzed.

4. Notes

1. Single use aliquots may be stored at 4°C for up to 1 month or at a nominal temperature of –20°C.

2. Store at 4°C protected from light for no longer than 1 month. Before use, warm the medium in a water bath.
3. To test whether the nanoparticles interfere with the phagocytosis of zymosan, a second set of the zymosan positive control can be prepared (not shown in Fig. 3). In this second set, the zymosan is reconstituted in nanoparticle solution/suspension to a final concentration of 2 mg/mL (see Fig. 4).
4. Always wear appropriate personal protective equipment and take appropriate precautions when handling your nanomaterial. Many occupational health and safety practitioners recommend wearing two layers of gloves when handling nanomaterials. Also, be sure to follow your facility's recommended disposal procedure for your specific nanomaterial.
5. This assay requires 600 µL of nanoparticles dissolved/resuspended in PBS (i.e. three 100 µL nanoparticle dilutions each tested in duplicate). The following questions have to be considered when selecting the concentration: For the initial run, a concentration of 1 mg/mL or one approaching the limit of solubility should be used and at three serial 1:5 dilutions.

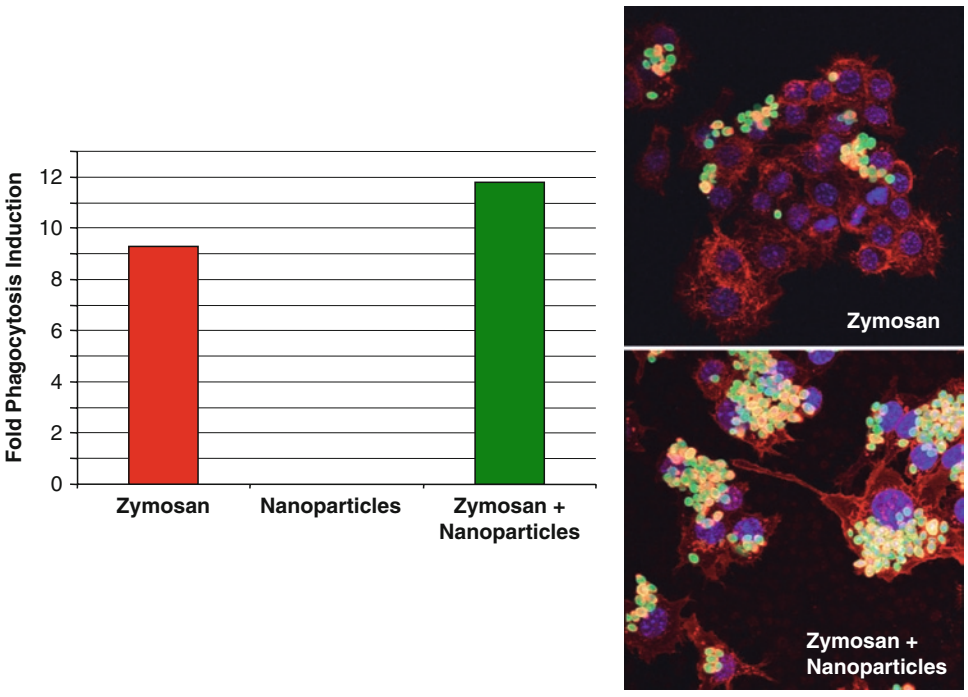

Fig. 4. The graph shows the results of this chemiluminescence assay for polymer-based nanoparticles alone and in the presence of Zymosan A. Though the nanoparticles do not seem to be taken up without Zymosan, they appear to significantly increase Zymosan uptake. Further investigation by real-time confocal microscopy showed that the nanoparticles caused the Zymosan to aggregate, leading to its increased uptake in the presence of nanoparticles. Confocal micrographs are shown in the *panels to the right.*

However, when nanoparticles are known to be cytotoxic at 1 mg/mL, lower concentrations should be evaluated. The nanoparticle-to-serum (or plasma) volume ratio and incubation conditions are the same as described for preparation of the positive control. Separation of the nanoparticles from bulk plasma/serum is performed by centrifugation at a speed and time deemed appropriate for a particular sample of nanoparticles. If ultracentrifugation is not feasible to separate particles, unincubated particles can be tested in the presence of 20% human serum/plasma.

6. Important: the temperature of the cells will affect the rate of uptake. Keep the plate warm during sample aliquoting (e.g. a plate warmer or warm gel pack should be used).

Acknowledgments

This project has been funded in whole or in part by federal funds from the National Cancer Institute, National Institutes of Health, under contract N01-CO-12400. The content of this publication does not necessarily reflect the views or policies of the Department of Health and Human Services, nor does the mention of trade names, commercial products, or organizations imply endorsement by the U.S. Government.

References

1. Aderem A., Underhill D. M. (1999) Mechanisms of phagocytosis in macrophages. *Annu. Rev. Immunol.* **17**, 593–623.
2. Shukla R., Bansal V., Chaudhary M., Basu A., Bhonde R. R., Sastry M. (2005) Biocompatibility of gold nanoparticles and their endocytotic fate inside the cellular compartment: a microscopic overview. *Langmuir* **21**(23), 10644–54.
3. Chithrani B. D., Ghazani A. A., Chan W. C. (2006) Determining the size and shape dependence of gold nanoparticle uptake into mammalian cells. *Nano Lett.* **6**(4), 662–8.
4. Chithrani B. D., Chan W. C. (2007) Elucidating the mechanism of cellular uptake and removal of protein-coated gold nanoparticles of different sizes and shapes. *Nano Lett.* **7**(6), 1542–50.
5. Antonini J. M., van Dyke K., Ye Z., DeMatteo M., Reasor M. J. (1994) Introduction of luminol dependent chemiluminescence as a method to study silica inflammation in the tissue and phagocytic cells of rat lung. *Environ. Health Perspect.* **102**(Suppl 10), 37–42.
6. Gref R., Luck M., Quellec P., et al. (2000) Stealth corona-core nanoparticles surface modified by PEG: influences of corona (PEG chain length and surface density) and of the core composition on phagocytic uptake and plasma protein absorption. *Colloids Surf. B Biointerfaces* **18**, 301–13.
7. Leroux J. C., Gravel P., Balant L., et al. (1994) Internalization of poly(D,L,-lactic acid) nanoparticles by isolated human leukocytes and analysis of plasma proteins absorbed onto particles. *J. Biomed. Mater. Res.* **28**, 471–81.
8. Mold C., Gresham H. D., DuClos T. W. (2001) Serum Amyloid P component and C-reactive protein mediate phagocytosis through murine FcγRs. *J. Immunol.* **166**, 1200–5.

INDEX

Scott E. McNeil (ed.), *Characterization of Nanoparticles Intended for Drug Delivery*, Methods in Molecular Biology, vol. 697, DOI 10.1007/978-1-60327-198-1, © Springer Science+Business Media, LLC 2011

D

E

F

G

H

I

L

M

N

U

X

Z